Human stem cell metabolomics; headspace volatile gas analysis as an indicator of self-renewal and differentiation status

---

Mohammed Abdulridha Al-Zubaidi

Thesis submitted to Keele University for the Degree of Doctor of Philosophy

March 2018

Keele University

Keele University

SUBMISSION OF THESIS FOR A RESEARCH DEGREE

Part I. DECLARATION by the candidate for a research degree. To be bound in the thesis

Degree for which thesis being submitted Doctor of Philosophy

Title of thesis Human stem cell metabolomics; headspace volatile gas analysis as an indicator of self-renewal and differentiation status

This thesis contains confidential information and is subject to the protocol set down for the submission and examination of such a thesis. NO

Date of submission 15.12.2017 Original registration date 06.01.2014

(Date of submission must comply with Regulation 2D)

Name of candidate Mohammed Abdulridha Al-Zubaidi

Research Institute Institute for Science and Technology in Medicine

Name of Lead Supervisor Professor Nicholas R Forsyth

I certify that:

(a) The thesis being submitted for examination is my own account of my own research
(b) My research has been conducted ethically. Where relevant a letter from the approving body confirming that ethical approval has been given has been bound in the thesis as an Annex
(c) The data and results presented are the genuine data and results actually obtained by me during the conduct of the research
(d) Where I have drawn on the work, ideas and results of others this has been appropriately acknowledged in the thesis
(e) Where any collaboration has taken place with one or more other researchers, I have included within an 'Acknowledgments' section in the thesis a clear statement of their contributions, in line with the relevant statement in the Code of Practice (see Note overleaf).
(f) The greater portion of the work described in the thesis has been undertaken subsequent to my registration for the higher degree for which I am submitting for examination
(g) Where part of the work described in the thesis has previously been incorporated in another thesis submitted by me for a higher degree (if any), this has been identified and acknowledged in the thesis
(h) The thesis submitted is within the required word limit as specified in the Regulations

Total words in submitted thesis (including text and footnotes, but excluding references and appendices) ……

Signature of candidate …….. Date……

Abstract

Self-renewal and an ability to differentiate are key hallmarks of stem cells. Pluripotent stem cells (PSC) have the capacity to differentiate into all cell types found within the three germ layers; ectoderm, endoderm, mesoderm. Multipotent stem cells including mesenchymal stem cells (MSC) customarily differentiate into cell types representative of one germ layer only.

Metabolomics focusses on characterising the low molecular weight organic compounds which are by-products of protein-protein interactions and metabolic enzymatic processes; volatile organic compounds (VOCs) emitted from or consumed by cells can be correlated with metabolic status. Selected Ion Flow Tube Mass Spectrometry (SIFT-MS) has been used to identify and discriminate between metabolites (VOCs) from both undifferentiated and differentiated stem cells in specific cell culture oxygen conditions (air (21% O_2) and physiological oxygen (2% O_2)).

The suitability of SIFT-MS for detecting and identifying VOCs from hPSCs was evaluated with SIFT-MS spectral data analysed via OPLS-DA. hPSCs cultured in 2% O_2 displayed a distinct metabolic profile to those cultured in 21% O_2. Metabolite markers differing between culture conditions for undifferentiated hPSCs included ethanol and acetaldehyde. Inhibition of ethanol/acetaldehyde conversion enzymes revealed mechanistic control of ethanol and acetaldehyde levels linked to environmental oxygen. hPSC differentiation-linked differences in metabolic profiles included immediate reductions in acetaldehyde and DMS/ethanethiol levels upon onset of differentiation.

For hMSCs, OPLS-DA score plots indicated that hMSCs cultured in a controlled, hermetic, workstation maintained at 2% O_2 were distinct to those cultured in either 2% O_2

or 21% O_2. The VOC profile of hMSCs varied with oxygen condition and degree of differentiation during osteogenic differentiation.

In summary, this thesis demonstrates that SIFT-MS can detect and discriminate VOC profiles in two distinct stem cell populations. These profiles are sensitive to oxygen and differentiation status and therefore provide a potential valuable tool for non-invasive explorations of stem cell biology.

Contents

Index of Figures

Chapter 1

Chapter 2

Chapter 3

Index of Tables

Chapter 2

Chapter 3

Chapter 4

Abbreviations

4-MP	4-methyl pyrazole
ACTB	β-Actin
ADH	Alcohol dehydrogenase
AFP	Alpha-fetoprotein
ALDH	Aldehyde dehydrogenase
ALPL	Alkaline Phosphatase
ANOVA	Analysis of variance
BGLAP	Gamma-carboxyglutamic acid-containing protein
BMA	Bone marrow aspirate
BMCs	Bone marrow cells
BSA	Bovine serum albumin
CAT	Catalase
CD	Cluster of differentiation
CFU-F	Colony forming unit-fibroblast
COL1A1	Collagen, type 1, alpha 1
CYP2E1	Cytochrome P450 2E1
DAPI	4',6-diamidino-2-phenylindole
dH_2O	Distilled water
DMEM	Dulbecco's Modified Eagle Medium
DMEM/F12	Dulbecco's Modified Eagle Medium:Nutrient Mixture F-12
DMS	Dimethyl sulphide
DMSO	Dimethyl sulphoxide
E8M	Essential 8 Medium
EDTA	Ethylenediaminetetraacetic acid
FBS	Fetal bovine serum
FS	Full scan
GC-MS	Gas chromatography-mass spectrometry
hESCs	Human embryonic stem cells
HIFs	Hypoxia inducible factor
hiPSCs	Human induced pluripotent stem cells
HLA-DR	Human Leukocyte Antigen-antigen D Related
hMSCs	Human mesenchymal stem cells
HOC	Hypoxic conditioned media
hPSCs	Human pluripotent stem cells
HS	Headspace
HSCs	Haematopoietic stem cells
hTERT	Human telomerase reverse transcriptase
IBMX	3-isobutyl-1-methylxanthine
ICM	Inner cell mass
IgG	Immunoglobulin G
KO-DMEM	Knockout Dulbecco's Modified Eagle Medium
LC-MS	Liquid chromatography-mass spectrometry
L-Glut	L-Glutamine
m/z	Mass to charge ratio
MIM	Multiple ion monitoring
MTT	3-(4,5-dimethylthiazol-2-yl)-2,5-diphenyltetrazolium bromide

NEAA	Non-essential amino acid
OCT-4	Octamer-binding transcription factor 4
OPLS-DA	Orthogonal partial least squares discriminant analysis
OTX	Orthodenticle homeobox 2
PBS	Phosphate buffer saline
PCA	Principal component analysis
PSA	Penicillin, streptomycin, amphotericin B
RT-PCR	Reverse transcription polymerase chain reaction
RUNX2	Runt related transcription factor 2
SD	Standard deviation
SIFT-MS	Selected ion flow tube-mass spectrometry
SOX	SRY (sex determining region)-box
SPARC	Secreted protein acidic and cysteine rich
SSEA	Stage-specific embryonic antigen
TAE	Tris acetate EDTA
TRA	Keratan-sulphate-antigen
VIP	variable importance in the project
VOCs	Volatile organic compounds
WS	Work station

Publications and presentations

Publications

1. Agrawal, R., Dale, T.P., Al-zubaidi, M.A., Malgulwar, P.B., Forsyth, N.R. and Kulshreshtha, R., 2016. Pluripotent and Multipotent Stem Cells Display Distinct Hypoxic miRNA Expression Profiles. *PloS one*, 11(10), pp. e0164976.

Oral presentations

1. Mohammed A Al-Zubaidi, Josep Sulé-Suso, Nicholas R Forsyth. The production of volatile organic compounds by human embryonic stem cells. Mercia Stem Cell Alliance (MSCA) conference, UK (September 2014).
2. Mohammed A Al-Zubaidi, Josep Sulé-Suso, Nicholas R Forsyth. Precision control of dissolved oxygen in mammalian cell culture media impacts on in situ volatile generation and promotes improved mesenchymal stem cell yield accompanied by reduced transcriptional variability. SFRR-E/SNFS Conference, Germany 2015.

Posters

1. Mohammed A Al-Zubaidi, Josep Sulé-Suso, Nicholas R Forsyth. The production of volatile organic compounds by human embryonic stem cells. Mercia Stem Cell Alliance (MSCA) conference, UK (September 2014)
2. Mohammed A Al-Zubaidi, Josep Sulé-Suso, Nicholas R Forsyth. Determination of headspace volatile levels: potential roles in mesenchymal stem cell biology. TCES conference, UK (July 2015).
3. Mohammed A Al-Zubaidi, Josep Sulé-Suso, Nicholas R Forsyth. Determination of headspace volatile levels: potential roles in mesenchymal stem cell biology. The 9th UK mesenchymal stem cell meeting, UK (December 2015).

Acknowledgements

I would like to thank sincerely my lead supervisor Professor Nick Forsyth who has guided me constantly throughout my PhD, for his patience, motivation and immense knowledge. Professor Nick Forsyth has not only contributed to scientific guidance towards my work but has also helped me in the development of my career as a researcher. I would like to thank my co-supervisor Professor Josep Sulé-Suso who has supported me from the beginning of my scientific study.

Beside my supervisors, I would also like to express my gratitude for those who helped me with SIFT-MS, Professor David Smith and Dr Thomas Chippendale. It is with particular thanks to Professor David Smith who provided me invaluable advices.

I would like to thank my country Iraq and then my sponsor (Ministry of Higher Education and Scientific Research, Republic of Iraq) for offering me the opportunity for this study. I thank the College Pharmacy, Al-Mustansiriyah University.

Last but not the least, I would like to thank my family: my parents and to my brother and my sisters for supporting me spiritually throughout my study.

Chapter 1-Introduction

1.1 Stem cells

Stem cells are defined as undifferentiated or unspecialised cells from the embryo (i.e. embryonic stem cells) or from adult tissue (i.e. adult stem cells). Embryonic stem cells have two important characteristics; the ability to divide and generate new identical copies of themselves (i.e. self-renewal) and under the proper physiological or experimental condition, can specialise or differentiate into a diverse range of cell types found in the body (Evans and Kaufman, 1981; Martin, 1981; Thomson et al., 1998). Like embryonic stem cells, some adult stem cells are capable of self-renewal and differentiation into various cell types. Conversely, unlike embryonic stem cells, adult stem cells are not pluripotent (i.e. multipotent) as well as having a limited self-renewal ability. Self-renewal and potency to differentiate into specialised cells allow them to serve as building blocks in developmental processes. (Ullah et al., 2015).

Stem cells are classified based on their potential for differentiation (Figure 1.1). Accordingly, they can be defined as:

- Totipotent stem cells are the most primitive and have the potential to develop into trophectoderm cell lineages in addition to the three germ layers; ectoderm, mesoderm and endoderm. These cells are yielded at the moment of fertilization of the egg (early progeny of the zygote) and remain until the embryo reaches the 4 to 8 cell stage (Mitalipov and Wolf, 2009).

- Pluripotent stem cells can differentiate into cells of all three germ layers, ectoderm, mesoderm and endoderm; e.g. embryonic stem cells and induced pluripotent stem cells (Mitalipov and Wolf, 2009).

- Multipotent stem cells can differentiate into multiple cell types in germ layer; e.g. mesenchymal stem cells and haematopoietic stem cells. (Bianco, 2011).

Currently, all mammalian stem cells can be classified based on their origin into two categories: embryonic stem cells (ESCs) and adult or somatic stem cells (e.g. mesenchymal stem cells (MSCs)) (Lodi et al., 2011). Recently, new stem cells have been added to the list of stem cells and were named induced pluripotent stem cells (iPSCs). (Mitalipov and Wolf, 2009).

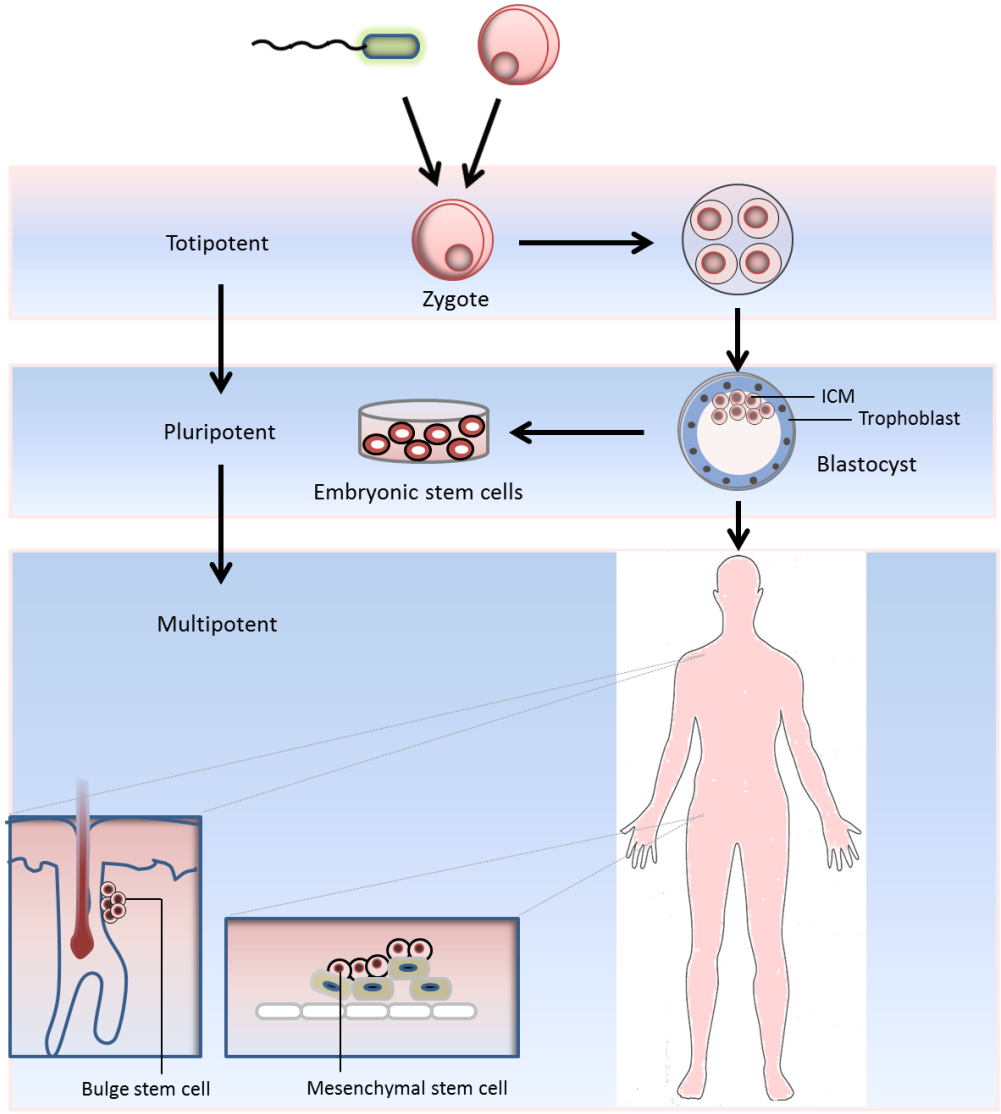

Figure 1.1. Types of stem cells. The formation of totipotent zygote following fusion of egg and sperm to form the inner cell mass (ICM) and trophoblast of the blastocyst.

Following ICM isolation from blastocyst, the cells of the inner cell mass (ICM) can be maintained in culture as pluripotent (i.e. embryonic stem cells). During the development of the embryo, the pluripotent stem cells in the inner cell mass (ICM) become multipotent stem cells and generate tissue-specific. These include epidermal stem cells (bulge cells) and mesenchymal stem cells. Eckfeldt et al., 2005.

1.2 Human pluripotent stem cells:

As mentioned above, due to their unique ability to differentiate into cells of all three germ layers and their unlimited self-renewal capacity, human PSCs hold a huge potential for a number of different scientific and clinical applications, including new drugs screening and cell-based therapies and regenerative medicine. Currently, two types of pluripotent stem cells have been described; embryonic stem cells (ESCs) and induced pluripotent stem cells (iPSCs) (Avior et al., 2016).

1.2.1 Human embryonic stem cells:

The first type of identified and isolated human pluripotent stem cells, hESCs are valuable tools in the area of biological development and regenerative medicine. Prior to the derivation of ESCs, embryonal carcinoma cells (ECCs) were isolated from teratocarcinomas formed following the implantation of early stage mouse embryos and used as a model for developing embryo *in vitro* (Martin, 1981). After a number of efforts, a breakthrough evolved and arose in 1981 when ESCs were isolated from murine embryos (Evans and Kaufman, 1981; Martin, 1981), before isolation of ESCs from non-human primate embryo's in 1995 (Thomson et al., 1995). In 1998, Thomson and colleagues isolated and cultured the first derivation of human ESCs from human embryos produced by *in vitro* fertilisation (IVF). These cells were isolated by immunosurgery from the inner cell mass (ICM) of the blastocyst stage embryo and cultured on irradiated mouse embryonic

fibroblasts. The resulting cells were grown as colonies and individual undifferentiated colonies were dissociated into clumps until the cell line was established. Five different hESC lines were derived, three of them had a normal XY karyotype (H1, H13 and H14) and two had a normal XX karyotype (H7 and H7) (Thomson et al., 1998). Both human embryonic stem cells and mouse embryonic stem cells have various signalling features and culture conditions, but they both maintain pluripotency via the expression of the same core transcription factors (Pera et al., 2000). Nowadays, those hESCs generated in 1998 are still utilized in research and regarded as the gold standard hESC lines.

A large number of hESC lines have now been generated besides the original five lines. There is a considerable heterogeneity between lines in addition to the differences in gene expression signatures (Abeyta et al., 2004), differentiation propensity (Osafune et al., 2008) and population doubling time; this variation possibly reflecting differences in derivation methods and timing, initial culture conditions, or original genetics of the source embryo. hESC lines must meet a number of criteria (Hoffman and Carpenter, 2005), including expression of a number of cell surface antigens and internal transcription factors associated with pluripotency for example stage specific antigens 3 and 4 (SSEA3 and SSEA4), tumour receptor antigens 1-60 and 1-81 (TRA1-60 and TRA1-81), octamer-binding transcription factor 4 (OCT4), Nanog and SRY-box 2 (SOX2). Another definition of pluripotency in hESC is being able to form all three germ layers derivatives in immunocompromised mice *in vivo* (Allegrucci and Young, 2006). Moreover, hESCs must possess the capacity for unlimited self-renewal and normal karyotype.

In spite of their promise, there are numerous issues to be considered before any strategy for use in routine clinical applications. Firstly, there are a number of ethical issues, which must be taken into account when deriving hESCs, including the destruction of fertilised embryos. Secondly, it is essential to confirm that all pluripotent stem cells are removed

from the transplanted cell population, as the presence of these cells increases the prospect of teratoma formation. The potential of immunogenicity also presents an issue for consideration (Wert and Mummery, 2003).

1.2.2 Induced pluripotent stem cells:

The best way to overcome the issue of hESCs immunorejection is by using autologous cells. Yamanaka and colleagues reprogrammed both mouse and human adult fibroblast to pluripotency via transduction of four defined factors, including Oct4, Sox2, Klf4 and c-Myc (Takahashi and Yamanaka, 2006; Takahashi et al., 2007) (figure 1.2). The generated pluripotent cells were known as induced pluripotent stem cells (iPSCs) which are similar to hESCs in morphology, proliferation capacity, expression of hESCs specific cell surface antigens (SSEA3, SSEA4, TRA1-60 and TRA1-81) and endogenous genes (Oct4, Nanog, Sox2), and the ability to generate any cell from all three germ layers *in vitro* and teratoma formation *in vivo*.

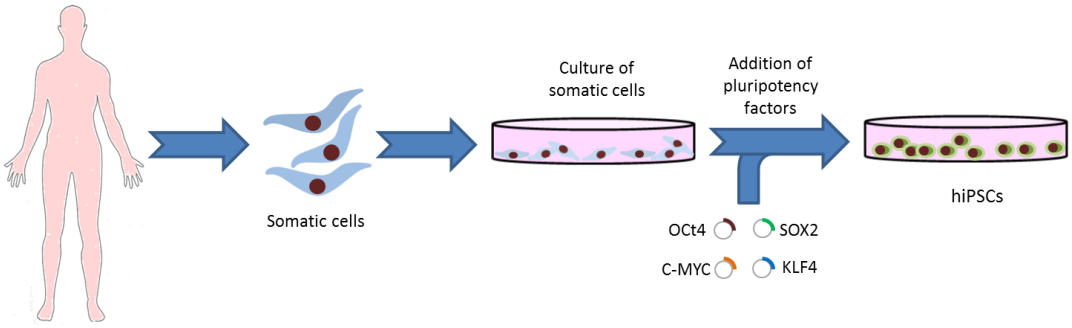

Figure 1.2. Schematic diagram represent stages of hiPSC generation. Following isolation, fibroblasts or other somatic cells are cultured *in vitro* and transduced with four pluripotent factors (OCT-4, SOX2, KLF4, and c-MYC). Adapted from Yamanaka and Blau, 2010.

1.3 Adult stem cells:

Adult stem cells are undifferentiated cells found in various tissues of the human body which are capable of differentiating into more mature cell of that tissue (Fujimaki et al., 2013). Adult stem cells can be classified depending on the germ layer they come from: the ectoderm layer of an early embryo lead to the nervous system, mammary glands, hair and skin; the endoderm layer give rise to the intestine, pancreas, liver and lung. Circulatory system muscle and mesenchymal stem cells come from the mesodermal layer (Haasters et al., 2009). Unlike ES cells, adult stem cells are only multipotent and are not derived by destruction of an embryo; consequently, avoiding many of the ethical issues involved in the research of embryonic stem cells. The clinical use of adult stem cells e.g. transplantation of bone marrow for treating blood disorder, has been used for decades (Kinner et al., 2002) and therefore holds great opportunity for regenerative medicine.

The bone marrow introduces several adult stem cell populations that serve to maintain the tissue homeostasis by generate new cell types in adult human body; haematopoietic stem cells (HSCs), mesenchymal stem cells (MSCs), multipotent adult progenitor cells and endothelial progenitor cells (EPCs). These cells differentiate into cells of the vascular and musculoskeletal systems (Saeed et al., 2016).

1.3.1 Mesenchymal stem cells:

The first evidence supporting the presence of distinct stem cell populations within the bone marrow was in 1968, when Friedenstein and colleagues found a set of cells that were tissue culture plastic adherent, colonogenic, nonphagocytic, and fibroblastic that were coined Colony Forming Unit-Fibroblast (CFU-F) (Friedenstein et al., 1968). Since then, a number of research groups have discovered MSCs and their particular properties that raised the need to establish general agreement on their definition (Dominici et al., 2006). The study

of hMSCs is dependent, in some part, on the morphology and expression of surface antigens. The cells are constituted of a heterogeneous population; three cell types commonly observed are rapidly self-renewing cells, slowly replicating, large, cuboidal or flattened cells and elongated fibroblastic-like, spindle shaped cells (Haasters et al., 2009).

There is no single marker for the detection and recognition of mesenchymal stem cells, therefore the Mesenchymal and Tissue Stem Cell Committee of the International Society for Cellular Therapy suggested a minimum set of criteria to define this population, based on the adherence to tissue culture plastic when cultured in standard culture condition, positive expression for several surface markers including CD105, CD90 and CD73, and negative surface marker expression for CD14, CD45, CD34, CD11b, CD79α, CD19 and HLA-DR, and multipotent differentiation potential (Dominici et al., 2006).

Human mesenchymal stem cells can be isolated from several tissues. The most popular are bone marrow (Friedenstein et al., 1968), adipose tissue (Zuk et al., 2001), placenta (In'T Anker et al., 2004) and umbilical cord structure or blood (Erices et al., 2000; Kim et al., 2004). Other adult tissue or organ sources of this population or similar ones are synovium (Fickert et al., 2003), cartilage (Alsalameh et al., 2004), dermis (Riekstina et al., 2009). MSCs might also be found during the fetal development in the lung, liver and spleen (In'T Anker et al., 2003). Although MSCs present in all above tissues, they appear to have some differences in their differentiation potential in accordance to their source (Cavallo et al., 2011; Peng et al., 2008).

The first reported source of MSCs was bone marrow (Friedenstein et al., 1968), which is considered to be the gold standard source, even though the frequency of MSCs is only 1/10000-1/100000 of nucleated cells (Peng et al., 2008). The harvesting of mesenchymal stem cells from bone marrow is painful and usually requires anaesthesia (Zuk et al., 2001)

as well as the low frequency of MSCs which decline with age (Penge et al., 2008) suggest an expansion step *in vitro* (Zuk et al., 2001). The expansion step is time consuming, expensive, and subject to cell contamination risk and loss (Zuk et al., 2001). Adipose tissue seems to be an alternative to the standard source of MSCs, which is usually discarded from abdominoplasties and lipoaspirations as a medical waste (Bourin et al., 2013), easily accessible with less invasive method (Cavallo et al., 2011; Peng et al., 2008), and richer in stem cells when compared to bone marrow (~ 500 fold) (Hass et al., 2011), which might result in reducing the expansion time of cells *in vitro* (Richardson et al., 2013).

Osteoprogenitors, chondrogenic progenitors and adipocyte progenitors are amongst a mixture of isolated MSCs from bone marrow that can be observed as partially defined in terms of their stem cell fate (Muraglia et al., 2000). MSCs have been reported to differentiate into adipocyte, osteoblast, chondrocyte, myoblast and fibroblast cells (Pittenger et al., 1999; Barry et al., 2001; Gang et al., 2004). However, in recent years some controversial studies reported cases of transdifferentiation across tissue types, for example neuronal cells and hepatocytes (Song and Tuan, 2004; Sato et al., 2005). Therefore MSCs offer great therapeutic potential for use in clinical applications, which is dependent on further understanding the regulation between self-renewal and lineage commitment.

1.4 Stem cell niche:

The stem cell niche concept was suggested by Schofield over 30 years ago to characterize the particular microenvironment where a stem cell resides *in vivo* (Wang and Wagers, 2011). The niche is basically a tissue microenvironment (Morrison and Spradling, 2008), including cells (including stem cells), the extracellular matrix, and soluble molecules present around the stem cells (Kolf et al., 2007). The niche is essential to give stem cells

cues to maintain them in an undifferentiated state and external cues to induce their differentiation whenever needed to replace and repair injured tissue (Kolf et al., 2007). Therefore, the niche will regulate stem cell behaviour and function via a balance between protection and interaction (Wang and Wagers, 2011). One of the important components of the niche is a group of proteins called cadherins, which are responsible for cell-cell adhesion, migration, differentiation, polarity and interaction with the mammalian homologue of Drosophila wingless (Wnts), which are believed to be involved in the maintenance of undifferentiated state and the differentiation paths of MSCs (Kolf et al., 2007).

Stem cell niches can be divided into three types based on the specific function; simple cell niches, complex cell niches and storage cell niches. The simple cell niche is a microenvironment which contains one stem cell type which is locked to the extracellular matrix via adhesion junctions and integrin mediated interactions. In this niche, paracrine signals promote stem cell growth while inhibiting differentiation. The complex niches contain two or more different stem cells that are supported by one or more different partner cells. The activity of the complex niches is controlled by regulatory signals to produce multiple progeny cells. Storage niches are specific locations in which stem cells are maintained until external signals are received to repair injured tissue (Ohlstein et al., 2004).

The compositions of extracellular matrix are fibres, laminin polymer, cell adhesion protein (e.g. fibronectin, proteoglycans) and growth factors (Chen, 2010). There are two types of extracellular matrix which exist together in the bone, the calcified bone matrix that is created by osteoblasts, and the marrow extracellular matrix that is created by MSCs (Chen, 2010). Datta and colleagues showed that the extracellular matrix is very important for MSCs differentiation (Datta et al., 2005). They observed that deposited extracellular matrix produced by osteoblastic cells on decellularized scaffold displayed higher proliferation of

MSCs, higher deposition of calcium and increased levels of osteopontin, indicating stem cells differentiation into bone progenitor cells (Datta et al., 2005).

The central and epiphysis region of bone is the bone marrow region where haematopoiesis occurs comprising extracellular matrix and a meshwork of thin walled capillaries (Zhao et al., 2012). The niche within this structure contains both haematopoietic stem/progenitor cells and mesenchymal stem cells along with adipocytes and stromal cells (Chen, 2010). MSCs are perivascular and usually present in the central area of the bone marrow, and they are also found at lower frequency in the vicinity of the endosteum (Krause et al., 2013) (Figure 1.3). The bone marrow niche is physioxic, and this low oxygen level, ranging from 1% in the niche itself to 6% in the sinusoidal cavity (Eliasson and Jonsson, 2010), participates in increasing the proliferation capacity, as well as maintaining the naïve state and the plasticity of mesenchymal stem cells (Makino et al., 1999). The physioxic environment of haematopoietic cells is associated with a more quiescent state because it occurs far away from blood capillaries and closer to bone surface (Eliasson and Jonsson, 2010).

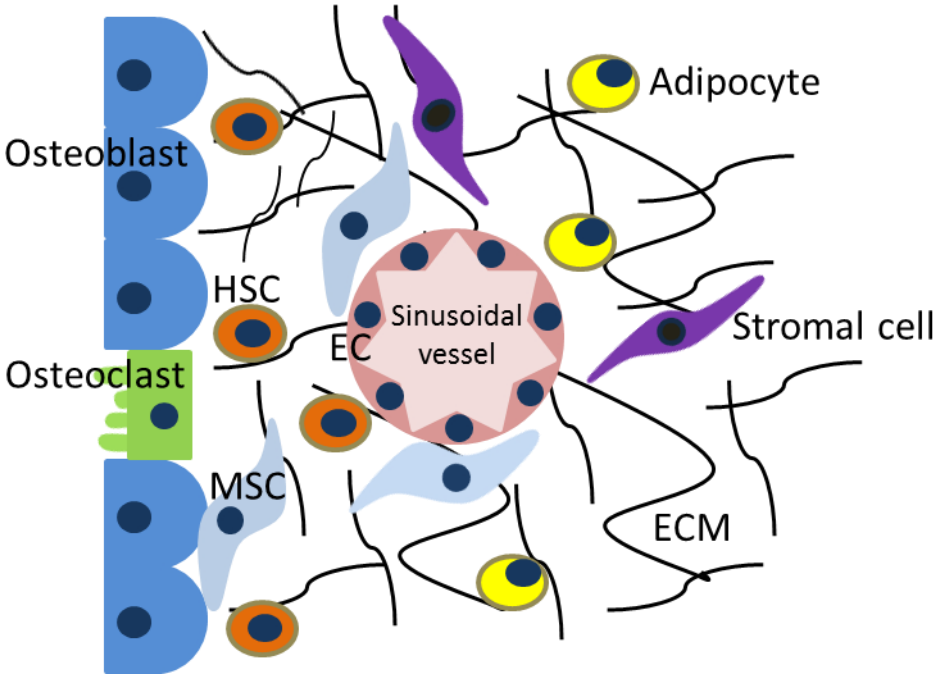

Figure 1.3. MSCs niche in bone marrow. The bone marrow cells including stromal cells, adipocyte and osteoblasts are derived from MSCs, while HSCs have the ability to differentiate into all haematopoietic cells including monocyte-derived osteoclasts. Adapted from Schraufstatter et al., 2011.

1.5 Oxygen and stem cells:

Oxygen is crucial for life with almost all organisms relying on oxygen for energy production. In humans, it is recognized as playing a key role as a vital electron acceptor during ATP production (Konigsberg et al., 2013). Although tissue specific oxygen tension is dependent on the distance away from the vasculature, 1% - 8% O_2 has been recognized as a general estimate for most tissues (Jez et al., 2015). In the early stages of human's pregnancy (6-7 days post fertilisation), in which the blastocyst can be explanted for development of hESC lines (Camarasa et al., 2012), the intrauterine fluid has an oxygen concentration far lower than that found at atmospheric condition. Direct measurements of oxygen concentration in human uterine fluids are difficult due to the invasive technique of the electrodes and catheters used to quantify its concentration but the mid-point of the

menstrual cycle has been assessed to reside at about 3% O_2 (Ottosen et al., 2006). Furthermore, the dissolved oxygen in the peripheral maternal venous blood was measured and showed a gradual increase in parallel with advancing pregnancy due to the establishment of circulatory system (Rodesch et al., 1992; Simon and Keith, 2008). Under low oxygen tension, the alterations to embryonic and fetal development have often been related to the actions of a family of transcriptional regulators (i.e. Hypoxic Inducible Factors (HIFs)), which are hypothesised to regulate critical phases of normal embryonic development under low oxygen. *In vitro*, the physioxic condition was investigated by Ezashi and colleagues, in order to maintain human embryonic stem cells in undifferentiated state. They showed that human embryonic stem cells cultured in the physioxic condition (3%-5%) O_2 contained less differentiated cells. Furthermore, air oxygen cultured cells had produced more chorionic gonadotropin after day five and progesterone after day nine in the media, indicating further differentiation (Ezashi et al. 2005). Additionally, Forsyth and colleagues reported that culture in 2% O_2 increased hESCs clonal recovery, and flow cytometry analysis showed that physioxia cultured cells were smaller and less granular than those in air oxygen condition. Moreover, they reported that the early and late passage culture reduced the spontaneous chromosomal aberration of hESCs in physioxic culture (Forsyth et al. 2006).

In vivo, mesenchymal stem cells reside in perivascular niches that associate closely with blood vessels in virtually all tissues. The various tissues where mesenchymal stem cells reside exhibit low oxygen tensions, even though these stem cells are located close to the blood vessels (Mohyeldin et al. 2010). For example, mesenchymal stem cells, found within the bone marrow, reside under 1-7% of oxygen level (Sheehy et al. 2012; Holzwarth et al. 2010) which is lower than the oxygen level in peripheral blood of healthy people (Jing et al. 2012).

In vitro, mesenchymal stem are traditionally expanded in air culture condition where 5% CO_2 is used to help buffer the medium's pH and for cellular metabolism. However, it was shown that expansion of stem cells in a low oxygen environment leads to more population doublings while maintaining the potential of stem cell differentiation (Moussavi-Harami et al 2004; Dellatore et al. 2008; Ma et al. 2009; Cicione et al. 2013). It was also shown that their growth rate could be improved by culturing under a hypoxic condition (5% O_2). In addition, the multipotency of mesenchymal stem cells was maintained and less apoptosis was observed (Hung et al. 2007).

It is suggested that more population doublings are obtained at low oxygen concentration as a result of less and delayed cellular senescence (DiGirolamo et al. 1999; Moussavi-Harami et al. 2004). Cell death or senescence is induced by DNA damage and/or by shortening of telomeres (Herbig et al. 2004; Bakkenist et al. 2004; Nakamura et al. 2008), which may happen via oxidative stress (Tchirkov and Lansdorp, 2003; Boesten et al. 2013). Reactive oxygen species (ROS), such as oxygen free radicals (O_2^-) and hydrogen peroxide (H_2O_2) are produced by oxidative phosphorylation when cells produce energy (Kondoh et al. 2007). Usually, cells have the ability to protect themselves against reactive oxygen species through cellular antioxidants. However, cells can be damaged by reactive oxygen species production if there is insufficient antioxidant. Premature aging of the cell can occur as a result of the production of ROS. However, when less ROS are produced by redirecting the metabolism of cells with lower oxygen concentration in the cell culture, the cellular senescence can be reduced and cell expansion is prolonged (Kondoh et al. 2005).

1.6 Metabolomics:

Metabolomics comprises both qualitative and quantitative analysis of all metabolites present in a biological system (Fiehn, 2001). Metabonomics was coined by Nicholson and

colleagues, and defined as the quantitative measurement of the dynamic multiparametric response of a biological system to pathophysiological stimuli or genetic modification (Nicholson et al., 1999). Practically, both terms overlap by a large degree and are frequently utilized interchangeably. The whole set of intracellular and extracellular metabolites produced by cells are known as the metabolome (Oliver et al., 1998). While metabolites are the downstream products of other omics (e.g. transcriptomics and proteomics), metabolomics of the biological system under study provides complementary knowledge for a better understanding of the cellular process (Villas-Boas et al., 2005). Metabolomics analyses have been divided into two major approaches: targeted and untargeted methods. Targeted metabolomics is a quantitative approach wherein a number of pre-determined metabolites belonging to a particular set of compounds (e.g. carbohydrates, lipids, amino acids) or to specific metabolic pathway (e.g. glycolysis) are quantitated (Roberts et al., 2012). Usually, this approach is hypothesis-driven study and needs *a priori* knowledge of the biological system under study. An example of this strategy was the analysis of 20 amino acids in cancer cells (Tomita et al., 2016). Because researchers concentrated on the measurement of the amino acids other metabolites present in the cell extracts were neglected. Targeted methods provide quantitative information about the selected number of metabolites.

The untargeted metabolomics approach (also known as global metabolomics or metabolite profile), on the other hand, aims to detect all metabolites in a biological sample, including unknown compounds. Usually, the untargeted approach compares the metabolite profile of the studied groups (control and altered groups) allowing the identification of the interesting metabolites which are the further investigated with a targeted approach (Leon et al., 2013). Therefore, untargeted and targeted metabolomics approaches can complement each other and if utilized in combination can provide more details about the metabolic events

occurring in the biological system. Untargeted metabolomics has been applied in the discovery of potential biomarkers in Alzheimer's disease (Li et al., 2010), cancer (Lin et al., 2011; Xie et al., 2012), onchocerciasis (Denery et al., 2010) and metabolic disorders (e.g. diabetes and obesity) (Zhang et al., 2009; Kim et al., 2010), amongst other conditions.

Additionally, untargeted metabolomics can be sub-divided into: metabolomics fingerprinting, which aims to analyse all the intracellular metabolites (endo-metabolome) (Fiehn, 2001) and metabolomics footprinting, which aims to analyse all extracellular metabolites (exo-metabolome) (Allen et al., 2003) (Figure 1.4). Footprinting analysis is technically simple when compared with metabolomics fingerprinting because it requires minimal sample preparation, only filtration or centrifugation to separate culture media from cells before the analysis. Metabolomics fingerprinting requires a much more technical procedure to extract the metabolites from cells and the protocols are also extensively improved in order to obtain suitable metabolite recoveries (Leon et al., 2013).

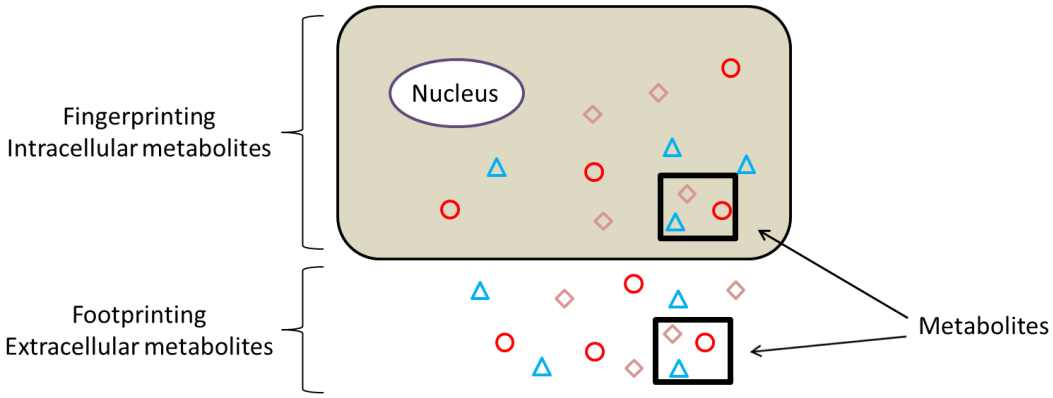

Figure 1.4. Untargeted metabolomics strategies for the analysis of extra- and intra-cellular metabolites. The figure shows the site of the extracellular (outside the cell) and intracellular (inside the cell) metabolites. Circles, diamonds and triangles represent metabolites.

Metabolites are intermediate products of catabolic and anabolic pathways and build the linkage between utilisation of nutrients and the production of cellular components, energy and waste products (Ussher et al., 2016). Metabolites are generally labile species, their chemical nature is very diverse, and they exist in a wide dynamic range (Hollywood et al., 2006). The diverse chemical properties and concentration ranges in living systems make all metabolites measurement hard to achieve. Hence, most of untargeted approaches are well-matched for a specific subset of compounds based on their chemical properties and concentration ranges.

Any biological system produces both volatile and non-volatile compounds (Whittle et al., 2007). In recent years, volatile organic compounds have received considerable interest (Filipiak et al., 2016). Hence, volatile organic compounds released from living cells are able to provide crucial information about different metabolic processes or pathways as well as the physiological condition of the cells (Pasini et al. 2004). Therefore, the concept arises of using volatile organic compounds or metabolite characteristics, which are a class of biomarkers, to establish metabolic changes due to different diseases, particularly cancer (Abaffy et al. 2013). Importantly, there are a wide range of volatile organic compounds present in trace amounts across a range of samples, including breath, urine and blood samples of human (Rudnicka et al., 2011; Silva et al., 2011; Xue et al., 2008). Generally volatile compounds are defined by a molecular weight range between 50-200 Daltons and have an appreciable vapour pressure under ambient conditions (Rowan, 2011). The advantages of volatile organic compounds are the fact that they are easily and non-invasively obtainable, and the analysis of VOC profiling is relatively inexpensive (Filipiak et al., 2016; Wang et al., 2016). However, the main drawback of VOCs in comparison to other markers e.g. nucleic acid and protein-based markers is the current incomplete information on the total number of volatile organic compounds produced by human cells.

Furthermore, many of the biochemical pathways leading to VOCs production and degradation within human cells are missing (Filipiak et al., 2016). In many and various cancer states, for example, lung and breast cancer, breath sample analysis has been used in several studies to determine which volatile organic compounds (metabolites) can serve as potential biomarkers. Additionally, other studies on cancers such as ovarian, liver, stomach and prostate cancers have been investigated using chemical analysis of exhaled breath (Abaffy et al. 2013). It has been reported in a recent study that there are nine urinary volatile organic compounds presented in patients with lung cancer at higher concentrations than those in control groups (Hanai et al 2012). In addition, studies have demonstrated that the concentration of hexanal and heptanal, which are volatile organic compounds, in the blood of patients suffering from lung cancer are elevated as compared with those in the control group (Deng et al. 2004).

Smith and colleagues showed that acetaldehyde is present in the headspace of the cell cultures of SK-MES and CALU-1 lung cancer cells lines in a proportion to the cells number (Smith et al. 2003). Acetaldehyde level was also found to be higher in a 3D model containing CALU-1 cancer cells line and non-malignant lung cells NL20 when compared to that of the same cells grown in 2D model (Rutter e al. 2013). High concentrations of acetone were also found in the headspace of lung cancer cells as compared to the growth medium (Filipiak et al. 2010).

1.7 Metabolomics and enzyme function identification:

Stem cells are the basic of all multicellular organisms. Several factors, from transcriptional to epigenetic, have been shown to play a role in fate determination; in addition, increasing consideration is being given to the responsibility of metabolism as a regulator of stem cell fate (Arnold et al., 2015). The research for novel enzymes is one of the tasks in functional

genomics. Metabolites can be used to assign or validate the function of enzyme activities because they are often the ultimate downstream products of gene expression (Baran et al., 2009). The chemical reactions that are processed by enzymes in all process of life are organised in response to the environment; in addition, the abundance of each metabolite depends on the specific physiological and state of a cell. Therefore, the intermediate metabolites reflect the phenotype of a cell, resulting in response to various environmental or genetic influences (Arnold et al., 2015).

Most of the traditional enzyme assays are used to establish enzyme activity, but a major drawback of this technique is that the enzyme function has to be known (Liesener and Karst, 2005). Integrated metabolomic and transcriptomic approaches can be used to assist identification of unknown enzymes (Fridman and Pichersky, 2005), however, pre-knowledge of the biochemical reaction was still necessary. Recent development in Mass spectrometry-based techniques in the analysis of intermediate metabolites has become a valuable technique for enzyme discovery and validation of their functional assignment (Baran et al., 2009).

1.8 Volatile organic compound sampling and extraction:

As with metabolomics, the measurement of the profile of volatiles generated by a living system needs an alteration of the analysis from the selective quantitative analysis of particular metabolite, which has been the core of analytical chemistry, to the measurement of several metabolites with corresponding balance in the precision, accuracy and sensitivity with single metabolites measurement. As different metabolites within a volatile profile will vary in their physical and chemical properties, the efficiency of extraction of these volatiles from the sample will also differ and will be extremely dependent on the sampling methods used. Thus, the choice of the most suitable strategy for volatile sampling and extraction is

the most important step. In general, a complete sample needs to be in an enclosed system with air circulation (dynamic headspace collection) and without air circulation (static headspace collection) (Rowan, 2011).

In a dynamic (purge and trap) headspace sampling method, a known volume of ultra-purified air is passed over the biological sample and the entrained volatiles are concentrated onto an adsorbent trapping graphite or organic polymer such as Tenax. VOCs may then be extracted from the adsorbent trap by elution with organic solvent transferred directly to instrument for analysis by rapid heating of the adsorbent material in a flow of inert gas (Rowan, 2011).

In static headspace analysis, air is not circulated and the volatiles in the sample are allowed to equilibrate with the air in an enclosed container. After the equilibration, a known volume of air is collected from the headspace of the sample using a needle and introduced to the instrument for analysis (Rowan, 2011).

1.9 Analytical platforms for metabolomics:

At present, there is no single analytical platform that can fully achieve the analysis of all metabolites in a given sample. Amongst the analytical platforms, both mass spectrometry (MS) (e.g., GC-MS) and nuclear magnetic resonance (NMR) are advanced analytical tools applied to metabolomic investigations. However, both techniques have different analytical advantages and disadvantages (Dunn et al., 2011). Each analytical platform has specific characterisation features, which enables analysis and detection of a specific range of metabolites (Zhang et al., 2012). Amongst the analytical techniques used for analysis of volatile metabolites is selected ion flow tube-mass spectrometry (SIFT-MS).

1.9.1 Overview of the SIFT-MS technique:

In 1976, Smith and Adam conceived and developed the Selected Ion Flow Tube (SIFT) to study the chemical reactions between ions and molecules at thermal energies (Adams and Smith, 1976; Smith and Adams, 1988), this was basic to the development of interstellar ion chemistry and developing an understanding of reactions that happen in the ionized terrestrial atmosphere (Smith and Adams, 1980; Smith and Spanel, 1995). The analytical method for the SIFT-MS technique was born as a direct mass spectrometric analysis of volatile compounds in the air and/or vapour samples by chemical ionisation (Smith and Spanel, 2005) (Figure 1.5).

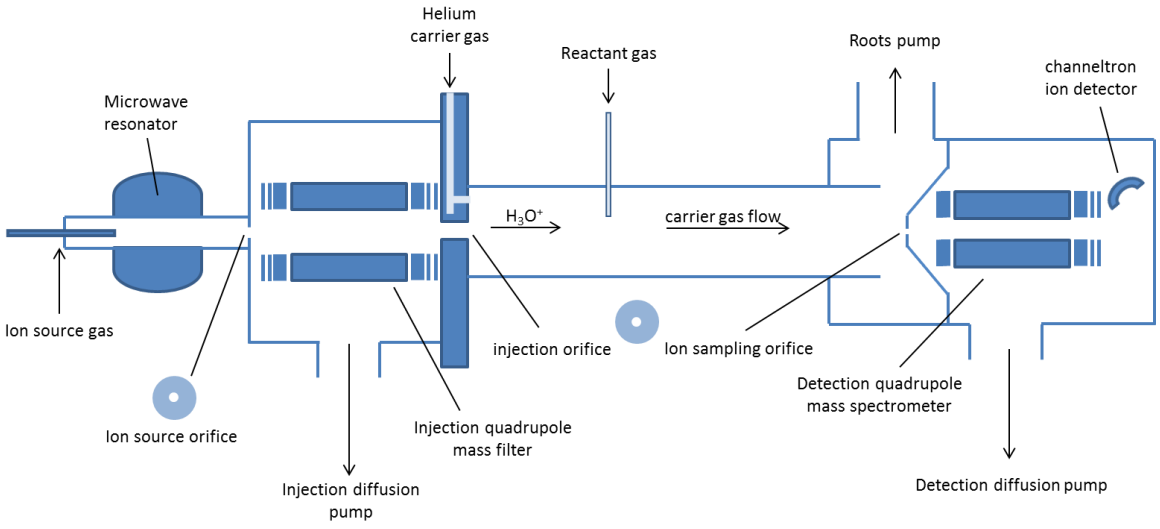

Figure 1.5. Schematic diagram of the SIFT-MS. The diagram showing the microwave resonator, injection quadrupole mass filter and three orifices through which (1) ions pass from ion source into the injection quadrupole mass filter, (2) mass selected precursor ions enter flow tube reactor, (3) product and precursor ions pass from flow tube reactor into the detection quadrupole mass spectrometer. Adapted from Smith et al.,1999.

A precursor ion is selected according to the mass to charge ratio (m/z) by an upstream quadrupole mass filter after formation of a mixture of positive ions in a microwave discharge source, the precursor ions are injected into flowing inert carrier gas (helium) at a pressure of ~ 100 Pa through a venture-type inlet (diameter 1 mm) where they are converted as a thermalized swarm along the flow tube (Smith and Spanel, 2005). The chosen precursor ions (H_3O^+, NO^+ and O_2^+) are utilised to ionize the trace gases in either air or vapour samples. These precursor ions are injected into flowing helium carrier gas, and the gas/vapour from the sample of interest is introduced at high speed via the heated sample inlet port; the capillary within the inlet port is heated to 80 ^oC to prevent water vapour condensation. The flow speed of helium gas transporting the ion swarm and the flow tube length determines the reaction time of the analyte molecules with the precursor ions. The chemical reaction occurs when a specific precursor ion reacts with the trace compounds in the introduced sample, a small fraction of reagent ions converting into product ions that are specific of the analytes (Smith and Spanel, 2005). The large fraction of the reagent ions (residual) together with the distinctive product ions travel from the flowing swarm through a pinhole orifice (diameter of ~ 0.3 mm) located at the downstream quadrupole mass spectrometer. Following mass analysis, quantification of the volatile compounds is accomplished by detection and counting at the channeltron multiplier/pulse counting system (Smith and Spanel, 2005).

In the methods utilized to ionize gaseous compounds, chemical ionisation (soft ionisation) in combination with mass spectrometry was developed to reduce the fragmentation of analyte molecules, leading to simpler distinct product ions thus helping the analyte compound identification and quantification. However, not many precursor ions are appropriate for ambient gas analysis as these precursors must be relatively unreactive with the major components of air (N_2, O_2, H_2O, CO_2 and Ar) but very reactive with the trace

gases being quantified (Smith and Spanel, 2005). The only appropriate precursor ions for SIFT-MS are H_3O^+, NO^+ and O_2^+; these ions do not undergo biomolecular reactions with the major components of air while reacting only very slowly with these neutrals via slow termolecular association (Spanel and Smith, 1995; Spanel and Smith, 1996a; Smith and Spanel, 1996; Spanel and Smith, 1996b). The availability of these ions in SIFT-MS provides advanced accuracy for identification of compounds, where important isobaric product ions are formed. Furthermore, the ability to rapidly switch between these reagent ions within milliseconds allows one to obtain data for each precursor ion without delay, which is valuable in the analysis of transient gaseous samples. In addition, the efficient generation of these reagent ions is from simple discharge ion sources (Spanel et al., 2004). The potential use of anions has been previously explored as precursor ions for SIFT-MS, but the reactivity of OH^- was found to be far less in comparison with H_3O^+ and the difficulty in obtaining a large sufficient current of OH^- ions; thus negative ions would restrict the level of analytical sensitivity of SIFT-MS (Spanel et al., 1995).

In 1997, SIFT-MS had developed to be a transportable SIFT-MS instrument, MK1, which weighed 350 Kg. This mobility allowed it to be worked for the first time outside of the analytical chemistry laboratory. Online gas analysis was performed for exhaled breath samples of pre and post haemodialysis patients in hospital (Davies et al., 2001). In 2001, SIFT-MS became the first commercial SIFT-MS instrument, MK2, and consisted of the latest pump and quadrupole mass spectrometers with improved specifications (Spanel and Smith, 2011). This allowed for a moderation in critical parameters such as orifice diameters and improved the limit of detection for the samples of exhaled breath to 2 parts per billion by volume (ppbv) for a 1 second integration time (Spanel and Smith, 2011). The thinking and continuous efforts of Professors Smith and Spanel regarding the flow dynamics, venturi design, pumping systems, vacuum housings and the fundamental ion

chemistry of SIFT-MS led to the production of the profile 3 instrument, which was introduced in 2006 in the UK. In particular, the large pumps that were used in previous versions of SIFT-MS were replaced with rotary backing pumps, leading to reduced weight and size of the profile 3 instrument (weight ~ 120 Kg), resulting in a more easily moved instrument (Smith et al., 2009).

The SIFT-MS instrument can be worked in two different modes. The first is the full-scan mode (FS); breath or liquid headspace gases are introduced into the carrier gas, and the downstream analytical mass spectrometer system is scanned over predetermined mass to charge ranges for a selected time period (Smith and Spanel., 2005). The count rates of the ions are then computed from the numbers of counts and the total sampling time for each ion. The count rates are kept, and then displayed on a linear or semi-logarithmic scale. The interpretation of the mass spectra relates the product ion peaks with the trace gases in the sample. The concentrations of the volatile compounds are computed from the count rates of the precursor ions and their distinct product ions and the proper k values (from standardized kinetics library) and the flow rates of the helium gas and of the breath or headspace sample. In the second, multi-ion monitoring mode (MIM), the downstream analytical mass spectrometer is quickly switched between selected mass to charge values to mark selected trace gas species (Smith and Spanel., 2005). The targeted volatile compounds are quantified in real-time from the obtained data and the rate coefficients of the reactions as included in the kinetic library. This real-time monitoring is possible because of the quick time response of SIFT-MS, which is approximately 20 ms; the quick response time is dictated by the fast flow rates of the helium gas along the flow tube and the sample gas along the inlet tube. In addition to the count rates of the selected product ions, the count rates for the precursor ions (e.g., H_3O^+ and $H_3O^+(H_2O)n$) are also recorded simultaneously, because they frequently change with the humidity of the sample gas. This

is achieved by rapidly switching between several m/z values of the precursor and product ions in the downstream mass spectrometer (Smith and Spanel., 2005).

1.10 Aims

Metabolomics studies can yield powerful biochemical data at the cellular level, giving a snapshot view of the phenotype of cell population under any state.

There are two main hypotheses to be explored in this thesis. Firstly, the physioxic condition can show changes in the metabolism of stem cells and subsequently differences in metabolite content of the cell culture media. Secondly, when stem cells differentiate, the metabolic profile of cells will shift from that characteristic of stem cells to that of the cell type into which the stem cells is differentiating.

In this thesis, the aim is to investigate the ability of using volatile organic compounds (metabolites) released from or consumed by human stem cells as a profiling tool within metabolomics and to identify potential volatile organic compound biomarkers of stem cells differentiation. Selected Ion Flow Tube Mass Spectrometry (SIFT-MS) has been employed in the analysis of volatile organic compounds to yield a broad set of data which will increase our understanding of the metabolism of self-renewal and differentiation of stem cells.

Chapter 2-Materials and Methods

2.1 Pluripotent stem cells:

2.1.1 Thawing:

Early passage cryovials of human pluripotent stem cells (hPSCs), including SHEF1 and SHEF2 human embryonic stem cells (hESCs) (obtained under licence, from the UK Stem Cell Bank (UKSCB)) (Alfatoonian et. al., 2010) and human induced pluripotent stem cells (ZK2012L) (kindly supplied by Prof Sue Kimber) (Cheng et. al., 2014), were removed from liquid nitrogen and thawed in a 37 ^{o}C water bath with gentle agitation. Vials were then sterilized with 70% (v/v) IMS followed by transfer into the cell culture hood and transfer of the thawed cells into a 15 ml conical tube followed by dilution with 10 ml of pre-warmed medium with medium added dropwise while gently shaking the tube back and forth to reduce osmotic shock. To remove the DMSO present in freezing medium, cells were pelleted by centrifugation (200 g for 4 min). Then the supernatant was removed and the cells re-suspended in 2 ml of medium and plated into one well of a vitronectin pre-coated 6-well plate (see section 2.1.3). The next day of the thawing and plating the cells into a 6-well-coated culture plate, 95% of the medium was aspirated to avoid drying out the cells and added 2 ml of fresh medium/well by gently adding to the side of the well, after 4-5 days cells were about 85% confluent.

2.1.2 Routine culture conditions:

All cell harvesting and culture procedures were carried out in Class II microbiological safety cabinets using disposable sterile plastic consumables. All objects entering the cabinet were first sprayed with 70% (v/v) IMS to disinfect. Human pluripotent stem cells (hPSCs) were cultured in a xeno-free culture system using Essential 8 Medium (Gibco, Cat. No. A15169-01) and a truncated recombinant human vitronectin (rh VTN-N) (Gibco, Cat. No. A14701SA) substrate (see section 2.1.3) (Figure 2.1) with routine passaging by

ethylene diamine tetra acetic acid (EDTA) (Life Technologies, Cat. No. 15575-038) (see section 2.1.4). The morphology of the cells was observed daily under inverted light microscope (Nikon Eclipse TS100, Japan) to ensure the maintenance of an undifferentiated phenotype and evaluate the confluency level.

Human ES cell lines SHEF1 and SHEF2, and iPSC from passage 35 to 65 were maintained under sterile conditions in a humidified incubator at 37 ^{o}C in the presence of 5% CO_2 at either 2% (physioxia) or 21% O_2 (air oxygen).

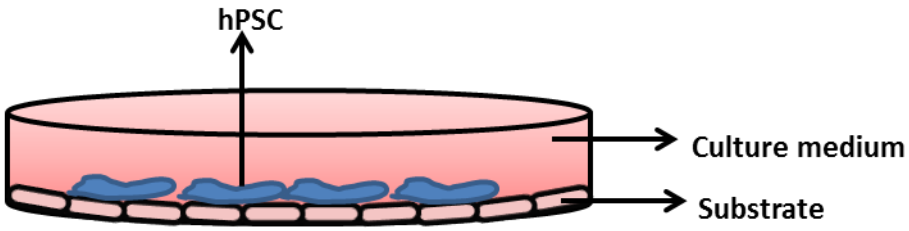

Figure 2. 1. *In vitro* culture requirements of hPSCs. The figure showing the requirement for an extracellular matrix (vitronectin substrate) to support hPSCs self-renewal in culture medium.

2.1.3 Substrate coating:

To prepare the coated wells of a 6-well plate, a 0.5 mg/ml vitronectin solution was first removed from the -80 ^{o}C freezer, thawed at room temperature, and 60 µl added into a 15 ml conical tube containing 6 ml of Dulbecco's phosphate-buffer saline (DPBS) without calcium and magnesium (Gibco, Cat. No. 14190-094). The solution was then mixed gently by pipetting up and down to obtain a 5 µg/ml working vitronectin solution which was distributed equally across each well of 6-well plate (0.5 µg/cm^2 as recommended by manufacturer) and incubated at room temperature for one hour prior to use. The plates were then used directly after the incubation or stored at 2-8 ^{o}C wrapped in parafilm for no more than one week.

2.1.4 Passaging:

hPSCs were passaged upon reaching 85% confluency to avoid death and/or spontaneous differentiation roughly every 4-5 days at a 1:6 split ratio (3.3×10^5) using 0.5 mM EDTA (Life Technologies, Cat. No. 15575-038) in DPBS. To harvest hPSCs, they were washed twice with DPBS to remove the culture media and 1 ml of 0.5 mM EDTA solution added followed by incubation at room temperature for 5-8 minutes or until the cells started to separate and round up. After this time the EDTA was aspirated followed by the addition of 1 ml pre-warmed E8M and the cells removed by gently pipetting media onto the plate surface. hPSCs media was changed 48 hrs after splitting and the spent medium replaced daily thereafter and maintained in a continuous culture during the whole experimental period.

2.1.5 Haemocytometer cell counting:

Cell count analysis was performed using Trypsin/EDTA (Lonza, Cat No. BE02-007E) to obtain a single cell suspension. The trypsinisation was carried out by diluting one volume of 5g/L trypsin and 2g/L EDTA stock solution in 10 volume of calcium and magnesium-free DPBS. hPSCs were washed twice with DPBS and 1 ml/well of diluted trypsin/EDTA solution was added followed by incubation at 37 ^{o}C for 3-5 minutes. After the incubation period, a ten-fold excess of medium was added to halt the trypsin activity. The cells suspension was then transferred into a centrifuge tube and pelleted at 200 g. The supernatant was aspirated and the cells re-suspended in 1 ml medium.

hPSC suspensions for counting were stained with Trypan blue (Sigma-Aldrich, Cat. No. T8154) by mixing 1 volume of cells suspension with 1 volume of Trypan blue. Cells were counted under a microscope in 4 of the large corner squares of the haemocytometer after introduce approximately 10 µl of the mixture (cell suspension and Trypan blue) very

gently between haemocytometer and coverslip by capillary action. The number of cells/ml in the original cell suspension was determined by the following equation: the mean number of cells of four square X 10^4 X 2 (dilution factor of Trypan blue added).

2.1.6 Crypreservation of cells:

A 70-80% confluent well of a 6-well culture plate of hPSC was harvested with EDTA as described in section 2.1.4; after aspirating the EDTA from the well, 1 ml of 10% (v/v) dimethyl sulfoxide (DMSO) (Fisher Scientific, Cat. No. D/4120/PB08) in Essential 8 medium was added and the cryoprotectant solution gently washed over the well to dislodge the cells from the surface which were then transferred into a cryovial. Each well of 6-well culture plate of hPSCs was collected in one cryovial before quickly placing the cryovials into Mr Frosty container for storage at -80 ^oC overnight before transfer them into liquid nitrogen.

2.2 Characterisation assays:

2.2.1 MTT assay:

The MTT (3-(4,5-dimethylthiazol-2-yl)-2,5-diphenyltetrazolium bromide) cell proliferation assay performed using MTT powder Thiazolyl Blue Tetrazolium Bromide (Sigma-Aldrich, Cat. No. M5655). The MTT powder was dissolved in dH_2O at a concentration of 5 mg/ml and then filtered using a 0.2 um filter. Briefly, 10^4 hPSCs were seeded into each well of 6 X 96-well plates and cells were allowed to attach for 48 hours at either 2% O_2 or 21% O_2 at 37 ^oC in a humidified incubator. Every day thereafter, MTT was performed on one plate in each condition. 150 µl of a 0.5 mg/ml MTT reagent-containing Essential 8 medium solution was added to each well followed by incubation at 37 ^oC for 4 hours. After incubation 125 µl MTT solution was removed. The MTT-formazan product

was subsequently dissolved by addition of 100% DMSO (50 µl/well) in the dark, followed by further incubation for 45 minutes in the incubator at 37 ^{o}C. The absorption was then measured with a microplate reader (BioTek, synergy 2) at a 570 nm wavelength. Triplicate experiments were performed at both 2% and 21% oxygen conditions.

2.2.2 Immunocytochemistry:

Immunocytochemistry of hPSC markers of pluripotency was performed using live, unfixed cell staining (R&D system, GloLIVE Human Pluripotent Stem Cell Live Cell Imaging Kit, Cat. No. SC023). Briefly, 3.3 x10^5 hPSCs were seeded into each well of a 6-well plate and grown for 96 hours in E8M. The antibodies were diluted to 1X concentration (1:50) in E8M, media aspirated and 1 ml fresh media containing 1X of the desired antibody (SSEA-4, TRA-1-60, SSEA-1) added to each well before returning to the incubator for 30 minutes incubation. Thereafter, the antibody-containing media were removed, hPSCs rinsed with fresh medium, and then re-fed with the medium. Labelled cells were imaged via fluorescence microscope (Nikon Eclipse Ti-S, Japan) with a Nikon DS-Qi1Mc camera. The NIS-elements BP software was used for image acquisition.

2.2.3 Flow cytometry:

Human PSCs were prepared for analysis by flow cytometry by dissociating to a single cell solution using trypsin-versene (EDTA) (Lonza, Cat No. BE02-007E). Approximately 5x10^5 human PS cells were labelled with the antibodies (SSEA-4, TRA-1-60, SSEA-1) as described in section (2.2.2). When the antibody-containing medium was removed, cells were washed using PBS, trypsinised, and centrifuged at 300 g for 3 minutes. The supernatant was then aspirated and the pellet washed in flow cytometry buffer (PBS with 0.5% (w/v) BSA (Fisher Scientific, Cat No. BP9703-100) and 2 mM EDTA (Fisher Scientific, Cat. No. BP2482-1) followed by centrifugation at 300 g. Samples were then re-

suspended in PBS and analysed by flow cytometry utilizing a Cytomics FC 500 (Beckman Coulter). Data analysis was performed using Flowing Software (version 2.5.1). The pluripotent markers expression of SSEA-4 was determined in the FL1 channel, while TRA-1-60 and SSEA-1 were determined in the FL2 channel.

2.2.4 Bioinformatics:

A gene expression data set generated for hESCs (cell lines, H1, H9 and RH1) cultured on Matrigel^{TM} in two conditions (2% and 21% O_2) until 90% confluent was exploited via *in silico* analysis (Forsyth et al., 2008). Focussed analysis was performed based on observations made during hPSC SIFT-MS analysis (see Section 2.3.3).

According to the KEGG `pathway database, the metabolic pathways for ethanol and acetaldehyde were recognised for further analysis. Since the complete pathway is separated into a several enzymatic reactions, NCBI web-based server was used to identify the genes to a specific enzymatic reaction. Based on the genes assignment, a list of genes was constructed by matching the identified genes for ethanol and acetaldehyde pathway to the (H1, H9 and RH1) gene expression data set. All expressed genes in ethanol and acetaldehyde metabolic pathway were then compared between 2% O_2 and 21% O_2 using t-test to identify the significant genes. All of the genes that showed significant differences ($P<0.05$) were selected for further consideration.

2.3 Spontaneous differentiation of human pluripotent stem cells:

hPSCs were differentiated as previously described (Kumar et al., 2015). In brief, hPSCs (around $5x10^5$) were cultured in 6-well vitronectin-coated culture plates in two different conditions (2% O_2 and 21% O_2) for 48 hours in Essential 8 medium to allow them to attach to the culture plates' surface. Thereafter, the medium was switched to spontaneous

differentiated media consisting of Knockout DMEM (KO-DMEM) (GIBCO, Cat No. 10829-018) supplemented with 10% (v/v) FBS, 2mM L-Glutamine (Lonza, Cat. No. BE17-605E), 1% (v/v) NEAA (Lonza, Cat. No. BE13-114E) and 0.1 mM β-mercaptoethanol (Gibco, Cat. No. 31350-010).

2.3.1 Evaluation of pluripotent markers expression in human pluripotent stem cells and their progeny:

hPSCs were cultured and expanded on vitronectin-coated 24-well plates in both 21% O_2 and 2% O_2 in E8M for 0 day and in spontaneous differentiation media for a 21 day period. Pluripotent marker analysis was performed during the differentiation period at days 0, 5, 10 and 20. For immunolabeling media was first removed, hPSC washed with PBS and fixed in 4% paraformaldehyde in PBS for 30 minutes at room temperature, and then washed 3 times with 1% BSA (Sigma-Aldrich, Cat. No. A1595) in PBS. The cells were then permeabilized and blocked with 10% normal donkey serum (Sigma-Aldrich, Cat. No. D9663), 0.3% triton X-100 (Sigma-Aldrich, Cat. No. T8787) and 1% BSA (Sigma-Aldrich, Cat. No. A1595) in PBS for 45 minutes at room temperature. hPSCs and their progeny were then incubated with 1 µg/100 µl working solution of primary anti-human monoclonal antibodies; mouse anti-alkaline phosphatase, mouse anti-SSEA-4, goat anti-Nanog and goat anti-Oct 3/4 (R&D system, Cat. No. SC008) overnight at 2-8 ^{o}C. hPSCs were washed 3 times with 1% BSA in PBS; antibodies Nanog and Oct 3/4 were treated using secondary antibody donkey anti-goat IgG (R&D system, Cat. No. NL003); alkaline phosphatase and SSEA-4 were treated with secondary antibody, donkey anti-mouse IgG (R&D system, Cat. No. NL557) at 5 µg/ml for 1 hour at room temperature. All immuno-stained samples were further counterstained with DAPI (100ng/ml) (Sigma-Aldrich, Cat. No. D9542) in order to visualise nuclei of the cells and imaged using a fluorescence microscope (Nikon Eclips Ti-S, Japan).

2.3.2 RT-PCR:

Gene expression analysis (RT-PCR) was performed at days 0, 5, 10 and 20 of differentiation; cell lysis at each time point was performed *in situ* for subsequent RNA extraction. Cell lysates were prepared and homogenised by following the manufacturer's protocol (Qiagen, RNeasy Mini Kit, Cat. No. 74104). Briefly, prior to lysis cell monolayers were washed with PBS after which cells were lysed in 350 µl RLT buffer supplemented with 10 µl/ml of β-mercaptoethanol (Gibco, Cat. No. 31350010), a cell scraper was used to ensure cells were detached from the culture plate and the lysate was then transferred to a QIAshredder mini-spin column (Qiagen, Cat. No. 79656) for homogenisation and removal of insoluble material. This was centrifuged for 2 minutes at 17000 g followed by removing and discarding the mini-spin column; the cell lysate was stored at -80 ^{o}C until RNA extraction was performed.

2.3.2.1 RNA extraction:

Undifferentiated and differentiated cell lysates were removed from the -80 ^{o}C freezer and thawed on ice. Total RNA extraction was carried out using the RNeasy mini kit (GIAQEN, Cat. No. 74104). One volume of 70% ethanol was added to the lysate and the mixed solution transferred to RNeasy mini-spin column. Samples were centrifuged for 15 seconds at 8000 g and the flow-through discarded with total RNA bound to the column membrane. To wash the membrane, 700 µl of RW1 buffer was added and the tube centrifuged for 15 seconds at 8000 g after which the flow-through was discarded. This was repeated once before performing an RPE buffer (500 µl) wash at 8000 g for 15 seconds followed by a second 500 µl RPE wash of 2 minutes, the flow-through following each centrifugation was discarded. The residual fluid was then removed by centrifugation of the mini-spin column at 17000 g. The collection tube was discarded and replaced with a 1.5 ml lidded collection

tube. The RNA was eluted from the membrane by adding 25 µl of RNase-free water to the spin column membrane and standing for 5 minutes before being centrifuged for 1 min at 17000 g. To increase the quantity of RNA, the eluent was re-pipetted on to the membrane and the column centrifuged for 1 minute at 17000 g. The concentration of the extracted RNA was measured using Nanodrop 2000 spectrometer (Thermo scientific) and transferred to store at -80 ^{o}C until required.

2.3.2.2 One step reverse transcription polymerase chain reaction:

RNA samples were diluted in ultrapure RNAse/DNAse-free dH_2O to a concentration of 25 ng/µl for gene expression analysis. Reverse transcription-polymerase chain reaction (RT-PCR) was carried out with a one-step RT-PCR kit (Qiagen, Cat. No. 210210). Briefly, all primers were designed using the NCBI website, the primer sequences and the annealing temperature for each gene is listed in Table 2.1. All RT-PCR mixtures contained 2.5 µl of RT-PCR buffer, 0.5 µl dNTP, 2.5 µl of Q-solution, 1 µl (25ng/µl) of RNA sample, 1 µl of each forward and reverse relevant primer (10 µM), 0.5 µl of RT-PCR enzyme mix and final volume made up to 12.5 µl with RNAse/DNAse free water. All RT-PCR reactions consisted of one cycle of 50 ^{o}C for 30 minutes (reverse transcription step), one cycle of 95 ^{o}C for 15 minutes, 39 cycles: 94 ^{o}C for one minute (DNA melting), primer specific annealing temperature (Table 2.1) for one minute, and 72 ^{o}C for one minute (DNA extension); one cycle of 72 ^{o}C for 10 minutes and finally 15 ^{o}C On hold. Following completion of amplification, samples (cDNA) were either fractionated directly on agarose gels or stored at 4 ^{o}C prior to fractionation.

Table 2. 1. Table of primer sequence, annealing temperatures and product size.

Gene name	Sense sequence (5' to 3')	Antisense sequence (5' to 3')	Annealing temperature (°C)	Product size (bp)
ACTB	GCCACGGCTGCTTCCAGC	AGCCATGCCAATCTCATCTT	57	528
POU5F1 (Oct-4)	GCAATTTGCCAAGCTCCTGAAGCAG	CATAGCCTGGGGTACCAAAATGGGG	55	536
NANOG	GGTGGCAGAAAAACAACTGGC	TGCAGGACTGCAGAGATTC	56	300
SOX1	CCAGGAGAACCCCAAGAGGC	CGGCCAGCGAGTACTTGTCC	56	206
AFP	AAGGATACCAGGAGTTATTGG	GTTGGCATATGAAGAAGTGC	56	398
Brachyury	GCATAAGTATGAGCCTCGAA	GTTGTCAGAATAGGATTGGGA	56	256
OTX2	CTCGCCACATCTACTTTGATA	GGCGGTTGCTTAAGATAAGA	57	226
SOX17	GCAAGATGCTGGGCAA	GCCGGTACTTGTAGTTGG	56	120
hTERT	GCAGCTCCCATTTCATCAGC	CAGGATGGTCTTGAAGTCTG	55	343
ADH4	CGCATTCAGATCATTGCTAC	ACTGGTTCCAAAGAAATGGT	56	339
ADH5	CGAATCAAGATCATTGCCAC	CTGGCATTAATCCTTTCCCT	56	268
CYP2E1	CTGGCTCCAGCTTTACAATA	AGAATCAGGAGCCCATATCT	56	306
ALDH1A1	TCATTCCTTGGAATTTCCCG	GCCCATAACCAGGAACAATA	57	183
ALDH1A3	GAAGAAGGAGATAAGCCCG	CTGCAAAGTATCTGAGGGTT	56	247
ALDH6A1	CTTGCTCCGCTATCAACAA	AGGAAGGTATTTCCACACAC	57	309

2.3.2.3 Agarose gel electrophoresis:

RT-PCR amplification products were confirmed by agarose gel electrophoresis. Agarose gels (Fisher Scientific, Cat. No. BP1356) were prepared at a 2% concentration in 1X tris-acetate-EDTA (TAE) buffer (Thermo Fisher Scientific, Cat. No. B49) supplemented with 0.3 µg/ml ethidium bromide (Sigma-Aldrich, Cat. No. E1510). Ethidium bromide which binds to a double strand DNA helix will increase its fluorescence 25-fold as compared to non-binding ethidium bromide (Severini and Morgan; 1991) following UV excitation allowing the visualisation of ethidium bromide binding DNA band within the gel. Agarose gels were poured into a gel tray with a gel comb and allowed to set for approximately 1 hour prior to use, after which the set gel was transferred into the electrophoresis chamber containing 1X TAE buffer. Each sample was mixed with 2 µl aliquot of gel loading buffer (Sigma-Aldrich, Cat. No. G2526) and then pipetted into the gel wells. At the same time, DirectLoad wide range DNA marker (Sigma-Aldrich, Cat. No. D7058) was run to allow the determination of fragments size. All gels were run for 1 hour at 100 V in 1X TAE buffer. Following completion of electrophoresis, gels were transferred to UV transilluminator (Syngene) to visualise by fluorescence at 254 nm where images were captured using Syngene GenSnap software).

2.3.3 Headspace analysis of pluripotent stem cells and their progeny by SIFT-MS:

In order to prepare samples of each of the pluripotent stem cell types [hESCs (SHEF1 and SHEF2) and hiPSCs] in this study for headspace analysis, following expansion in 6-well tissue culture plate to around 70-80% confluence, the cells (around $12x10^6$ cells) were incubated in 20 ml Essential 8 Medium in 2% and 21% O_2 conditions for 24 hours before samples acquisition. In parallel 6-well tissue culture plates containing only 20 ml Essential

8 Medium without cells were incubated in 2% and 21% O_2 for 24 hours as a control. After the incubation period, cell-free cell culture media and incubated cell culture media were transferred to clean, sterile 150 ml glass bottles, 20 ml fresh media were transferred to another bottle as a further control. The headspace of the bottles was then purged with dry and sterile air (20% oxygen and 80% nitrogen mixture; BOC, UK) for 1 minute and capped tightly with septum caps and parafilm and incubated for an additional 16 hours at 37 ^{o}C, this incubation period was chosen to allow accumulation of volatile organic compounds before a SIFT-MS measurement was taken.

In order to prepare spontaneous differentiation samples of each human pluripotent stem cell, the differentiated progenitor cells in 6-well tissue culture plate at each time point (5, 10 and 20 days) (Figure 2.2) were incubated in 20 ml differentiated medium for 24 hours in both conditions 2% and 21% O_2 before sample acquisition. 6-well tissue culture plates containing 20 ml of the differentiated media without cells were incubated for 24 hours in relevant oxygen conditions in parallel. After the incubation period, the cell culture media were transferred into bottles as described above.

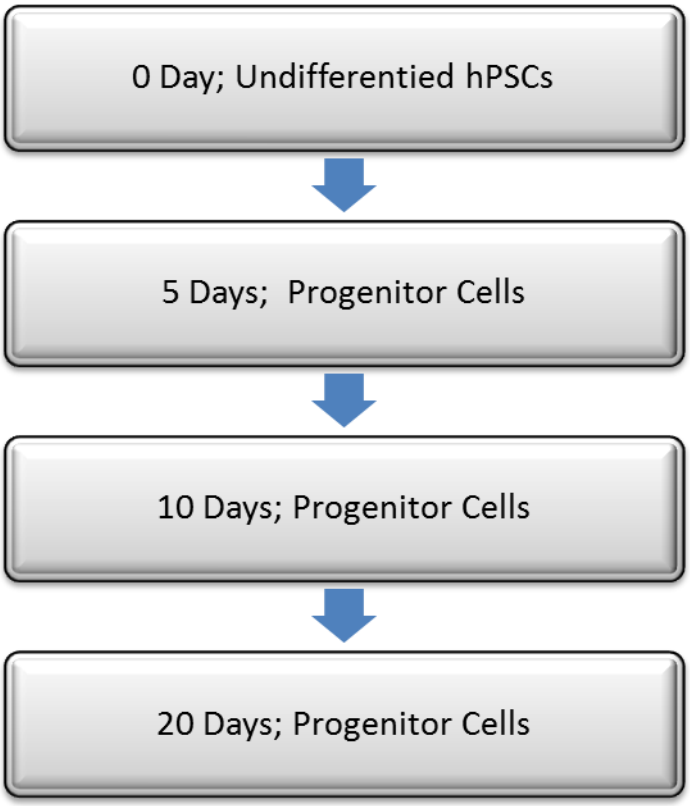

Figure 2. 2. The process flow of hPSCs and their progenitors' VOCs extraction. The flow showing the time points of volatiles extracted from headspace (HS) of culture media throughout hPSCs differentiation period.

Following the 16-hour incubation period for undifferentiated pluripotent stem cells and their differentiated progeny media samples, the headspace was measured using the Profile 3 SIFT-MS instrument (Figure 2.3). The samples were placed in a water bath (37 ^{o}C) to maintain the temperature of the samples throughout the analysis.

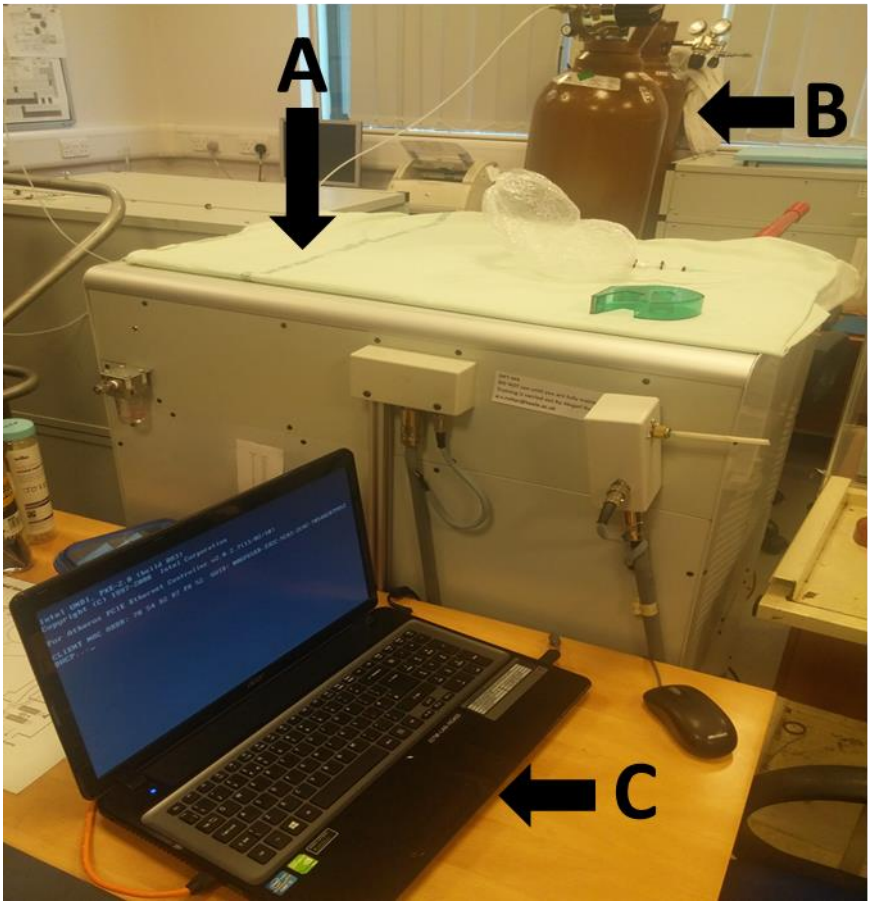

Figure 2. 3. Photograph illustrating the SIFT-MS instrument set up. (A) SIFT-MS, (B) Helium cylinder and (C) laptop.

The H_3O^+ precursor (reagent) ion was applied to analyse the headspace gases using both Multi Ion Monitoring mode (MIM) and Full Scan mode (FS) operation of the instrument. Prior to analysis the samples, the water level of the operator's exhaled breath (6% +/- 0.1) was achieved as a calibration procedure to check the flow rate of the sample into the instrument using flow rate adjustment incorporated into the software and post analysis the Excel was used to normalise the data to 6% exactly. In order to introduce the headspace gases of the samples into the flow tube of the instrument, the septa of the caps were punctured using a needle attached to the sampling arm of the SIFT-MS instrument. For each headspace measurement, the time for sampling was 1 minute.

2.4 Human pluripotent stem cells and application of both ADH and CYP2E1 inhibitor:

The routine culture of each human pluripotent stem cells types [hESCs (SHEF1 and SHEF2) and iPSC] in 6-well tissue culture plate was performed as described in section 2.1.2 with Essential 8 Medium in two oxygen conditions (2% and 21% O_2). Alcohol dehydrogenase (ADH) and cytochrome P450 2E1 (CYP2E1) inhibitor 4-methyl pyrazole (4-MP) (Alfa Aesar, Cat. No. A18083) was dissolved in filtered dH_2O prior to the experiments and stored as a 2.5 M stock inhibitor solution. Water solvent was selected to prevent any effect on the cells biochemistry and any interference with the SIFT-MS analysis and results. Fresh inhibitor (5 mM) / media solutions were prepared for each media replacement.

2.4.1 Cell viability:

The effect of the ADH and CYP2E1 inhibitor (4-MP) on the viability of each human pluripotent stem cell ((ESCs(SHEF1), ESCs(SHEF2), iPSCs) was assessed with the cells attached to 96-well plates and cultured in two oxygen conditions by determining the mitochondrial dehydrogenase activities in the living cells using the MTT assay. MTT (Sigma-Aldrich, Cat. No. M5655) solution was prepared as described in section 2.2.1. Equal numbers of cells (10^4 cells) were plated per well in 96-well plates and incubated for 72 hours in two oxygen conditions. Three different concentrations of 4-MP inhibitor were used (0.5 mM, 5 mM and 50 mM). After this time, 150 µl/well of MTT reagent containing E8 medium solution was added with a final concentration 0.5 mg/ml of MTT and the cells were incubated at 37 ^oC for 4 hours. Thereafter, 125 µl of the MTT solution was removed. The MTT-formazan product was subsequently dissolved by addition of 100% DMSO (50 µl/well) in the dark, followed by incubation for 45 minutes in the incubator at 37 ^oC. The

absorption was then measured with a microplate reader (BioTek, synergy 2) at a 570 nm wavelength. Triplicate experiments were performed at both oxygen conditions.

2.4.2 Headspace analysis by SIFT-MS:

Before commencing the ADH and CYP2E1 inhibition experiments, each human pluripotent stem cell was divided into two experimental groups: the first group was untreated cells serving as the control group and the second group was treated cells with 5 mM 4-MP inhibitor; additional E8M containing 6-well tissue culture plates without cells were incubated in relevant oxygen condition with and without 5 mM 4-MP in parallel and processed as a control for the corresponding group. In this case, 70-80% confluence, the cells in one 6-well tissue culture plate were treated by applying the inhibitor (4-MP, 5 mM) containing E8 medium (20 ml) and the cells in the second 6-well tissue culture plate were treated with the E8 medium without inhibitor, while cell-free 6-well tissue culture plates were incubated with inhibitor (4-MP, 5 mM) containing E8 medium and E8M without inhibitor for 24 hours in relevant oxygen condition, prior to transferring the media to the 150 ml glass bottles. The bottles were then purged with dry and sterile air (20% oxygen and 80% nitrogen mixture; BOC, UK) for 1 minute and capped tightly with septum caps and parafilm and incubated for an additional 16 hours at 37 ^{o}C, this incubation period was chosen to allow accumulation of volatile organic compounds before a SIFT-MS measurement was taken. Following the 16 hour incubation period for media samples, the headspace was measured using profile 3 SIFT-MS instrument as described in section 2.3.3.

2.5 Human mesenchymal stem cells:

2.5.1 Isolation of mesenchymal stem cells from bone marrow aspirate and culture:

Human mesenchymal stem cells (hMSCs) were isolated and cultured from whole bone marrow aspirates (BMA) by modification of the plastic adherent culture technique described by Kay et al, 2015. Commercially sourced (Lonza, USA) whole bone marrow aspirates aspirated from the bilateral iliac crest from 3 different healthy donors (Table 2.2) were and supplemented with 100 U heparin/ml to prevent coagulation.

Table 2. 2. Donor details of human bone marrow aspirates.

No	BMA label	Donor description	Supplier
1	BMA-15	Human Bone Marrow, Female, Age-36 years	Lonza, MD, USA
2	BMA-16	Human Bone Marrow, Male, Age-29 years	Lonza, MD, USA
3	BMA-17	Human Bone Marrow, Female, Age-50 years	Lonza, MD, USA

The aspirate was seeded within 48 hours of aspiration at a density of 10^5 total cells/cm^2, according to the total cell count provided by the supplier with the aspirate, onto fibronectin-coated 75 cm^2 tissue culture flasks. Fibronectin coating of flasks was performed with a 10 ng/ml solution of fibronectin in PBS for at least one hour at room temperature after which the fibronectin solution was aspirated and BMA added to a total volume of 20ml per T75. of Dulbecco's Modified Eagle Medium (DMEM) (Lonza, Cat. No. BE12-709F) supplemented with 5% (v/v) Fetal Bovine Serum (FBS) (biosera, Cat. No. FB-1001/500), 2mM L-Glutamine (L-Glut) (Lonza, Cat. No. BE17-605E), 1% (v/v) non-essential amino acid (NEAA) (Lonza, Cat. No. BE13-114E) and 1% (v/v) (PSA)

penicillin-streptomycin-amphotericin B (Lonza, Cat. No. 17-745E) (100 U/ml penicillin, 100 µg/ml streptomycin, 0.25 µg/ml amphotericin B) at 37 ^{o}C in three different oxygen conditions (21% O_2, 2% O_2, 2% O_2 Work Station (WS)) and 5% CO_2. After one week of culture 50% media was removed and replaced with freshly prepared media as described above. Following this cells were incubated for a further week after time a whole media change was performed. hMSC isolation was complete at the end of the third week as evidenced by the appearance of colony forming units – fibroblastic (CFU-F) following the removal of all non-adherent cell populations. Once isolated hMSC media changes were carried out twice a week with freshly completed media as described above (Figure 2.4).

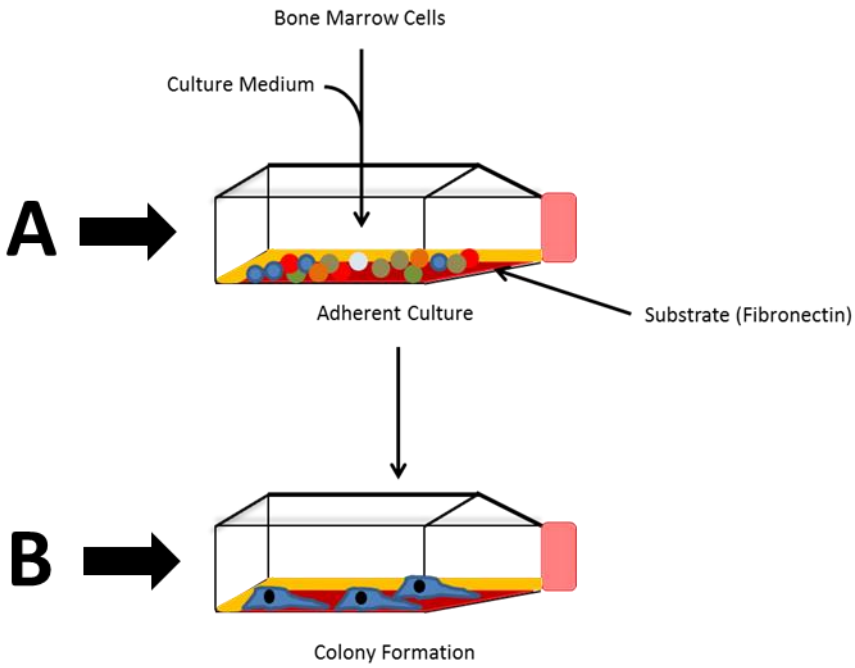

Figure 2. 4. Experimental design showing MSCs isolation by adherent culture using plastic tissue culture. (A) MSCs isolation from heparinized human bone marrow aspirate by seeding all bone marrow cells on fibronectin-coated flask and (B) colony forming units-fibroblast (CFU-F) appeared in flask after removing all non-adherent cells.

2.5.1.1 Mesenchymal stem cells sub-culture:

As necessary, confluent T75 flasks of hMSCs were sub-cultured enzymatically using trypsin/EDTA (Lonza, Cat No. BE02-007E). Trypsinisation was carried out by diluting one volume of 5g/L trypsin and 2g/L EDTA stock solution in 10 volume of calcium and magnesium-free PBS; the cells were rinsed twice with PBS and 5 ml of diluted trypsin/EDTA solution was added to cover the cells before 3-5 minutes incubation at 37 ^{o}C for. After the incubation period, flasks were tapped to encourage cell detachment, and once microscopically confirmed, 10 ml of complete medium added to halt the trypsin activity. The cells suspension was then transferred into a centrifuge tube and pelleted at 200 g for 3 minutes. The supernatant was aspirated and the cells re-suspended in medium for passage.

2.5.1.2 Surface markers characterisation of mesenchymal stem cells:

hMSCs surface marker expression was characterised on passage 1 cells. hMSCs were washed with PBS and then trypsinised using trypsin/EDTA as described in section 2.5.1.2. Thereafter, cells were counted and re-suspended in flow cytometry buffer (PBS with 0.5% (w/v) BSA (Fisher Scientific, Cat No. BP9703-100) and 2 mM EDTA (Fisher Scientific, Cat. No. BP2482-1) for 10 minutes and approximately $1x10^6$ cells distributed equally across 10 x 1.5 ml eppendorf tubes for specific cell surface marker staining, centrifuged at 300 g for 5 minutes and the supernatant discarded. 100 µl flow cytometry buffer and 10 µl of either CD73 (Miltenyi Biotech, Cat. No. 130-097-943), CD90 (Miltenyi Biotech, Cat. No. 130-097-932), CD105 (Miltenyi Biotech, Cat. No. 130-098-906), CD14 (Miltenyi Biotech, Cat. No. 130-098-067), CD19 (Miltenyi Biotech, Cat. No. 130-098-068), CD34 (Miltenyi Biotech, Cat. No. 130-098-140), CD45 (Miltenyi Biotech, Cat. No. 130-098-141), HLA-DR (Miltenyi Biotech, Cat. No. 130-098-177), IgG1 isotype control (Miltenyi Biotech, Cat. No. 130-098-845) or IgG2a isotype control (Miltenyi Biotech, Cat. No. 130-

098-849) phycoerythrin-conjugated antibodies were added to the cells followed by incubation in the dark at (2-8 ^{o}C) for 10 minutes. Following incubation, flow cytometry buffer was added to a total volume of 1 ml and hMSC centrifuged at 300 g for 5 minutes, the supernatant removed and finally the cell re-suspended in 1 ml of flow cytometry buffer for analysis in the flow cytometer (Cytomics FC 500, Beckman Coulter), with at least 50000 events count. The acquired data were analysed using Flowing Software (version 2.5.1). IgG1 was the isotype control for CD19, CD73, CD90 and CD105, while IgG2a was the isotype control for CD14, CD34, CD45 and HLA-DR). FL2 channel was used for analysis.

2.5.1.3 Tri-lineage differentiation:

To determine the multipotency of hMSCs cells were seeded into a 24-well plate at a density of $2x10^4/cm^2$ in MSCs complete culture media and allowed to attach overnight. Following this the media was replaced with differentiation media and this marked as the first day of differentiation. hMSCs were then cultivated for 21 days in adipogenic differentiation medium, osteogenic differentiation medium and chondrogenic differentiation medium with medium changes twice a week whereas control culture, hMSCs were maintained in complete culture media for the same period with media changes twice a week.

2.5.1.3.1 Adipogenic differentiation:

Adipogenic differentiation media was made by supplementing Dulbecco's Modified Eagle Medium (DMEM) (Lonza, Cat. No. BE12-709F) with 10% (v/v) FBS (biosera, Cat. No. FB-1001/500), 1% (v/v) NEAA (Lonza, Cat. No. BE13-114E), 2mM L-Glut (Lonza, Cat. No. BE17-605E), 0.5 µM dexamethasone (Sigma-Aldrich, Cat. No. D2915), 0.5 mM 3-isobutyl-1-methylxanthine (IBMX) (Sigma-Aldrich, Cat. No. I7018), 10 µg/ml insulin

(Sigma-Aldrich, Cat. No. I9278) and 0.1 mM indomethacin (Sigma-Aldrich, Cat. No. I7378).

2.5.1.3.2 Osteogenic differentiation:

Osteogenic differentiation media was made by supplementing Dulbecco's Modified Eagle Medium (DMEM) (Lonza, Cat. No. BE12-709F) with 10% (v/v) FBS (biosera, Cat. No. FB-1001/500), 1% (v/v) NEAA (Lonza, Cat. No. BE13-114E), 2mM L-Glut (Lonza, Cat. No. BE17-605E), 50 µM ascorbic acid phosphate (Sigma-Aldrich, Cat No. A8960), 10 mM β-glycerophosphate (Sigma-Aldrich, Cat. No. G5422) and 0.1 µM dexamethasone (Sigma-Aldrich, Cat. No. D2915).

2.5.1.3.3 Chondrogenic differentiation:

Chondrogenic differentiation media was made by supplementing Dulbecco's Modified Eagle Medium (DMEM) (Lonza, Cat. No. BE12-709F) with 1% (v/v) FBS (biosera, Cat. No. FB-1001/500), 1% (v/v) NEAA (Lonza, Cat. No. BE13-114E), 2 mM L-Glut (Lonza, Cat. No. BE17-605E), 1% (v/v) Insulin, Transferrin, Sodium Selenite (ITS) (Sigma-Aldrich, Cat. No. I3146), 1% (v/v) sodium pyruvate (Sigma-Aldrich, Cat. No. S8636), 0.1 µM dexamethasone (Sigma-Aldrich, Cat. No. D2915), 50 µM ascorbic acid phosphate (Sigma-Aldrich, Cat. No. A8960), 40 µg/ml L-Proline (Sigma-Aldrich, Cat. No. P5607) and 10 ng/ml TGF-β3 (PeproTech, Cat. No. AF-100-36E).

2.5.1.3.4 Histological staining of differentiated hMSCs:

To confirm hMSCs differentiation after 21 days hMSC were washed twice with PBS and fixed with 4% paraformaldehyde in PBS for 20 minutes after which fixed cells were washed twice with PBS before being stored in PBS at 4 ^{o}C. Calcium deposition by differentiated osteoblasts, lipid accumulation in adipocytes and glycosaminoglycan-rich

matrix secreted by chondrocytes was detected by histological stains; Alizarin Red S, Oil Red O and Alcian Blue respectively.

2.5.1.3.5 Alizarin Red:

Fixed cells were stained with Alizarin Red S (Sigma-Aldrich, Cat. No. A5533) to detect calcium deposition. A 2% (w/v) of Alizarin Red S solution was prepared in distilled water (dH_2O), filtered with 0.4 porous filter paper and the pH adjusted to 4.1 with the 10% ammonium hydroxide. For staining PBS was first removed from fixed cells followed by a dH_2O wash and immersion in alizarin red s solution for 10 minutes. The cells were then washed five times with tap water to remove excess dye and covered with tap water before viewing the cells with an inverted microscope (OLYMPUS CKX41) with a colour camera attachment using Image-Pro Insight software.

2.5.1.3.6 Oil Red O:

A stock solution of Oil Red O was prepared by dissolving 175 mg Oil Red O (Sigma-Aldrich, Cat. No. O0625) in 50 ml of 99% isopropanol (Fisher Scientific, Cat. No. P/7500/17) which was then left overnight to ensure saturation of the solution. The solution was then filtered with a 0.22 µm syringe filter. The working solution was prepared immediately prior to staining by mixing 6 ml of stock solution with 4 ml of dH_2O. To stain fixed cells PBS was removed followed by two 60% isopropanol washes for 5 minutes each. Oil Red O working solution was then added for 10 minutes after which the stain was removed, cells washed 5 times with tap water before finally being immersed in tap water before being viewed with an inverted microscope (OLYMPUS CKX41) with a colour camera attachment using Image-Pro Insight software.

2.5.1.3.7 Alcian Blue:

To detect glycosaminoglycan production by the differentiated chondrocytes a 1% Alcian blue stain solution (pH 1.5) was prepared by dissolving 500 mg of Alcian Blue 8GX (Sigma-Aldrich, Cat. No. A5268) in 3% acetic acid (Sigma-Aldrich, Cat. No. A6283). The solution was filtered using 0.2 µm porous paper filter. To stain PBS was removed from fixed cells which were then washed once with dH_2O and then stained with 1% Alcian blue solution overnight at room temperature. The stain was then removed and cells washed gently with running tap water for 2 minutes. Images were captured via an inverted microscope (OLYMPUS CKX41) with a colour camera attachment using Image-Pro Insight software.

2.5.2 Headspace analysis of human bone marrow aspirate and bone marrow-derived mesenchymal stem cells by SIFT-MS:

BMA were seeded in three conditions (21% O_2, 2% O_2 and 2% O_2 WS) as described in section 2.5.1. After 24 hours incubation BMA in cell culture media (total volume 20 ml) was removed and placed into a 150 ml glass bottle and the volume raised to 50 ml with freshly prepared complete culture media. Media was again collected after 7 and 14 days incubation where either the collection was performed by transferring 50% (7 days' time point) of the culture media (10 ml each flask) or 100% (14 days' time point) of the culture media (20 ml each flask) into bottles and the volume raised to 50 ml with freshly prepared complete culture media. After 21 days, cell-free supernatant media (20 ml each flask) was collected and transferred into 150 ml glass bottles and completed to 50 ml with freshly complete culture media. For hMSCs, cells were detached from the flask with trypsin/EDTA as described in section 2.5.1.1, re-suspended in 50 ml freshly complete culture media and immediately transferred into 150 ml glass bottles. In parallel, incubated

cell culture media without cells and freshly prepared complete culture media were collected at each time point in the same fashion as described above (Figure 2.5). Once the media/cells were added to the bottles, the samples were purged with dry and sterile air (20% oxygen and 80% nitrogen mixture; BOC, UK) for 1 minute, sealed tightly with septum caps and parafilm, and incubated for 16 hour at 37 ^{o}C. This incubation period was to allow accumulation of volatile organic compounds before a SIFT-MS measurement was taken. Following the 16 hour incubation period the headspace was measured using profile 3 SIFT-MS instrument as described in section 2.3.3. Each time point was evaluated in triplicate from three independent donors.

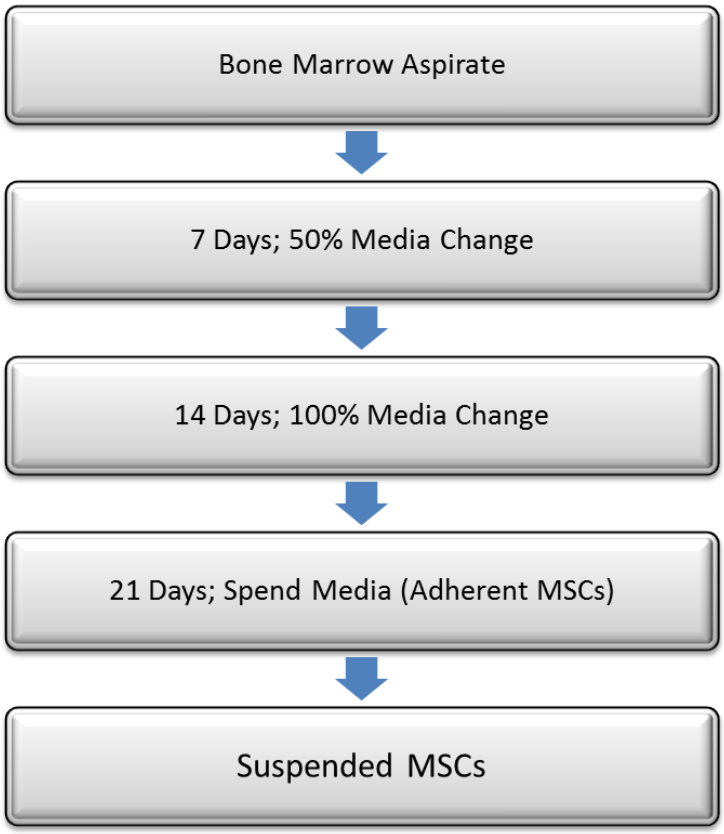

Figure 2. 5. The process flow of VOCs extraction of bone marrow aspirate and BM-MSCs. Volatile extraction using headspace (HS) was performed for culture media at bone marrow aspirate time point and days 7, 14 and 21 (adherent MSCs) of isolation and suspended MSCs.

2.6 Osteogenic differentiation of mesenchymal stem cells:

For gene expression and volatile organic compound determination in response to osteogenic differentiation hMSC at P1 were harvested by trypsinisation using trypsin/EDTA (Lonza, Cat. No. BE02-007E) and subsequently seeded at densities of $2x10^4$ cells/cm^2 into 24-well culture plates for histological characterisation (see section 2.5.1.3.5), 6-well culture plates for RNA extraction (see section 2.3.2.1) and T75 culture flasks for volatile organic compound determination in the MSCs complete culture medium consisting of Dulbecco's Modified Eagle's Medium (DMEM) (Lonza, Cat. No. BE12-709F), 5% (v/v) FBS (biosera, Cat. No. FB-1001/500), 1% (v/v) NEAA (Lonza, Cat. No. BE13-114E) and 2mM L-Glut (Lonza, Cat. No. BE17-605E), and incubated in a humidified atmosphere at 37 ^oC in three different oxygen conditions 21% O_2, 2% O_2 and 2% O_2 WS, and 5% CO_2 for 24 hours. Osteogenic differentiation was induced by addition of osteogenic induction medium consisting of Dulbecco's Modified Eagle Medium (DMEM) (Lonza, Cat. No. BE12-709F) supplemented with 10% (v/v) FBS (biosera, Cat. No. FB-1001/500), 1% (v/v) NEAA (Lonza, Cat. No. BE13-114E), 2mM L-Glut (Lonza, Cat. No. BE17-605E), 50 µM ascorbic acid phosphate (Sigma-Aldrich, Cat No. A8960), 10 mM β-glycerophosphate (Sigma-Aldrich, Cat. No. G5422) and 0.1 µM dexamethasone (Sigma-Aldrich, Cat. No. D2915). Uninduced control cultures were maintained in the MSCs complete culture media throughout and used as control samples. Osteogenic and maintenance media were changed twice a week over the culture period.

2.6.1 Histological Characterisation of osteogenic differentiation:

At each time point (7, 14 and 21 days), hMSCs were either expanded or induced to undergo osteogenic lineage commitment. The histological characterisation was performed as described in section 2.5.1.3.

2.6.2 RT-PCR:

Semi-quantitative RT-PCR assay was performed to determine the expression levels of osteoblast-specific marker genes osteonectin (SPARC), collagen 1A1 (COL1A1), alkaline phosphatase liver/bone/kidney (ALPL), runt-related transcription factor 2 (RUNX2), and osteocalcin (BGLAP) at Days 0, 7, 14 and 21 of differentiation. The primers were designed using human gene sequences from NCBI Map Viewer. Customised primer sets were purchased from Invitrogen, USA. Primers are listed below (Table 2.2).

Table 2. 3. Table of primers sequences, annealing temperatures and product size.

Gene name	Sense sequence (5' to 3')	Antisense sequence (5' to 3')	Annealing Temperature (°C)	Product size (bp)
ACTB	GCCACGGCTGCTTCCAGC	AGCCATGCCAATCTCATCTT	57	528
ALPL	TGCGCAGAGAAAGAGAAAG	CATTGGTGTTGTACGTCTTG	56	259
COL1A1	TGCTCGTGGAAATGATGG	AATACCAGGAGCACCATTG	56	256
SPARC	GGATGAGGACAACAACCTTC	GATCCTTGTCGATATCTCTGC	57	357
RUNX2	TCCCAGTATGAGAGTAGGTG	GGCAGTGTCATCATCTGAAA	56	274
BGLAP	CAAATAGCCCTGGCAGATTC	CTTGGACACAAAGGCTGC	57	278

2.6.2.1 RNA extraction:

At each time point (0, 7, 14, 21 days) the RNA isolation was performed as described in section 2.3.2.1.

2.6.2.2 One-step Reverse Transcription Polymerase Chain Reaction:

At each time point of osteogenic differentiation 0, 7, 14 and 21 days, RT-PCR was performed as described in section 2.3.2.2.

2.6.2.3 Gel electrophoresis:

All the amplicons were confirmed by agarose gel electrophoresis as described in section 2.3.2.3.

2.6.3 Headspace analysis of mesenchymal stem cells and osteogenic cells by SIFT-MS:

hMSC were seeded into 6X T75 cell culture flasks containing 20 ml MSCs complete culture media (DMEM, 2mM L-glutamine, 1% (v/v) NEAA and 5% (v/v) FBS) after trypsinisation as described in section 2.5.1.1 at a density of $2x10^4$ cells/cm^2. Cells were grown in an incubator for 24 hours at 37 ^oC in humidified, 5% CO_2 and three different oxygen condition 21% O_2, 2% O_2 and 2% O_2 Work Station (WS) atmosphere. After 24 hours incubation, three cell culture flasks out of six in each condition were induced towards osteogenesis by addition of osteogenic differentiation media as described in section 2.5.1.3.2, for up to 21 days where the medium was changed every 2-3 days. hMSCs grown in MSCs medium were used as a control samples. At days 7, 14 and 21 (Figure 2.6), cells were incubated for 24 hours with 20 ml of MSCs culture media after which medium was removed from each flask (from hMSCs control and differentiation e) and transferred into 150 ml glass bottles. In parallel, incubated MSCs culture media without cells was

collected at each time point in the same fashion as described above. The volume of media in each bottle was raised to 50 ml and the samples were prepared for SIFT-MS as described in section 2.5.2.

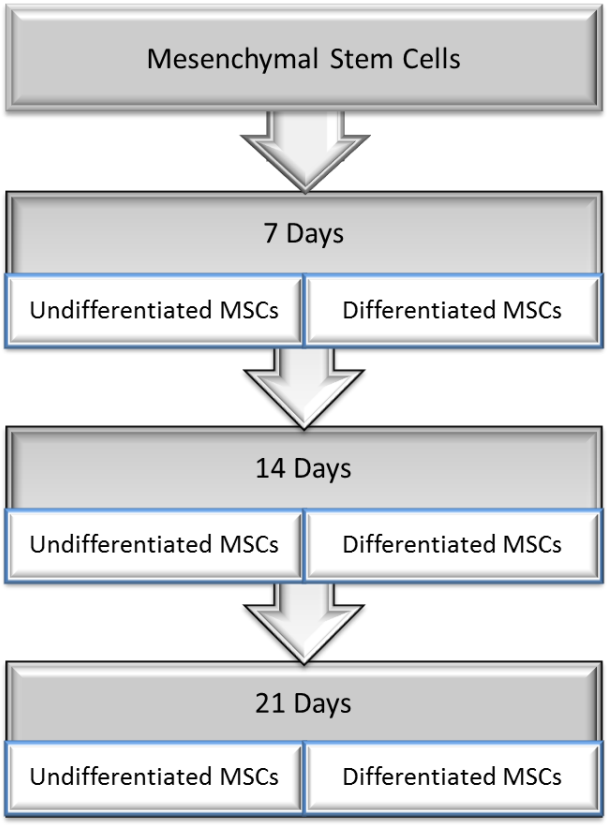

Figure 2. 6. The process flow showing key steps for VOCs extraction from MSCs culture media in standard and osteogenic treatment. MSCs were seeded in 6 X T75 flasks, MSCs in three flasks induced into osteogenic while kept MSCs in the others in standard MSCs medium, volatile extraction using headspace (HS) was performed for cell culture media in standard and treated cells at days 7, 14, 21 of induction.

2.7 Headspace analysis of cell culture media:

Dulbecco's Modified Eagle Medium (DMEM) (Lonza, Cat. No. BE12-709F) supplemented with 1% (v/v) NEAA (Lonza, Cat. No. BE13-114E) and 2mM L-Glut (Lonza, Cat. No. BE17-605E); Essential 8 Medium (Gibco, Cat. No. A15169-01); Dulbecco's Modified Eagle Medium/F12 (DMEM/F-12) (Gibco, Cat. No. 31330-038) and Knockout DMEM (KO-DMEM) (GIBCO, Cat No. 10829-018) supplemented with 2mM L-Glutamine (Lonza, Cat. No. BE17-605E), 1% (v/v) NEAA (Lonza, Cat. No. BE13-114E) were used in this experiments. 20 ml of each media was incubated in 6-well tissue culture plates in 21% O_2, 2% O_2 and 2% O_2 Work Station (WS) at 37 ^oC and 5% CO_2 for 24 hours and then transferred into 150 ml glass bottles. Similarly, non-incubated media was added to 150 ml glass bottles. Once the media added to the bottles, the samples were purged with dry and sterile air (20% oxygen and 80% nitrogen mixture; BOC, UK) for 1 minute and sealed tightly with septum caps and parafilm, and incubated for further 16 hours at 37 ^oC, this incubation period was chosen to allow accumulation of volatile organic compounds before a SIFT-MS measurement was taken. Following the 16 hour incubation period for the samples, the headspace was measured using profile 3 SIFT-MS instrument as described in section 2.3.3. Each time point was made in triplicate.

2.8 Data pre-treatment:

Spectral datasets of full scan (FS) mode, obtained from analysis of the headspace vapour of samples, were analysed using multivariate statistical analysis using SIMCA 14.1 software (MKS Umetrics AB, Umeå, Sweden). Initially, principal component analysis (PCA) was applied as unsupervised clustering then orthogonal projection least squares discriminant analysis (OPLS-DA) as a supervised multivariate analyses. The data were transformed and

scaled before computing the PCA and OPLS-DA using log transformation and unit variance (UV) scaling.

In addition to the multivariate analysis, ANOVA or t-test was also performed by investigating the spectra to identify significant variables (ions) in different cell culture media and conditions after removing m/z 19 precursor ion (H_3O^+) and its isotopologues at m/z 20, m/z 21, plus water clusters (because of the aqueous nature of samples) and their isotopologues at m/z 37, m/z 38, m/z 39, m/z 55, m/z 56, m/z 57, m/z 73, m/z 74, m/z 75, m/z 91 (Spanel and Smith, 2000; Spooner et al., 2009; Shestivska et al., 2015) in addition to variables with zero values.

Chapter 3-Cell functionality characterisation

3.1 Introduction:

Stem cells are functionally undifferentiated cells that have the ability to self-renew and to differentiate into specialised cell types. Stem cells may be isolated from embryo, bone marrow and several adult tissues, and the potential for differentiation of these stem cells into committed and more mature specialized cell varies depending on the source of stem cells (Ullah et al., 2015).

Pluripotent stem cells have the potential to differentiate into three embryonic germ layers and give rise to all the cell types of the embryo proper. These cells include both embryonic stem cells, which derived from blastocyst stage embryo, and induced pluripotent stem cells, pluripotency has been induced via the reprogramming of somatic cell. (Avior et al., 2016). The capability of hPSCs for application in cell replacement therapy and for treatment of disease has been discussed previously (Wu and Hochedlinger, 2011). Scale up and expansion of hPSC relies on *in vitro* culture and this includes a number of environmental limitations which place undue stresses onto the cells. Among these stresses is the routine use of non-physiological air oxygen concentrations (21% O_2) (Stover et al., 2016).

In contrast, adult stem cells are multipotent stem cells, which are able to give rise to a subset of cell linages, and of these, the mesenchymal stem cells (MSCs) are an example of adult stem cells (Haasters et al., 2009). MSCs can be isolated from a wide range of adult tissues such as umbilical cord blood, adipose tissue, bone marrow and dental pulp (Erices et al., 2000; Lund et al., 2009; Shi and Gronthos, 2003).

The two distinct stem cells populations that generally reside in bone marrow are haematopoietic and mesenchymal stem cells (Dawn and Bolli, 2005). Bone marrow-derived MSCs are usually isolated via their physical adherence to the plastic tissue culture

plate (Meirelles and Nardi, 2003). An aspect of the utility of MSCs in cell-based therapies includes their differentiation capacity where, for instance, bone repair resides in their capacity to differentiate into osteoblasts (Im, 2015). It therefore becomes important to maintain multipotency in clinical mesenchymal stem cells prior to transplantation into the target tissue (Otte et al., 2013).

The functional characterisation of cells in this first result chapter was essential before any further studies are carried out, to ensure the quality and the current status of the cells.

3.2 Aims:

1. To characterise hPSCs and assess their proliferation, metabolic activity and differentiation in two different oxygen conditions (21% O_2 and 2% O_2).
2. To isolate mesenchymal stem cells (MSCs) from human bone marrow aspirate and culture them in three different oxygen conditions (21% O_2, 2% O_2 and 2% O_2 WS).
3. To characterise bone marrow derived mesenchymal stem cells (BM-MSCs) and assess their osteogenic differentiation in three different oxygen conditions (21% O_2, 2% O_2 and 2% O_2 WS).

3.3 Materials and methods:

hPSCs were cultured and expanded in xeno-free E8M under air (21% O_2) and physiological normoxia (physioxia) (2% O_2) (See chapter 2 for more details). hPSCs growth analysis was evaluated via cell counts and MTT while detailed characterisation of hPSCs was carried out to confirm pluripotency. Immunofluorescence- and FACS-based methods were applied to identify and quantify SSEA1, SSEA-4, TRA-1-60 expression. Pluripotency marker expression was also evaluated over 20 days of differentiation via both immunofluorescence and RT-PCR (Full methodology is detailed in chapter 2).

hMSCs isolation, characterisation and osteo-induction were carried out in three oxygen conditions (21% O_2, 2% O_2 and 2% O_2 WS) (Full methodology in detailed in chapter 2).

3.4 Results:

3.4.1 Influence of physioxia (2% O_2) on proliferation of hPSCs

To determine the effect of oxygen on the proliferation of hPSC (ESCs and iPSCs) cells were seeded into multiple wells of a 6-well plate and cell counts performed daily over a 6-day period. From analysis of two hESC lines (SHEF1 and SHEF2) and a single hiPSC line (ZK2012L) it was apparent that no consistent pattern emerged (Figure 3.1). SHEF1 cell number increased significantly from day 3 onwards in physioxia vs. air oxygen ($P<0.05$). Conversely, SHEF2 and ZK2012L displayed increases from day 2 onwards in air oxygen vs. physioxia, with significant increases for ZK2021L cells at two, four and five days of counting($P<0.05$).

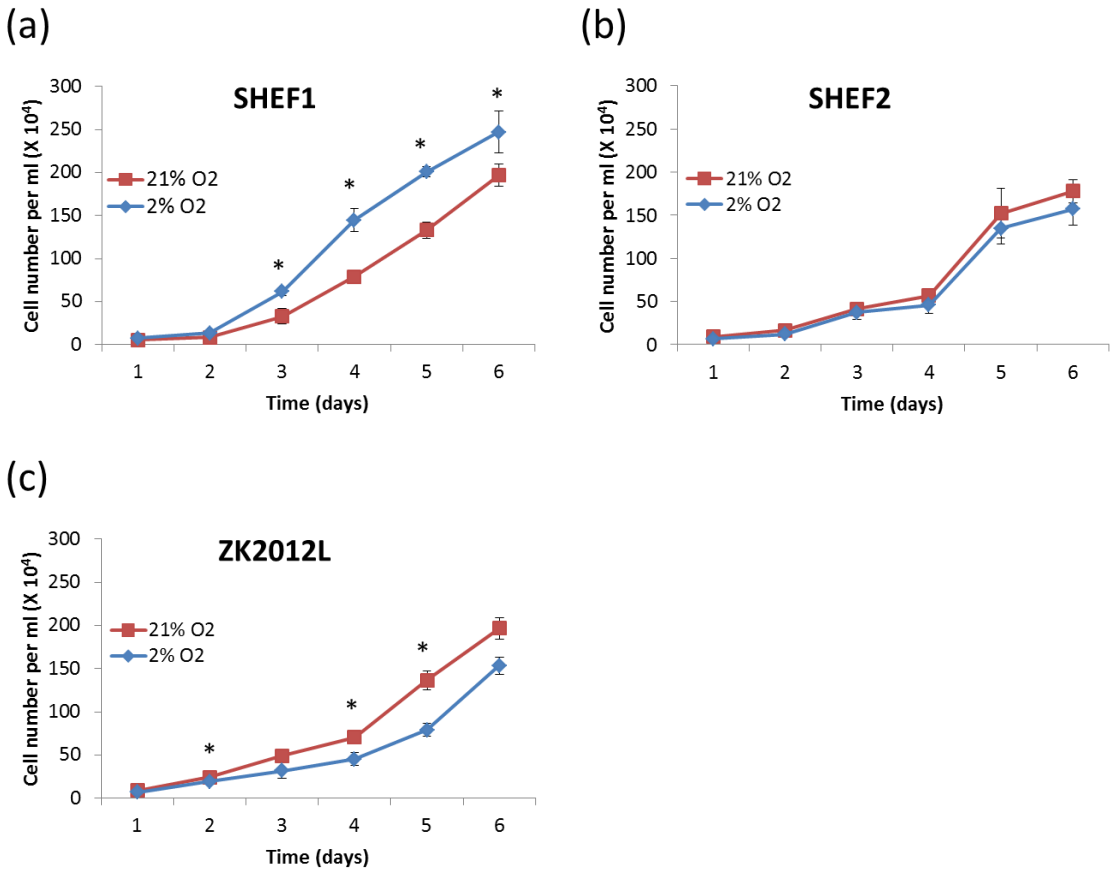

Figure 3. 1. hPSCs display cell line specific proliferation responses to physioxia. a) SHEF1 b) SHEF2 and c) ZK2012L in air oxygen (21% O_2) and physioxia (2% O_2). The x-axis indicates time (days), y-axis indicates cells x 104/ml. Red and blue lines represent cells cultured under 21% O_2 and 2% O_2. Error bars represent +/- SD. Asterisk (*) indicates $p<0.05$ between conditions

3.4.2. Influence of physioxia (2% O_2) on hPSCs metabolic activity

The impact of oxygen condition on mitochondrial metabolic activity was investigated via the MTT assay. Cells were seeded as described for the cell counting experiment (Section 3.4.1) and MTT performed at each day post seeding in 2% O_2 and 21% O_2 conditions. Similar to influence of physioxia on proliferation of hPSCs (section 3.4.1) it was apparent that individual cell lines displayed distinct responses to a physioxia environment (Figure 3.2). SHEF1 displayed a significant increase in MTT at Day 6 in physioxia only (Figure 3.2a) whereas SHEF2 and ZK2012L (Figure 3.2b and c) both exhibited significant MTT decreases in physioxia across the bulk of the time points tested (only Day 5 for SHEF2 and Day 1 for ZK2012L were not significant).

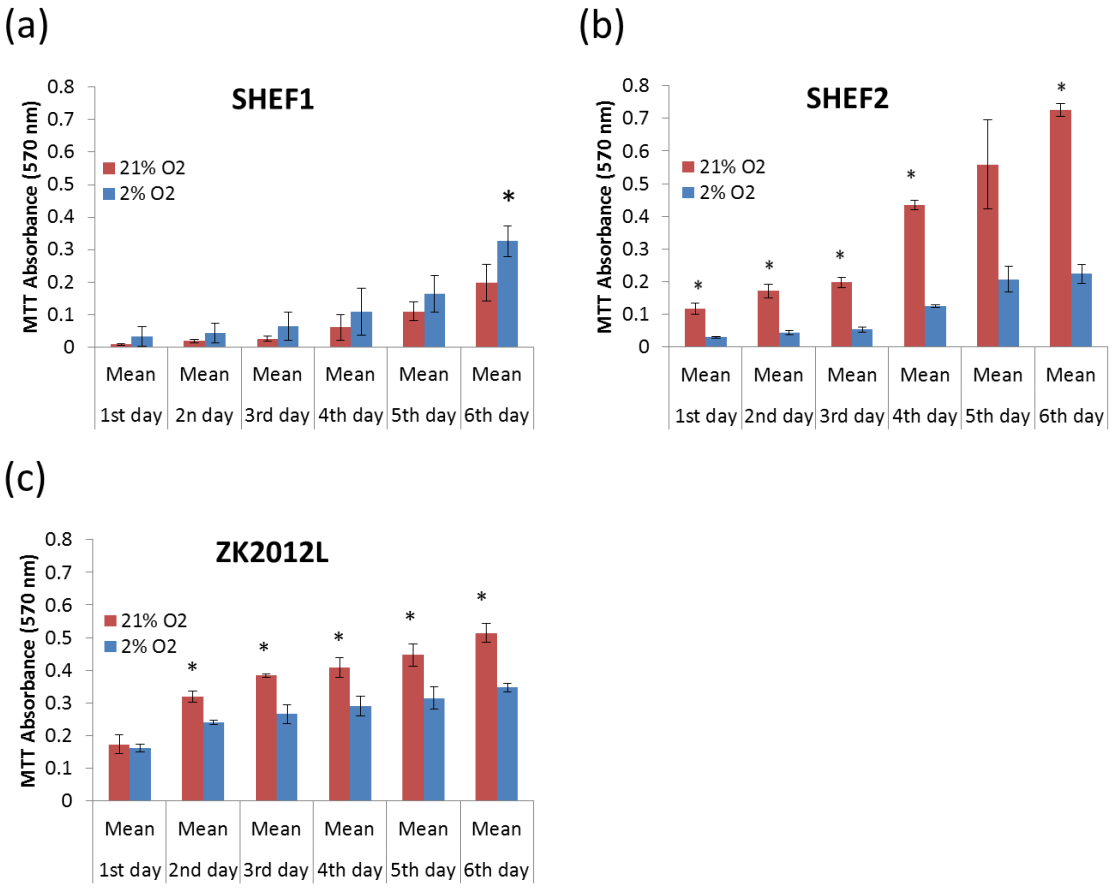

Figure 3. 2. hPSCs display cell line specific metabolic responses to physioxia. a) SHEF1, b) SHEF2, and c) ZK2012L in air oxygen (21% O_2) and physioxia (2% O_2). The x-axis indicates Time (days), y-axis indicates MTT absorbance (570 nm). Red and blue bars represent cells cultured under 21% O_2 and 2% O_2, respectively. Error bars represent +/- SD. Asterisk (*) indicates $p<0.05$ between conditions.

3.4.3. Characterisation of hPSCs by immunofluorescence staining and flow cytometry

hPSCs expression of surface markers associated with retention of pluripotency was explored via immunostaining of live cells with SSEA-4, TRA-1-60, and the marker of differentiation, SSEA-1. The immunofluorescent staining of live, unfixed hPSCs showed positive expression of the pluripotent surface markers SSEA-4 and TRA-1-60 alongside negative expression of the SSEA-1 surface marker (figure 3.3a-c). These characteristics are typical of the surface antigen of hPSCs and distinct from the differentiated hPSCs.

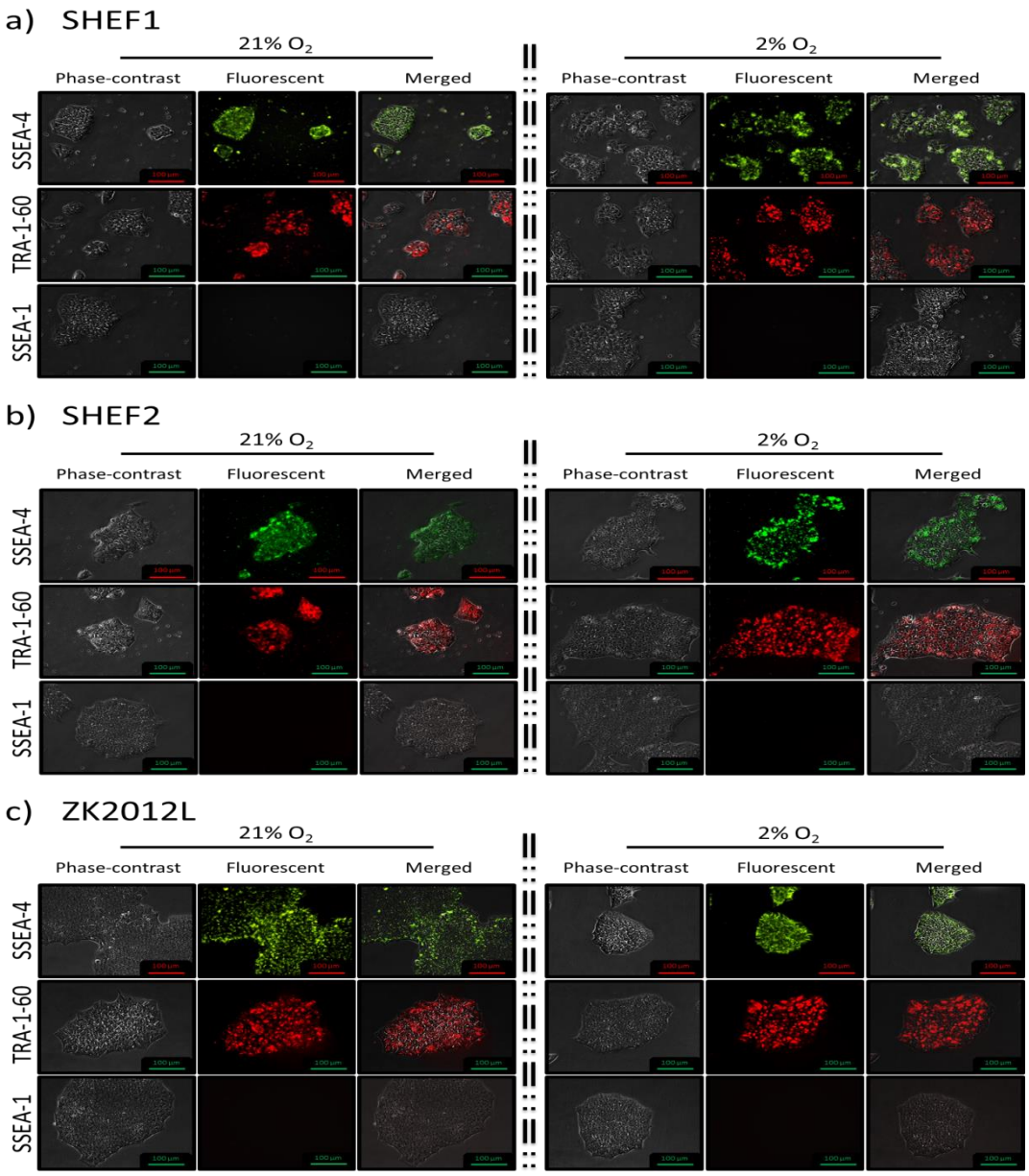

Figure 3. 3. Analysis of SSEA-4, TRA-1-60 and SSEA-1 expression in live hPSCs cultured in 21% and 2% O_2. a) SHEF1, b) SHEF2, and c) ZK2012L. For each pluripotent stem cell, the left panel shows cells cultured in 21% O_2 and the right panel shows cells cultured in 2% O_2. In each panel, the top row shows images stained with SSEA-4 antibody, the middle row shows images stained with TRA-1-60 antibody and the bottom row shows images stained with SSEA-1 antibody, whereas the left column shows phase-contrast images, the middle column shows fluorescent images and the right column shows merged images. Scale bars represent 100 µm.

Following on from marker expression by immunofluorescence, expression levels of each marker were quantified via flow cytometry analysis (Figure 3.4) and (Table 3.1).

Table 3. 1. Mean ± SD percentage of hPSCs for each marker in 21% O_2 and 2% O_2 conditions.

Cell	Oxygen condition	Marker		
		SSEA-4	**TRA-1-60**	**SSEA-1**
SHEF1	**21%**	97.86 ± 2.66	70.16 ± 14.4	2.55 ± 0.6
	2%	98.6 ± 1.17	76.2 ± 12.85	2.5 ± 0.3
SHEF2	**21%**	83.43 ± 15.36	64.71 ± 12.87	4.54 ± 3.68
	2%	90.91 ± 6.89	68.76 ± 11.99	3.74 ± 1.5
ZK2012L	**21%**	91.08 ± 2.61	52.25 ± 7.1	6.12 ± 4.46
	2%	92.07 ± 7.86	57.64 ± 5.13	5.82 ± 3.31

No significant changes in expression levels of SSEA-4, TRA-1-60, or SSEA-1 were noted between cells cultured under physioxia and air oxygen. Previous reports have indicated that physioxia can reduce both size and complexity of hPSCs vs. air oxygen. The panel of cell lines was investigated using forward scatter (FS) and side scatter (SS) as surrogate markers for size and complexity, respectively. Overall reductions were noted in each instance but the associated variance made the bulk of these decreases non-significant. The only +exceptions to this were with ZK2012L (FS) and SHEF2 (SS).

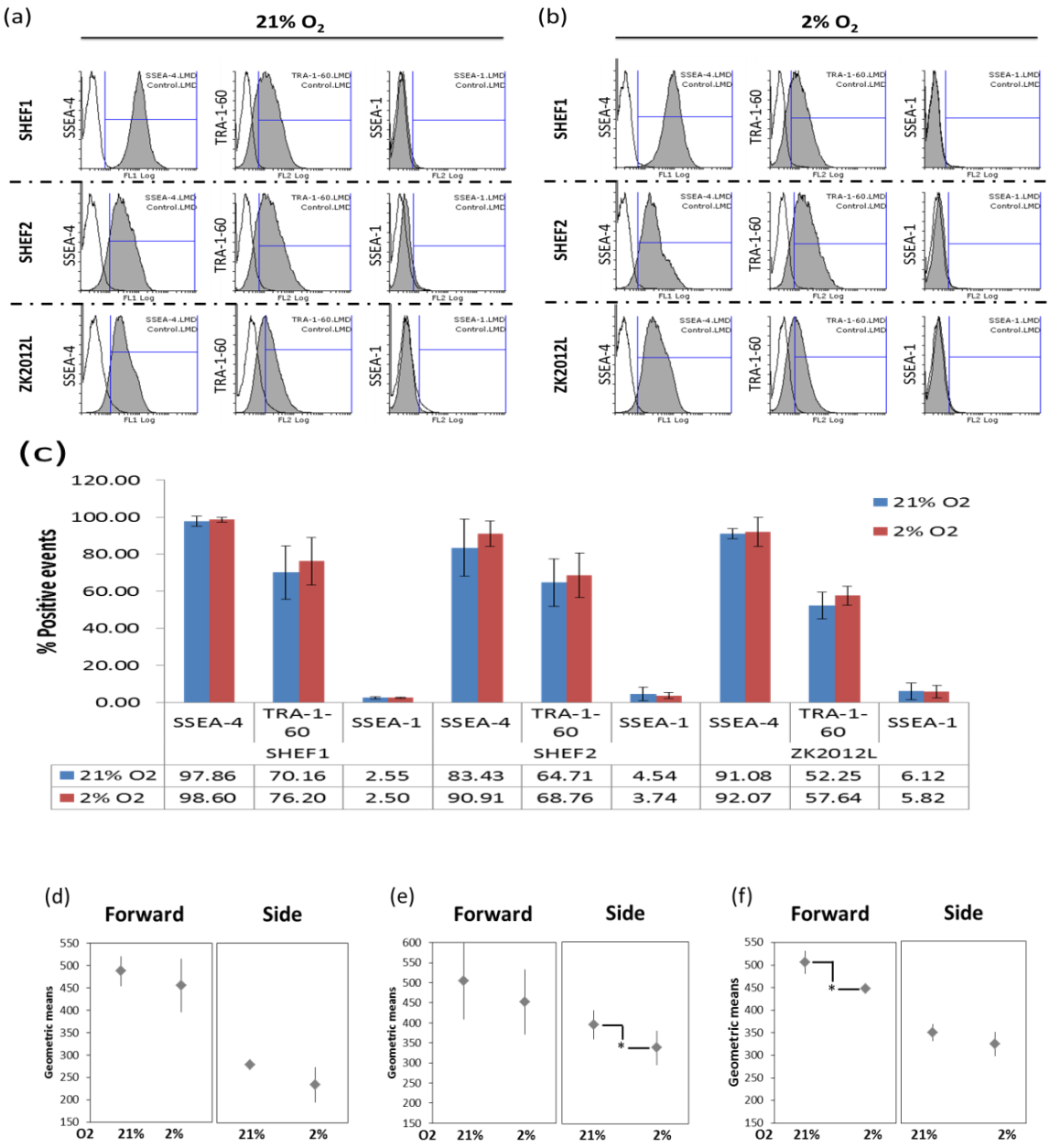

Figure 3. 4. Analysis of SSEA-4, TRA-1-60 and SSEA-1 expression in hPSCs by flow cytometry analysis. Overlay histograms of pluripotent marker expression for SHEF1 (top panel), SHEF2 (middle panel) and ZK2012L (bottom panel) cultured in air oxygen (21% O_2) (a) and physioxia (2% O_2) (b). Percentage of positive cells identified from (a) and (b). (c). FS and SS graphs of SHEF1 (d), SHEF2 (e), and ZK2012L (f) where geometric mean of FS (size) and SS (complexity) for cells in 21% and 2% O_2 (x-axis) are shown on y-axis. Error bar represent +/-SD.

3.4.4. Genes related to ethanol/acetaldehyde metabolism

Acetaldehyde sits as a midpoint on the Ethanol to Acetate metabolic pathway controlled by expression of specific enzymes (Figure 3.5 and Table 3.2). In summary Ethanol is oxidised to acetaldehyde where the reaction is catalysed by ADH, CYP2E1 and CAT enzymes and the resultant acetaldehyde is further oxidised to acetate by the ALDH enzyme (Seitz and Stickel, 2007). The conversion involves 7 alcohol dehydrogenase (ADH) family members, a single cytochrome P4502E1 (CYP2E1), a single catalase (CAT), and 19 acetaldehyde dehydrogenase family members (ALDH).

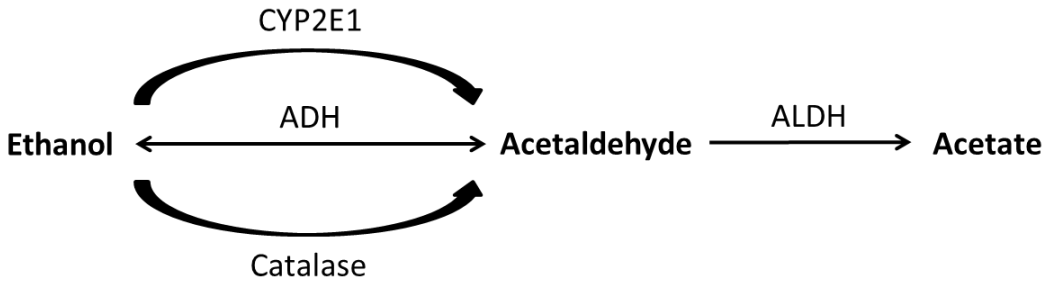

Figure 3. 5. Pathways of ethanol/acetaldehyde metabolism in human. The oxidation of ethanol by ADH and/or CYP2E1 and/or catalase produces acetaldehyde which is converted in turn into Acetate by ALDH.

Table 3. 2. Ethanol/acetaldehyde metabolism genes (NCBI).

No.	Metabolic reaction	Enzyme	Gene
1	Ethanol → Acetaldehyde	Alcohol dehydrogenase	ADH1B, ADH1C, ADH1A, ADH5, ADH4, ADH7, ADH6
2	Ethanol → Acetaldehyde	Cytochrome P450 2E1 (CYP2E1)	CYP2E1
3	Ethanol → Acetaldehyde	Catalase	CAT
4	Acetaldehyde → Acetate	Aldehyde dehydrogenase	ALDH2, ALDH1A1, ALDH1B1, ALDH7A1, ALDH3A1, ALDH1L1, ALDH3A2, ALDH5A1, ALDH1A2, ALDH1A3, ALDH18A1, ALDH4A1, ALDH9A1, ALDH3B1, ALDH6A1, ALDH1L2, ALDH16A1, ALDH8A1, ALDH3B2

Our research group has previously noted that culture of hPSC in physioxia results in substantial modulation of the transcriptome vs. air oxygen cultured cells (Forsyth et al, 2008). This microarray data was reanalysed via *in silico* analysis to determine if any significant changes in gene expression level were noted for the enzymes identified above. CAT, CYP2E1, ALDH1L2, ADH4, ADH5 and ALDH18A1 were all significantly upregulated in 2% O_2, while ALDH9A1, ALDH4A1, ALDH7A1, ALDH16A1, ALDH1B1, ALDH1A2, ALDH3A2, ALDH5A1, ALDH6A1, ALDH1A3, ALDH1A1 were all significantly downregulated in 2% O_2 (Figure 3.6a). RT-PCR supported the upregulation of ADH4, ADH5 and CYP2E1 and downregulation of ALDH1A1, ALDH1A3 and ALDH6A1 in 2% O_2 (Figure 3.6b).

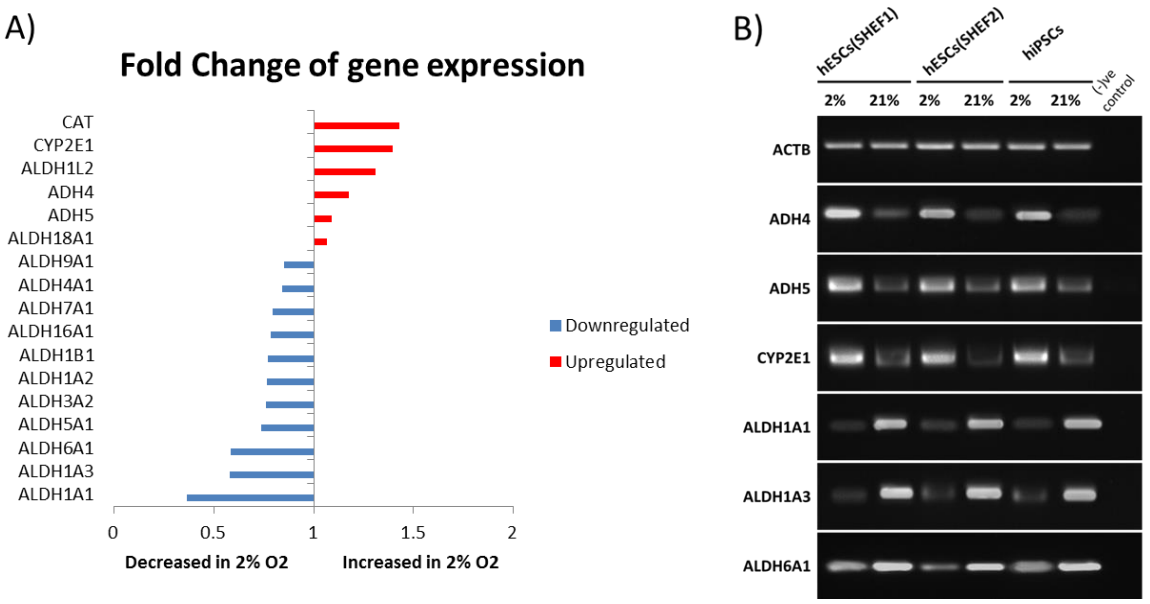

Figure 3. 6. Ethanol/acetaldehyde metabolic pathway linked gene expression. A) The fold change in microarray gene expression level in hESCs was plotted on scale 0 to 2 (>1 for upregulation, while <1 for downregulation). Red bars represent the upregulated genes and blue bars represent downregulated genes in hESCs cultured in 2% O_2 relative to 21% O_2. B) RT-PCR of selected gene expression involved in ethanol/acetaldehyde metabolism of hPSCs. ACTB confirmed the presence of amplifiable RNA in all samples.

3.4.5. Assessment of cell viability in hPSCs cultures

The effects of treating the cells with the 4-methyl pyrazole (4-MP), inhibitor of ADH and CYP2E1, on the viability of hPSCs were assessed under physioxia and air oxygen conditions, with the cells attached to 96-well plates, using MTT assay. MTT data indicated that 0.5 mM and 5 mM 4-MP inhibitor had no significant effect on the viability of hPSCs with the exception of ZK2012L cells treated with 0.5 mM 4-MP in 21% O_2, which led to significant increase in the MTT reduction, while 50 mM was toxic (Figure 3.7). Therefore, the 4-MP concentration of 5 mM was selected in the subsequent SIFT-MS experiment.

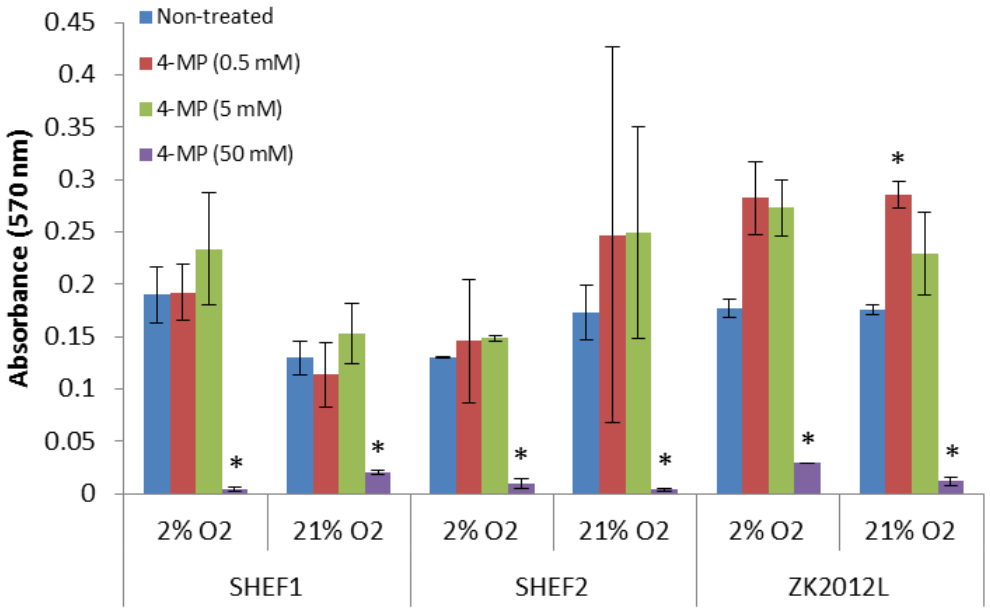

Figure 3. 7. Viability of hPSCs exposed to different concentration of 4-MP. X-axis represent each hPSCs in both 2% O_2 and 21% O_2 conditions. Y-axis represents MTT absorbance at 570 nm. Blue bars indicate control untreated cells, whereas red, green and purple bars indicate 0.5, 5 and 50 mM 4-MP concentrations, respectively.

3.4.6. RT-PCR analysis of undifferentiated and spontaneous differentiated hPSCs

Having established the headspace profile of undifferentiated hPSCs alterations during the process of differentiation were established and characterised. To achieve this hPSCs were spontaneously differentiated by switching media and supplementing with serum. During differentiation RNA was extracted over a 20 day period and RT-PCR amplification of pluripotency associated and germ layer specific transcripts was performed. In addition to this retention of expression of pluripotency-linked proteins via immunofluorescence was determined. POU5F1, NANOG, and hTERT expression were detected over the entire 20 day period in all hPSCs tested. Some evidence of down-regulation was apparent but this was not quantified further (Figure 3.8a, b, c). A pluripotent differentiation capacity requires evidence of expression of genes associated with the three germ layers. Expression of ectoderm (OTX2), endoderm (AFP) and mesoderm (Brachyury) in differentiating hPSCs was therefore evaluated. SHEF1 showed a notable gradual increase in AFP expression which though stronger in 21% was also apparent in 2% O_2 throughout the differentiation period (Figure 3.8a). Brachyury gene expression shows upregulation in both 21% O_2 and 2% O_2 which was subsequently down-regulated and virtually lost by day 20 (Figure 3.8a). OTX2 expression was also noted at virtually all time points.

Similar to SHEF1, SHEF2 displayed POU5F1 and NANOG expression at all points tested (Figure 3.8b). hTERT appeared to undergo some downregulation in 2% O_2 culture only at Days 10 and 20. AFP and Brachyury displayed similar expression profiles in 21% O_2 SHEF2 ranging from being undetectable, or at very low levels, at Day 0 to upregulation at Day 5 and maintenance thereafter. Conversely in 2% O_2 Brachyury was maintained at low

levels throughout the period while AFP, apart from a transient upregulation at Day 10, was absent. OTX2 was expressed in both undifferentiated and differentiated cells with some upregulation in the latter.

ZK2012L was again similar to the above displaying continuous expression of POU5F1, NANOG, hTERT, and OTX2 in both 21% O_2 and 2% O_2 across the entire time-course (Figure 3.8c). AFP displayed a gradual increase in expression in 21% O_2, while in 2% O_2 the expression of AFP increased through to Day 10 and decreased thereafter (Figure 3.8c). Brachyury expression was noted at Day 20 only in 21% O_2 and at Days 10 and 20 only in 2% O_2.

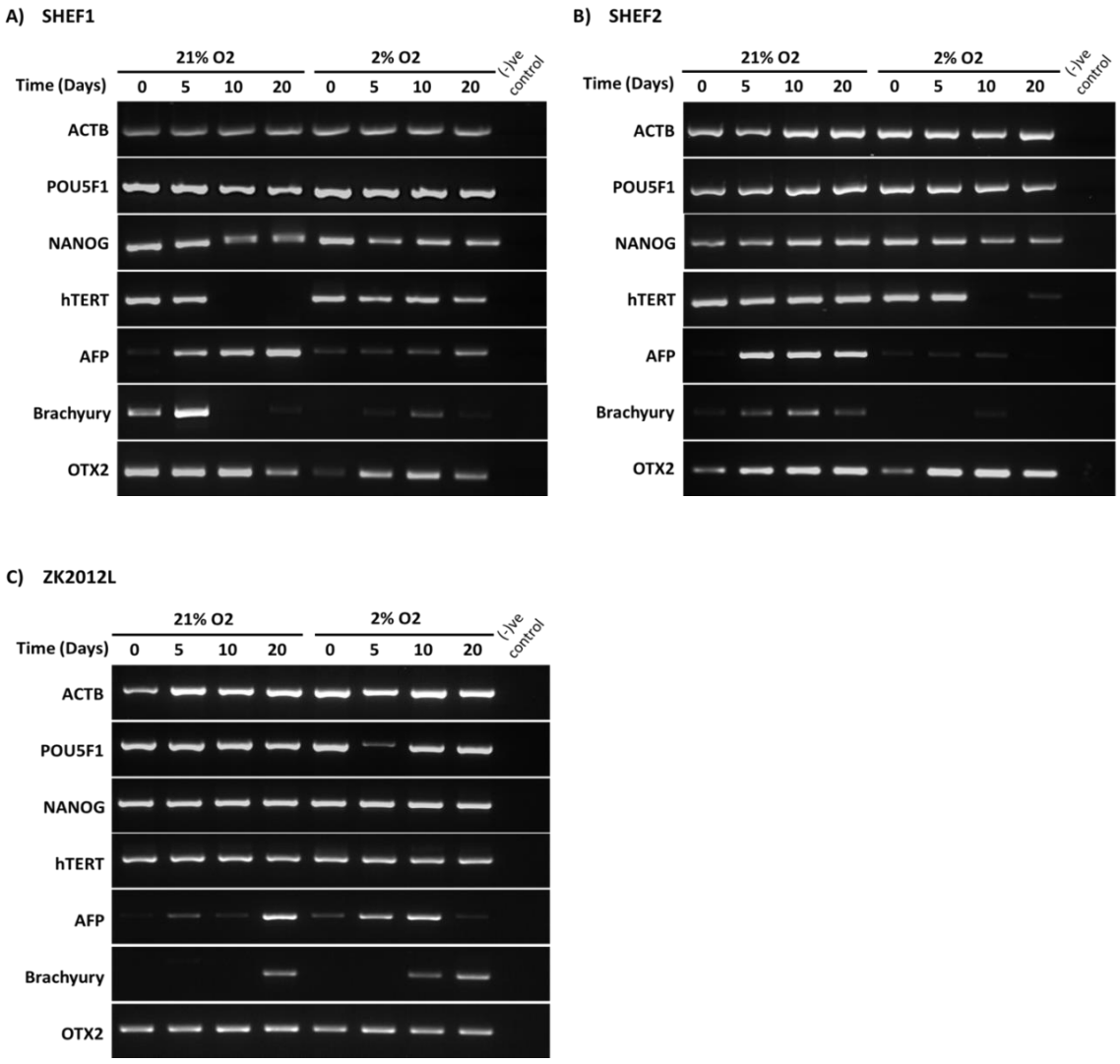

Figure 3. 8. Expression of pluripotency and differentiation-linked genes in hPSCs from day 0 to day 20 of differentiation in 21% O_2 and 2% O_2. A) SHEF1. B) SHEF2. C)ZK2012L. ACTB confirms the presence of amplified RNA in all samples. POU5F1, NANOG, hTERT are markers of embryonic stem cell pluripotency. AFP is endoderm marker gene. Brachyury is mesoderm marker gene. OTX2 is ectoderm marker gene.

3.4.7. Pluripotency marker expression via immunofluorescence in undifferentiated and differentiated hPSCs

Evaluation of transcript expression only indicates that the gene is being transcribed. Evidence was therefore next sought to identify that the translated proteins for both POU5F1 (OCT-4) and NANOG along with ALP and the SSEA-4 glycoprotein peptides were also downregulated during differentiation (Figure 3.9). It was clear that all undifferentiated hPSCs expressed high level of OCT-4, NANOG, ALP, and SSEA-4 in both 2% and 21% O_2 conditions. During spontaneous differentiation, expression of pluripotent markers was decreased in a time-dependent manner from 0 to 20 days. SHEF1 in 2% O_2 showed notable reduction in OCT-4, NANOG, ALP and SSEA-4 expression after 10, 5, 10 and 20 days of differentiation (Figure 3.9a), respectively, while SHEF1 in 21% O_2 showed notable reduction in OCT-4 and NANOG after 5 days, and ALP and SSEA-4 after 10 days of differentiation (Figure 3.9b). SHEF2 in 2% O_2 showed notable reduction in OCT-4 and NANOG after 5 days, and ALP and SSEA-4 after 10 days of differentiation (Figure 3.9c), while SHEF2 in 21% O_2 showed notable reductions in OCT-4, NANOG, ALP and SSEA-4 after 5 days of differentiation (Figure 3.9d). ZK2012L in 2% and 21% O_2 conditions showed notable reduction in OCT-4, NANOG and ALP after 5 days, and SSEA-4 after 10 days of differentiation (Figure 3.9e and 3.9f).

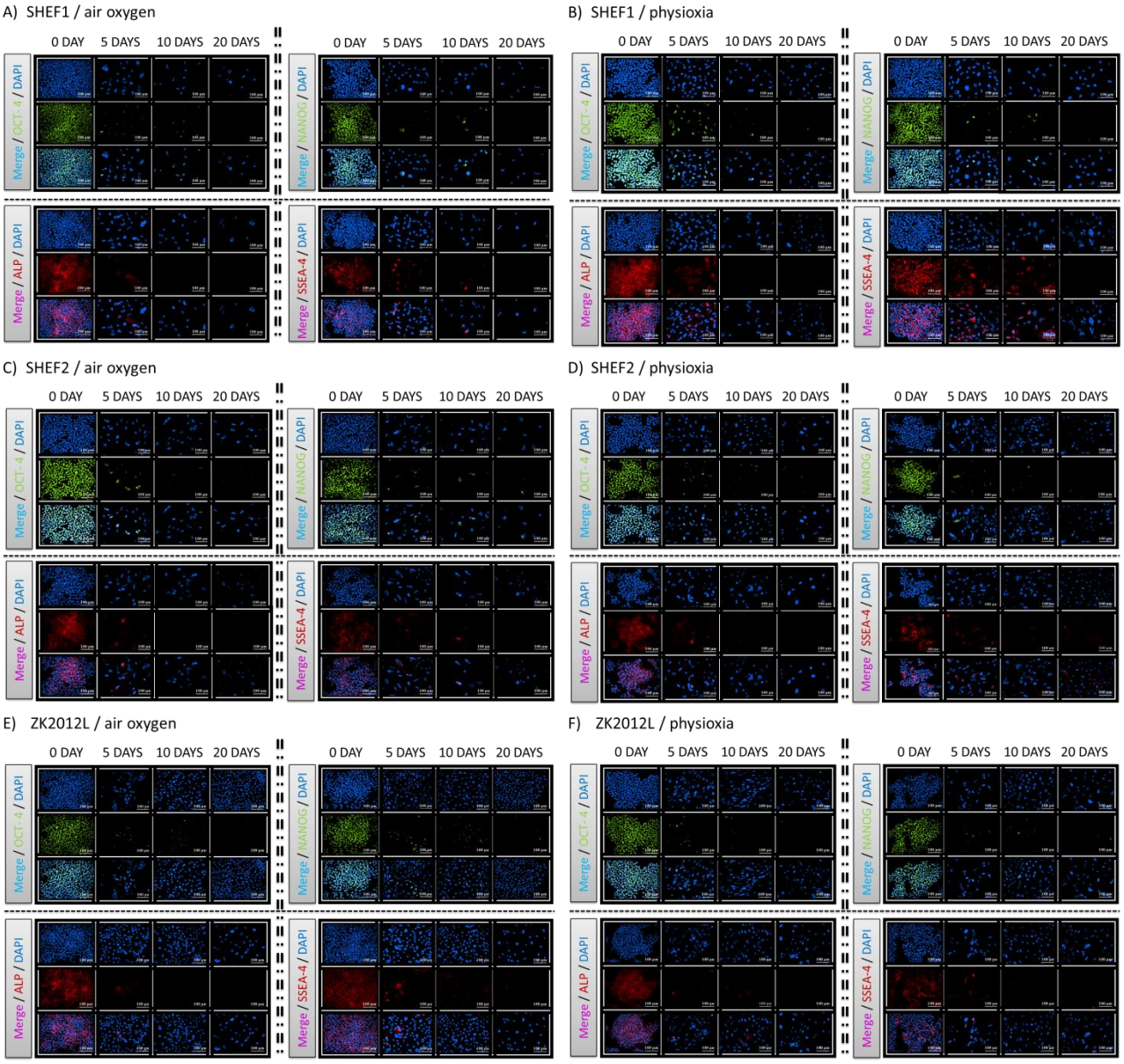

Figure 3. 9. Pluripotency marker expression in undifferentiated and differentiating hPSCs. Oct-4, Nanog, ALP, and SSEA-4 expression was evaluated in hPSCs at selected time points of differentiation (0, 5, 10 and 20 days) in SHEF1 (21% O_2) (A) and (2% O_2) (B), SHEF2 (21% O_2) (C) and (2% O_2) (D), and ZK2012L (21% O_2) (E) and2% O_2 (F). Green fluorescence represents Oct-4 and Nanog expression, red fluorescence represents ALP and SSEA-4 expression whereas blue fluorescence represents DAPI staining for nuclei in all images. Each scale bar represents 100 µm.

3.4.8. Influence of incubation condition on isolation of hMSCs

At the culmination of the isolation procedure on day 28 cells were counted and quantified. In agreement with previous observations (Kay et al 2015) the highest number of cells were recovered under 2% O_2 WS condition with a reduced, though not significantly so, number in 2% O_2 and the least cells recovered under 21% O_2 (Figure 3.10).

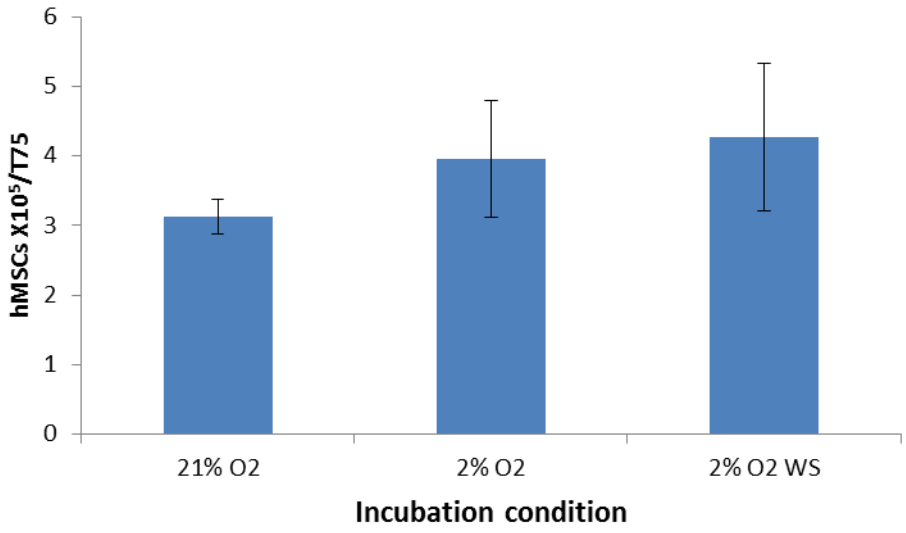

Figure 3. 10. Oxygen conditions effects on human hMSCs recovery. Bars represent the number of cells recovered per T75 flask at first trypsinisation. X-axis indicates oxygen conditions and Y-axis indicates cell x 10^5 per T75 flask. Error bars represent +/- SD.

3.4.9. Immunophenotypic characterisation by flow cytometry

To determine the immunophenotype of isolated cells flow cytometry was used to determine expression levels of a panel of cell surface markers, according to ISCT guidelines (Dominici et al., 2006) (Figure 3.11). Table 3.3. below indicates that the cells isolated displayed an immunophenotype characteristic of an hMSC and that there were no significant differences between isolation conditions.

Table 3. 3. Mean ± SD percentage of hMSCs for each marker in three oxygen conditions (21% O_2, 2% O_2 and 2% O_2 WS).

Marker		**Oxygen condition**		
		21%	**2%**	**2% WS**
Positive	**CD105**	94.4 ± 4.2	96.5 ± 5.4	96.6 ± 4.2
	CD73	99.6 ± 0.3	99.8 ± 0.1	98.8 ± 1.1
	CD90	93.1 ± 10.7	95.9 ± 6.4	97.1 ± 3.8
Negative	**CD19**	3.9 ± 3.2	2.7 ± 2.4	0.8 ± 0.5
	CD45	1.2 ± 0.3	0.9 ± 0.8	0.4 ± 0.1
	CD34	1 ± 0.5	0.5 ± 0.4	0.3 ± 0.2
	CD14	5 ± 2.7	6.6 ± 4.5	5.3 ± 3.4
	HLA-DR	3.2 ± 1.2	2.1 ± 1.6	3.7 ± 3.1

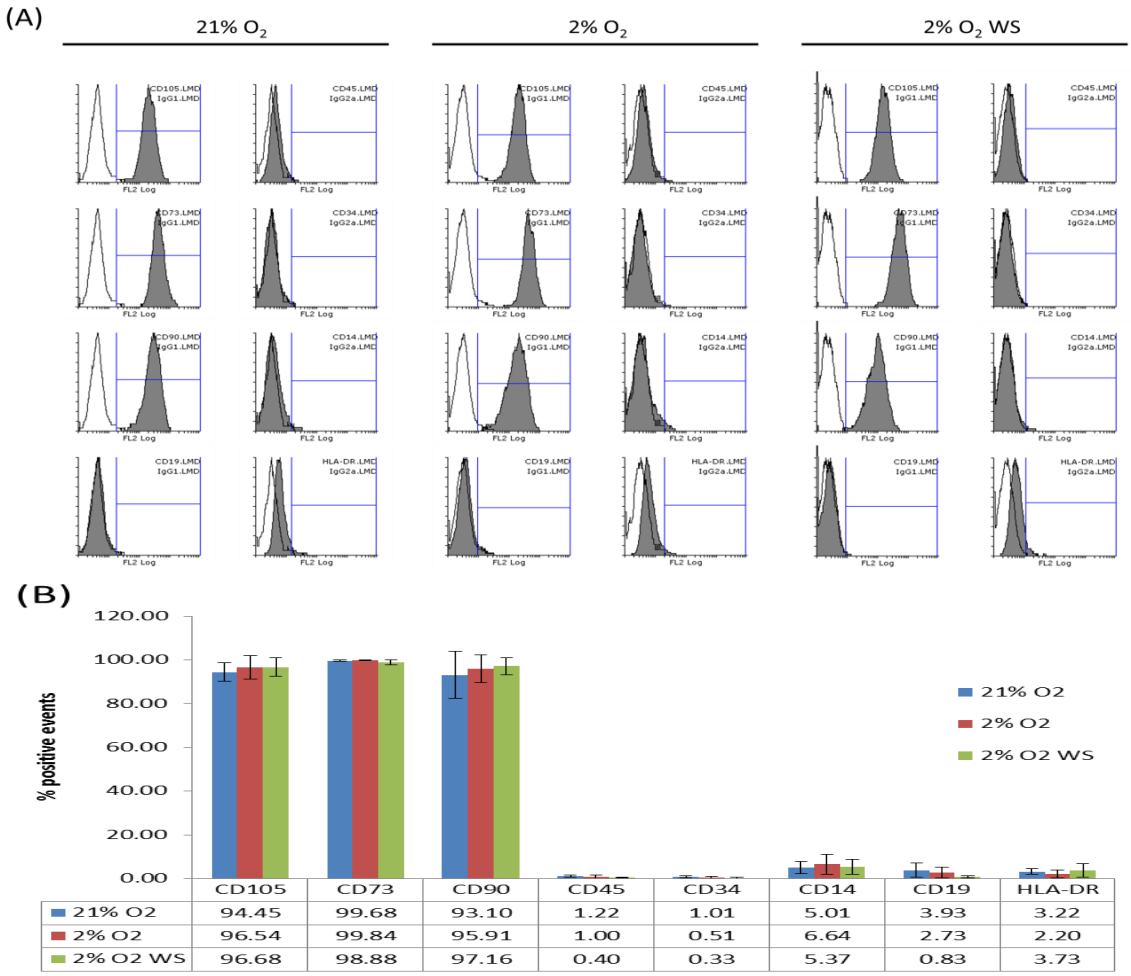

	CD105	CD73	CD90	CD45	CD34	CD14	CD19	HLA-DR
21% O2	94.45	99.68	93.10	1.22	1.01	5.01	3.93	3.22
2% O2	96.54	99.84	95.91	1.00	0.51	6.64	2.73	2.20
2% O2 WS	96.68	98.88	97.16	0.40	0.33	5.37	0.83	3.73

Figure 3. 11. Immunophenotypic characterisation of BM-hMSCs. A) Flow cytometry analysis of cell surface antigens showed that the hMSCs in three oxygen conditions positively expressed CD105, CD73 and CD90, but were negative for CD34, CD45, CD14, and HLA-DR expression. Unfilled region is isotype control IgG1 or IgG2a, grey region is antibody marker. B) Percentage of positive events relative to relevant isotype control marker for each immunophenotype marker in each oxygen condition. Bar graph showing summary of flow cytometry result for hMSCs. X-axis indicates cell surface markers and y-axis indicates the percentage of cells staining positive for each marker. Blue bars represent average cells in 21% O_2, red bars represent average cells in intermittent 2% O_2 and green bars represent average cells in 2% O_2 WS. Error bars represent +/-SD, n=3 for each marker.

3.4.10. Differentiation of BM-hMSCs into mesenchymal lineage

Bone marrow isolated cells displayed an hMSC guideline immunophenotype but it remained to be determined if they possessed a multipotent differentiation capacity. The cells were then exposed to either adipogenic, osteogenic, or chondrogenic differentiation cocktails. When cells were cultured in an adipogenic differentiation media, cells showed the formation of adipocytes, which were detected by staining the lipid droplet with Oil Red O stain; cells grown in control medium did not stain for Oil Red O. When cells were induced in osteogenic differentiation media, cells revealed mineralisation with calcium deposition confirmed by Alizarin red stain; there was no Alizarin red stain in the cells cultured in control media. When cells were differentiated into chondrocytes, cartilage matrix formation was demonstrated by Alcian blue staining of proteoglycans; cells grown in control media did not stain with Alcian blue (Figure 3.12). Taken together with the immunophenotype data the evidence of a tri-lineage differentiation potential allows us to refer to the cells as hMSC or BM-hMSC.

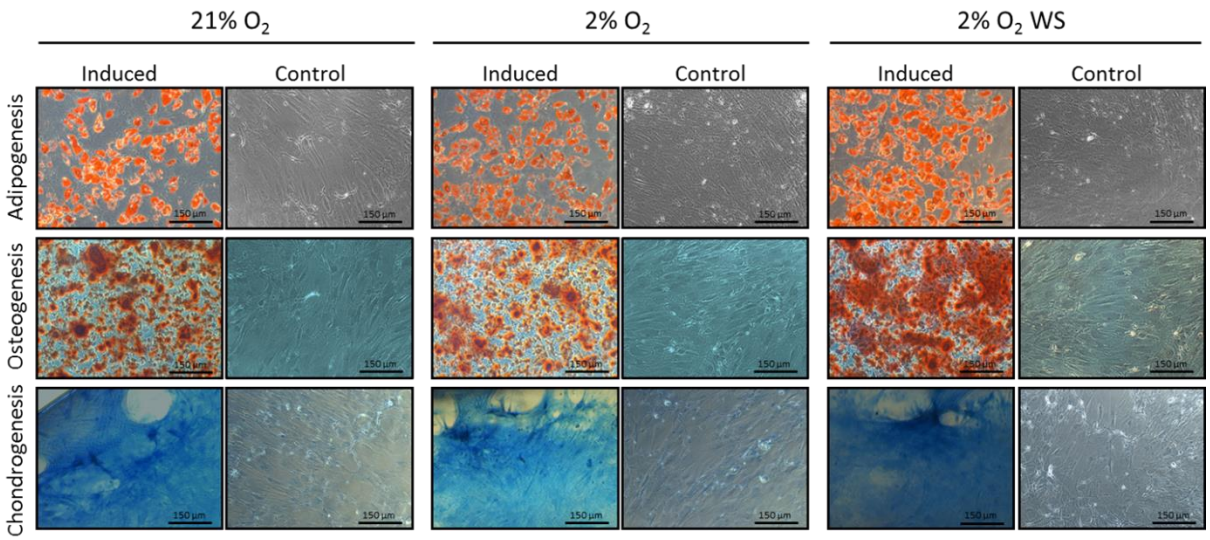

Figure 3. 12. Tri-lineage differentiation of bone marrow derived mesenchymal stem cells (BM-hMSCs). Adipogenic differentiation was characterised by the staining of lipid droplet with Oil Red O. Osteogenic differentiation was characterised by matrix mineralisation identification using the Alizarin Red stain. Chondrogenic differentiation was characterised by Alcian blue staining detection of proteoglycans. The first column in each condition stained cells following differentiation in induction media, while the second column shows control cells. The first row shows cells stained with Oil Red O; the second cells stained with Alizarin Red and the third cells stained with Alcian blue. The scale bar was 150 µm.

3.4.11. Assessment of cell viability in hMSCs cultures

The potential effects of the overnight incubation (16 hours) in the sealed bottles on the viability of hMSCs were assessed using the Trypan blue method. The result revealed that hMSCs showed little or no decline in viability following the incubation period of 16 hours.

Table 3. 4. Mean viable cell number prior and following 16 hours' period of incubation in sealed glass bottles.

	21% O_2	**2% O_2**	**2% O_2 WS**
Prior incubation	300000	300000	300000
Following incubation	285000	287500	290000

3.4.12. Assessment of osteogenic differentiation of hMSCs

For detection of deposited mineralised matrix in the differentiated hMSCs, cells that were cultured in growth and osteogenic induction media were stained with Alizarin Red. The results of the staining directly indicated that osteogenic ability was enhanced in induced hMSCs as compared with controls on day 7, 14 and 21 in intermittent physioxia (2% O_2), physioxia (2% O_2 WS) and air oxygen (21% O_2) (Figure 3.13a).

RT-PCR results confirmed differentiation by showing that hMSC expression profiles matched osteogenic phenotype. RUNX2 was not upregulated but rather maintained and the expression over the time-period of differentiation was similar to its expression at day 0 in 2% O_2, 2% O_2 WS and 21% O_2. COL1A1 expression in 2% O_2 increased on day 7 above the undifferentiated time-point and subsequently decreased and increased on day 14 and 21, respectively. COL1A1 expression in 2% O_2 WS and 21% O_2 was maintained at the same level with the exception of day 21 in 21% O_2 where expression of COL1A1 dropped below the previous time-points. ALPL expression in 2% O_2 increased on day 7 post differentiation and decreased thereafter but was still higher than its expression in undifferentiated hMSCs, whereas ALPL expression in 2% O_2 WS increased continuously over the period of differentiation. ALPL in 21% O_2 expressed the same level at day 0 and day 7 of differentiation, whereas its level at day 14 dropped below the starting two points

and return increased at day 21. SPARC expression in 2% O_2 decreased after 7 days of differentiation as compared with undifferentiated hMSCs and increased after 14 and 21 days of differentiation, whereas its expression in 2% O_2 WS was high in day 0 and day 7 of differentiation and dropped below the starting two points and then increased at time-point day 21 of differentiation. In 21% O_2 SPARC expression was the same at day 0 and day 7 of differentiation, and slightly decreased on day 14 and 21 of differentiation. BGLAP, a marker of an osteoblast, was expressed on day 21 of differentiation in all oxygen conditions with a maximum expression in physioxia (2% O_2 WS) (Figure 3.13b).

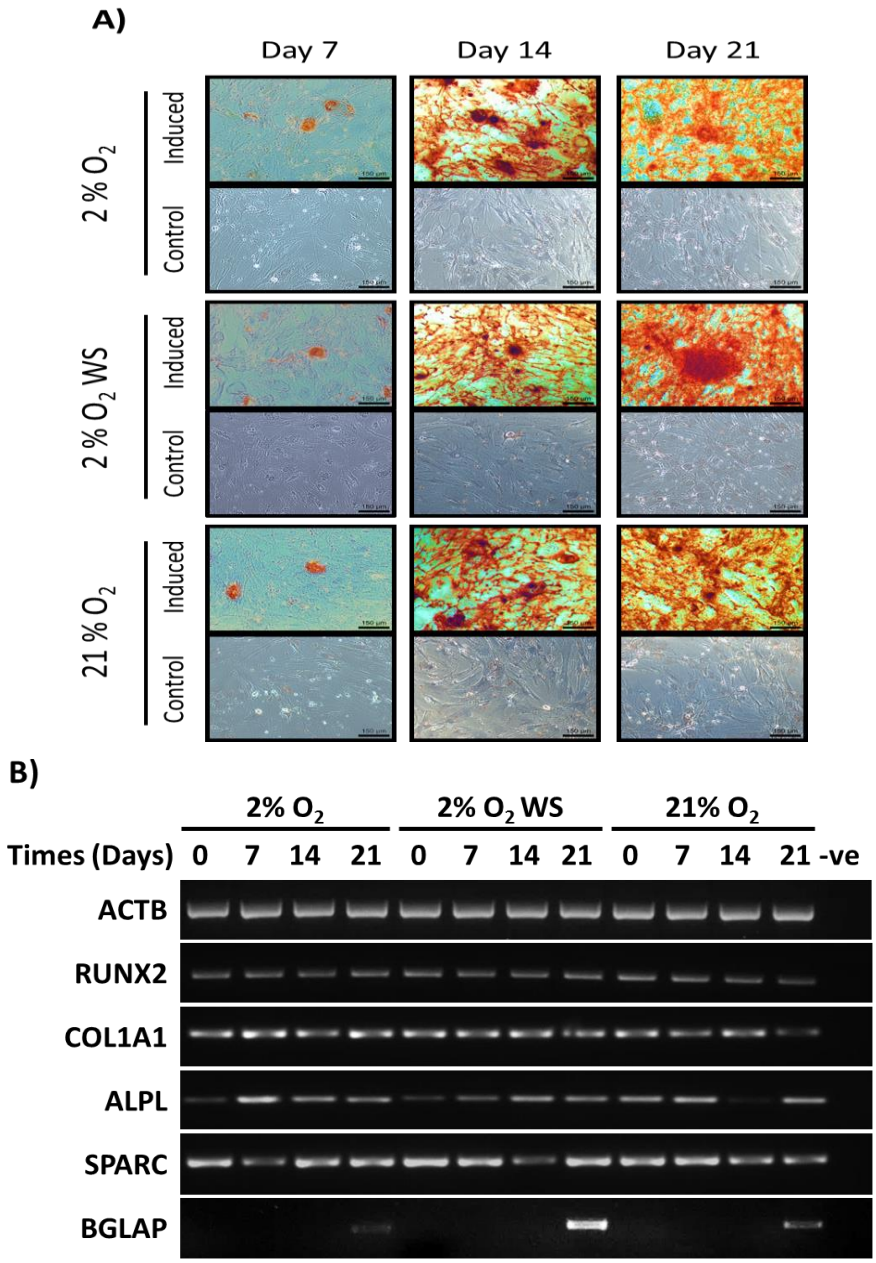

Figure 3. 13. Osteogenic differentiation in hMSCs cultured in 2% O_2, 2% O_2 WS and 21% O_2 after 7, 14 and 21 days. (A) Alizarin red staining for osteo-induced hMSCs (top rows) and undifferentiated hMSCs (bottom rows) for 2% O_2 (top panel), 2% O_2 WS (middle panel) and 21% O_2 (bottom panel). (B) RT-PCR of selected genes expression involved in osteogenic differentiation of hMSCs. ACTB confirmed the presence of amplifiable RNA in all samples.

3.5 Discussion:

The morphology of hESC and hiPSC colonies was expected, exhibiting characteristics of human pluripotent stem cells, for instance, high nucleus-to-cytoplasm ratio, flat, dense, colonies and well-defined colony borders.

Several studies have reported on the valuable effects of culturing hPSCs under physioxic condition, including improved morphology, increased pluripotency markers and reduction in chromosomal abnormalities (Ezashi et al., 2005; Forristal et al., 2010; Forsyth et al., 2006). Other studies showed that low oxygen tension (1-5%) allow cell proliferation via adapted mitochondrial respiration (Jiang et al., 1996; Guzy and Schumacker, 2006). In order to determine whether oxygen level affected proliferation and maintenance of undifferentiated state, the growth rate, MTT, and surface expression of SSEA-4, TRA-1-60 and SSEA-1 was measured.

Previous studies upon the effects of physioxic conditions on hPSCs were controversial in relation to proliferation and prevention of spontaneous differentiation. The MTT assay here revealed that SHEF1-hESCs during prolonged culture in physioxia stayed more or less the same in terms of proliferation curve when compared with those in air oxygen condition. This might be an indication of balance between proliferation and metabolic activity. The results are in agreement with previous papers in which hESCs were cultured at 21% O_2 or 5% O_2 tension (Rajala et al., 2011; Forristal et al., 2010). In contrast, SHEF2-hESCs and ZK2012L-hiPSCs in air oxygen showed that the cell growth curve remained more or less the same as MTT results, again this might be an indication of balance between proliferation and metabolic activity. A similar result was also observed for mouse embryonic stem cells cultured under both 2% and 21% O_2 (Fernandes et al., 2011). However, researchers observed that oxygen level as low as 1% leads to decreased

proliferation of hESCs, 3-5% O_2 showing no difference in the proliferation of hESCs when compared with 21% O_2 (Ezashi et al., 2005). The variability of these contrasting responses of hPS cell lines to oxygen may be due to the different cell line in addition to inadvertent re-oxygenation during the experiments.

The characterisation of hPSCs is important for the stem cell community. Flow cytometry technique and fluorescence image-based analysis are useful to assess the undifferentiated state of hPSCs by cell surface and nuclear marker expression. Cell surface stemness markers SSEA4, SSEA3, TRA-1-60 and TRA-180 are routinely used in many laboratories. Recent studies have reported that hESCs did not show differences in expression of SSEA-4, SSEA-1, TRA-1-60, TRA-1-81 when cultured in low oxygen tension (Chen et al., 2008; Forristal et al., 2010; Narva et al., 2013). Similarly, the study here was not able to observe any statistical difference for hPSCs between air oxygen (21% O_2) and 2% O_2 concentration in the expression of SSEA-4 and TRA-1-60, although there was a consistent trend for increasing SSEA-4 and TRA-1-60 indicators of the undifferentiated state. Consistently, expression of the differentiation markers SSEA-1 was low.

In vitro differentiation assays are useful and important for demonstrating the pluripotent nature of hPSCs by formation of progenitor cells from all three germ layers.

The pluripotent phenotype of both hESC lines and hiPSCs during the differentiation was confirmed by the detection of stemness markers, by RT-PCR (Figure 3.8) and by immunocytochemistry (Figure 3.9).

The observation of hPSCs differentiation was monitored in a timely manner by both RT-PCR and immunocytochemistry analyses to determine the differentiated state of hPSCs cultured in two oxygen conditions. Observation of the expression of pluripotent gene markers including POU5F1 and Nanog, could not distinguish between undifferentiated

hPSCs and their progeny. The explanation for this observation may be that some undifferentiated hPSCs still remain in cultures. hTERT disappeared after 10 days of differentiation in SHEF1-hESCs and SHEF2-hESCs in 21% O_2 and 2% O_2 respectively, while ZK2012L-hiPSCs progeny still appeared. A previous study reported that different hPSC lines expressed similar genes in the undifferentiated state; however, the expression of these genes might become variable when the cells started to differentiated (Toivonen et al., 2013). In contrast to pluripotent gene markers, the variability in expression of gene markers for all three germ layers (ectoderm, endoderm and mesoderm) was noted in hPSCs. The difference in culture conditions appears to affect the differentiation capacity of the hPSCs that has been detected by RT-PCR. The effect of physioxia on embryonic stem cell differentiation is controversial (Millman et al., 2009). The study here reveals that 21% O_2 condition improve endodermal lineage differentiation (AFP gene) which is in agreement with a previous study (Hakim et al., 2014) which reported that high oxygen was useful for efficient creation of insulin-producing cells. For mesodermal lineage differentiation, the results here show that physioxia improved expression of mesodermal gene (Brachyury) during the differentiation of ZK2012L-hiPSC, which is in agreement with previous studies (Niebruegge et al., 2009; Correia et al., 2014). In contrast, hESC lines showed that 21% O_2 improved expression of mesodermal gene during the time-course of differentiation. Ectodermal differentiation (OTX2 gene) showed progenitor cells expressed the OTX2 gene. However, it was noticed that all undifferentiated hPSC lines visualised the OTX2 gene with some variation while undifferentiated SHFE1-hESCs in 21% O_2 visualised Brachyury. The variation between hPSC lines differentiation was not correlated with the method used for hPSCs induction. Both hESC and hiPSC lines were successfully differentiated into three germ layers regardless of the oxygen conditions. However, previous studies reported the differences between the differentiation propensities

within hESC and hiPSC lines (Bock et al., 2011; Kim et al., 2011; Boulting et al., 2011; Osafune et al., 2008; Lappalainen et al., 2010) and between hESC and hiPSCs lines (Hu et al., 2010). Results here are in agreement with these views. Furthermore, the expression of pluripotent markers Oct-4, Nanog, SSEA-4 as well as ALP were monitored for hPSCs cultured in two oxygen conditions by analysing the cellular expression of pluripotent markers (Oct-4, Nanog, ALP and SSEA-4) over the time-course of differentiation. Expression of theses markers gradually decreased over the time-course of differentiation which indicates that across all time points, cells gradually lost their pluripotency.

This study investigated the effect of physioxia (intermittent and uninterrupted) on the isolation and metabolomics of human bone marrow-derived MSCs. Stem cells-based therapies require viable and high cell numbers for regenerative medicine. Evaluation of the cell number of the isolated MSCs, though not significant, showed that the number of isolated MSCs under continuous physioxia (2% O_2) was higher than those isolated under intermitted physioxia (2% O_2) and air oxygen (21% O_2). Indeed the number of MSCs was higher in intermitted physioxia (2% O_2) versus air oxygen (21% O_2). These findings are in agreement with a recent study (Kay et al., 2015). In contrast, a previous study concluded that reduced oxygen tension (2% or 5% O_2) decreased the number of bone marrow-isolated MSCs with a maximum at 20% O_2 (Pattappa et al., 2012). The interpretation of this contrast may be due to different culture medium and its composition as well the exact oxygen tension.

Human mesenchymal stem cells have gained wide interest in MSC-based tissue engineering of bone, due to their potential to differentiate into osteoblasts (Im, 2015). The results in figure 3.12 demonstrated that the cells confirmed the tri-lineage differentiation potential which is characteristic of mesenchymal stem cells.

Along with the positive results for differentiation into adipogenic, osteogenic and chondrogenic lineages, the surface protein profile was assessed according to the criteria established by the International Society for Cellular Therapy (ISCT) (Dominici et al., 2006). hBM-MSCs were positive for CD105, CD 73 and CD 90 and negative for CD 45, CD34, CD14, CD19 and HLA-DR and no significant difference was detected between the three experimental oxygen conditions. Also under both conditions of intermittent physioxia and physioxia, the positive markers CD105, CD73 and CD90 were higher than 95%, whereas under normoxic condition only CD73 was higher than 95% but CD105 and CD 90 were slightly lower than 95%. This lower CD105 and CD90 percentage of cells in normoxia may be related to prolonged enzymatic time exposure during cell detachment (Brown et al., 2007; Temtem et al., 2009). On the other hand, CD45 and CD34 markers showed lower than 2%, while CD14, CD19 and HLA-DR showed higher than 2% in three environmental conditions with the exception of CD19 in physioxia which showed lower than 2%. This may be due to impurity of MSCs with monocytes, which express CD14 (Hubacek and Poledne, 1999). The increase of CD 19 may be due to adherence of B cells to MSCs in culture (Dominici et al., 2006). Although the surface expression of HLA-DR is negative on MSCs, they have been revealed to contain an intracellular HLA-DR that can be detected at the cell surface after stimuli by IFN-γ (Le Blanc et al., 2003). Other studies reported that HLA-DR surface marker was observed more on cells isolated from whole bone marrow when compared with those isolated from separated mononuclear cells (Tarte et al., 2010). Indeed, Immunogenicity of MSCs was poor *in vitro* regardless of the expression level of HLA-DR, and thus the expression of HLA-DR does not appear to be a critical criterion for MSCs (Tarte et al., 2010).

In terms of mineralisation, a higher amount of mineralised matrix was deposited at day 14 and 21 compared with day 7 of the time-course of the osteogenic differentiation. The cells cultured in MSCs growth media revealed no mineralisation nodule formation.

On the other hand, RUNX2 is the earliest marker of osteogenic differentiation and is described to be important for osteogenic lineage commitment of mesenchymal progenitors (Wang et al., 2015); the results here show expression before and during the osteogenic differentiation. A previous study reported that no major changes of RUNX2 level occurred during the time-course of human osteoblast differentiation (Shui et al., 2003). SPARC, also known as an osteogenic marker, whose expression appears from pre-osteoblastic to the osteoplastic phase, has an essential role in bone formation (Delany et al., 2000). SPARC shows expression during osteogenic differentiation, although undifferentiated MSCs also seem to express it. The expression of SPARC in undifferentiated MSCs is reported by a previous study (Silva et al., 2003). In the studies reported here RUNX2 is also expressed in undifferentiated MSCs. A recent study described the expression of RUNX2 in WRO and TCP-1 cells and showed that its expression is influenced by fetal bovine serum (FBS) (Niu et al., 2012). Hence, it is possible that the RUNX2 gene expression is directly related to fetal bovine serum.

ALP and COL1A1 are known as early markers of osteogenic differentiation and BGLAP is described to be a later-stage marker (Jaiswal et al., 1997). The osteo-induction of MSCs in culture caused a constant high level of ALP expression from initiation. The increased expression of ALP is an indicator for osteogenic differentiation because ALP is responsible for mineralisation of extracellular matrix (Marom et al., 2005). Collagen I is important for mineralisation of bone matrix (Khosla et al., 2008) and its expression at a high level would be observed during the differentiation. Although there is no difference between day 0 and the whole process of differentiation, COL1A1 exhibits constant high expression levels

throughout. This result is also verified by previous study that showed COL1A1 was expressed before and during osteogenic differentiation (Friedman et al., 2006), indicating that MSCs are in the biosynthesis and maintenance of extracellular matrix.

The BGLAP gene was described as a late osteogenic differentiation marker appearing with matrix mineralisation (Kulterer et al., 2007) and was expressed at late stage (day 21) of osteogenic differentiation of MSCs.

Chapter 4-Analysis of full scan spectra of VOCs in the headspace of cells

4.1 Introduction

In the context of regenerative medicine there is an emergent interest in the application of metabolomics to better understand the biology of hPSCs and their progeny, with respect to proteomics and transcriptomics. Incorporation of physiological normoxia into this process may help better elucidate a genuine vs. artefact-driven biology in the hPSC culture system.

There is currently a limited knowledge of the extracellular metabolites released by human stem cells which have potential as biomarkers of stem cell activity. Metabolomics studies have been employed to investigate the culture media of bacteria (Villas-Boas et al., 2006) and yeast (Allen et al., 2003). Mammalian cell-based studies have included metabolic profiling of human hepatoma cell culture media in relation to cell growth (Miccheli et al., 2006), and the identification of hESC-secreted molecules with the potential to serve as biomarkers of pharmacological efficacy (Cezar et al., 2007). NMR (Miccheli et al., 2006), GC-quadrupole MS (Villas-Boas et al., 2006) and LC-TOF MS (Allen et al., 2003; Cezar et al., 2007) instruments have been used in previous metabolomics studies. For this study, SIFT-MS was selected for real time and on-line volatile organic compounds analysis.

4.2 Aims:

1. To compare the metabolic profile of hPSCs cultured in two different oxygen conditions (21% O_2 and 2% O_2).
2. To compare the metabolic profile of hPSCs and their progenitor cells in two oxygen conditions (21% O_2 and 2% O_2).

3. To compare the metabolic profile of bone marrow-derived mesenchymal stem cells throughout the isolation process in three different oxygen conditions (21% O_2, 2% O_2 and 2% O_2 WS).
4. To compare the metabolic profile of MSCs during the time-course of osteogenic differentiation in three different oxygen conditions (21% O_2, 2% O_2 and 2% O_2 WS).

4.3 Materials and methods

In order to study volatile organic compounds headspace analysis experiments were performed using full scan (FS) mode of SIFT-MS (see Section 2.3.3). It is worth mentioning that about $8x10^6$ hPSCs and their progeny were incubated for 24 hours with E8M and KO-DMEM respectively (more details in chapter 2).

hMSCs isolation, characterisation and osteo-induction were carried out in three oxygen conditions (21% O_2, 2% O_2 and 2% O_2 WS) (Full methodology in detailed in chapter 2). In order to study headspace trace gases of human bone marrow cells (BMCs) and MSCs (see section 2.3.3) it is important to note cell numbers. The numbers of BMCs collected at day 0 were around $7.5x10^6$, while for experimental reasons (using syringe and needle) cell numbers are unknown at days 7 and 14. One-half of the media was aspirated by syringe and needle from the flasks and dispensed straight into sealed glass bottles at day 7 and the second-half at day 14. For suspended hMSCs, cells were counted and $3x10^5$ transferred into the glass bottles.

The VOCs from plastic tissue culture plate containing media (appendix 1) were examined and the spectra of incubated media without cells were subtracted (normalised) from the spectra of cells exposed media.

4.4 Results

4.4.1 Analysis of SIFT-MS mass spectra derived from the headspace of hPSCs cultures

SIFT-MS has been used to successfully differentiate between a range of cell types as described elsewhere (Smith et al., 2003; Sule-Suso et al., 2009). However there are no studies described thus far which have sought to use SIFT-MS to identify metabolomics profiles in hPSCs in either air oxygen or physioxia conditions. Cell-free control media samples and media which had been incubated for 24 hours on adherent hPSC cultures in either air oxygen or physioxia conditions (See Section 2.3.3 for methodology) were therefore compared. PCA scores from the collected SIFT-MS hPSC datasets showed that all samples lay within the 95% confidence region (Hotelling T^2 ellipse) (Figure 4.1). SHEF1 score plots showed that control media and cell-exposed media in both 21% O_2 and 2% O_2 are separated. Control media samples clustered tightly whereas cell-exposed media in both 21% O_2 and 2% O_2 did not display well-defined clusters (Figure 4. 1a). SHEF2 score plots again indicated an independent and distinct, tight, clustering of cell-free media but in contrast to above cell exposed media displayed substantial overlap in clustering between both 21% O_2 and 2% O_2 (Figure 4. 1b). Finally, and similar to SHEF1, ZK2012L score plots indicated that control cell-free media and cell-exposed medias all clustered in a distinct manner (Figure 4. 1c). Control media samples clustered together tightly while 21% O_2 and 2% O_2 cell exposed media displayed a loose, distinct, clustering pattern.

Figure 4. 1. PCA scores plot of hPSCs cultured in air oxygen (21% O_2) and physioxia (2% O_2). a) SHEF1. (t[1]= 26.3%, t[2]= 17.1%). b) SHEF2. (t[1]= 61.6%, t[2]= 29.2%). c) ZK2012L. (t[1]= 41%, t[2]= 20.3%). X and Y axes represent the second and first principal components, respectively. Ellipses represent the 95% confidence interval. Circles represent control media group (n=5), squares represent incubated media with cells in 21% O_2 (n=5), triangles represent incubated media with cells in 2% O_2 (n=5).

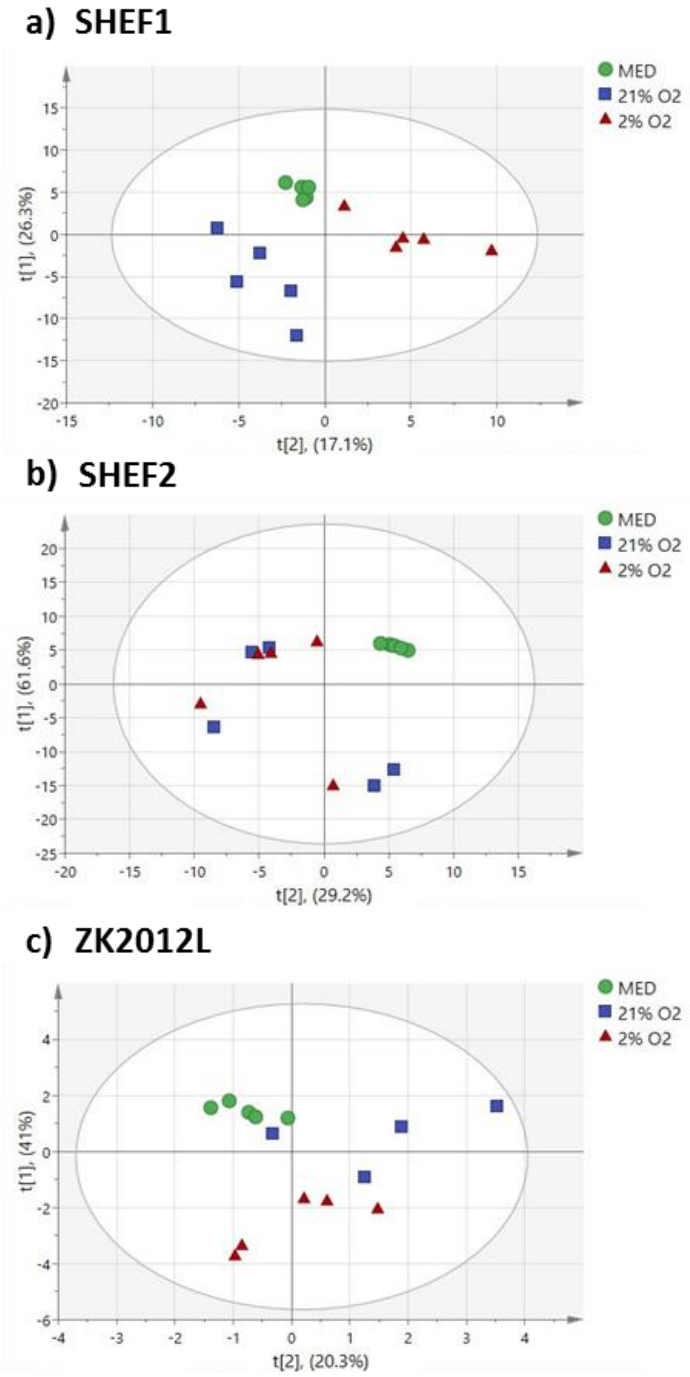

In the OPLS-DA models, all data lay inside the 95% confidence region (Hotelling T2 ellipse) (Figure 4.2) SHEF1 displayed tight sample clustering within groups and clear separation across groups (Figure 4.2a). SHEF2 score plots showed distinct clustering for all groups. Clustering was tight for control cell-free media and 2% O_2 cell-exposed media but in contrast was loose for 21% O_2 cell-exposed samples (Figure 4.2b). ZK2012L displayed a similar clustering to SHEF1 with all groups occupying distinct regions of clustering though not as tightly as seen with SHEF1 samples (Figure 4.2c).

Table 4. 1. Results of the cross validation and CV-ANOVA for OPLS-DA models of hPSCs media.

OPLS-DA model	R2Y (cum)	Q2 (cum)	P-value (CV-ANOVA)
SHIF1	0.998	0.917	0.007
SHEF2	0.876	0.76	0.004
ZK2012L	0.946	0.8	0.04

Figure 4. 2. Scores plot from the OPLS-DA discrimination of SIFT-MS spectra of hPSCs cultured in 21% and 2% O_2. a) SHEF1. b) SHEF2. c) ZK2012L. X-axis, t[2] and Y-axis, t[1], indicate the second and first principal components, respectively. Ellipses represent the 95% confidence intervals. Circles represent control media group (n=5), squares represent incubated media with cells in 21% O_2 (n=5), triangles represent incubated media with cells in 2% O_2 (n=5).

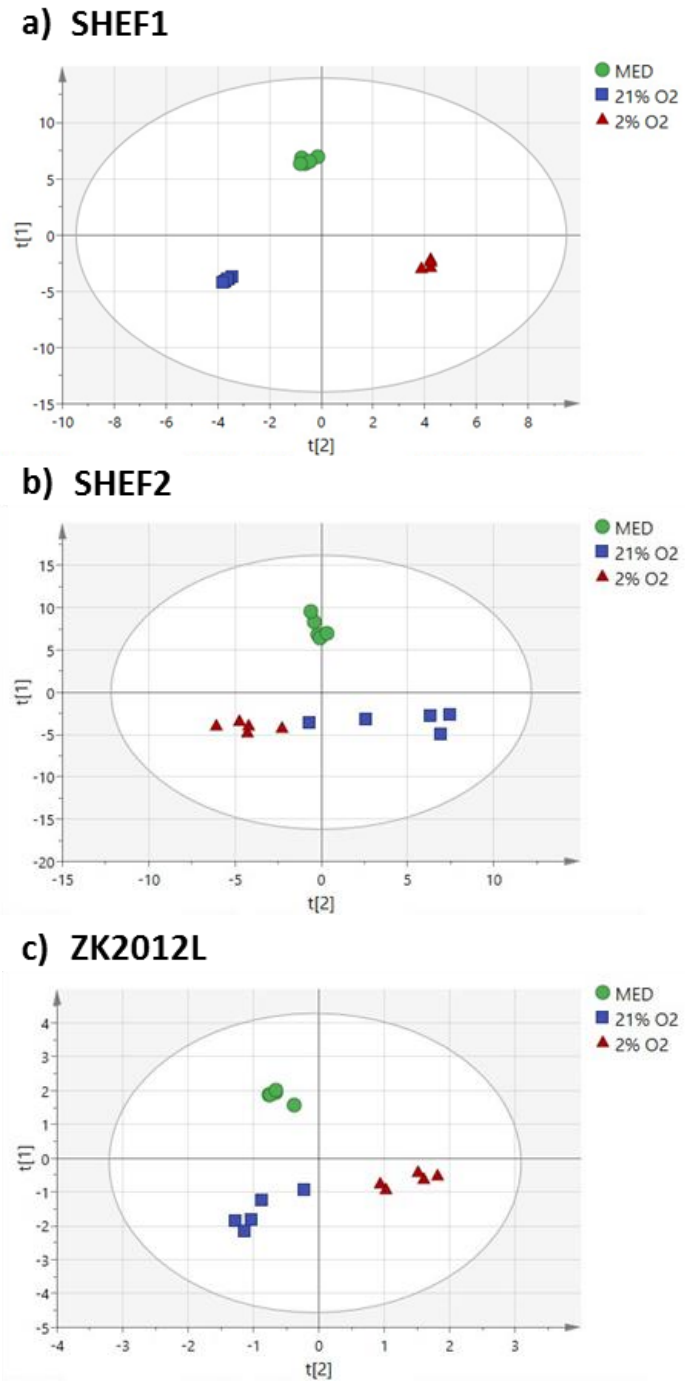

The variables relevant for discrimination in OPLS-DA models were identified from their variable importance in the projection (VIP) values for each of the hPSCs lines explored. Large VIP values (≥1) are the most relevant for predicted variables.

The number of VIP variables (≥1) shared and unique across the hPSC lines examined are indicated (Figure 4.3, Table 4.2). SHEF1, SHEF2 and ZK2012L shared by 2 unique variables. Variables shared across two lines were; SHEF1 and SHEF2 shared 11 unique variables, ZK2012L shared 4 unique variables with both SHEF1 andSHEF2, whereas SHEF1, SHEF2 and ZK2012L had 12, 36 and 5 unique variables, respectively.

Figure 4. 3. Venn diagram showing statistically-selected discriminating variables (ions) in hPSCs. Overlap between SHEF1, SHEF2, and ZK2012L OPLS-DA models are indicated. As indicated in the diagram, there are unique and shared (ions) variables from the three hPSCs models. Blue circle represent the number of variables (m/z) in SHEF1, red circle represent the number of variables (m/z) in SHEF2 and green circle represent the number of variables (m/z) in ZK2012L.

Table 4. 2. Significant variables (ions) mass to charge ratio (m/z) accountable for class discrimination of hPSCs by OPLS-DA (with VIP score ≥1).

hPSCs	No. of m/z ions	Variable (ions) m/z
SHEF1, SHEF2, ZK2012L	2	m/z 54, m/z 18
SHEF1, SHEF2	11	m/z 45, m/z 125, m/z 113, m/z 34, m/z 32, m/z 90, m/z 97, m/z 30, m/z 58, m/z 115, m/z 49
SHEF1, ZK2012L	4	m/z 101, m/z 81, m/z 69, m/z 63
SHEF2, ZK20212L	4	m/z 111, m/z 43, m/z 84, m/z 33
SHEF1	12	m/z 44, m/z 123, m/z 176, m/z 72, m/z 60, m/z 128, m/z 161, m/z 119, m/z 71, m/z 52, m/z 141, m/z 88
SHEF2	36	m/z 95, m/z 134, m/z 41, m/z 86, m/z 92, m/z 142, m/z 155, m/z 110, m/z 136, m/z 169, m/z 145, m/z 129, m/z 147, m/z 132, m/z 124, m/z 79, m/z 94, m/z 61, m/z 40, m/z 106, m/z 109, m/z 68, m/z 146, m/z 78, m/z 70, m/z 135, m/z 117, m/z 107, m/z 153, m/z 31, m/z 139, m/z 103, m/z 50, m/z 67, m/z 126, m/z 157
ZK2012L	6	m/z 47, m/z 83, m/z 51, m/z 65, m/z 99, m/z 82

Metabolite profiling associated with hPSCs culture in physioxia and air oxygen was derived from VIP plots where metabolites (ions) that fulfilled the criteria (VIP≥1) were subjected to univariate analysis (t-test). Significant variables (P<0.05) which presented increases in either 21% O_2 and 2% O_2 are illustrated in Figure 4.4 and listed in Table 4.3.

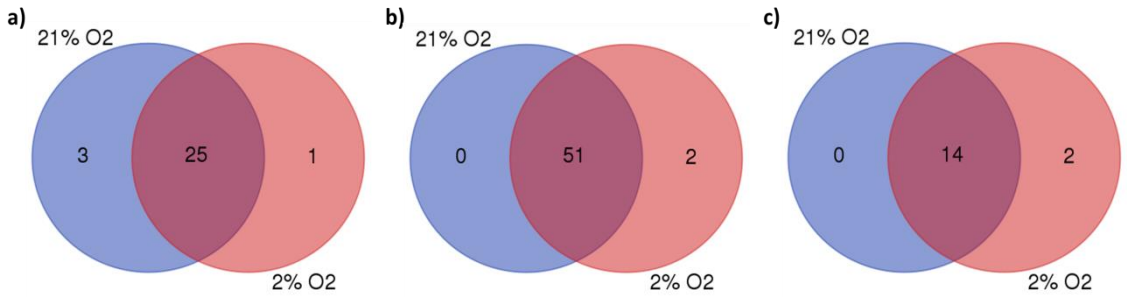

Figure 4. 4. Increased variables in hPSC-conditioned media. Venn diagram showing the number of variables (ions) that increased significantly (P<0.05) in 21% O_2 and 2% O_2 conditions within the analysed variables. a) SHEF1. b) SHEF2. c) ZK2012L. Blue circle represent the number of variables (m/z) in21% O_2 condition, red circle represent the number of variables (m/z) in 2% O_2 condition.

Table 4. 3. Expected compounds at each protonated mass (m/z) where significant differences in the headspace gases of media of hPSCs were noted between 21% O_2 and 2% O_2 conditions over the m/z ranges 10 to 180.

hPSCs	Conditions	Statistics	m/z	Proposed compounds
SHEF1	21% O_2	Significantly increased	m/z 18	(Ammonia, 2-methylbutylamine (50%), 2-methyl-2-butylamine (90%), 3-methylbutylamine (5%), 3-methyl-2-butylamine (65%), 2-pentylamine (60%), 3-pentylamine (70%))
			m/z 54	(2-propenenitrile, ammonia with hydrates)
			m/a 123	(4-ethylphenol, 1-phenylethanol, 2-phenylethanol)
	2% O_2	Significantly increased	m/z 72	(2-methyl-2-propen-1-amine, N-ethyl-azitidine, Pyrrolidine, N-thylidene-ethanamine, ethyl azide, acrylamide, methoxyacetonitrile, 2-azetidinone)
SHEF2	21% O_2	Significantly increased	NI	
	2% O_2	Significantly increased	m/z 18	(Ammonia, 2-methylbutylamine (50%), 2-methyl-2-butylamine (90%), 3-methylbutylamine (5%), 3-methyl-2-butylamine (65%), 2-pentylamine (60%), 3-pentylamine (70%))
			m/z 94	(aniline)
ZK2012L	21% O_2	Significantly increased	NI	
	2% O_2	Significantly increased	m/z 63	(Carbon dioxide, ethanediol (35%), ethanethiol, dimethyl sulphide)
			m/z 81	(1,1-dichloroethane (50%), 1,2-dichloroethane (35%), cis-3-hexenal (65%), camphene (14%), 2-carene (18%), 3-carene (24%), s-limonene (30%), myrcene (30%), ocimene (25%), α-pinene (39%), β-pinene (40%), α-terpinene (10%), Y-terpinene (16%))

NI: no ions (m/z) increased significantly were found.

4.4.2. Analysis of SIFT-MS mass spectra derived from the headspace of hPSCs and their progenitors cultures

PCA scores were produced for collected datasets of hPSCs in air oxygen (21% O_2) and physioxia (2% O_2) (Figure 4.5). The score plot of SHEF1 in 21% O_2 indicated considerable overlap between control undifferentiation and differentiation media samples (Figure 4.5a). Cell exposed media revealed relatively distinct and tight clustering for media from differentiating cells at Days 5, 10, and 20 while undifferentiated Day 0 cell exposed media did not fall into well-defined clusters but remained distinct. Control media for SHEF1 in 2% O_2 again showed a considerable evidence of overlap and associated clustering (Figure 4.5b). Similar to 21% O_2 undifferentiated cell exposed media clustered distinct to that of the differentiated cell exposed media which clustered together tightly with a minimum of overlap. SHEF2 score plots in 21% O_2 indicated that control media samples were clearly separated from differentiated cell media and from all cell exposed media (Figure 4.5c). Undifferentiated 21% O_2 SHEF2 exposed media displayed a loose and disperse clustering profile while all differentiated cell media (Day 5, 10, and 20) clustered tightly together but remained distinct with little or no overlap. The score plot of SHEF2 in 2% O_2 indicated that control media samples clustered together with little or no overlap and were distinct from cell exposed samples (Figure 4.5d). Clear separation between undifferentiated cells and differentiated cells media was again noted where the differentiated cell samples clustered tightly together with no overlap noted. Finally, the score plots of ZK2012L in 21% O_2 indicated a previously noted overlap between control undifferentiation and differentiation media which was distinct to all cell exposed media samples (Figure 4.5e). Unlike the previous cell lines; SHEF1 and SHEF2, ZK2012L cell exposed media samples did not cluster together but were instead loosely dispersed across the plot. This pattern was repeated for ZK2012L samples cultured in physioxia (Figure 4.5f).

Figure 4. 5. PCA score plots of hPSCs exposed culture media headspace. a) SHEF1 in 21% O_2 (t[1]=33.9%, t[2]=14.3%). b) SHEF1 in 2% O_2 (t[1]=33.3%, t[2]=14.5%). c) SHEF2 in 21% O_2 (t[1]=24.6%, t[2]=14.7%). d) SHEF2 in 2% O_2 (t[1]=21.5%, t[2]=16.1%). e) ZK2012L in 21% O_2 (t[1]=9.4%, t[2]=47.4%). f) ZK2012L in 2% O_2 (t[1]=11.7%, t[2]=45.8%). For each score plot X and Y axes represent the second and first principal components, respectively. Ellipses represent the 95% confidence intervals for each PCA score plot. The control undifferentiated media (n=5), differentiation media (n=9) are shown as circles and squares, respectively whereas undifferentiated cells media (day 0), differentiated cell media (day 5), differentiated cell media (day 10) and differentiated cell media (day 20) are shown as triangles inverted triangles, diamonds and pentagons, respectively.

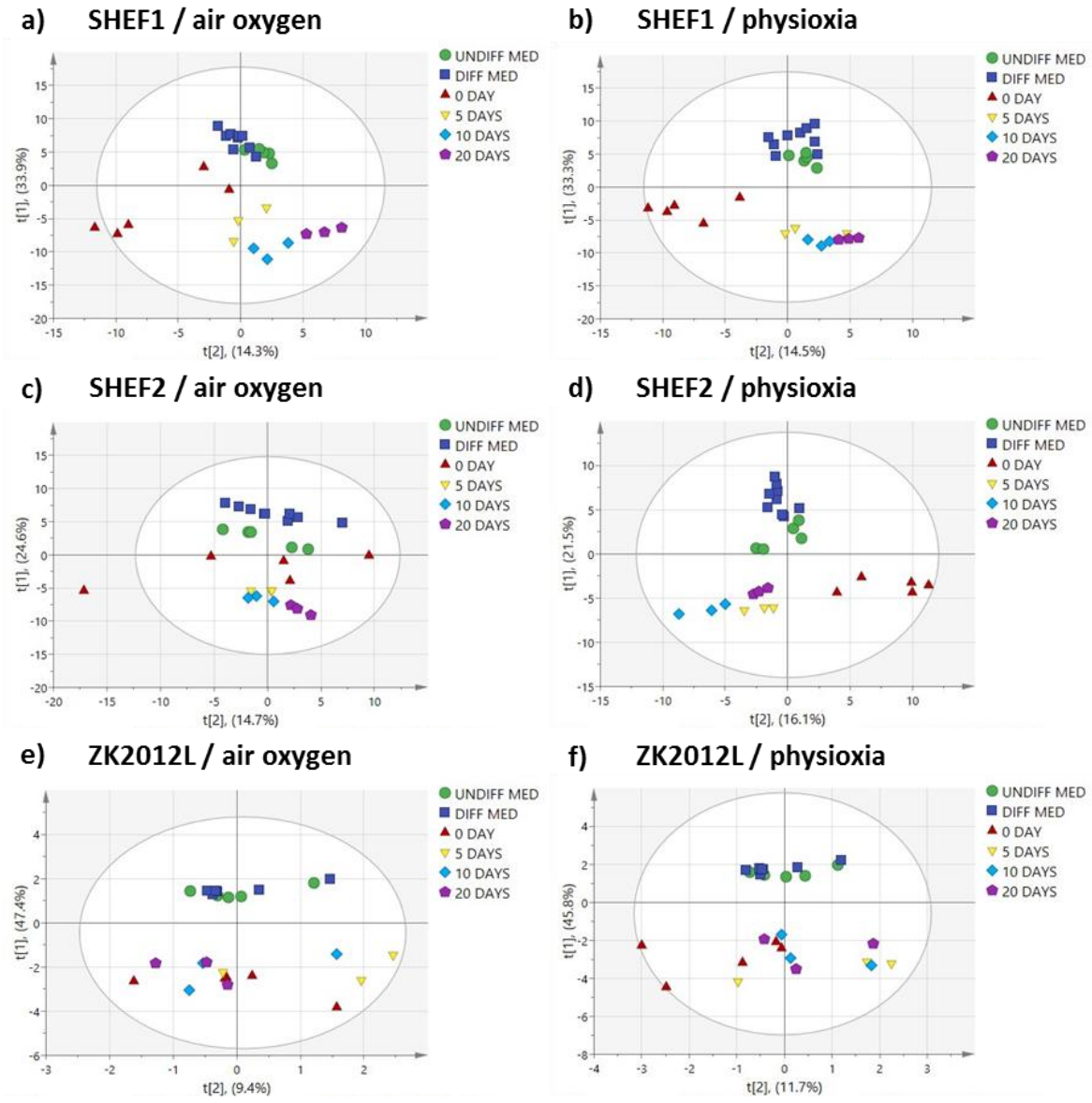

In the OPLS-DA models, all samples lay within the 95% confidence region (Hotelling T2 ellipse) (Figure 4.6). SHEF1 score plots for both in 21% O_2 and 2% O_2 indicated that undifferentiated and differentiated control media were distinct from undifferentiated and differentiated cell exposed media and that they overlapped with each other.(Figure 4.6a, b). Similarly, in both settings undifferentiated cell exposed media clustered distinctly from differentiated cell exposed media. In 21% O_2 differentiated cell exposed media clustered distinctly while in 2% O_2 tight clustering with some overlap was noted. SHEF2 21% O_2 and 2% O_2 OPLS-DA score plots indicated clear separation between all groups, distinct clustering and no overlap (Figure 4.6c, d). The score plots of ZK2012L in 21% O_2 and 2% O_2 again showed that undifferentiated and differentiated control media were clearly separated, and overlapping with each other, from undifferentiated and differentiated cell exposed media (Figure 4.6e, f). Undifferentiated cell exposed media displayed distinct clustering in both conditions and while this was also true of differentiated cell exposed media in air oxygen some overlap was noted in physioxia.

Table 4. 4. Results of the cross validation and CV-ANOVA for OPLS-DA models of hPSCs media.

OPLS-DA model	R2Y (cum)	Q2 (cum)	P-value (CV-ANOVA)
SHEF1/ air oxygen	0.778	0.612	0.001
SHEF1/ physioxia	0.774	0.584	0.001
SHEF1/ air oxygen	0.827	0.0.605	0.03
SHEF1/ physioxia	0.836	0.677	0.0005
ZK2012L/ air oxygen	0.803	0.603	0.008
ZK2012L/ physioxia	0.795	0.647	0.002

Figure 4. 6. Scores plot from the OPLS-DA discrimination of SIFT-MS spectra of hPSCs cultured in 21% and 2% O_2. a) SHEF1 in 21% O_2 score plot. b) SHEF1 in 2% O_2 score plot. c) SHEF2 in 21% O_2 score plot. d) SHEF2 in 2% O_2 score plot. e) ZK2012L in 21% O_2 score plot. f) ZK2012L in 2% O_2 score plot. For each score plot X-axis, t[2] and Y-axis, t[1], represent the second and first principal components, respectively. Ellipses represent the 95% confidence intervals for each OPLS-DA score plot. The control undifferentiated media (n=5), differentiation media (n=9) are shown as circles and squares, respectively, whereas undifferentiated cells media (day 0), differentiated cells media (day 5), differentiated cells media (day 10) and differentiated cells media (day 20) are shown as triangles, inverted triangles, diamonds and pentagon, respectively.

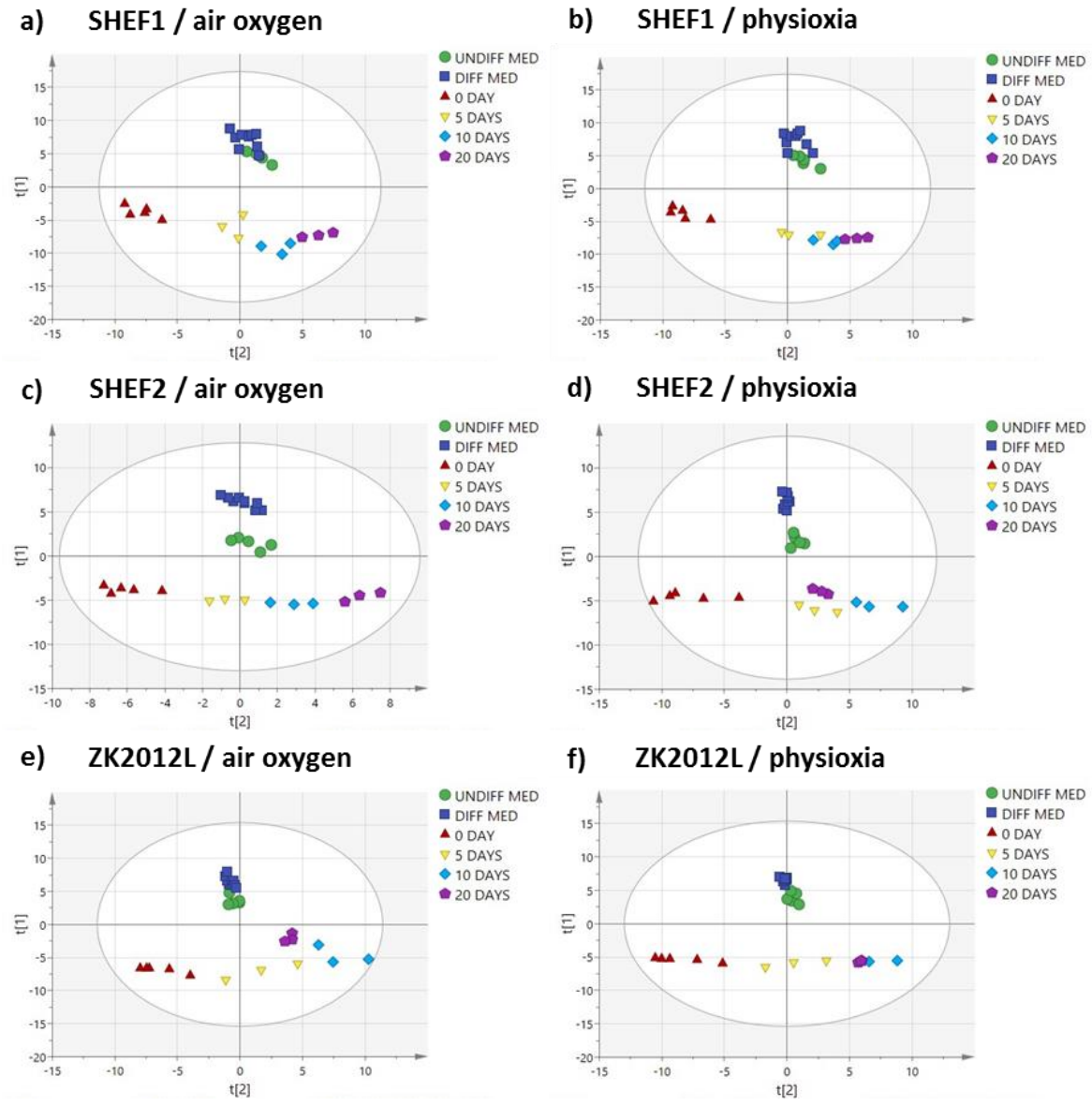

The number of shared and unique VIP≥1 variables for each hPSC and between each oxygen condition across the entire differentiation course were determined (Figure 4.7 and Table 4.5).

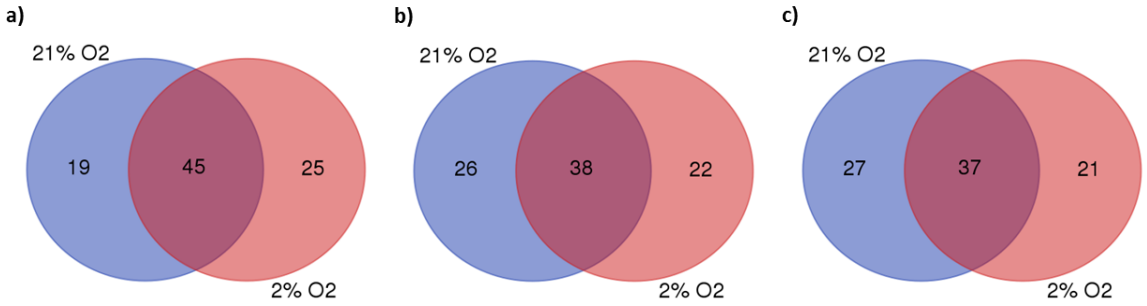

Figure 4. 7. Discriminating variables (ions) from OPLS-DA models for hPSCs cultured in 21% O_2 and 2% O_2. a) SHEF1. b) SHEF2. c) ZK2012L. As indicated in the diagrams, there are unique and shared variables (ions) for each hPSCs cultured in both oxygen conditions. Blue circle represent the number of variables (m/z) in 21% O_2 and red circle represent the number of variables (m/z) in 2% O_2

Table 4. 5. The significant variables (ions) mass to charge ratio (m/z) accountable for class discrimination of hPSCs cultured in 21% O_2 and 2% O_2 by OPLS-DA (with VIP score ≥1).

PSCs	Conditions	m/z No.	Variables
SHEF1	21% O_2, 2% O_2	45	m/z 167, m/z 95, m/z 122, m/z 44, m/z 112, m/z 123, m/z 142, m/z 162, m/z 155, m/z 45, m/z 105, m/z 76, m/z 169, m/z 72, m/z 29, m/z 124, m/z 113, m/z 94, m/z 114, m/z 40, m/z 104, m/z 128, m/z 106, m/z 161, m/z 143, m/z 53, m/z 68, m/z 131, m/z 78, m/z 119, m/z 107, m/z 43, m/z 118, m/z 54, m/z 120, m/z 31, m/z 63, m/z 103, m/z 90, m/z 141, m/z 30, m/z 42, m/z 18, m/z 115, m/z 163
	21% O_2	19	m/z 86, m/z 77, m/z 176, m/z 133, m/z 145, m/z 138, m/z 60, m/z 61, m/z 93, m/z 71, m/z 52, m/z 28, m/z 177, m/z 80, m/z 139, m/z 67, m/z 148, m/z 49, m/z 82
	2% O_2	25	m/z 164, m/z 100, m/z 111, m/z 41, m/z 171, m/z 101, m/z 87, m/z 110, m/z 125, m/z 83, m/z 137, m/z 32, m/z 81, m/z 70, m/z 35, m/z 99, m/z 98, m/z 151, m/z 85, m/z 48, m/z 50, m/z 97, m/z 165, m/z 116, m/z 88
SHEF2	21% O_2, 2% O_2	38	m/z 159, m/z 167, m/z 111, m/z 87, m/z 105, m/z 77, m/z 136, m/z 169, m/z 145, m/z 129, m/z 108, m/z 113, m/z 79, m/z 94, m/z 114, m/z 61, m/z 109, m/z 34, m/z 143, m/z 81, m/z 68, m/z 135, m/z 35, m/z 71, m/z 107, m/z 43, m/z 31, m/z 177, m/z 85, m/z 48, m/z 139, m/z 59, m/z 62, m/z 97, m/z 141, m/z 67, m/z 82, m/z 126
	21% O_2	26	m/z 123, m/z 86, m/z 142, m/z 162, m/z 125, m/z 124, m/z 173, m/z 60, m/z 40, m/z 121, m/z 106, m/z 149, m/z 53, m/z 146, m/z 69, m/z 119, m/z 52, m/z 154, m/z 120, m/z 84, m/z 80, m/z 90, m/z 50, m/z 115, m/z 49, m/z 157
	2% O_2	22	m/z 164, m/z 100, m/z 64, m/z 101, m/z 110, m/z 76, m/z 175, m/z 137, m/z 131, m/z 28, m/z 54, m/z 63, m/z 96, m/z 165, m/z 30, m/z 58, m/z 148, m/z 116, m/z 18, m/z 163, m/z 88, m/z 117
ZK2012L	21% O_2, 2% O_2	37	m/z 95, m/z 47, m/z 123, m/z 111, m/z 64, m/z 46, m/z 142, m/z 45, m/z 77, m/z 129, m/z 83, m/z 113, m/z 102, m/z 40, m/z 89, m/z 109, m/z 34, m/z 137, m/z 143, m/z 81, m/z 32, m/z 78, m/z 135, m/z 178, m/z 117, m/z 52, m/z 43, m/z 153, m/z 65, m/z 99, m/z 84, m/z 63, m/z 85, m/z 59, m/z 96, m/z 141, m/z 18
	21% O_2	27	m/z 122, m/z 112, m/z 100, m/z 86, m/z 168, m/z 150 m/z 155, m/z 110, m/z 108, m/z 132, m/z 173, m/z 94, m/z 106, m/z 93, m/z 68, m/z 119, m/z 70, m/z 51, m/z 107, m/z 80, m/z 33, m/z 48, m/z 139, m/z 103, m/z 97, m/z 30, m/z 49
	2% O_2	21	m/z 167, m/z 134, m/z 170, m/z 101, m/z 171, m/z 87, m/z 145, m/z 138, m/z 127, m/z 128, m/z 130, m/z 146, m/z 69, m/z 120, m/z 158, m/z 151, m/z 177, m/z 50, m/z 67, m/z 163, m/z 82

The number of VIP≥1 variables that were both shared and unique among hPSCs across each oxygen condition (Figure 4.8, Table 4.6) were then identified.

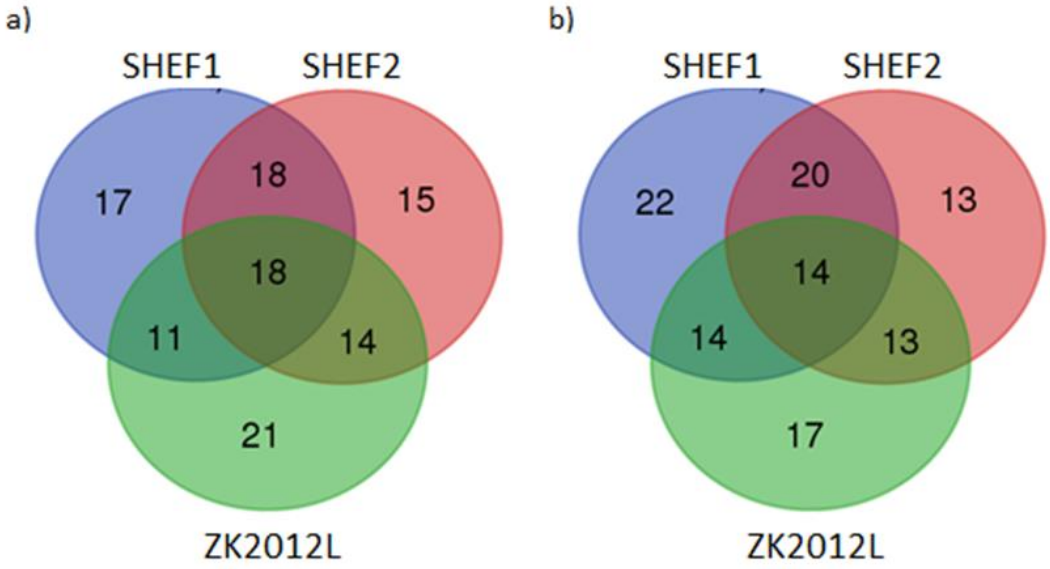

Figure 4. 8. hPSC line specific statistically-selected discriminating variables (ions) from OPLS-DA models. a) 21% O_2. b) 2% O_2 condition. As represented in the diagrams, there are shared and unique variables (ions) among hPSCs cultured in air oxygen (21% O_2) and physioxia (2% O_2). Blue circle represent the number of variables (m/z) in SHEF1, red circle represent the number of variables (m/z) in SHEF2 and green circle represent the number of variables (m/z) in ZK2012L

Table 4. 6. The significant variables (ions) mass to charge ratio (m/z) accountable for class discrimination of hPSCs cultured in 21% O_2 and 2% O_2 by OPLS-DA (with VIP score ≥1).

Condition	hPSCs	m/z No.	Variables
21% O_2	SHEF1, SHEF2, ZK2012L	18	m/z 123, m/z 86, m/z 142, m/z 77, m/z 113, m/z 94, m/z 40, m/z 106, m/z 143, m/z 68, m/z 119, m/z 52, m/z 107, m/z 43, m/z 80, m/z 139, m/z 141, m/z 49
	SHEF1, SHEF2	18	m/z 167, m/z 162, m/z 105, m/z 169, m/z 145, m/z 124, m/z 60, m/z 114, m/z 61, m/z 53, m/z 71, m/z 120, m/z 31, m/z 177, m/z 90, m/z 67, m/z 115, m/z 82
	SHEF1,	11	m/z 95, m/z 122, m/z 112, m/z 155, m/z 45, m/z 93, m/z 78, m/z 63, m/z 103, m/z 30, m/z 18
	SHEF2), ZK2012L	14	m/z 111, m/z 129, m/z 108, m/z 173, m/z 109, m/z 34, m/z 81, m/z 135, m/z 117, m/z 84, m/z 48, m/z 85, m/z 59, m/z 97
	SHEF1	17	m/z 44, m/z 176, m/z 76, m/z 133, m/z 72, m/z 29, m/z 138, m/z 104, m/z 128, m/z 161, m/z 131, m/z 28, m/z 118, m/z 54, m/z 42, m/z 148, m/z 163
	SHEF2	15	m/z 159, m/z 87, m/z 125, m/z 136, m/z 79, m/z 121, m/z 149, m/z 146, m/z 69, m/z 35, m/z 154, m/z 62, m/z 50, m/z 126, m/z 157
	ZK2012L	21	m/z 47, m/z 100, m/z 168, m/z 64, m/z 46, m/z 150, m/z 110, m/z 132, m/z 83, m/z 102, m/z 89, m/z 137, m/z 32, m/z 70, m/z 178, m/z 51, m/z 153, m/z 65, m/z 99, m/z 33, m/z 96
2% O_2	SHEF1, SHEF2, ZK2012L	14	m/z 167, m/z 111, m/z 101, m/z 87, m/z 113, m/z 137, m/z 143, m/z 81, m/z 43, m/z 63, m/z 85, m/z 141, m/z 18, m/z 163
	SHEF1, SHEF2	20	m/z 164, m/z 100, m/z 105, m/z 110, m/z 76, m/z 169, m/z 94, m/z 114, m/z 68, m/z 131, m/z 35, m/z 107, m/z 54, m/z 31, m/z 48, m/z 97, m/z 165, m/z 30, m/z 116, m/z 88
	SHEF1), ZK2012L	14	m/z 95, m/z 123, m/z 171, m/z 142, m/z 45, m/z 83, m/z 40, m/z 128, m/z 32, m/z 78, m/z 99, m/z 120, m/z 151, m/z 50
	SHEF2, ZK2012L	13	m/z 64, m/z 77, m/z 145, m/z 129, m/z 109, m/z 34, m/z 135, m/z 117, m/z 177, m/z 59, m/z 96, m/z 67, m/z 82
	SHEF1	22	m/z 122, m/z 44, m/z 112, m/z 41, m/z 162, m/z 155, m/z 125, m/z 72, m/z 29, m/z 124, m/z 104, m/z 106, m/z 161, m/z 53, m/z 70, m/z 119, m/z 118, m/z 98, m/z 103, m/z 90, m/z 42, m/z 115
	SHEF2	13	m/z 159, m/z 136, m/z 175, m/z 108, m/z 79, m/z 61, m/z 71, m/z 28, m/z 139, m/z 62, m/z 58, m/z 148, m/z 126
	ZK2012L	17	m/z 47, m/z 134, m/z 170, m/z 46, m/z 138, m/z 127, m/z 102, m/z 89, m/z 130, m/z 146, m/z 69, m/z 178, m/z 52, m/z 153, m/z 65, m/z 158, m/z 84

Metabolite profiling associated with hPSCs and their progenitors cultured in two different oxygen conditions (air oxygen and physioxia) was obtained based on VIP scores. These metabolites (ions) that fulfilled the criteria (VIP≥1) were subjected to one-way ANOVA with post-hoc Tukey. The proposed compounds for each variable (ion) (from m/z10 to 180) that significantly (P< 0.05 or 0.01) decreased or increased in the headspace of each hPSC during the differentiation in 21% O_2 and 2% O_2 are listed in Table 4.7.

Table 4. 7. Expected compounds at each protonated mass (m/z) shows a significant difference by one-way ANOVA with post-hoc Tukey test, in headspace gases between undifferentiated hPSCs and their progenitors throughout the differentiation over the m/z ranges 10 to 180.

hPSCs and their progenitors	Condition	m/z	ANOVA (p-value)	Post Hoc Tukey (p-value) (significant)	Proposed Compounds
SHEF1 and their progenitors	21% O_2	m/z 44	0.001	Undiff Vs. 5 days (0.001) ↓ Undiff Vs. 10 days (0.005) ↓ Undiff Vs. 20 days (0.001) ↓	isocyanic acid, n-methyl methanimine, acetaldimine, ethenamine, ethylenimine)
		m/z 45	0.001	Undiff Vs. 5 days (0.005) ↓ Undiff Vs. 10 days (0.005) ↓ Undiff Vs. 20 days (0.005) ↓	(Acetaldehyde, ethanediol (65%), lactic acid (75%), 1,1-dichloroethane (50%))
		m/z 61	0.021	Undiff Vs. 5 days (0.047) ↓ Undiff Vs. 10 days (0.03) ↓	(acetic acid, methyl formate (95%), 1-propanol (10%), 2-propanol (2-%))
		m/z 67	0.033	Undiff Vs. 10 days (0.047) ↑	(water cluster of methanethiol)
		m/z 123	0.031	Undiff Vs. 10 days (0.029) ↑	(4-ethyl phenol, 1-phenyl ethanol, 2-phenyl ethanol)
	2% O_2	m/z 44	0.024	Undiff Vs. 20 days (0.03) ↓	(1-propanol (isotope of main fragment), 2-propanol (isotope of main fragment), isocyanic acid, n-methyl methanimine, acetaldimine,

					ethenamine, ethylenimine)
		m/z 45	0.009	Undiff Vs. 5 days (0.028) ↓ Undiff Vs. 10 days (0.022) ↓ Undiff Vs. 20 days (0.028) ↓	(Acetaldehyde, ethanediol (65%), lactic acid (75%), 1,1-dichloroethane (50%))
		m/z 48	0.045	Undiff Vs. 20 days (0.044) ↓	o-methylhydroxylamine
		m/z 54	0.022	Undiff Vs. 20 days (0.022) ↑	(2-propenenitrile, $NH4^{+}.2H_2O$)
		m/z 63	0.004	Undiff Vs. 5 days (0.016) ↓ Undiff Vs. 10 days (0.011) ↓ Undiff Vs. 20 days (0.013) ↓	(Carbon dioxide, Ethanediol (35%), ethanethiol, dimethyl sulphide)
		m/z 71	0.045	ND	(2-butenal, 2-methyl-2-butene, 1-pentene, trans-2-pentene, iso-butyric acid (10%), n-butyric acid (5%), 2-methyl-2-butanol, 3-methyl-1-butanol, 1-pentanol, 3-pentanol, methyl butyrate (10%), tert-pentyl (amyl) methyl ether (95%), 1-octene (35%), trans-2-octene (35%), 1-nonene (30%), trans-2-nonene (25%), 3-methyl-1-butyl acetate (40%), 1-octanol (35%), 2-octanol (15%), 1-decene (20%))
		m/z 81	0.025	ND	(1,1-dichloroethane (50%), 1,2-dichloroethane (35%), cis-3-hexenal (65%), camphene (14%), 2-carene (18%), 3-carene (24%), s-limonene (30%), myrcene (30%), ocimene (25%), α-pinene (39%), β-pinene (40%), α-terpinene (10%), Y-terpinene (16%))
		m/z 89	0.02	Undiff Vs. 20 days (0.027) ↓	(Pyruvic acid (80%), iso-butyric acid (90%), n-butyric acid (95%), 1,4-dioxane, ethyl acetate, 3-hydroxybutanone, methyl propionate (95%), butyl methyl

					ether (40%))
		m/z 97	0.048	ND	(fluorobenzene, 2-furancarboxaldehyde, 1,1,1-trichloroethane)
		m/z 113	0.032	ND	(Chlorobenzene, trans-2-heptenal, 1-octene (30%), trans-2-octene (35%), 1-octanol (40%), 2-octanol (75%))
		m/z 123	0.01	Undiff Vs. 5 days (0.009) ↑	(4-ethylphenol, 1-phenylethanol, 2-phenylethanol)
SHEF2 and their progenitors	21% O_2	m/z 45	0.001	Undiff Vs. 5 days (0.001) ↓ Undiff Vs. 10 days (0.001) ↓ Undiff Vs. 20 days (0.001) ↓	(Acetaldehyde, ethanediol (65%), lactic acid (75%), 1,1-dichloroethane (50%))
		m/z 63	0.001	Undiff Vs. 5 days (0.002) ↓ Undiff Vs. 10 days (0.001) ↓ Undiff Vs. 20 days (0.002) ↓	(Carbon dioxide, ethanediol (35%), ethanethiol, dimethyl sulphide)
		m/z 67	0.006	Undiff Vs. 20 days (0.014) ↓	(Water cluster of methanethiol)
		m/z 81	0.001	Undiff Vs. 5 days (0.001) ↓ Undiff Vs. 10 days (0.001) ↓ Undiff Vs. 20 days (0.001) ↓	(1,1-dichloroethane (50%), 1,2-dichloroethane (35%), cis-3-hexenal (65%), camphene (14%), 2-carene (18%), 3-carene (24%), s-limonene (30%), myrcene (30%), ocimene (25%), α-pinene (39%), β-pinene (40%), α-terpinene (10%), Y-terpinene (16%))
	2% O_2	m/z 45	0.015	Undiff Vs. 5 days (0.04) ↓ Undiff Vs. 10 days (0.038) ↓ Undiff Vs. 20 days (0.047) ↓	(Acetaldehyde, ethanediol (65%), lactic acid (75%), 1,1-dichloroethane (50%))
		m/z 63	0.011	Undiff Vs. 5 days (0.029) ↓ Undiff Vs. 10 days (0.03) ↓ Undiff Vs. 20 days (0.039) ↓	(Carbon dioxide, ethanediol (35%), ethanethiol, dimethyl sulphide)
		m/z 81	0.002	Undiff Vs. 5 days (0.005) ↓ Undiff Vs. 10 days (0.005) ↓ Undiff Vs. 20 days (0.013) ↓	(1,1-dichloroethane (50%), 1,2-dichloroethane (35%), cis-3-hexenal (65%), camphene (14%), 2-carene (18%), 3-carene (24%), s-limonene (30%), myrcene (30%), ocimene (25%), α-pinene (39%), β-pinene

					(40%), α-terpinene (10%), Y-terpinene (16%))
ZK2012L and their progenitors	21% O_2	m/z 18	0.029	Undiff Vs. 5 days (0.026) ↓	(Ammonia, 2-methylbutylamine (50%), 2-methyl-2-butylamine (90%), 3-methylbutylamine (5%), 3-methyl-2-butylamine (65%), 2-pentylamine (60%), 3-pentylamine (70%))
		m/z 45	0.006	Undiff Vs. 10 days (0.011) ↓ Undiff Vs. 20 days (0.013) ↓	(Acetaldehyde, ethanediol (65%), lactic acid (75%), 1,1-dichloroethane (50%))
		m/z 48	0.008	Undiff Vs. 20 days (0.035) ↑	o-methylhydroxylamine
		m/z 63	0.001	Undiff Vs. 5 days (0.003) ↓ Undiff Vs. 10 days (0.007) ↓ Undiff Vs. 20 days (0.001) ↓	(Carbon dioxide, ethanediol (35%), ethanethiol, dimethyl sulphide)
		m/z 81	0.004	Undiff Vs. 20 days (0.002) ↓	(1,1-dichloroethane (50%), 1,2-dichloroethane (35%), cis-3-hexenal (65%), camphene (14%), 2-carene (18%), 3-carene (24%), s-limonene (30%), myrcene (30%), ocimene (25%), α-pinene (39%), β-pinene (40%), α-terpinene (10%), Y-terpinene (16%))
		m/z 84	0.009	Undiff Vs. 5 days (0.027) ↓	(1-methylpyrrolidine (25%), piperidine (10%))
		m/z 99	0.005	Undiff Vs. 5 days (0.012) ↓ Undiff Vs. 10 days (0.011) ↓ Undiff Vs. 20 days (0.037) ↓	(1,2-dichloroethane (10%), cyclohexanone, trans-2-hexenal, cis-3-hexenal (35%), 1-heptene (25%), trans-2-heptene (35%), methylcyclohexane (5%), 1-decene (10%), trichloronitromethane (2%), iso-flurane (10%))
	2% O_2	m/z 59	0.008	Undiff Vs. 20 days (0.005) ↓	(Acetone, propanal, allyl ethyl ether (15%), 1-nitropropane (5%), 2-nitropropane (60%))
		m/z 72	0.032	Undiff Vs 5 days (0.02) ↑	(pyrrolidine,

					diethylamine (5%))
		m/z 77	0.011	Undiff Vs. 20 days (0.02) ↓	(carbon disulphide, thioacetic acid (77%), 1,2-propanediol (5%), 1,3-propanediol (30%))
		m/z 82	0.033	Undiff Vs. 5 days (0.031) ↑	(2,2-difluoro-ethylamine)
		m/z 83	0.031	Undiff Vs. 20 days (0.035 ↑	(4-methyl-1,3-pentadiene, 1,5-pentanedial (glutyraldehyde)(30%), hexanal (50%), cyclohexane (50%))
		m/z 101	0.006	Undiff Vs. 5 days (0.018) ↑ Undiff Vs. 10 days (0.024) ↑ Undiff Vs. 20 days (0.016) ↑	(1,5-pentanedial (glutyraldehyde) (50%), Y-valerolactone, 2-hexanone, 3-hexanone, hexanal (50%))
		m/z 111	0.02	Undiff Vs. 5 days (0.039) ↑	(2-fluorotoluene, 4-fluorotoluene, 2-hydroxyphynol, 5-methyl-1,2-furancarboxaldehyde, n-octanal (15%))

ND: no significant difference were found

4.4.3. Analysis of SIFT-MS mass spectra derived from the headspace of bone marrow cells and bone marrow-derived mesenchymal stem cells

The hMSCs were successfully isolated from bone marrow aspirates. Isolated hMSCs were able to attach to surfaces of culture flask and expand in air oxygen (21% O_2), intermittent physioxia (2% O_2) and physioxia (2% O_2) work station (WS). The impact of oxygen tension on hMSCs isolation throughout the isolation from bone marrow aspirate was assessed with SIFT-MS analysis of the headspace of human bone marrow cells and MSCs. PCA scores from the collected SIFT-MS human bone marrow cells (BMCs) and MSCs datasets during different time points of isolation showed that all samples lay within the 95% confidence region (Hotelling T^2 ellipse) (Figure 4.9). Score plot of day 0 time point

indicated distinct clustering of control media from incubated BMCs; samples of incubated BMCs in 21% O_2 clustered more tightly than incubated cells in 2% O_2, whereas incubated cells in 2% O_2 WS showed that all samples do not cluster well (Figure 4.9a). Day 7 score plot again showed clear separation between control media and incubated BMCs clusters. Incubated cells in 2% O_2 WS showed that all samples do not cluster well, whereas samples of incubated cells in either 21% O_2 group or 2% O_2 group displayed clustering. In addition, incubated cells groups displayed substantial overlap (Figure 4.9b). The Day 14 score plot showed that control media samples were clustered tightly and separated from incubated cells groups. Incubated cells samples in either 21% O_2 group or 2% O_2 group displayed little evidence of tight clustering with broad dispersal while 2% O_2 WS displayed tight and distinct clustering (Figure 4.9c). Adherent hMSCs score plot revealed control media samples clustered and separated from incubated cells groups but little beyond that where all cell groups displayed substantial overlap and loose distribution (Figure 4.9d). Suspended hMSCs score plot indicated distinct clustering over groups with substantial overlap between groups of incubated cells in 21% O_2 and 2% O_2 (Figure 4.9e).

Figure 4. 9. PCA scores plot of hBMCs and hMSCs cultured in air oxygen (21% O_2), intermittent physioxia (2% O_2) and physioxia (2% O_2) work station (WS). a) Day 0 (t[1]= 40%, t[2]= 19.3%). b) Day 7 (t[1]= 36.4%, t[2]= 24.9%). c) Day 14 (t[1]= 27.2%, t[2]= 23.1%). d) Adherent hMSCs (t[1]= 26.6%, t[2]= 19.5%). e) suspended hMSCs (t[1]= 30.2%, t[2]= 19%). X and Y axes represent the second and first principal components, respectively. Ellipses represent the 95% confidence intervals. Circles represent control media group (n=3), squares represent incubated media with cells in 21% O_2 (n=3), triangles represent incubated media with cells in 2% O_2 (n=3), inverted triangles represent incubated media with cells in 2% O_2 WS (n=3).

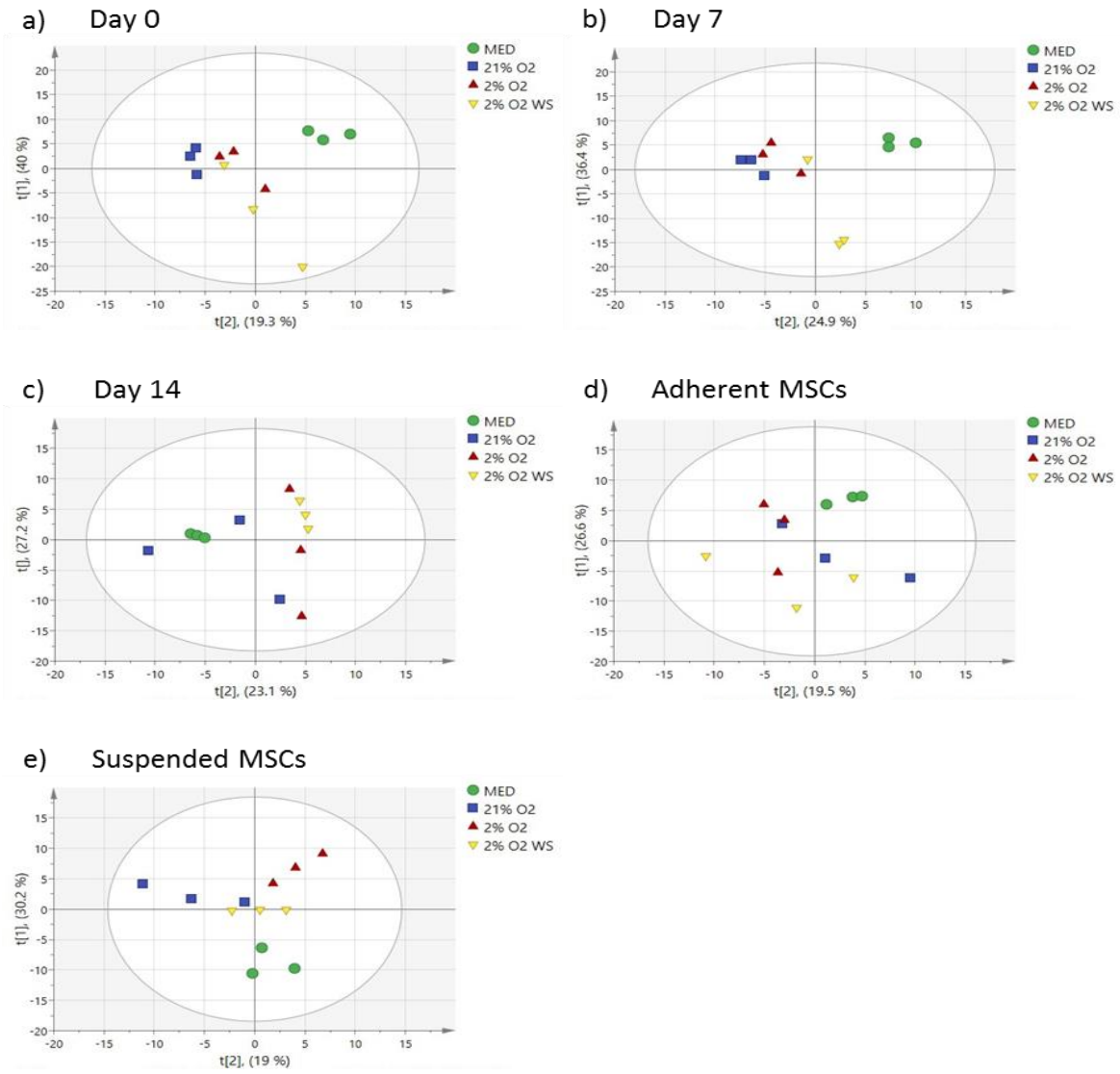

In the OPLS-DA models, all data lay inside the 95% confidence region (Hotelling T2 ellipse) (Figure 4.10). Day 0 (Figure 4.10a) and day 7 (Figure 4.10b) scores plot displayed tight samples clustering within groups and clear separation over groups; 21% O_2 and 2% O_2 groups appeared close to each other. Day 14 score plots again showed clear group separation between groups with tight sample clustering for media control, incubated cells in 21% O_2 and 2% O_2 groups (Figure 4.10c). Adherent hMSCs (Figure 5.5d) and suspended hMSCs (Figure 4.10e) again showed clear cluster separation between groups with close sample clustering for media control group and cells cultured in 2% O_2 WS group.

Table 4. 8. Results of the cross validation and CV-ANOVA for OPLS-DA models of hBMCs and hMSCs media.

OPLS-DA model	R2Y (cum)	Q2 (cum)	P-value (CV-ANOVA)
Day 0	0.941	0.798	0.0288
Day 7	0.921	0.682	0.0381
Day 14	0.966	0.784	0.028
Adherent MSCs	0.913	0.652	0.0427
Suspended MSCs	0.927	0.729	0.0261

Figure 4. 10. Scores plot from OPLS-DA discrimination of SIFT-MS spectra of hBMCs and hMSCs cultured in 21% O_2, 2% O_2 and 2% O_2 WS. a) Day 0. b) Day 7. c) Day 14. d) Adherent hMSCs. e) suspended hMSCs. X-axis, t[2] and Y-axis, t[1], indicate the second and first principal components, respectively. Ellipses represent the 95% confidence intervals. Circles represent control media group (n=3), squares represent incubated media with cells in 21% O_2 (n=3), triangles represent incubated media with cells in 2% O_2 (n=3). Inverted triangles represent incubated media with cells in 2% O_2 WS (n=3).

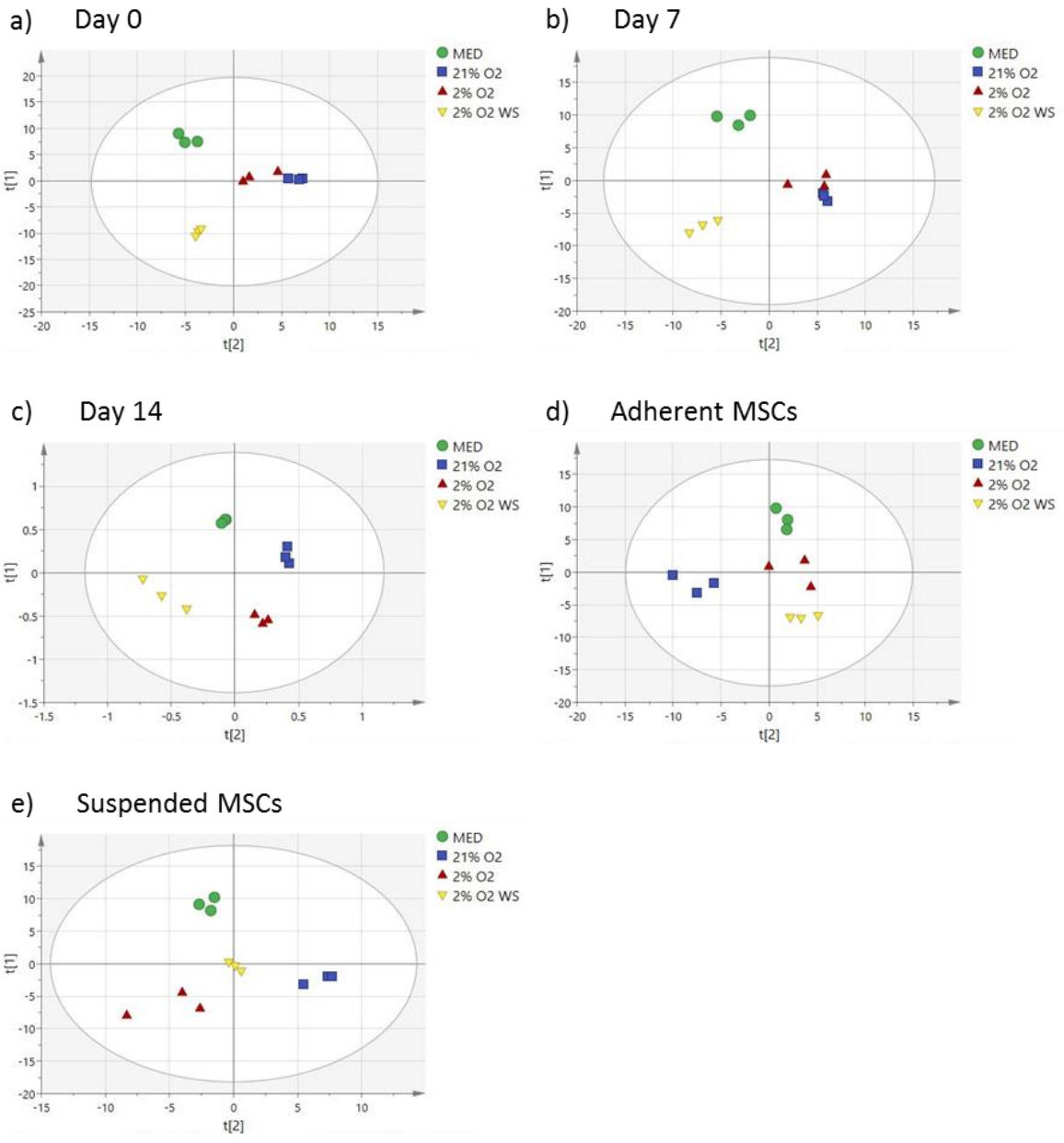

The variables relevant for discrimination in OPLS-DA models were identified from their VIP values for each time point during hMSCs isolation and isolated hMSCs. Large VIP values (≥1) are the most relevant for predicted variables.

The number of VIP variables (≥1) shared and unique across the time points examined throughout hMSCs isolation are indicated (Figure 4.11, Table 4.9).

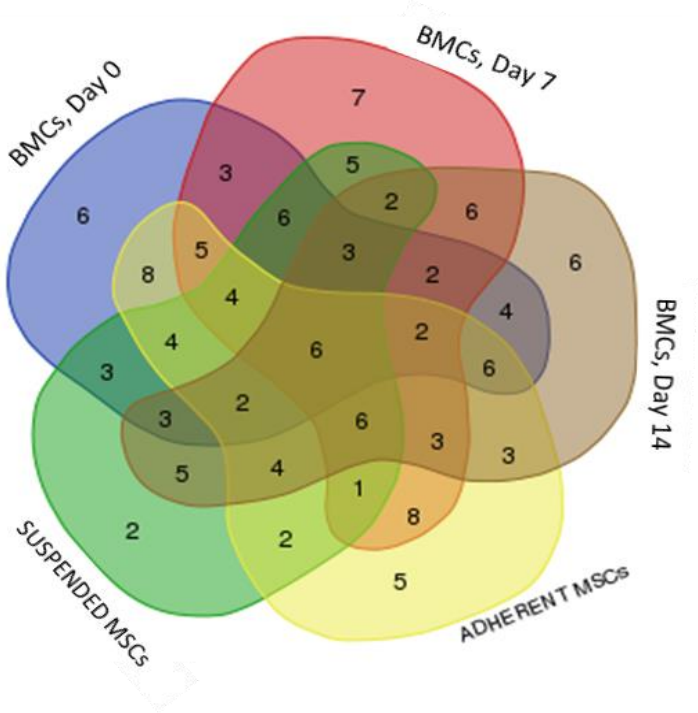

Figure 4. 11. Venn diagram showing statistically-selected discriminating variables (ions) in human BMCs and MSCs. Overlap of time points of hMSCs isolation and isolated hMSCs OPLS-DA models are indicated. As indicated in the diagram, there are unique and shared (ions) variables from the five cells models. Blue shape represent the number of variables (m/z) in BMCs (Day 0), red shape represent the number of variables (m/z) in BMCs (Day 7), brown shape represent the number of variables (m/z) in BMCs (Day 14), yellow shape represent the number of variables (m/z) in adherent MSCs and green shape represent the number of variables (m/z) in suspended MSCs.

Table 4. 9. Significant variables (ions) mass to charge ratio (m/z) accountable for class discrimination of BMCs over time-course of hMSCs isolation and isolated hMSCs by OPLS-DA (with VIP score ≥1).

Cells	No. of m/z ions	Variables (ions) m/z
BMCs (day 0), BMCs (day 7), BMCs (day 14), Adherent hMSCs, suspended hMSCs	6	m/z 146, m/z 169, m/z 140, m/z 44, m/z 105, m/z 40
BMCs (day 0), BMCs (day 7), BMCs (day 14), Adherent hMSCs	2	m/z 124, m/z 113
BMCs (day 0), BMCs (day 7), BMCs (day 14), suspended hMSCs	3	m/z 138, m/z 31, m/z 147
BMCs (day 0), BMCs (day 7), Adherent hMSCs, suspended hMSCs	4	m/z 32, m/z 61, m/z 123, m/z 78
BMCs (day 0), BMCs (day 14), Adherent hMSCs, suspended hMSCs	2	m/z 114, m/z 34
BMCs (day 7), BMCs (day 14), Adherent hMSCs, suspended hMSCs	6	m/z 41, m/z 155, m/z 93, m/z 82, m/z 98, m/z 84
BMCs (day 0), BMCs (day 7), BMCs (day 14)	2	m/z 104, m/z 117
BMCs (day 0), BMCs (day 7), Adherent hMSCs	5	m/z 134, m/z 170, m/z 132, m/z 177, m/z 115
BMCs (day 0), BMCs (day 7), suspended hMSCs	6	m/z 77, m/z 59, m/z 151, m/z 142, m/z 63, m/z 87
BMCs (day 0), BMCs (day 14), Adherent hMSCs	6	m/z 88, m/z 103, m/z 119, m/z 167, m/z 165, m/z 76
BMCs (day 0), BMCs (day 14), suspended hMSCs	3	m/z 86, m/z 45, m/z 99
BMCs (day 0), Adherent MSCs, suspended hMSCs	4	m/z 171, m/z 96, m/z 90, m/z 148
BMCs (day 7), BMCs (day 14), Adherent hMSCs	3	m/z 111, m/z 159, m/z 139
BMCs (day 7), BMCs (day 14), suspended hMSCs	2	m/z 47, m/z 101
BMCs (day 7), Adherent hMSCs, suspended hMSCs	1	m/z 58
BMCs (day 14), Adherent hMSCs, suspended hMSCs	4	m/z 18, m/z 175, m/z 89, m/z 50
BMCs (day 0), BMCs (day 7)	3	m/z 160, m/z 127, m/z 178
BMCs (day 0), BMCs (day 14)	4	m/z 158, m/z 136, m/z 68, m/z 130
BMCs (day 0), Adherent hMSCs	8	m/z 60, m/z 153, m/z 97, m/z 125, m/z 156, m/z 168, m/z 30, m/z 43
BMCs (day 0), suspended hMSCs	3	m/z 179, m/z 137, m/z 143
BMCs (day 7), BMCs (day 14)	6	m/z 94, m/z 80, m/z 69, m/z 42, m/z 35, m/z 129

BMCs (day 7), Adherent hMSCs	8	m/z 106, m/z 53, m/z 133, m/z 173, m/z 161, m/z 154, m/z 62, m/z 131
BMCs (day 7), suspended hMSCs	5	m/z 46, m/z 71, m/z 128, m/z 174, m/z 79
BMCs (day 14), Adherent hMSCs	3	m/z 141, m/z 85, m/z 112
BMCs (day 14), suspended hMSCs	5	m/z 65, m/z 92, m/z 48, m/z 28, m/z 66
Adherent hMSCs, suspended hMSCs	2	m/z 33, m/z 145
BMCs (day 0)	6	m/z 180, m/z 164, m/z 72, m/z 107, m/z 162, m/z 176
BMCs (day 7)	7	m/z 157, m/z 126, m/z 81, m/z 135, m/z 120, m/z 52, m/z 109
BMCs (day 14)	6	m/z 149, m/z 150, m/z 121, m/z 110, m/z 100, m/z 49
Adherent hMSCs	5	m/z 163, m/z 116, m/z 95, m/z 122, m/z 118
suspended hMSCs	2	m/z 70, m/z 102

Metabolite profiling associated with BMCs and hMSCs culture in 21% O_2, 2% O_2 and 2% O_2 WS was derived from VIP scores where metabolites (ions) that fulfilled the criteria (VIP≥1) were subjected to ANOVA analysis.

Table 4. 10. Expected compounds at each protonated mass (m/z) where significant differences in the headspace gases of media of BMCs or hMSCs were noted over 21% O_2, 2% O_2 and 2% O_2 WS conditions over the m/z ranges 10 to 180.

Samples	m/z	ANOVA (p-value)	Post Hoc Tukey (p-value) (significant)	Proposed Compounds
BMCs (day 0)	m/z 125	0.033	21% O_2 Vs. 2% O_2 (0.028)	(4-fluorobenzaldehyde, 5,5-dimethyl-2-cyclohexenone, (methylthio)-benzene, 2,3,4,5-tetramethylfuran)
	m/z 127	0.041	21% O_2 Vs. 2% O_2 WS (0.034)	(2-chlorotoluene, 4-chlorotoluene, dimethyl trisulphide, trans-2-octenal, 1-nonene (30%), trans-2-nonene (40%))
BMCs (day 7)	m/z 31	0.028	21% O_2 Vs. 2% O_2 (0.049) 2% O_2 Vs. 2% O_2 WS (0.037)	(Formaldehyde, ethylene glycol dimethyl (5%))
	m/z 71	0.029	21% O_2 Vs. 2% O_2 (0.025)	(2-butenal, 2-methyl butane, 1-pentene, trans-2-pentene, isobutyric acid (10%), butyric acid (5%), 2-methyl-2-butanol, 3-methyl-1-butanol, 1-pentanol, 3-pentanol, tert-pentyl methylether (95%), 1-octene (35%), trans-2-octene (35%), 1-nonene (30%), trans-2-nonene (25%), 3-methyl-1-butyl acetate (40%), 1-octanol (35%), 2-octanol (15%), 1-decene (20%))
	m/z 80	0.016	21% O_2 Vs. 2% O_2 (0.019) 21% O_2 Vs. 2% O_2 WS (0.037)	(pyridine)
	m/z 127	0.038	21% O_2 Vs. 2% O_2 (0.037)	(2-chlorotoluene, 4-chlorotoluene, dimethyl trisulphide, trans-2-octenal, 1-nonene (30%), trans-2-nonene (40%))
BMCs (day 14)	m/z 44	0.047	ND	(Isocyanic acid, n-methyl methanimine, acetaldimine, ethenamine, ethylenimine)
Adherent hMSCs	m/z 97	0.013	21% O_2 Vs. 2% O_2 WS (0.012) 2% O_2 Vs. 2% O_2 WS (0.048)	(Fluorobenzene, 2-furancarboxaldehyde, methylcyclohexane (95%), 1,1,1-trichloroethane)
suspended hMSCs	m/z 79	0.021	21% O_2 Vs. 2% O_2 (0.02)	(Benzene, dimethyl sulphoxide, 2-thioethanol (5%))
	m/z 93	0.045	21% O_2 Vs. 2% O_2 (0.048)	(Toluene)

ND: No significant difference were found

4.4.4. Analysis of SIFT-MS mass spectra derived from the headspace of hMSCs and osteogenic differentiation of hMSCs

To investigate the metabolic changes occurring in the BM-hMSCs during osteogenesis and to compare with undifferentiated hMSCs SIFT-MS analysis of the media headspace was performed. PCA score plot from the collected SIFT-MS hMSCs and hMSCs after osteoinduction showed that all samples lay within the 95% confidence region (Hotelling T^2 ellipse) (Figure 4.12, 4.13 and 4.14). The score plot of undifferentiated and differentiated hMSCs in 21% O_2 showed a clear cluster separation of control media samples. Undifferentiated and differentiated hMSCs media at Day 7 showed broad overlaps between groups, day 14 cell-exposed media showed some separation between undifferentiated and differentiated clusters, while day 21 cell-exposed media again showed a high degree of overlap (Figure 4.12a). The score plot of 21% O_2 undifferentiated hMSCs over the time course revealed clear cluster separation of control media samples. hMSCs exposed media revealed distinct separation for day 7 but some overlap for days 14 and 21 (Figure 4.12b). In contrast to 21% O_2 undifferentiated hMSCs, 21% O_2 differentiated hMSCs exposed media showed clustered distinct groups over the time course of differentiation and separate from control media which clustered together tightly (Figure 4.12c).

The score plot of undifferentiated and differentiated hMSCs in 2% O_2 showed a clear cluster separation of control media samples. Undifferentiated and differentiated hMSCs Day 7 exposed media showed overlap and associated clustering, whereas undifferentiated and differentiated hMSCs Days 14 and 21 showed strong overlap between samples and were distinct from Day 7 cells (Figure 4.13a). The score plot of 2% O_2 Undifferentiated hMSCs over the time course revealed clear cluster separation of control media samples. Undifferentiated hMSCs exposed media showed strong evidence of overlap at Days 14 and 21 while undifferentiated Day 7 hMSCs exposed media revealed distinct clustering (Figure

4.13b). Similar to 2% O_2 undifferentiated hMSCs, 2% O_2 differentiated hMSCs exposed media showed overlap at Days 14 and 21 while differentiated Day 7 hMSCs exposed media revealed a distinct cluster (Figure 4.13c).

The score plot of undifferentiated and differentiated hMSCs in 2% O_2 WS showed a clear cluster separation of control media samples. Undifferentiated and differentiated hMSCs Day 7 exposed media revealed clustering with strong overlap between them, whereas undifferentiated and differentiated hMSCs Days 14 and 21 showed distinct clustering (Figure 4.14a). The score plot of 2% O_2 WS undifferentiated hMSCs over the time course revealed clear cluster separation of control media samples. Undifferentiated hMSCs exposed media showed distinct cluster separation at Days 7 and 21 while undifferentiated Day 14 hMSCs exposed media displayed a looser organisation (Figure 4.14b). Similar to 2% O_2 WS undifferentiated hMSCs, 2% O_2 WS differentiated hMSCs exposed media showed clear cluster separation at Days 7 and 21 while differentiated Day 14 hMSCs exposed media displayed a looser organisation (Figure 4.14c).

Figure 4. 12. PCA scores plot of hMSCs and osteo-induced hMSCs media over the time-course of differentiation in air oxygen (21% O_2). a) undifferentiated and differentiated hMSCs (t[1]= 20.3%, t[2]= 15.7%). b) undifferentiated hMSCs (t[1]= 30.2%, t[2]= 21.5%). c) differentiated hMSCs (t[1]= 33.1%, t[2]= 25.2%). X and Y axes represent the second and first principal components, respectively. Ellipses represent the 95% confidence intervals. Circles represent control media group (n=3), squares represent incubated media with undifferentiated hMSCs (day 7) (n=3), triangles represent undifferentiated hMSCs media (day 14) (n=3), inverted triangles represent undifferentiated hMSCs media (day 21) (n=3) whereas differentiated hMSCs media at day 7 (n=3), 14 (n=3) and 21 (n=3) represent as diamonds, pentagons and hexagons, respectively.

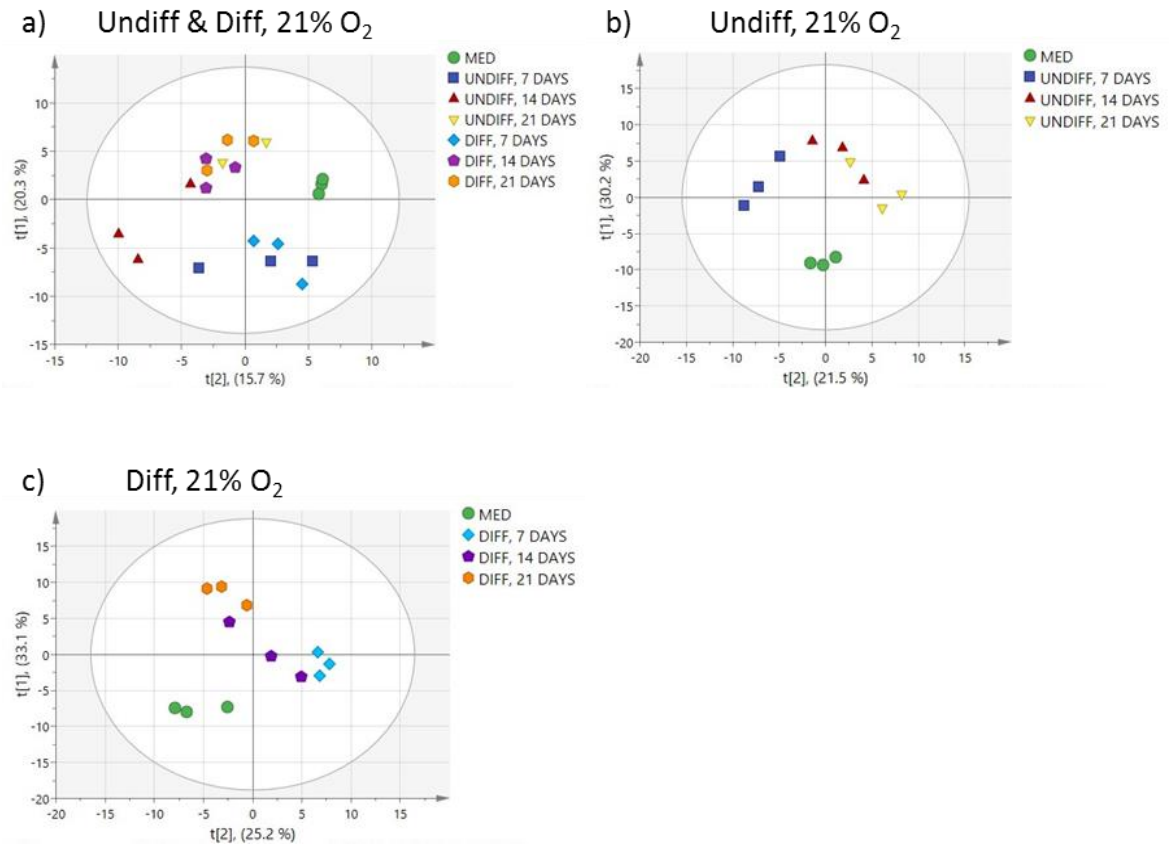

Figure 4. 13. PCA scores plot of hMSCs and osteo-induced hMSCs media over the time-course of differentiation in intermittent physioxia (2% O_2). a) undifferentiated and differentiated hMSCs (t[1]= 24.4%, t[2]= 18.1%). b) undifferentiated hMSCs (t[1]= 29.3%, t[2]= 26%). c) differentiated hMSCs (t[1]= 28.5%, t[2]= 26.6%). X and Y axes represent the second and first principal components, respectively. Ellipses represent the 95% confidence intervals. Circles represent control media group (n=3), squares represent incubated media with undifferentiated hMSCs (day 7) (n=3), triangles represent undifferentiated hMSCs media (day 14) (n=3), inverted triangles represent undifferentiated hMSCs media (day 21) (n=3) whereas differentiated hMSCs media at day 7 (n=3), 14 (n=3) and 21 (n=3) represent as diamonds, pentagons and hexagons, respectively.

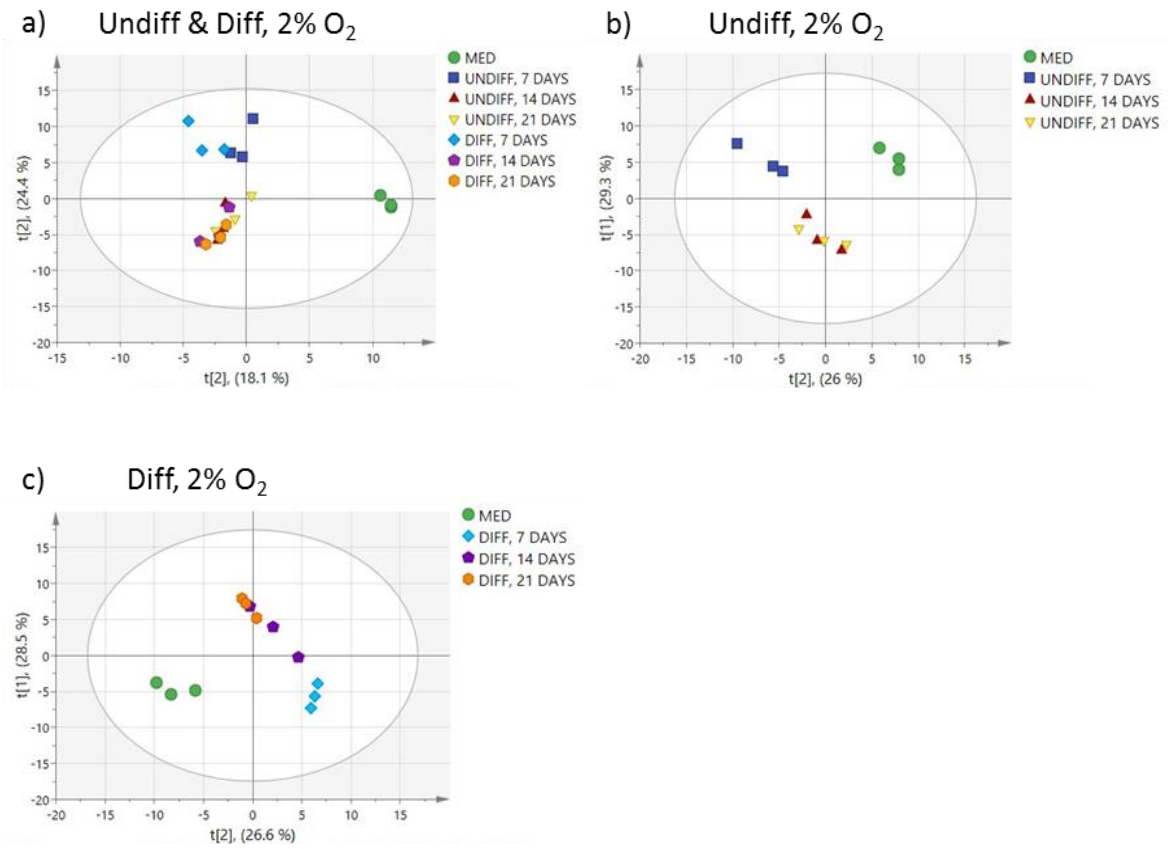

Figure 4. 14. PCA scores plot of hMSCs and osteo-induced hMSCs media over the time-course of differentiation in physioxia (2% O_2 WS). a) undifferentiated and differentiated hMSCs (t[1]= 26.8%, t[2]= 22.6%). b) undifferentiated hMSCs (t[1]= 28%, t[2]= 24.7%). c) differentiated hMSCs (t[1]= 31.3%, t[2]= 24.9%). X and Y axes represent the second and first principal components, respectively. Ellipses represent the 95% confidence intervals. Circles represent control media group (n=3), squares represent incubated media with undifferentiated hMSCs (day 7) (n=3), triangles represent undifferentiated hMSCs media (day 14) (n=3), inverted triangles represent undifferentiated hMSCs media (day 21) (n=3) whereas differentiated hMSCs media at day 7 (n=3), 14 (n=3) and 21 (n=3) represent as diamonds, pentagons and hexagons, respectively.

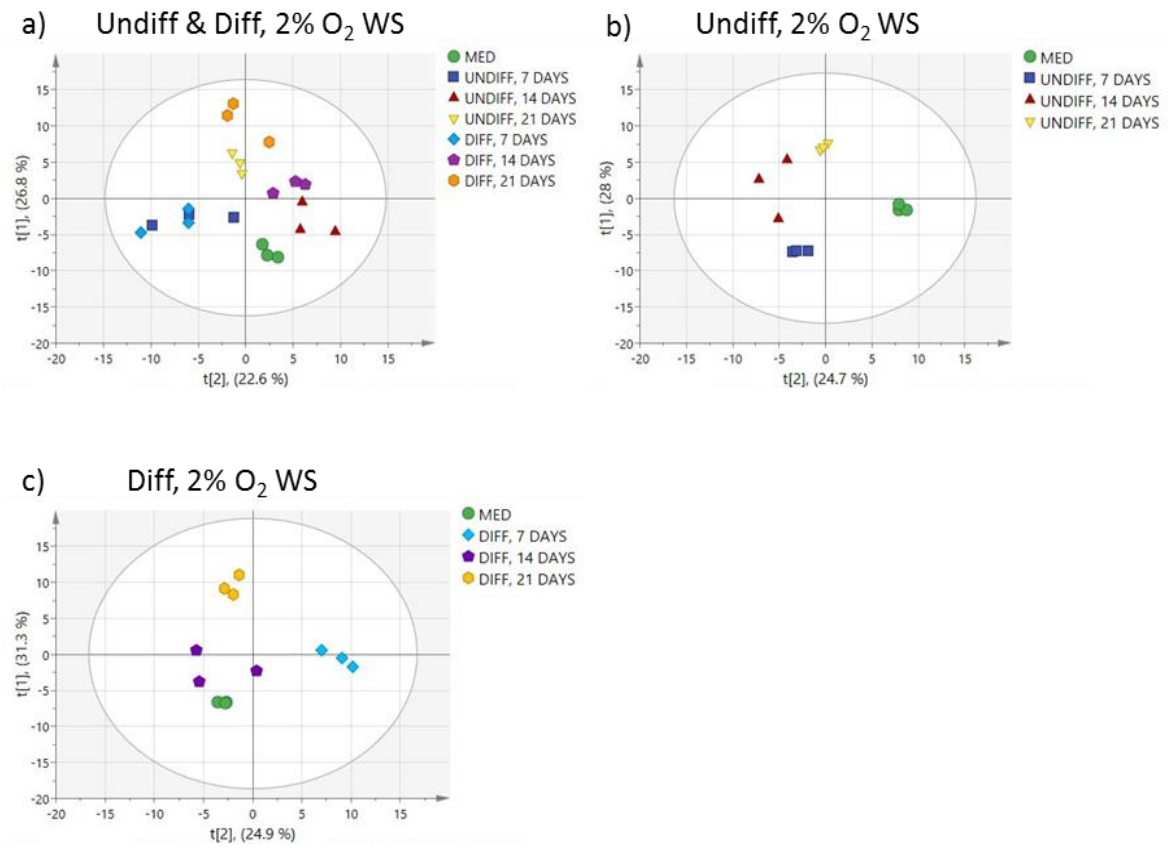

In the OPLS-DA models for cells cultured in 21% O_2, all samples lay within the 95% confidence region (Hotelling T2 ellipse) (Figure 4.15). The two-dimensional (2D) and three-dimensional (3D) score plot for 21% O_2 control media was distinct from undifferentiated and differentiated cell exposed media. The 2D (Figure 4.15ai) and 3D (Figure 4.15aii) scores plot showed clustering but not good separation between undifferentiated and differentiated hMSCs at Day 7. Differentiated hMSCs at Days 14 overlapped with differentiated and undifferentiated hMSCs at Day 21 but revealed separation from undifferentiated hMSCs at Day 14 based on the 2D score plot. Differentiated and undifferentiated hMSCs at Day 21 could not be distinguished by the 2D score but an obvious cluster separation of undifferentiated hMSCs from differentiated hMSCs was revealed based on the 3D score plot. The 2D and 3D score plots of undifferentiated hMSCs revealed clear cluster separation of control media and cells exposed media at Days 7, 14 and 21 (Figure 4.15bi, bii). 2D and 3D scores plot of differentiated hMSCs indicated distinct control media from differentiated cell exposed media. Exposed cell media at Day 7 revealed distinct from cell exposed media at Days 14 and 21 by 2D and 3D scores. Exposed cell media at Day 14 and 21 revealed some overlap by 2D score plot but an obvious cluster separation was revealed by 3D score plot (Figure 4.15ci, cii).

Table 4. 11. Results of the cross validation and CV-ANOVA for OPLS-DA models of hMSCs and osteo-induced hMSCs media in air oxygen (21% O_2).

OPLS-DA model	R2Y (cum)	Q2 (cum)	P-value (CV-ANOVA)
Undifferentiated and differentiated hMSCs	0.883	0.621	0.0389
Undifferentiated hMSCs	0.916	0.755	0.0074
Differentiated hMSCs	0.89	0.68	0.0265

Figure 4. 15. OPLS-DA discrimination score plots of SIFT-MS spectra of hMSCs and osteo-induced hMSCs media over the time-course of differentiation in air oxygen (21% O_2). Undifferentiated and differentiated hMSCs (2D score plot) (ai) and (3D score plot) (aii). Undifferentiated hMSCs (2D score plot) (bi) and (3D score plot) (bii). Differentiated hMSCs (2D score plot) (ci) and (3D score plot) (cii). X-axis, t[2] and Y-axis, t[1], indicate the second and first principal components, respectively. Ellipses represent the 95% confidence intervals. Circles represent control media group (n=3), squares represent incubated media with undifferentiated hMSCs (day 7) (n=3), triangles represent undifferentiated hMSCs media (day 14) (n=3), inverted triangles represent undifferentiated hMSCs media (day 21) (n=21) whereas diamonds, pentagons and hexagons represent differentiated hMSCs media at day 7 (n=3), 14 (n=3) and 21 (n=3), respectively.

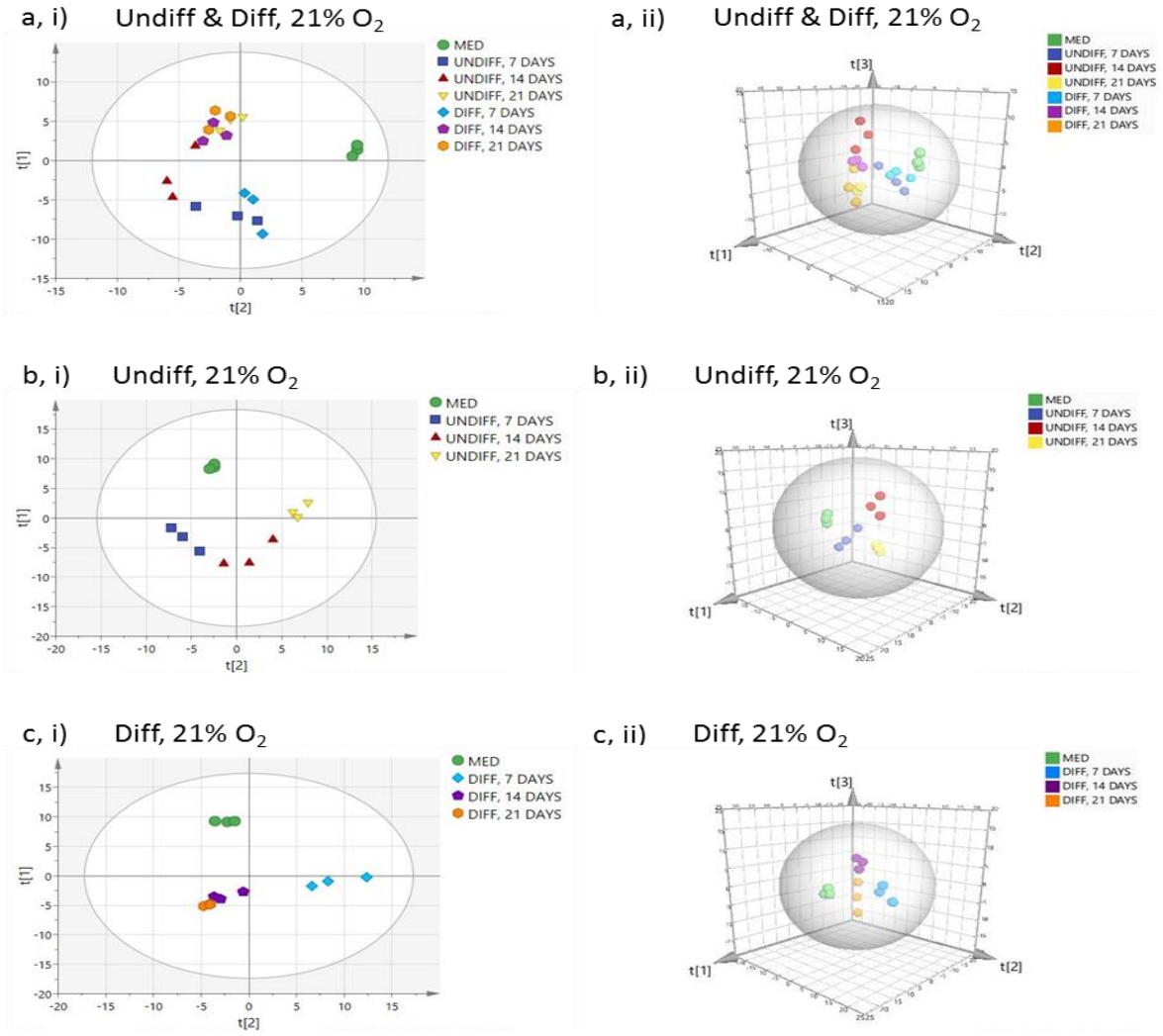

In the OPLS-DA models for cells cultured in 2% O_2, all samples lay within the 95% confidence region (Hotelling T2 ellipse) (Figure 4.16). The two-dimensional (2D) and three-dimensional (3D) score plot for control media was distinct from undifferentiated and differentiated cell exposed media. The 2D and 3D scores plot indicated undifferentiated hMSCs exposed media distinct with little or no overlap from differentiated hMSCs exposed media at Day 7. Both undifferentiated and differentiated hMSCs at Day7 were located farther away from undifferentiated and differentiated hMSCs at Days 14 and 21 that revealed strong overlap by 2D score plot (Figure 4.16ai), whereas the 3D score plot revealed cluster separation between undifferentiated and differentiated hMSCs exposed media for both Days 14 and 21 with strong evidence of overlap and associated clustering between differentiated hMSCs exposed media at Day 14 and Day 21 (Figure 4.16aii). The 2D and 3D score plot of undifferentiated hMSCs revealed cluster separation among groups with little or no overlap between Day 14 and Day 21 by 2D score plot (4.16bi, bii). The 2D and 3D score plot of differentiated hMSCs revealed cluster separation among groups with partial overlap between Day 14 and Day 21 by 2D score plot (Figure 4.16ci, cii).

Table 4. 12. Results of the cross validation and CV-ANOVA for OPLS-DA models of hMSCs and osteo-induced hMSCs media intermittent physioxia (2% O_2).

OPLS-DA model	R2Y (cum)	Q2 (cum)	P-value (CV-ANOVA)
Undifferentiated and differentiated hMSCs	0.862	0.655	0.0079
Undifferentiated hMSCs	0.923	0.722	0.00749
Differentiated hMSCs	0.886	0.709	0.0102

Figure 4. 16. OPLS-DA discrimination score plots of SIFT-MS spectra of hMSCs and osteo-induced hMSCs media over the time-course of differentiation in intermittent physioxia (2% O_2). Undifferentiated and differentiated hMSCs (2D score plot) (ai) and (3D score plot) (aii). Undifferentiated hMSCs (2D score plot) (bi) and (3D score plot) (bii). Differentiated hMSCs (2D score plot) (ci) and (3D score plot) (cii). X-axis, t[2] and Y-axis, t[1], indicate the second and first principal components, respectively. Ellipses represent the 95% confidence intervals. Circles represent control media group (n=3), squares represent incubated media with undifferentiated hMSCs (day 7) (n=3), triangles represent undifferentiated hMSCs media (day 14) (n=3), inverted triangles represent undifferentiated hMSCs media (day 21) (n=21) whereas diamonds, pentagons and hexagons represent differentiated hMSCs media at day 7 (n=3), 14 (n=3) and 21 (n=3), respectively.

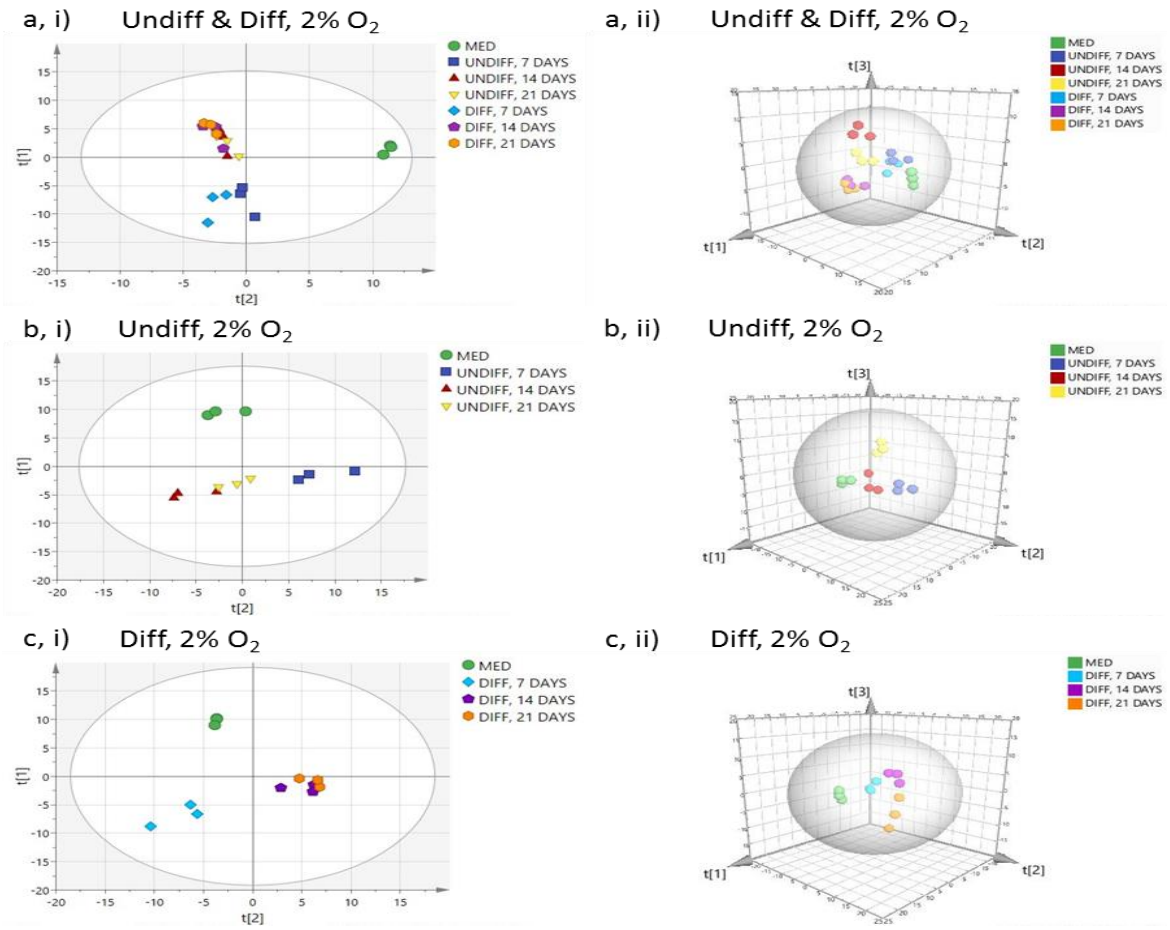

In the OPLS-DA models for cells cultured in 2% O_2 WS, all samples lay within the 95% confidence region (Hotelling T2 ellipse) (Figure 4.17). The two-dimensional (2D) and three-dimensional (3D) score plot for control media was distinct from undifferentiated and differentiated cell exposed media. The 2D and 3D scores plot of undifferentiated and differentiated hMSCs indicated undifferentiated hMSCs and differentiated hMSCs exposed media distinct with strong overlap between them at Day 7. Both undifferentiated and differentiated hMSCs at Day 7 were located farther away from undifferentiated hMSCs and differentiated hMSCs at Days 14 and 21 which revealed distinct cluster from each other by 2D and 3D score plot (Figure 4.17ai) and (Figure 4.17aii). The 2D score plot of undifferentiated hMSCs showed cluster separation for control media and cells exposed media at Day 14, whereas strong overlapping between cells exposed media at day 7 and day 21 (Figure 4.17bi); 3D score plot displayed distinct cluster separation among groups (Figure 4.17bii). The 2D and 3D score plot of differentiated hMSCs revealed cluster separation among groups with no overlap (Figure 4.17ci, cii).

Table 4. 13. Results of the cross validation and CV-ANOVA for OPLS-DA models of hMSCs and osteo-induced hMSCs media physioxia (2% O_2 WS).

OPLS-DA model	R2Y (cum)	Q2 (cum)	P-value (CV-ANOVA)
Undifferentiated and differentiated hMSCs	0.889	0.737	0.002
Undifferentiated hMSCs	0.924	0.823	0.00012
Differentiated hMSCs	0.928	0.822	0.0005

Figure 4. 17. OPLS-DA score plot discrimination of SIFT-MS spectra of hMSCs and osteo-induced hMSCs media over the time-course of differentiation in physioxia (2% O_2 WS). Undifferentiated and differentiated hMSCs (2D score plot) (ai) and (3D score plot) (aii). Undifferentiated hMSCs (2D score plot) (bi) and (3D score plot) (bii). Differentiated hMSCs (2D score plot) (ci) and (3D score plot) (cii). X-axis, t[2] and Y-axis, t[1], indicate the second and first principal components, respectively. Ellipses represent the 95% confidence intervals. Circles represent control media group (n=3), squares represent incubated media with undifferentiated hMSCs (day 7) (n=3), triangles represent undifferentiated hMSCs media (day 14) (n=3), inverted triangles represent undifferentiated hMSCs media (day 21) (n=21) whereas diamonds, pentagons and hexagons represent differentiated hMSCs media at day 7 (n=3), 14 (n=3) and 21 (n=3) as, respectively.

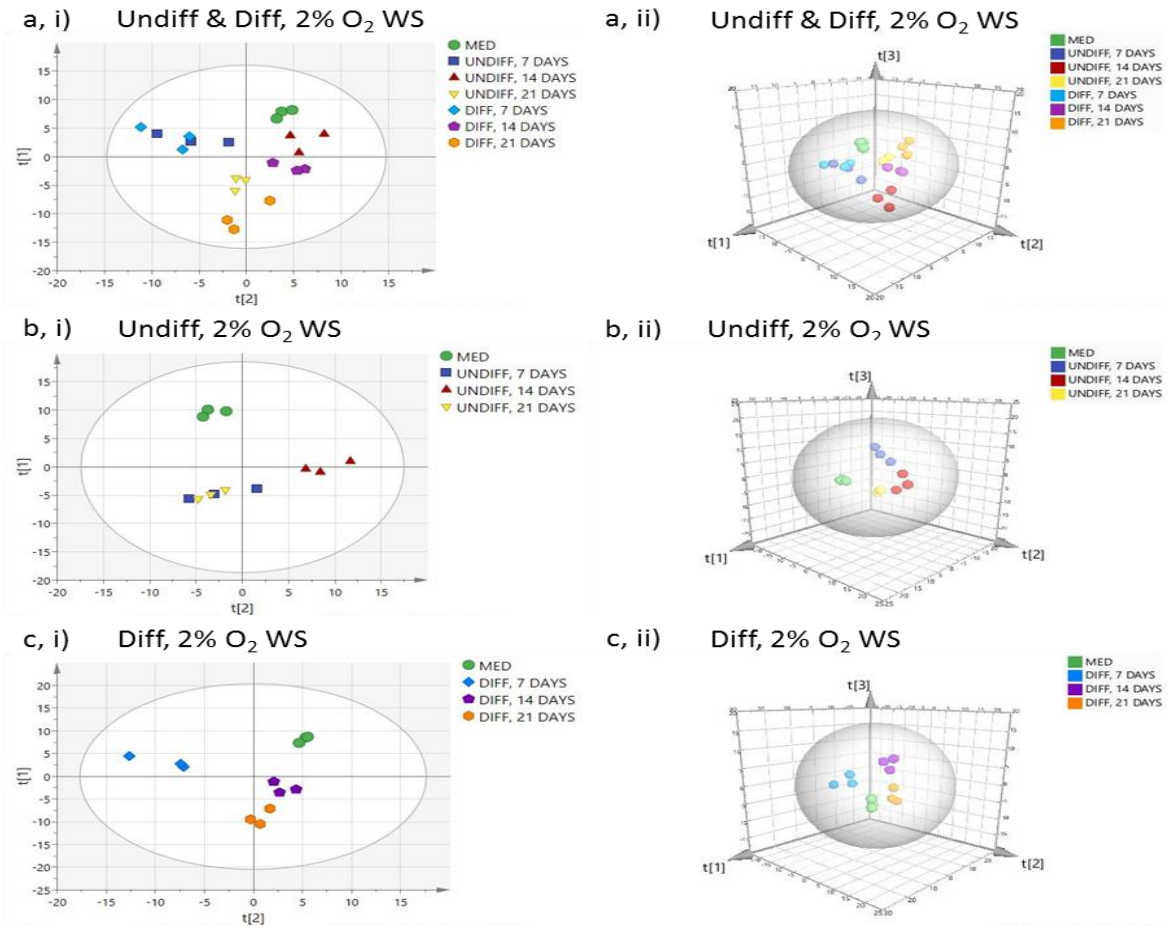

The variables relevant for discrimination in OPLS-DA models were identified from their VIP values for either both undifferentiated and differentiated hMSCs, or undifferentiated hMSCs alone and differentiated hMSCs alone over time-course in each oxygen condition. Large VIP values (≥1) are the most relevant for predicted variables.

The number of shared and unique VIP≥1 variables for undifferentiated and differentiated hMSCs among oxygen conditions were determined (Figure 4.18, Table 4.14).

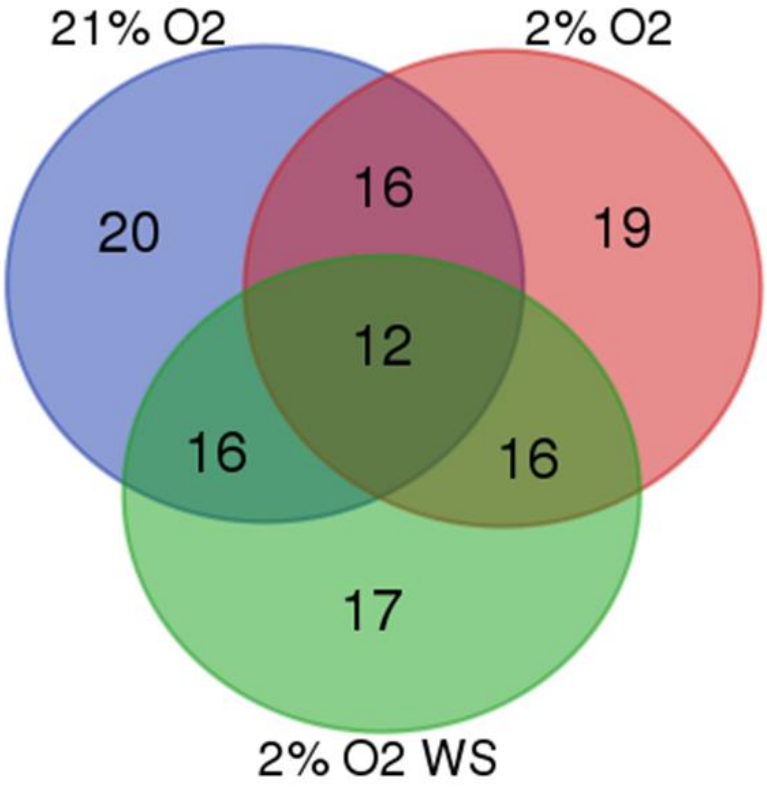

Figure 4. 18. Discriminating variables (ions) from OPLS-DA models for undifferentiated and differentiated hMSCs cultured in 21% O_2, 2% O_2 and 2% O_2 WS. As indicated in the diagram, there are unique and shared variables (ions) for cells cultured in each oxygen conditions. Blue circle represent the number of variables (m/z) in 21% O_2, red circle represent the number of variables (m/z) in 2% O_2 and green circle represent the number of variables (m/z) in 2% O_2 WS.

Table 4. 14. Significant variables (ions) mass to charge ratio (m/z) accountable for class discrimination of undifferentiated and differentiated hMSCs over time-course of differentiation by OPLS-DA (with VIP score ≥1).

Conditions	No. of m/z ions	Variables (ions) m/z
21% O_2, 2% O_2, 2% O_2 WS	12	m/z 114, m/z 167, m/z 85, m/z 87, m/z 168, m/z 88, m/z 147, m/z 45, m/z 59, m/z 115, m/z 165, m/z 63
21% O_2, 2% O_2	16	m/z 18, m/z 93, m/z 171, m/z 107, m/z 95, m/z 51, m/z 173, m/z 135, m/z 61, m/z 77, m/z 36, m/z 81, m/z 30, m/z 78, m/z 76, m/z 49
21% O_2, 2% O_2 WS	16	m/z 106, m/z 157, m/z 154, m/z 141, m/z 94, m/z 159, m/z 169, m/z 137, m/z 113, m/z 70, m/z 82, m/z 111, m/z 68, m/z 121, m/z 48, m/z 84
2% O_2, 2% O_2 WS	16	m/z 102, m/z 86, m/z 90, m/z 120, m/z 42, m/z 123, m/z 52, m/z 89, m/z 92, m/z 35, m/z 170, m/z 153, m/z 129, m/z 177, m/z 67, m/z 44
21% O_2	20	m/z 172, m/z 112, m/z 46, m/z 178, m/z 148, m/z 62, m/z 136, m/z 126, m/z 71, m/z 162, m/z 143, m/z 151, m/z 99, m/z 176, m/z 69, m/z 161, m/z 97, m/z 101, m/z 175, m/z 64
2% O_2	19	m/z 163, m/z 33, m/z 158, m/z 72, m/z 138, m/z 127, m/z 32, m/z 152, m/z 41, m/z 28, m/z 65, m/z 119, m/z 80, m/z 54, m/z 104, m/z 50, m/z 132, m/z 131, m/z 117
2% O_2 WS	17	m/z 130, m/z 125, m/z 145, m/z 146, m/z 105, m/z 155, m/z 40, m/z 96, m/z 22, m/z 109, m/z 34, m/z 79, m/z 58, m/z 164, m/z 108, m/z 144, m/z 43

The number of VIP≥1 variables that were both shared and unique between undifferentiated hMSCs and differentiated hMSCs across the time-course of differentiation in each oxygen condition were identified (Figure 4.19, Table 4.15).

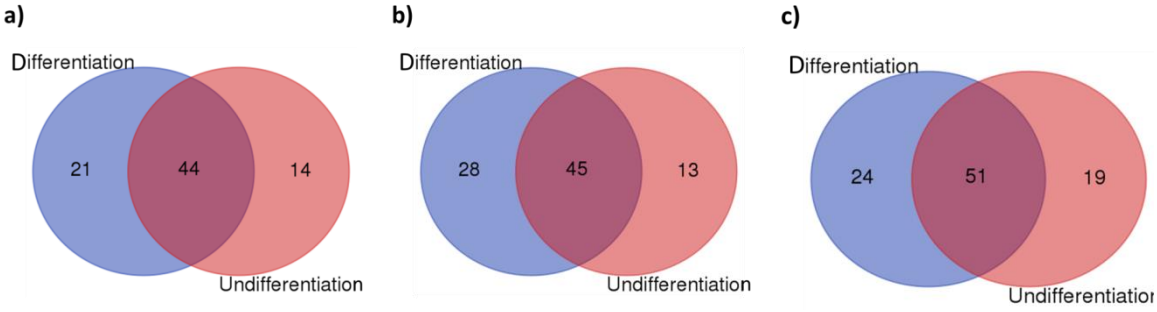

Figure 4. 19. Discriminating variables (ions) from OPLS-DA models for undifferentiated hMSCs and differentiated hMSCs. 21% O_2 (a), 2% O_2 (b) and 2% O_2 WS (c). As indicated in the diagrams, there are unique and shared variables (ions) for cells cultured in each oxygen condition. Blue circle represent the number of variables (m/z) in differentiation media and red circle represent the number of variables (m/z) in undifferentiation media.

Table 4. 15. Significant variables (ions) mass to charge ratio (m/z) accountable for class discrimination of undifferentiated hMSCs and differentiated hMSCs in 21% O_2, 2% O_2 and 2% O_2 WS over time-course of differentiation by OPLS-DA (with VIP score ≥1).

Conditions	21% O_2		2% O_2		2% O_2 WS	
	No. of m/z ions	Variables (ions) m/z	No. of m/z ions	Variables (ions) m/z	No. of m/z ions	Variables (ions) m/z
Unifferentiated, differentiated	44	m/z 172, m/z 18, m/z 106, m/z 93, m/z 114, m/z 171, m/z 157, m/z 141, m/z 107, m/z 94, m/z 95, m/z 46, m/z 32, m/z 159, m/z 169, m/z 105, m/z 51, m/z 85, m/z 113, m/z 87, m/z 135, m/z 168, m/z 82, m/z 147, m/z 178, m/z 65, m/z 126, m/z 136, m/z 143, m/z 45, m/z 77, m/z 59, m/z 36, m/z 151, m/z 79, m/z 99, m/z 69, m/z 97, m/z 175, m/z 63, m/z 76, m/z 83, m/z 49, m/z 64	45	m/z 18, m/z 33, m/z 114, m/z 93, m/z 72, m/z 125, m/z 107, m/z 102, m/z 86, m/z 90, m/z 32, m/z 159, m/z 60, m/z 41, m/z 105, m/z 51, m/z 87, m/z 173, m/z 168, m/z 88, m/z 96, m/z 147, m/z 65, m/z 126, m/z 68, m/z 45, m/z 77, m/z 59, m/z 36, m/z 179, m/z 81, m/z 54, m/z 92, m/z 78, m/z 35, m/z 104, m/z 153, m/z 69, m/z 129, m/z 177, m/z 101, m/z 67, m/z 63, m/z 76, m/z 43	51	m/z 18, m/z 106, m/z 33, m/z 93, m/z 72, m/z 171, m/z 116, m/z 107, m/z 95, m/z 32, m/z 60, m/z 169, m/z 51, m/z 149, m/z 87, m/z 173, m/z 82, m/z 47, m/z 147, m/z 65, m/z 62, m/z 22, m/z 61, m/z 150, m/z 68, m/z 52, m/z 45, m/z 119, m/z 77, m/z 34, m/z 59, m/z 81, m/z 89, m/z 98, m/z 100, m/z 48, m/z 78, m/z 142, m/z 84, m/z 99, m/z 69, m/z 129, m/z 161, m/z 165, m/z 175, m/z 44, m/z 144, m/z 63, m/z 83, m/z 43, m/z 64
Undifferentiated	14	m/z 167, m/z 154, m/z 173, m/z 47, m/z 162, m/z 68, m/z 81, m/z 30, m/z 78, m/z 84, m/z 58, m/z 176, m/z 177, m/z 101	13	m/z 158, m/z 171, m/z 95, m/z 152, m/z 82, m/z 42, m/z 52, m/z 89, m/z 30, m/z 132, m/z 131, m/z 49, m/z 117	19	m/z 141, m/z 145, m/z 102, m/z 159, m/z 137, m/z 85, m/z 75, m/z 113, m/z 135, m/z 168, m/z 70, m/z 40, m/z 88, m/z 96, m/z 123, m/z 92, m/z 170, m/z 153, m/z 108
Differentiated	21	m/z 33, m/z 133, m/z 102, m/z 112, m/z 41, m/z 88, m/z 111, m/z 62, m/z 71, m/z 61, m/z 123, m/z 52, m/z 119, m/z 121, m/z 89, m/z 48, m/z 100, m/z 153, m/z 165, m/z 67, m/z 31	28	m/z 160, m/z 138, m/z 167, m/z 141, m/z 127, m/z 134, m/z 169, m/z 85, m/z 28, m/z 120, m/z 178, m/z 111, m/z 61, m/z 123, m/z 109, m/z 119, m/z 34, m/z 80, m/z 98, m/z 48, m/z 79, m/z 115, m/z 58, m/z 84, m/z 170, m/z 165, m/z 83, m/z 64	24	m/z 172, m/z 167, m/z 154, m/z 125, m/z 86, m/z 46, m/z 90, m/z 41, m/z 111, m/z 126, m/z 42, m/z 118, m/z 36, m/z 80, m/z 121, m/z 30, m/z 54, m/z 79, m/z 58, m/z 177, m/z 97, m/z 101, m/z 67, m/z 76

The proposed compounds for each variable (ion) (from m/z10 to 180) that showed significant (P< 0.05 or 0.01) difference among groups by ANOVA and decreased or increased in the headspace of undifferentiated and osteo-induced hMSCs during the differentiation in 21% O_2 and 2% O_2 and 2% O_2 WS are listed in Table 4.16.

Table 4. 16. Expected compounds at each protonated mass (m/z) where significant differences in the headspace gases of undifferentiated and differentiated hMSCs media were noted in 21% O_2, 2% O_2 and 2% O_2 WS conditions over the m/z ranges 10 to 180.

Conditions	m/z	ANOVA (p-value)	Diff Vs. Undiff			Proposed compounds
			7 days	14 days	21 days	
21% O_2	m/z 36	0.004	↑	↑	↓	($NH_3.H_3O^+$)
	m/z 45	0.001	↓	↓	↓	(Acetaldehyde, ethanediol (65%), lactic acid (75%), 1,1-dichloroethane (50%))
	m/z 61	0.003	↑	↓	↓	(Propanol, acetic acid)
	m/z 63	0.017	↓	↓	↓	(Carbon dioxide, Ethanediol (35%), ethanethiol, dimethyl sulphide)
	m/z 65	0.001	↓	↑	↑	(ethanol)
	m/z 77	0.044	↓	↑	↑	(Carbon disulphide, thioacetic acid (80%), 1,2-propanediol (5%), 1,3-propanediol (30%)
	m/z 82	0.009	↓	↓	↓	(2,2-difluoro-ethylamine)
	m/z 83	0.001	↑	↑	↓	(4-methyl-1,3-pentadiene, 1,5-pentandial (glutyraldehyde) (30%), hexanal (50%), cyclohexane (50%), water cluster of ethanol)
	m/z 85	0.002	↑	↑	↓	(Trans-2-methyl-2-butenal, trans-2-pentenal, cyclohexane (50%), 1-hexene, trans-2-hexene, Pentanoic acid (10%), trimethylacetic acid (10%), 1-hexanol, 1,2-cyclo-propylether (94%), 1-nonene (20%), trans-2-nonene (15%), 1-decene (15%), hexyl acetate (7%))
	m/z 97	0.001	↓	↓	↑	(fluorobenzene, 2-furancarboxaldehyde, 1,1,1-trichloroethane)
	m/z 99	0.022	↓	↑	↓	(1,2-dichloroethane (10%), cyclohexanone, trans-2-hexenal, cis-3-hexenal (35%), 1-heptene (25%), trans-2-heptene (35%), methylcyclohexane (5%), 1-decene (10%), trichloronitromethane (2%), iso-flurane (10%))
	m/z 101	0.001	↑	↑	↑	(1,5-pentanedial (glutyraldehyde) (50%), Y-valerolactone, 2-hexanone, 3-hexanone, hexanal (50%))
	m/z	0.005	↑	↑	↓	(2-hydroxy butyric acid (95%), 3-hydroxy

	105					butyric acid (95%), 2-isohydroxy butyric acid (>5%), 1,5-pentanediol (10%))
	m/z 111	0.047	↑	↑	↑	(2-fluorotoluene, 4-fluorotoluene, 2-hydroxyphynol, 5-methyl-1,2-furancarboxaldehyde, n-octanal (15%))
	m/z 113	0.015	↓	↓	↑	(Chlorobenzene, trans-2-heptenal, 1-octene (30%), trans-2-octene (35%), 1-octanol (40%), 2-octanol (75%))
2% O_2	m/z 18	0.001	↓	↑	↓	(Ammonia, 2-methylbutylamine (50%), 2-methyl-2-butylamine (90%), 3-methylbutylamine (5%), 3-methyl-2-butylamine (65%), 2-pentylamine (60%), 3-pentylamine (70%))
	m/z 54	0.024	↑	↓	↑	(2-propenenitrile, $NH4^+.2H_2O$)
	m/z 63	0.006	↓	↑	↓	(Carbon dioxide, Ethanediol (35%), ethanethiol, dimethyl sulphide)
	m/z 65	0.032	↓	↑	↑	(ethanol)
	m/z 69	0.012	↓	↓	↑	(Chloromethane, furan, isoprene (2-methyl butadiene), cluster of methanol, cyclopropanecarboxylic acid (10%), 3-methylbutanal (30%), 1-pentanal (25%), myrcene (2%), ocimene (3%))
	m/z 72	0.001	↑	↓	↑	(2-methyl-2-propen-1-amine, N-ethyl-azitidine, Pyrrolidine, N-thylidene-ethanamine, ethyl azide, acrylamide, methoxyacetonitrile, 2-azetidinone)
	m/z 77	0.025	↓	↓	↑	(Carbon disulphide, thioacetic acid (80%), 1,2-propanediol (5%), 1,3-propanediol (30%)
	m/z 81	0.029	↓	↑	↓	(1,1-dichloroethane (50%), 1,2-dichloroethane (35%), cis-3-hexenal (65%), camphene (14%), 2-carene (18%), 3-carene (24%), s-limonene (30%), myrcene (30%), ocimene (25%), α-pinene (39%), β-pinene (40%), α-terpinene (10%), Y-terpinene (16%))
	m/z 82	0.048	↑	↓	↑	(2,2-difluoro-ethylamine)
	m/z 83	0.016	↑	↑	↑	(4-methyl-1,3-pentadiene, 1,5-pentandial (glutyraldehyde) (30%), hexanal (50%), cyclohexane (50%), water cluster of ethanol)
	m/z 101	0.001	↓	↑	↑	(1,5-pentanedial (glutyraldehyde) (50%), Y-valerolactone, 2-hexanone, 3- hexanone, hexanal (50%))
	m/z 105	0.003	↓	↓	↓	(2-hydroxy butyric acid (95%), 3-hydroxy butyric acid (95%), 2-isohydroxy butyric acid (>5%), 1,5-pentanediol (10%))
2% O_2 WS	m/z 33	0.002	↓	↑	↓	(methanol, butyl methyl ether (10%))
	m/z 36	0.0001	↑	↑	↑	($NH_3.H_3O^+$)
	m/z 43	0.0001	↓	↓	↓	(Cyclopropane, pyruvic acid (20%), 1,5-pentanedial (glutyraldehyde) (20%), propyl ether (5%))
	m/z 45	0.028	↑	↓	↑	(Acetaldehyde, ethanediol (65%), lactic acid (75%), 1,1-dichloroethane (50%))
	m/z 48	0.019	↑	↓	↓	(o-methylhydroxylamine)
	m/z 51	0.028	↑	↓	↓	(Water cluster of methanol)

	m/z 54	0.023	↑	↑	↑	(2-propenenitrile, $NH4^{+}.2H_2O$)
	m/z 61	0.001	↑	↓	↓	(acetic acid, methyl formate (95%), 1-propanol (10%), 2-propanol (2-%))
	m/z 69	0.0001	↑	↓	↓	(Chloromethane, furan, isoprene (2-methyl butadiene), cluster of methanol, cyclopropanecarboxylic acid (10%), 3-methylbutanal (30%), 1-pentanal (25%), myrcene (2%), ocimene (3%))
	m/z 77	0.004	↑	↑	↓	(Carbon disulphide, thioacetic acid (80%), 1,2-propanediol (5%), 1,3-propanediol (30%)
	m/z 81	0.03	↑	↓	↑	(1,1-dichloroethane (50%), 1,2-dichloroethane (35%), cis-3-hexenal (65%), camphene (14%), 2-carene (18%), 3-carene (24%), s-limonene (30%), myrcene (30%), ocimene (25%), α-pinene (39%), β-pinene (40%), α-terpinene (10%), Y-terpinene (16%))
	m/z 83	0.04	↑	↓	↑	(4-methyl-1,3-pentadiene, 1,5-pentandial (glutyraldehyde) (30%), hexanal (50%), cyclohexane (50%), water cluster of ethanol)
	m/z 84	0.0001	↑	↓	↑	(2,2-dimethyl-propanenitrile, ter-butyl isocyanide, 4-NH2-pyrazole, 3(5)-aminopyrazole, N,N-dimethyl-2-propyne-1-amine)
	m/z 97	0.015	↑	↑	↓	(fluorobenzene, 2-furancarboxaldehyde, 1,1,1-trichloroethane)

The proposed compounds for each variable (ion) (from m/z10 to 180) that shows significant (P< 0.05 or 0.01) difference among groups by ANOVA and decreased or increased in the headspace of osteo-induced hMSCs (Table 4.17) and undifferentiated hMSCs (Table 4.18) during time-course in 21% O_2 and 2% O_2 and 2% O_2 WS were identified.

Table 4. 17. Expected compounds at each protonated mass (m/z) where significant differences in the headspace gases of osteo-induced hMSCs media were noted in 21% O_2, 2% O_2 and 2% O_2 WS conditions over the m/z ranges 10 to 180.

Conditions	m/z	ANOVA (p-value)	Time-course of differentiation	Proposed compounds
21% O_2	m/z 45	0.004	Increased	(Acetaldehyde, ethanediol (65%), lactic acid (75%), 1,1-dichloroethane (50%))
	m/z 46	0.007	Decreased	(dimethylamine)
	m/z 61	0.001	Decreased	(Propanol, acetic acid)
	m/z 65	0.016	Decreased	(ethanol)
2% O_2	m/z 18	0.002	Decreased	(Ammonia, 2-methylbutylamine (50%), 2-methyl-2-butylamine (90%), 3-methylbutylamine (5%), 3-methyl-2-butylamine (65%), 2-pentylamine (60%), 3-pentylamine (70%))
	m/z 72	0.007	Increased	(2-methyl-2-propen-1-amine, N-ethyl-azitidine, Pyrrolidine, N-thylidene-ethanamine, ethyl azide, acrylamide, methoxyacetonitrile, 2-azetidinone)
	m/z 77	0.033	Increased	(Carbon disulphide, thioacetic acid (80%), 1,2-propanediol (5%), 1,3-propanediol (30%)
	m/z 83	0.012	Increased	(4-methyl-1,3-pentadiene, 1,5-pentandial (glutyraldehyde) (30%), hexanal (50%), cyclohexane (50%), water cluster of ethanol)
	m/z 93	0.019	Decreased	(Toluene)
2% O_2 WS	m/z 36	0.023	Decreased	($NH_3.H_3O^+$)
	m/z 72	0.007	Increased	(2-methyl-2-propen-1-amine, N-ethyl-azitidine, Pyrrolidine, N-thylidene-ethanamine, ethyl azide, acrylamide, methoxyacetonitrile, 2-azetidinone)

Table 4. 18. Expected compounds at each protonated mass (m/z) where significant differences in the headspace gases of undifferentiated hMSCs media were noted in 21% O_2, 2% O_2 and 2% O_2 WS conditions over the m/z ranges 10 to 180.

Conditions	m/z	ANOVA (p-value)	Time-course of differentiation	Proposed compounds
21% O_2	m/z 45	0.004	Increased	(Acetaldehyde, ethanediol (65%), lactic acid (75%), 1,1-dichloroethane (50%))
	m/z 81	0.041	Increased	Cluster of acetaldehyde
	m/z105	0.028	Increased	(2-hydroxy butyric acid (95%), 3-hydroxy butyric acid (95%), 2-isohydroxy butyric acid (>5%), 1,5-pentanediol (10%))
2% O_2	m/z 72	0.007	Increased	(2-methyl-2-propen-1-amine, N-ethyl-azitidine, Pyrrolidine, N-thylidene-ethanamine, ethyl azide, acrylamide, methoxyacetonitrile, 2-azetidinone)
2% O_2 WS	m/z 36	0.0001	Decreased	($NH_3.H_3O^+$)

4.5 Discussion

In this chapter the analysis of volatile organic compounds using full scan (FS) mode of the SIFT-MS technique has been used to compare and differentiate metabolic profiles of classes of stem cells.

In the regulation of cellular metabolism, oxygen plays a role, and it has been studied over long time (Henderson, 1969; Hu et al, 2016). Metabolomic analysis was conducted to characterise the metabolic profile in air oxygen (21% O_2) and physioxic (2% O_2) pluripotent stem cells. The distinctive metabolic profile of air oxygen (21% O_2) and physioxic (2% O_2) hPSCs was successfully demonstrated using OPLS-DA. This study is in agreement with a previous study on MEL2 hES cell that showed the effect of oxygen environment (5% O_2 and 20% O_2) on metabolic profiles and mitochondria using NMR spectroscopy (Less et al., 2015). Furthermore, the alteration of metabolic profile between physioxic and air oxygen HCT 116 cancer cell line have been documented by Frezza et al. who showed the metabolic profile of physioxic cells by using LC-MS (Frezza et al., 2011).

The metabolic profile of hPSCs and their progenitor cells over the time-course of differentiation was also investigated. Several studies reported large metabolic differences between pluripotent stem cells and somatic cells using ^{1}H NMR and LC-MS (Folmes et al., 2011; Panopoulos et al., 2012). A recent study has shown discriminated metabolic profile of human induced pluripotent stem cells from early neural progenitor cells and embryoid bodies during differentiation using GC-MS to investigate VOCs (Capuano et al., 2017). In accordance with these studies, the results presented here show large differences in metabolic profiles between hPSCs and their progenitor cells in air oxygen and physioxic conditions using SIFT-MS.

In conclusion, analysis of volatile organic compounds seems promising in comparing the metabolic profile of hPSCs in normoxic versus physioxic conditions *in vitro*. Furthermore, it seems that VOCs can be used as a distinguishing characteristic profile in the characterisation of hPSCs and their progenitor cells.

MSCs separation techniques generally depend on the pattern expression specific membrane protein markers. As a result, isolation of MSCs requires confirming by the presence or absence of the combination of several antibodies (Zhao et al., 2016). Although several studies have indicated the effect of low oxygen tension on MSCs behaviour and function (Das et al., 2010; Holzwarth et al., 2010; Efimenko et al., 2011; Rosova et al., 2008), this effect has not been exploited for identification of a unique metabolic profile of MSCs. On the basis of MSCs isolation protocol, a mass spectrometry approach was adopted to compare the three oxygen conditions of MSCs derivation here which may affect their isolation. The OPLS-DA score plot from metabolic profile of bone marrow cells and isolated MSCs at each time point suggest that the metabolic profile of 2% O_2 WS cells differs from those in 2% O_2 and 21% O_2 over the time-course of isolation. The spectra differences between 2% O_2 and 21% O_2 cells has been noted from day 14 time point toward suspended MSCs.

A comprehensive analysis of BM-MSCs metabolism during osteogenesis was studied employing three oxygen environments (21% O_2, 2% O_2 and 2% O_2 WS). 21% O_2 was shown to be less effective than 2% O_2 and 2% O_2 WS in inducing hMSCs osteogenesis. Importantly, metabolic profiling revealed differences in the osteogenic effect of three oxygen conditions and proved that cells undergo metabolic alterations before reaching a terminal metabolic state which revealed their degree of differentiation.

Metabolomics comparison of MSCs and *in vitro* osteogenic differentiation of MSCs over time course (OPLS-DA score plot 3D) demonstrated that metabolism has the potential to capture the degree of osteogenic differentiation. Although the variability of osteogenic differentiation depends upon oxygen tension, metabolomics described the overall process of differentiation and showed the stage of cells differentiation. This picture is suggesting that metabolic profiling can be used as a tool for the monitoring of MSCs maintenance and differentiation. Similar studies have been carried out to investigate the effects of different environmental oxygen culture on MSCs during the differentiation. Particularly, Munoz et al. revealed that the osteo-induction of MSCs was successfully carried out in 20% oxygen concentration for 21 days and subsequently cultured under either 21% O_2 or 2% O_2 for further 3 days (Munoz et al., 2014). Jang et al. suggested the metabolomic profiles as biomarkers of MSCs differentiation to monitor chondrogenesis by using nuclear magnetic resonance spectroscopy (Jang et al., 2013). Surrati et al. performed metabolomics of the culture media to monitor osteogenesis of mouse MSCs (Surrati et al., 2016).

In conclusion, the metabolic phenotype of isolated hMSCs outlined here is supportive of the discrimination of isolated MSCs in different oxygen conditions. Moreover, the metabolic profile changes upon osteogenic differentiation at three different oxygen tensions provide a picture for how hMSCs and osteo-induced hMSCs reveal a related metabolic profile, and the individual OPLS-DA score plots revealed clear discrimination between media headspace samples from undifferentiated and osteo-induced hMSCs and a gradual shift of metabolic profile during the differentiation.

Chapter 5-MIM analysis of selected VOCs in the headspace of cells

5.1 Introduction

In the previous chapter, the full scan (FS) mode of SIFT-MS technique was used and the acquired data were analysed using multivariate analysis. The results highlighted the differential metabolic profile associated with cell status.

In this chapter, the multiple ion monitoring (MIM) mode of selected Ion Flow Tube-Mass Spectrometry (SIFT-MS) technique is employed to quantify the metabolites in the headspace of stem cell culture and their progenitor in normoxic and physioxic conditions. Recently, SIFT-MS-based approaches have been employed for the quantification of volatile metabolites of cells above the growth medium (Sule-Suso et al., 2009; Rutter et al., 2013), it is therefore acceptable to use this technique, in which volatile compounds can be analysed using non-invasive measurement.

5.2 Aims:

1. To compare the volatile organic compounds (VOCs) of hPSCs cultured in two different oxygen conditions (21% O_2 and 2% O_2).
2. To investigate the activity of intracellular enzymes (ADH and CYP2E1) within hPSCs.
3. To compare the volatile organic compounds (VOCs) of hPSCs and their progenitor cells in two oxygen conditions (21% O_2 and 2% O_2).
4. To compare the volatile organic compounds (VOCs) of bone marrow-derived mesenchymal stem cells throughout the isolation process in three different oxygen conditions (21% O_2, 2% O_2 and 2% O_2 WS).

5. To compare the volatile organic compounds (VOCs) of MSCs during the time-course of osteogenic differentiation in three different oxygen conditions (21% O_2, 2% O_2 and 2% O_2 WS).

5.3 Materials and Methods:

In order to study volatile organic compounds headspace analysis experiments were performed using multiple ion monitoring (MIM) mode of SIFT-MS (see Section 2.3.3). It is worth mentioning that about $8x10^6$ hPSCs and their progeny were incubated for 24 hours with E8M and KO-DMEM respectively; and the same number of hPSCs was used for quantification of ethanol/acetaldehyde in the presence of the ADH & CYP2E1 enzymes inhibitor (more details in chapter 2).

hMSCs isolation, characterisation and osteo-induction were carried out in three oxygen conditions (21% O_2, 2% O_2 and 2% O_2 WS) (Full methodology in detailed in chapter 2). In order to quantify headspace trace gases of human bone marrow cells (BMCs) and MSCs (see section 2.3.3) it is important to note cell numbers. The numbers of BMCs collected at day 0 were around $7.5x10^6$, while for experimental reasons (using syringe and needle) cell numbers are unknown at days 7 and 14. One-half of the media was aspirated by syringe and needle from the flasks and dispensed straight into sealed glass bottles at day 7 and the second-half at day 14. For suspended hMSCs, cells were counted and $3x10^5$ transferred into the glass bottles.

As the VOCs from plastic tissue culture plate containing media (appendix 2) were examined the concentration of VOCs of incubated media without cells were subtracted (normalised) from the concentration of VOCs of cells exposed media.

5.4 Results:

5.4.1. Quantification of VOCs present in the headspace of hPSCs

A total of 10 volatile compounds (acetone, acetaldehyde, ethanol, butanol, pentanol, DMS/ethanethiol, hexanal, butyric acid, pentene, putresceine) in the headspace of media of three hPSCs cultured in 21% O_2 and 2% O_2 were analysed using MIM mode of the SIFT-MS (Figure 5.1) and (Table 5.1). Following normalisation of incubated media with cells to incubated media without cells a t-test was performed for all volatile organic compounds of two conditions to assess for any differences in the concentration of volatile compounds between 21% O_2 and 2% O_2 conditions.

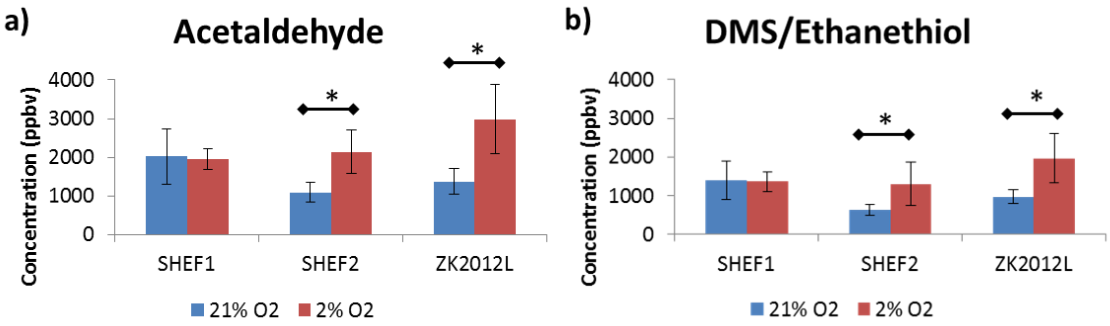

Figure 5. 1. Physioxia effects on the levels of volatile organic compounds in the headspace of SHEF1, SHEF2 and ZK2012L media. Bars represent normalised mean values of compounds for each hPSCs in both air oxygen (21% O_2) (blue bars) and physioxia (2% O_2) (red bars). Error bars represent +/-SD, asterisks represent significance at ($P<0.05$) between 21% O_2 and 2% O_2 conditions. X-axis indicates of hPSCs, and Y-axis indicates of concentration (ppbv) of volatile compounds (a=acetaldehyde, b=DMS/ethanethiol).

Table 5. 1. Summary of mean ± SD for VOCs detected in the headspace of SHEF1, SHEF2 and ZK2012L media in air oxygen (21% O_2) and physioxia (2% O_2). The concentrations are measured in parts per billion by volume (ppbv). The P-values were calculated by t-test.

VOC	Oxygen condition	SHEF1		SHEF2		ZK2012L	
		Mean ± SD	P-value	Mean ± SD	P-value	Mean ± SD	P-value
Acetone	**21%**	162.5 ± 688.4	0.73	18.1 ± 8.4	0.84	6.5 ± 13	0.86
	2%	55.9 ± 205.2		16.1 ± 16.3		5.2 ± 20.6	
Acetaldehyde	**21%**	2021.9 ± 715.4	0.85	1093.6 ± 253.7	0.001	1372.7 ± 329.9	0.001
	2%	1955.5 ± 279.6		2140.5 ± 560.2		2988.4 ± 902.1	
Ethanol	**21%**	22220.3 ± 13208.1	0.03	7848.6 ± 16707.9	0.75	3076.1 ± 3354.8	0.059
	2%	1479.3 ± 1594.8		4277.4 ± 15393.3		-436.1 ± 5795.9	
Butanol	**21%**	261.3 ± 338.8	0.11	84.1 ± 371.6	0.47	110.5 ± 71.6	0.051
	2%	52.3 ± 184.5		-67 ± 156.4		-10.3 ± 63.2	
Pentanol	**21%**	13.6 ± 9.5	0.51	7.1 ± 16	0.54	1.8 ± 16.8	0.14
	2%	12.7 ± 7.6		0.7 ± 13.2		11.9 ± 10	
DMS/Ethanethiol	**21%**	1383.6 ± 497.3	0.91	632.6 ± 138.1	0.03	967.8 ± 178.2	0.01
	2%	1356.7 ± 248.7		1301.3 ±559.5		1960.6 ± 636	
Hexanal	**21%**	240.6 ± 203.7	0.06	98.7 ± 219.3	0.57	-5.4 ± 67.8	0.50
	2%	0.6 ± 39.3		21.5 ± 160.9		23.4 ± 65.3	
Butyric acid	**21%**	1.4 ± 10.5	0.97	5.1 ± 14.2	0.98	2.1 ± 15.8	0.23
	2%	1.3 ± 4.9		5.3 ± 13.6		9 ± 8.8	
Pentene	**21%**	13.7 ± 7.5	0.82	2 ± 2.9	0.06	-0.3 ± 2.7	0.09
	2%	12.8 ± 3.4		-5.3 ± 6.9		3.1 ± 4	
Putresceine	**21%**	2.8 ± 13.5	0.49	6.1 ± 22.4	0.94	4.1 ± 19.5	0.29
	2%	7.2 ± 9.2		5.1 ± 15.3		13.8 ± 23.4	

5.4.2. Quantification of ethanol and acetaldehyde in the headspace of hPSCs treated with ADH and CYP2E1 inhibitor

From interpretation of the analysis above (section 5.4.1) significant increases in Acetaldehyde and DMS/Ethanthiol release were noted in physioxia in two of the three hPSC lines under investigation and comparable levels in the third. Acetaldehyde was then selected as a metabolite to explore further and to determine if its environmental modulation were reflected in altered transcriptional activity.

Having established the non-toxic dosage of 4-MP (section 3.4.5) alteration of headspace concentrations of Ethanol and/or acetaldehyde (Figure 5.2) were investigated to establish the effects of the inhibition of ADH and CYP2E1). The results of the SIFT-MS headspace analysis were again normalised to incubated media. Supplementation of SHEF1, SHEF2 and ZK2012L cultures with 4-MP resulted in increased ethanol headspace concentrations in both 2% and 21% O_2 as compared with untreated cells (Figure 5.2a). Conversely, an overall reduction was observed in acetaldehyde release from treated hPSCs in comparison to untreated cells in both 2% and 21% O_2 conditions (Figure 5.2b). The single exception to this was noted with SHEF2 where acetaldehyde levels in the media of treated SHEF2 was higher than that of untreated in 21% O_2. Furthermore, a significant difference ($p<0.01$) has been noticed between treated and non-treated ZK2012L in 21% O_2 condition.

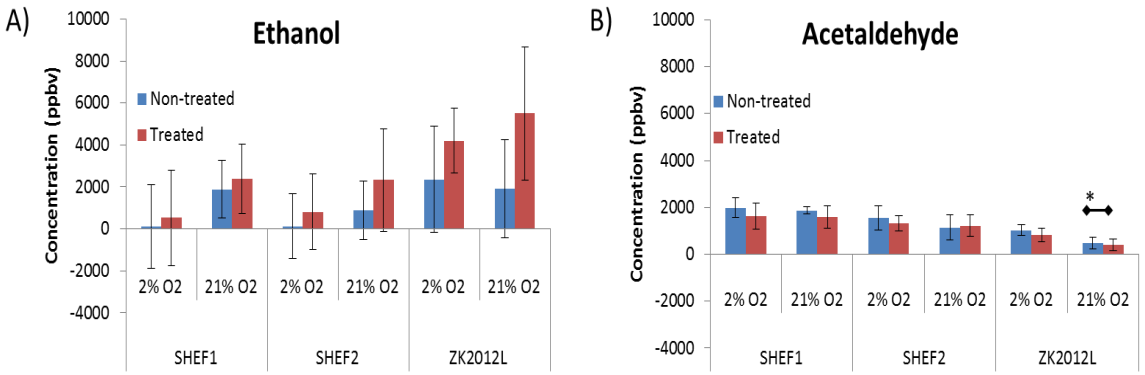

Figure 5. 2. 4-MP induced ethanol and acetaldehyde concentration changes in hPSC headspace. Concentrations of ethanol (A) and acetaldehyde (B), represented in part-per-billion by volume (ppbv) (Y-axis), measured in the headspace of samples of non-treated cells (blue bars) and cells treated with 5 mM 4-MP inhibitor (red bars). In this case the cells were SHEF1, SHEF2 and ZK2012L in both Physioxia (2% O_2) and air oxygen (21% O_2) conditions (X-axis). Error bars indicate +/-SD. Asterisk indicates significant difference between non-treated and 4-MP treated samples at ($P<0.01$).

5.4.3. Quantification of VOCs present in the headspace of hPSCs and their progenitors

A total of 10 volatile compounds (Acetone, acetaldehyde, ethanol, butanol, pentanol, DMS/Ethanethiol, hexanal, butyric acid, pentene, putresceine) in the headspace of hPSCs and their progenitors for each oxygen condition were analysed using MIM mode of the SIFT-MS (Table 5.2, 5.3, 5.4) and (Figure 5.3, 5.4, 5.5). Following normalisation of incubated media with cells to incubated media without cells One-way ANOVA and post-hoc Tukey were performed for all volatile compounds to assess for any difference in concentration over time-course of differentiation and between undifferentiated cells and each time point of differentiation for 21% O_2 and 2% O_2 conditions.

Table 5. 2. Summary of mean ± SD for VOCs detected in the headspace of SHEF1 and their progenitors media in air oxygen (21% O_2) and physioxia (2% O_2). The concentrations are measured in parts per billion by volume (ppbv). The P-values were calculated by ANOVA.

VOCs	Oxygen condition	(0 Day) Mean±SD	(5 Days) Mean±SD	(10 Days) Mean±SD	(20 Days) Mean±SD	ANOVA (P-value)
Acetone	21%	162.5 ± 600.8	-186.1 ± 657.6	486.6 ± 667.9	-372.7 ± 625.1	0.436
	2%	59 ± 177.9	-213. ± 49492.1	-6.9 ± 1053.8	617.6 ± 561.5	0.539
Acetaldehyde	21%	2021.9 ± 662.9	140 ± 188.1	27 ± 168.2	31.5 ± 140.7	0.001
	2%	1955.5 ± 378.7	168 ±185.7	44.6 ± 165.3	30.4 ± 95.4	0.001
Ethanol	21%	22220.2 ± 20639.4	9354.9 ± 14566.4	21562.6 ± 4915.2	6811.2 ± 2226.4	0.203
	2%	617 ± 2371.8	1584.7 ± 3004.5	1935 ± 4001	1622.8 ± 4984.5	0.998
Butanol	21%	261.3 ± 318.5	-1.5 ± 317.8	449.2 ± 95.4	-163.2 ± 274.3	0.097
	2%	67.7 ± 163.4	-41.7 ± 309.2	1.7 ± 396.4	-379.5 ± 226.8	0.271
Pentanol	21%	13.6 ± 11.9	1.7 ± 22	31.8 ± 27.3	-3.6 ± 30.4	0.29
	2%	13.7 ± 7	4.2 ± 21.7	9.7 ± 16.2	-21.3 ± 15.7	0.077
DMS/Ethanethiol	21%	1383.6 ± 473.9	33.8 ± 157.8	21.8 ± 118.2	16.3 ± 98.9	0.001
	2%	1254.3 ± 314.3	40.4 ± 161.4	17.4 ± 133.1	18.4 ± 90.3	0.001
Hexanal	21%	240.6 ± 284.8	-69 ± 224.2	344.3 ± 263.8	-5.6 ± 190.5	0.128
	2%	-2.9 ± 35	-63.4 ± 72.1	-28 ± 57.8	-40.9 ± 12.5	0.43
Butyric acid	21%	1.4 ± 9.1	-1.8 ± 10.4	20 ± 8	-8.5 ± 10.1	0.033
	2%	4.4 ± 8.2	-0.3 ± 10.4	2.2 ± 7.6	-15.5 ± 4.8	0.039
Pentene	21%	13.7 ± 12.8	3.9 ± 13.4	12.8 ± 22.5	5.5 ± 23.5	0.841
	2%	10.4 ± 6.1	5.2 ± 13.6	8.5 ± 10.2	-6.2 ± 16.2	0.234
Putresceine	21%	2.8 ± 12.1	-4.5 ± 13.1	24.8 ± 14.7	-2.6 ± 14.9	0.104
	2%	9.9 ± 10	-0.7 ± 19.7	9.6 ± 13	-16.6 ± 14.9	0.16

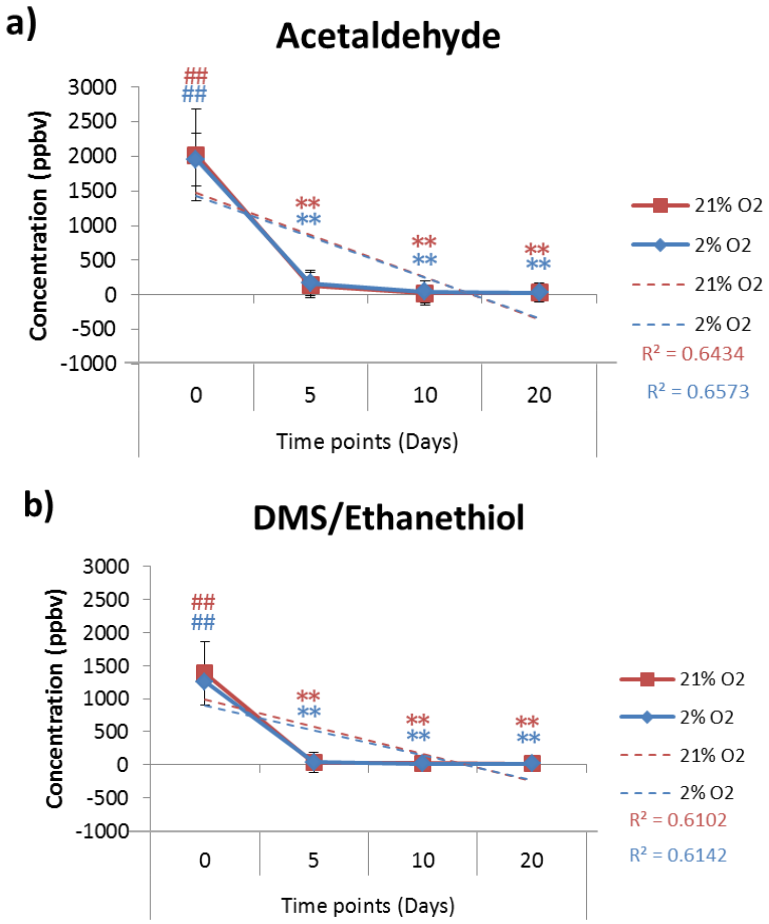

Figure 5. 3. Mean values of volatile organic compounds detected in the headspace of SHEF1 and their progenitors media over time-course of differentiation in air oxygen (21% O_2) and physioxia (2% O_2). Red and blue lines represent mean values of compounds in air oxygen (21% O_2) and physioxia (2% O_2), respectively, over time-course of differentiation. Error bars represent +/-SD. Hatched lines indicate of trendlines for 21% O_2 (red lines) and 2% O_2 (blue lines). Red R-squared and blue R-squared values indicate the correlation coefficient for 21% O_2 and 2% O_2, respectively. X-axis indicates time points (days) of differentiation, and Y-axis indicates concentration (ppbv) of volatile compounds (a=acetaldehyde, b=DMS/ethanethiol).

Table 5. 3. Summary of mean ± SD for VOCs detected in the headspace of SHEF2 and their progenitors media in air oxygen (21% O_2) and physioxia (2% O_2). The concentrations are measured in parts per billion by volume (ppbv). The P-values were calculated by ANOVA.

VOCs	Oxygen condition	(0 Day) Mean±SD	(5 Days) Mean±SD	(10 Days) Mean±SD	(20 Days) Mean±SD	ANOVA (P-value)
Acetone	21%	18.1 ± 8.4	56 ± 41.1	13.7 ± 17.3	16 ± 101.9	0.727
	2%	16.1 ± 16.3	66.5 ± 61.8	-0.08 ± 19.1	40.6 ± 54.1	0.318
Acetaldehyde	21%	1093.6 ± 253.7	-142.6 ± 95.2	-153 ± 161.3	-103 ± 53.8	0.001
	2%	2140.5 ± 560.2	-48.2 ± 40.3	-203.9 ± 215.2	-128 ± 91.5	0.001
Ethanol	21%	7848.6 ± 16707.9	-269 ± 3644.3	9423 ± 9158.4	344.4 ± 2158.4	0.615
	2%	4277.4 ± 15393.2	779.4 ± 2972.3	4707.4 ± 9821.8	407.8 ± 2107.5	0.922
Butanol	21%	84.1 ± 371.6	-35.2 ± 43.1	137.8 ± 109.9	-49 ± 72.1	0.725
	2%	-67 ± 156.4	-45.9 ± 73.8	67.2 ± 119.4	-27.8 ± 45.6	0.493
Pentanol	21%	7.1 ± 16	-11.2 ± 11	-16.9 ± 18.6	7 ± 5.8	0.111
	2%	0.7 ± 13.2	-6.4 ± 8.3	-0.6 ± 14.8	-6.2 ± 12.7	0.833
DMS/Ethanethiol	21%	632.6 ± 138.1	-100.9 ± 61.5	-87.2 ± 149.1	-80.1 ± 24.1	0.001
	2%	1301.3 ± 559.5	-87.9 ± 70.8	-89.8 ± 87.1	-78.5 ± 26.9	0.001
Hexanal	21%	98.7 ± 219.3	31.4 ± 126.1	64.8 ± 93.6	26.1 ± 61.9	0.908
	2%	21.5 ± 160.9	21.3 ± 6.5	39.1 ± 89.4	-12 ± 27.5	0.94
Butyric acid	21%	5.1 ± 14.2	-0.7 ± 9.4	-7.4 ± 15.2	6.8 ± 3	0.466
	2%	5.3 ± 13.6	-5.7 ± 7.7	-2.2 ± 7	-4.2 ± 8.4	0.495
Pentene	21%	2 ± 2.9	-11.7 ± 18.8	-10.5 ± 3.8	0.08 ± 3.4	0.142
	2%	-5.3 ± 6.9	-0.6 ± 12.7	1.8 ± 9.6	-2.1 ± 5.8	0.764
Putresceine	21%	6.1 ± 22.4	9.1 ± 7	-10.8 ± 23.4	-0.1 ± 12.4	0.572
	2%	5.1 ±15.3	-1.6 ± 3.2	6.6 ± 14.8	-0.03 ± 0.4	0.766

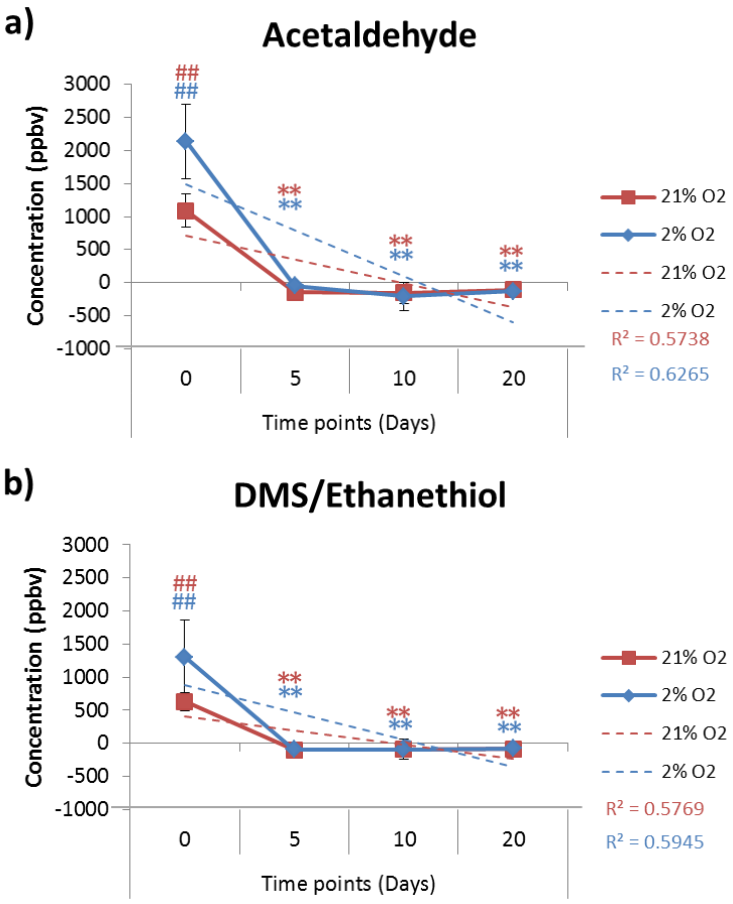

Figure 5. 4. Mean values of volatile organic compounds detected in the headspace of SHEF2 and their progenitors media over time-course of differentiation in air oxygen (21% O_2) and physioxia (2% O_2). Red and blue lines represent mean values of compounds in air oxygen (21% O_2) and physioxia (2% O_2), respectively, over time-course of differentiation. Error bars represent +/-SD. Hatched lines indicate trendlines for 21% O_2 (red lines) and 2% O_2 (blue lines). Red R-squared and blue R-squared values indicate the correlation coefficient for 21% O_2 and 2% O_2, respectively. X-axis indicates time points (days) of differentiation, and Y-axis indicates concentration (ppbv) of volatile compounds (a=acetaldehyde, b=DMS/ethanethiol).

Table 5. 4. Summary of mean ± SD for VOCs detected in the headspace of ZK2012L and their progenitors media in air oxygen (21% O_2) and physioxia (2% O_2). The concentrations are measured in parts per billion by volume (ppbv). The P-values were calculated by ANOVA.

VOCs	Oxygen condition	(0 Day) Mean±SD	(5 Days) Mean±SD	(10 Days) Mean±SD	(20 Days) Mean±SD	ANOVA (P-value)
Acetone	21%	6.5 ± 13	-52.6 ± 76.6	33.1 ± 22	25.3 ± 25	0.077
	2%	5.2 ± 20.6	-164.3 ± 106.4	-116.4 ± 18	-251.5 ± 22.2	0.001
Acetaldehyde	21%	1372.7 ± 329.9	698.4 ± 108.7	570.1 ± 104.6	173.2 ± 89.3	0.001
	2%	2988.4 ± 902.1	391.9 ± 303.2	-3188.5 ± 6277.4	497.1 ± 168.5	0.088
Ethanol	21%	3076.1 ± 3354.8	-15579.6 ± 31142.2	3479.1 ± 3893.1	4717.7 ± 3668.1	0.292
	2%	-436.1 ± 5795.9	6280.5 ± 6731.3	9335 ± 1232.3	16042.8 ± 8970	0.028
Butanol	21%	110.5 ± 71.6	-201.5 ± 410.4	44.6 ± 80.3	-5 ± 60.4	0.237
	2%	-10.3 ± 63.2	-41.4 ± 116.3	-2.5 ± 39.3	-14.2 ± 83.4	0.929
Pentanol	21%	1.8 ± 16.8	5.1 ± 16.2	10 ± 18	15 ± 12.7	0.714
	2%	11.9 ± 10	-8.5 ± 15.1	-16.3 ± 20.2	-7 ± 12.3	0.081
DMS/Ethanethiol	21%	967.8 ± 178.2	463.2 ± 51.2	388.4 ± 57.1	62.6 ± 84	0.001
	2%	1960.6 ± 636	252.4 ± 229.5	-1827.3 ± 3695.9	255.7 ± 74.5	0.075
Hexanal	21%	-5.4 ± 67.8	-247.1 ± 302.7	-60.4 ± 80.6	61.1 ± 151	0.165
	2%	23.4 ± 65.3	67.1 ± 49.6	109.5 ± 40	143 ± 60.5	0.073
Butyric acid	21%	2.1 ± 15.8	8.7 ± 9.9	10.4 ± 17.8	13.3 ± 9.2	0.716
	2%	9 ± 8.8	-3.3 ± 10.8	-14.3 ± 20	-6 ± 12.9	0.148
Pentene	21%	-0.3 ± 2.7	-4.1 ± 7.5	-0.6 ± 2.5	1.7 ± 3.7	0.445
	2%	3.1 ± 4	-5.8 ± 4.8	-2 ± 1.5	-1 ± 1.6	0.036
Putresceine	21%	4.1 ± 19.5	1 ± 7.5	1.4 ± 8.5	6.7 ± 7.3	0.95
	2%	13.8 ± 23.4	2.8 ± 12.4	-33.7 ± 43.8	-6.5 ± 8.6	0.144

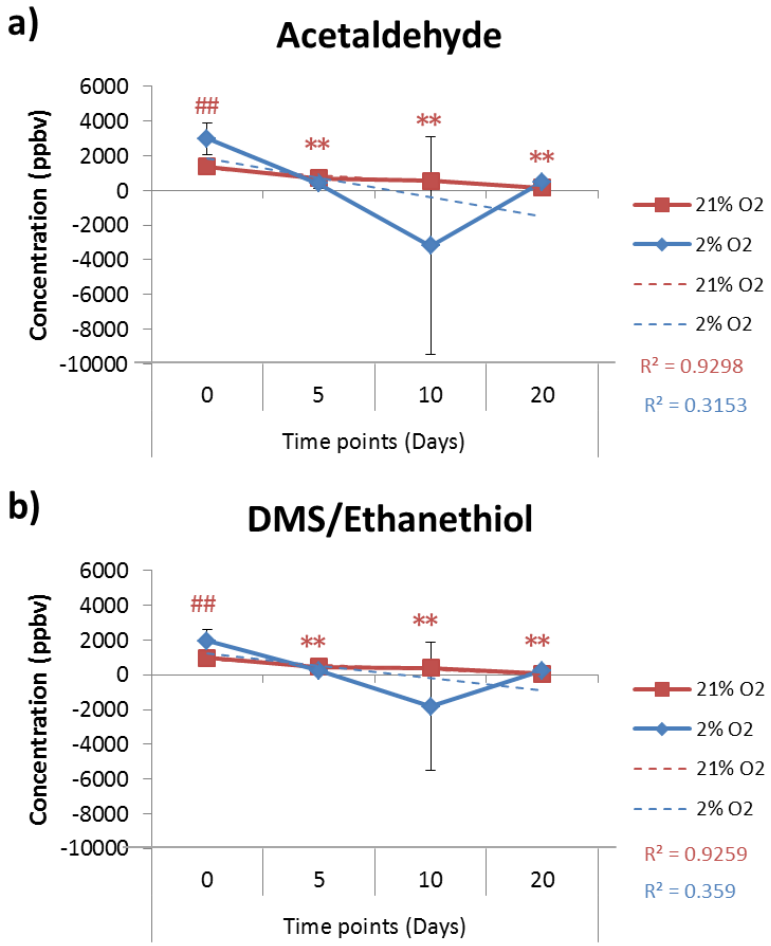

Figure 5. 5. Mean values of volatile organic compounds detected in the headspace of ZK2012L and their progenitors media over time-course of differentiation in air oxygen (21% O_2) and physioxia (2% O_2). Red and blue lines represent mean values of compounds in air oxygen (21% O_2) and physioxia (2% O_2), respectively, over time-course of differentiation. Error bars represent +/-SD. Hatched lines indicate trendlines for 21% O_2 (red lines) and 2% O_2 (blue lines). Red R-squared and blue R-squared values indicate the correlation coefficient for 21% O_2 and 2% O_2, respectively. X-axis indicates time points (days) of differentiation, and Y-axis indicates concentration (ppbv) of volatile compounds (a=acetaldehyde, b=DMS/ethanethiol).

5.4.4. Quantification of VOCs present in the headspace of BMCs and hMSCs across the time-course of isolation

A total of 9 volatile compounds (acetone, acetaldehyde, ethanol, pentanol, DMS/Ethanethiol, hexanal, butyric acid, pentene, putresceine) in the headspace of BMCs and MSCs cultured in 21% O_2 and 2% O_2 were analysed using MIM mode of the SIFT-MS (Table 5.5) (Figure 5.6, 5.7). Following normalisation of incubated media with cells to incubated media without cells in the relevant oxygen condition ANOVA and Post Hoc Tukey were performed for all volatile organic compounds of three conditions to assess for any differences in the concentration of volatile compounds among and between any oxygen conditions.

Table 5. 5. Summary of mean ± SD for VOCs detected in the headspace of BMCs and MSCs media in air oxygen (21% O_2), intermittent physioxia (2% O_2) and physioxia (2% O_2 WS). The concentrations are measured in parts per billion by volume (ppbv). The P-values were calculated by ANOVA.

VOCs	Cells	21% O_2 (Mean ± SD)	2% O_2 (Mean ± SD)	21% O_2 WS (Mean ± SD)	P-value
Acetone	**BMCs (0 Day)**	232.9 ± 476	252.7 ± 442.6	-150.9 ± 129.8	0.32
	BMCs (7 Days)	-447.5 ± 594.2	-46.6 ± 248.8	-77.1 ± 529	0.46
	BMCs (14 Days)	-694 ± 963.5	-898.9 ± 1418.2	-991.8 ± 1546.6	0.96
	Adherent MSCs	527 ± 551.7	540.6 ± 699.6	-341 ± 466.4	0.18
	Suspended MSCs	32.6 ± 75.8	1.9 ± 23.1	-20.3± 18.5	0.40
Acetaldehyde	**BMCs (0 Day)**	-37.1 ± 79	-153.5 ± 58.2	-2286.6± 1969.5	0.09
	BMCs (7 Days)	164.9 ± 161.3	-35.4 ± 83.5	-2071.5± 1894.5	0.03
	BMCs (14 Days)	628.2 ± 238.2	167 ± 777	-36.4 ± 388.6	0.42
	Adherent MSCs	47.6 ± 79.4	24.3 ± 76.5	-1026.4± 2220.6	0.53
	Suspended MSCs	-175.9 ± 220.3	-241.5 ± 212.4	33.7 ± 269.4	0.32
Ethanol	**BMCs (0 Day)**	523.6 ± 2059.5	572.9 ± 1677.7	40069 ± 57924.7	0.32
	BMCs (7 Days)	8473 ± 13931.7	-1840.1 ± 2013	32262.3 ± 28729	0.07
	BMCs (14 Days)	1674.3 ± 7307.4	2011.3 ± 5599.3	64283.6±90487.9	0.26

	Adherent MSCs	7950.6± 13563.4	1052 ± 2488.7	8371.7 ± 8028.5	0.52
	Suspended MSCs	229.2 ± 294.2	186.2 ± 317.6	112.5 ± 203.4	0.86
Pentanol	**BMCs (0 Day)**	-4.4 ± 12.5	-4.3 ± 13.5	-2.4 ± 19.4	0.96
	BMCs (7 Days)	27.8 ± 78.8	-10 ± 29.1	8 ± 18.9	0.61
	BMCs (14 Days)	-41.1 ± 75.1	-42.1 ± 61.3	-52.4 ± 86.2	0.61
	Adherent MSCs	19.9 ± 19	20.8 ± 28.9	-23.6 ± 14.1	0.07
	Suspended MSCs	-4.1 ± 5.8	-1.1 ± 14.2	1 ± 5.9	0.79
DMS/Ethanethiol	**BMCs (0 Day)**	-24.7 ± 33.3	-101.8 ± 37.1	-1467.3 ± 1184.2	0.07
	BMCs (7 Days)	539.7 ± 892.9	-14.1 ± 95.4	-1216.4 ± 1120	0.052
	BMCs (14 Days)	308.5 ± 160.5	155.6 ± 565.5	-92.6 ± 445.1	0.61
	Adherent MSCs	1 ± 104.3	24.3 ± 104.1	-627.2 ± 1397.6	0.56
	Suspended MSCs	-123.8 ± 109.2	-141.5 ± 117.9	-31.6 ± 198	0.578
Hexanal	**BMCs (0 Day)**	32.2 ± 51	24.5 ± 24.2	594.1 ± 654.5	0.19
	BMCs (7 Days)	30.3 ± 59.6	-5.2 ± 16.5	583.5 ± 652.1	0.09
	BMCs (14 Days)	22 ± 38.3	70.1 ± 144	72.4 ± 85.1	0.81
	Adherent MSCs	66.2 ± 119.9	14.1 ± 23.6	113.4 ± 114.8	0.49
	Suspended MSCs	0.1 ± 5.8	-4.4 ± 3.1	0.3 ± 5.7	0.36
Butyric acid	**BMCs (0 Day)**	-7.2 ± 8.4	-1.3 ± 7.4	6 ± 15.6	0.43
	BMCs (7 Days)	4.4 ± 24	-6.9 ± 11.9	5.8 ± 6.4	0.54
	BMCs (14 Days)	-18.6 ± 34	-21.8 ± 27.4	-23.1 ± 36.4	0.98
	Adherent MSCs	3.3 ± 3	4.8 ± 7.3	-14.1 ± 6.6	0.01
	Suspended MSCs	-4.6 ± 4	-8.1 ± 14.4	1.5 ± 4.8	0.44
Pentene	**BMCs (0 Day)**	3.3 ± 4.8	-3.3 ± 10.2	-9.6 ± 3.8	0.32
	BMCs (7 Days)	26.2 ± 61.8	-3.3 ± 22.1	2.3 ± 19.7	0.59
	BMCs (14 Days)	-24.7 ± 45.4	-22.3 ± 37.5	-36.2 ± 49.7	0.93
	Adherent MSCs	18.4 ± 18.6	17.9 ± 24.2	-10.4 ± 10.5	0.17
	Suspended MSCs	0.7 ± 5.7	7.9 ± 3	-0.5 ± 1.4	0.04
Putresceine	**BMCs (0 Day)**	-13.2 ± 13	-3.1 ± 12.3	-20.1 ± 21.6	0.46
	BMCs (7 Days)	14 ± 53	-2.3 ± 10.8	-7.4 ± 13	0.68
	BMCs (14 Days)	-27.3 ± 52	-21.9 ± 52.3	-28.5 ± 39.6	0.98
	Adherent MSCs	3.2 ± 4.8	8.5 ± 15.6	-10.6 ± 19.3	0.32
	Suspended MSCs	-7 ± 12	1.6 ± 8.4	5.4 ± 6.9	0.26

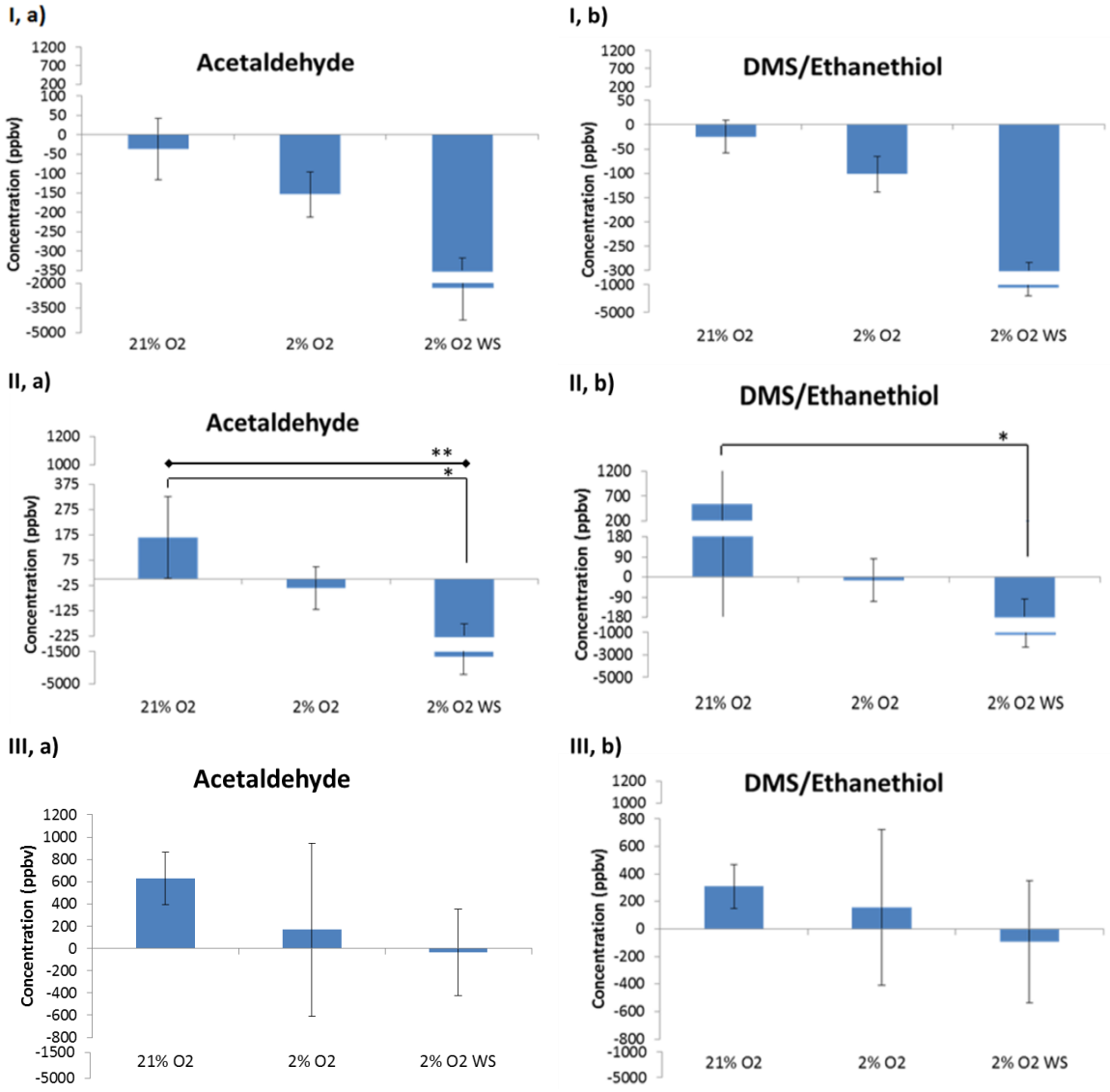

Figure 5. 6. Physioxia effects on the levels of volatile organic compounds in the headspace of BMCs media. Bars represent normalised mean values of compounds for cells in air oxygen (21% O_2) (n=3), intermittent physioxia (2% O_2) (n=3) and Physioxia (2% O_2 WS) (n=3) (X-axis). Error bars represent +/-SD, (*) represent significance at ($P<0.05$) of post-hoc Tukey test and (**) represent significance at ($P<0.05$) of ANOVA test. Y-axis indicates concentration (ppbv) of volatile compounds (a=acetaldehyde, b=DMS/ethanethiol). (I= Day 0, II= Day7, III= Day 14)

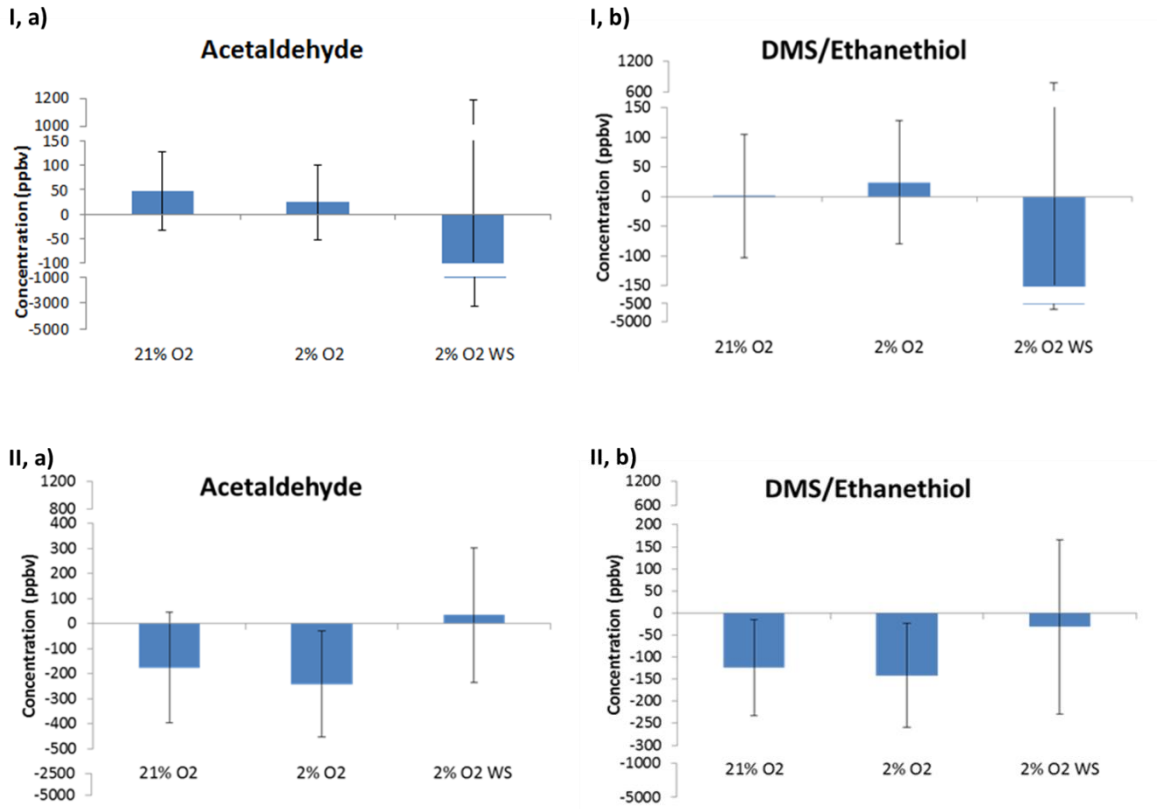

Figure 5. 7. Physioxia effects on the levels of volatile organic compounds in the headspace of MSCs media. Bars represent normalised mean values of compounds for BMCs at day 0 in air oxygen (21% O_2) (n=3), intermittent physioxia (2% O_2) (n=3) and Physioxia (2% O_2 WS) (n=3) (X-axis). Error bars represent +/-SD. Y-axis indicates concentration (ppbv) of volatile compounds (a=acetaldehyde, b=DMS/ethanethiol). (I=adherent MSCs, II=suspended MSCs).

5.4.1 Quantification of VOCs present in the headspace of hMSCs and osteo-induced hMSCs across time-course of differentiation

A total of 9 volatile compounds (acetaldehyde, ethanol, butanol, pentanol, DMS/Ethanethiol, hexanal, butyric acid, pentene, putresceine) in the headspace of media of hMSCs and osteo-induced hMSCs cultured in 21% O_2, 2% O_2 and 2% O_2 WS were analysed using MIM mode of the SIFT-MS (Table 5.6, 5.7, 5.8).and (Figure 5.8). Following normalisation of incubated media with cells to incubated media without cells a t-test was performed for all volatile organic compounds of both hMSCs and osteo-induced hMSCs to assess for any differences in the concentration of volatile compounds between them at each time-point throughout the differentiation.

Table 5. 6. Summary of mean ± SD for those VOCs that were detected in the headspace of hMSCs and osteo-induced hMSCs media over time-course of differentiation in air oxygen (21% O_2). The concentrations are measured in part per billion by volume (ppbv). The P-values were calculated by t-test.

VOCs	Cells	(7 Days) (Mean ± SD)	P-value	(14 Days) (Mean ± SD)	P-value	(21 Days) (Mean ± SD)	P-value
Acetaldehyde	**Undiff**	24 ± 66.5	0.58	192.3 ± 74.9	0.17	393.6 ± 407.4	0.16
	Diff	-7.6 ± 28		63.6 ± 117.7		133.2 ± 194.6	
Ethanol	**Undiff**	115.2 ± 1017	0.09	1409 ± 388.3	0.10	221.4 ± 1278.1	0.67
	Diff	1512.4 ± 719		684.2 ± 578.7		-111.6 ± 453.1	
Butanol	**Undiff**	-9.7 ± 37.8	0.99	-26 ± 53.1	0.33	-9.8 ± 34.3	0.26
	Diff	-9.6 ± 40.1		-52.9 ± 44.5		28.6 ± 9.4	
Pentanol	**Undiff**	-5.3 ± 5.1	0.58	17.5 ± 4.4	0.60	7 ± 1.6	0.74
	Diff	-0.7 ± 7.8		13.1 ± 8.2		4.5 ± 13.1	
DMS/Ethanethiol	**Undiff**	88.4 ± 99.2	0.95	85.5 ± 43.7	0.17	328.1 ± 178.9	0.02
	Diff	93 ± 49.9		-16.2 ± 96.6		215.8 ± 186.9	
Hexanal	**Undiff**	-4.5 ± 17.1	0.21	-19.4 ± 38.6	0.64	0.5 ± 12.7	0.79
	Diff	-34.2 ± 15		-28.8 ± 22		-6.5 ± 30.1	
Butyric acid	**Undiff**	-1.7 ± 3.2	0.96	9 ± 3.2	0.68	1.7 ± 6.9	0.25
	Diff	-1.5 ± 7.8		9.9 ± 2.8		-4.8 ± 0.3	
Pentene	**Undiff**	-4 ± 3.7	0.51	9.4 ± 6.9	0.49	5.9 ± 7.9	0.70
	Diff	1 ± 9.2		3.3 ± 5.9		10.6 ± 14.5	
Putresceine	**Undiff**	-5.2 ± 6.1	0.04	3.6 ± 6.4	0.83	16 ± 13.6	0.56
	Diff	1.6 ± 3.6		2.5 ± 2.2		9.9 ± 11	

Table 5. 7. Summary of mean ± SD for those VOCs that were detected in the headspace of hMSCs and osteo-induced hMSCs media over time-course of differentiation in intermittent physioxia (2% O_2). The concentrations are measured in part per billion by volume (ppbv). The p-values were calculated by t-test.

VOCs	Cells	(7 Days) (Mean ± SD)	P-value	(14 Days) (Mean ± SD)	P-value	(21 Days) (Mean ± SD)	P-value
Acetaldehyde	**Undiff**	10.7 ± 21.5	0.35	-5.6 ± 12.7	0.67	-65.5 ± 33.8	0.85
	Diff	21.8 ± 31.1		0.9 ± 16.3		-71.4 ± 24.4	
Ethanol	**Undiff**	-50.1 ± 222.5	0.20	52.1 ± 267	0.11	-286.2 ± 186.5	0.51
	Diff	96.3 ± 251.1		449.9 ± 106.2		20.1 ± 485.6	
Butanol	**Undiff**	-135.5 ± 4.7	0.95	-53.3 ± 17.7	0.87	-26.9 ± 67.5	0.14
	Diff	-134 ± 44.6		-51.2 ± 17		-76.6 ± 34	
Pentanol	**Undiff**	6.5 ± 8	0.85	-7.9 ± 17.3	0.81	-6.8 ± 14	0.57
	Diff	5.5 ± 2.7		-4.6 ± 4.2		-17.2 ± 20.3	
DMS/Ethanethiol	**Undiff**	21.5 ±	0.93	-54.2 ±22.3	0.80	27.5 ± 28.3	0.20
	Diff	-20 ± 44.5		-42.3 ± 60.8		45.6 ± 37.7	
Hexanal	**Undiff**	-20.5 ± 22.2	0.66	-1.9 ± 9.2	0.67	-8.1 ± 15.3	0.18
	Diff	-29.7 ± 15.7		3 ± 10.5		4.6 ± 8.1	
Butyric acid	**Undiff**	5.3 ± 5.7	0.47	4.3 ± 4.3	0.80	-8.6 ± 6.5	0.94
	Diff	1.4 ± 4.9		3.5 ± 0.29		-9.6 ± 16.4	
Pentene	**Undiff**	1.1 ± 4.1	0.52	-14 ± 14.6	0.72	2.2 ± 8.6	0.18
	Diff	4.5 ± 3.4		-9.4 ± 4.5		-8.3 ± 4	
Putresceine	**Undiff**	9.4 ± 8.2	0.49	3.9 ± 4.8	0.09	-26.8 ± 5.1	0.64
	Diff	4.6 ± 4.3		8.7 ± 2.5		-22.6 ± 9.2	

Table 5. 8. Summary of mean ± SD for those VOCs that were detected in the headspace of hMSCs and osteo-induced hMSCs media over time-course of differentiation in air oxygen (21% O_2). The concentrations are measured in part per billion by volume (ppbv). The P-values were calculated by t-test.

VOCs	Cells	(7 Days) (Mean ± SD)	P-value	(14 Days) (Mean ± SD)	P-value	(21 Days) (Mean ± SD)	P-value
Acetaldehyde	**Undiff**	-60.4 ± 36.8	0.49	-272.2 ± 403.5	0.75	-158.9 ± 132.2	0.06
	Diff	-84.2 ± 13.4		-340.8 ± 77.3		-22.3 ± 116.6	
Ethanol	**Undiff**	-631.2 ± 149.4	0.51	-996.5 ± 394.6	0.08	-264.6 ± 551.9	0.28
	Diff	-557.3 ± 83.5		-297.1 ± 157.3		363.9 ± 280.2	
Butanol	**Undiff**	38 ± 45.9	0.69	-21.3 ± 29.4	0.13	29.8 ± 73.4	0.69
	Diff	50.5 ± 14		-56.5 ± 25.4		-5.6 ± 61.7	
Pentanol	**Undiff**	8.9 ± 13.3	0.42	12 ± 10.7	0.56	-3.9 ± 47.6	0.88
	Diff	4.3 ± 9.4		7.2 ± 11.2		-7.3 ± 18.3	
DMS/Ethanethiol	**Undiff**	44.2 ± 9	0.001	-47.3 ± 285.6	0.78	-110.5 ± 89.9	0.04
	Diff	-2.1 ± 10.3		-97.4 ± 24.9		16.8 ± 77.3	
Hexanal	**Undiff**	9.8 ± 4.9	0.60	-5.5 ± 19	0.47	-12.1 ± 9.3	0.77
	Diff	6 ± 9.2		-11.8 ± 7		-7.8 ± 13.6	
Butyric acid	**Undiff**	7.8 ± 10.3	0.97	5.1 ± 3.4	0.58	-1.6 ± 43	0.46
	Diff	7.7 ± 6.4		2.7 ± 9.3		-20 ± 9.3	
Pentene	**Undiff**	1 ± 4.3	0.12	7.5 ± 8.2	0.78	-2.6 ± 4.3	0.13
	Diff	-4 ± 5.3		4.8 ± 8.9		14.5 ± 11	
Putresceine	**Undiff**	8.1 ± 13	0.98	-3.6 ± 4.7	0.33	16.1 ± 9.3	0.77
	Diff	8.3 ± 6.6		-9.8 ± 4.3		19.2 ± 8	

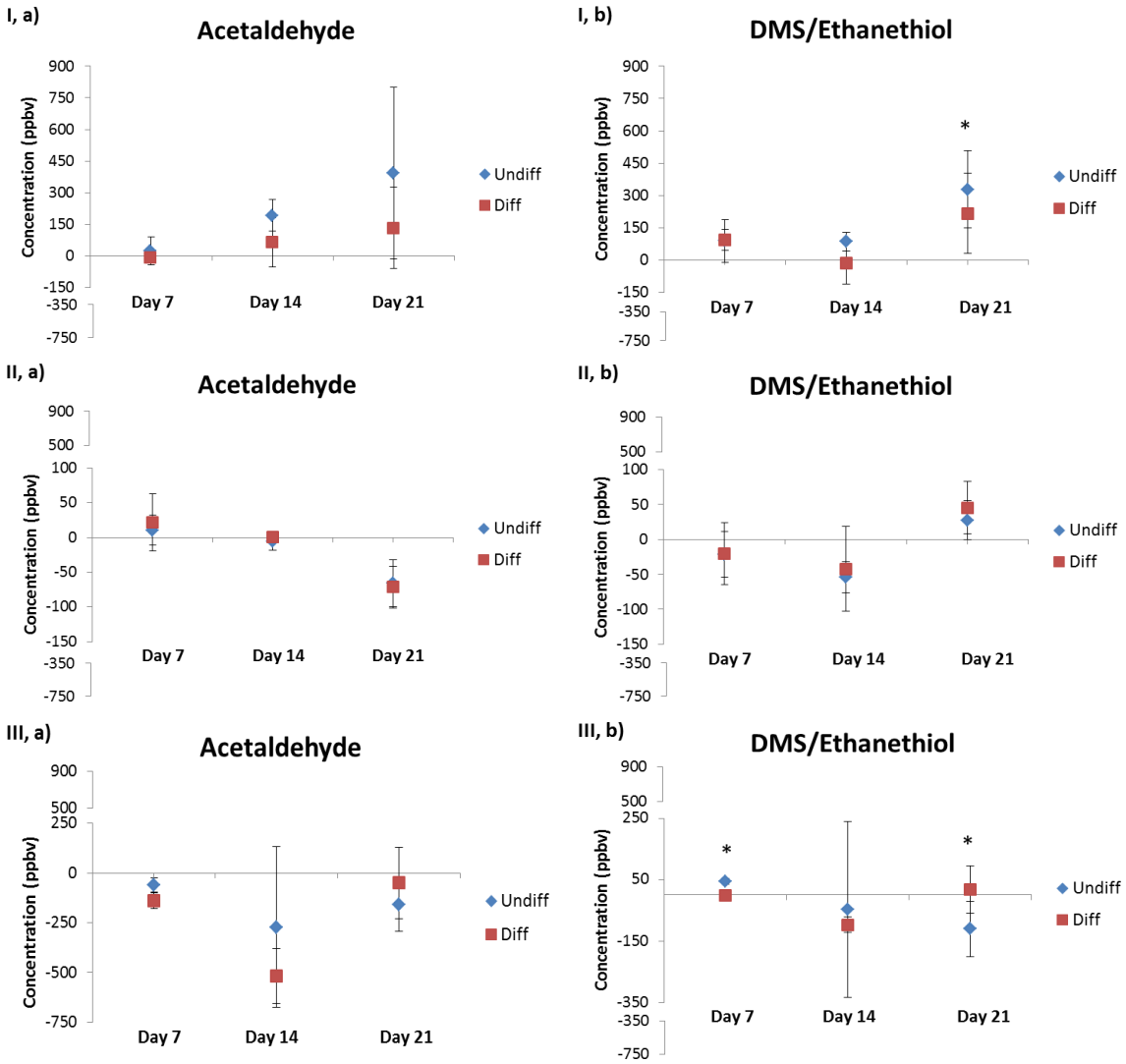

Figure 5. 8. Mean values of volatile organic compounds detected in the headspace of undifferentiated and osteo-induced hMSCs media during differentiation. Diamonds and squares represent normalised mean values of compounds for undifferentiated hMSCs (n=3) and osteo-induced hMSCs (n=3), respectively. Error bars represent +/-SD, asterisks represent significance at ($P<0.05$) between undifferentiated cells and osteo-induced cells. X-axis indicates time-course (days) of differentiation, and Y-axis indicates concentration (ppbv) of volatile compounds. (a=acetaldehyde, b=DMS/ethanethiol). (I= 21% O_2, II=2% O_2, III= 2% O_2 WS).

5.5 Discussion:

In this chapter a further understanding of the cells behaviour can be derived from the targeted analytical approach (MIM mode) of SIFT-MS technique to measure the concentration of different classes of volatile organic compounds and to investigate the biochemical pathways and metabolic changes caused by environment oxygen and induction to differentiate.

Short chain aldehyde, i.e., acetaldehyde, present in the headspace of cell culture media were quantified using SIFT-MS. There is a significant decrease in the mean concentration of acetaldehyde in 21% O_2 condition when comparing with 2% O_2 condition for HSEF2-hESCs and ZK2012L-hiPSCs, while in SHEF1-hESCs an equivalent level is observed in both conditions as shown in figure 4.10. Acetaldehyde has previously been detected in the exhaled human breath (Turner et al., 2006) and in the culture of human lung cancer cell line (Sule-suso et al., 2009; Smith et al., 2003). Until recently, it was believed that acetaldehyde in human cells is a metabolite predominantly from ethanol oxidation by the alcohol dehydrogenase enzyme (Shin et al., 2009), although other studies have also demonstrated that human blood cells metabolise ethanol to acetaldehyde or metabolise it further to acetate in an alcohol dehydrogenase-independent manner (Shin et al., 2009), which can be further metabolised through TCA to produce energy, or these compounds can accumulate in cells (Hernandez et al., 2016). In general, acetaldehyde formation from SHEF1-hESCs in both oxygen conditions was equivalent indicating that ADH was not affect by the oxygen condition, while increasing its level significantly in 2% O_2 as compared with 21% O_2 for SHEF2-hESCs and ZK2012L-hiPSCs was evidence of elevated ADH activity in 2% O_2. Actually, increases in acetate level but not acetaldehyde can be noticed in human plasma after ethanol intake (Hernandez et al., 2016).

VOCs discriminating between air oxygen (21% O_2) and physioxic (2% O_2) undifferentiated pluripotent stem cells have been identified *in vitro*. A combination of two classes of compounds (alcohols and aldehyde), ethanol and acetaldehyde, was able to discriminate between physioxic (2% O_2) and air oxygen (21% O_2) undifferentiated pluripotent stem cells. Acetaldehyde was previously identified by Chippendale and colleagues utilising SIFT-MS, in a model to study the volatile metabolites of the intracellular acetaldehyde dehydrogenase reaction (Chippendale et al., 2012). Crucially, it was observed that the hPSCs, specifically the ADH and CYP2E1 present within the cells, metabolised ethanol and effectively removed it from the media. When the ADH and CYP2E1 enzymes inhibitor 4-methylpyrazole (4-MP) was in the media of cell culture the headspace ethanol increased whereas acetaldehyde reduced, seemingly because the 4-MP concentration was sufficient to inhibit ADH and CYP2E1 oxidizing ethanol to acetaldehyde according to the reaction scheme outlined in Figure 4.11. Moreover, various studies have documented that human embryonic stem cells revealed similar changes in metabolite use in response to environmental oxygen (Christensen et al., 2014; Forristal et al., 2013; Turner et al., 2014).

Acetaldehyde was correlated with the differentiation of hPSCs. The activity of the metabolic pathways for releasing or consuming of acetaldehyde were reduced or activated, respectively, at the onset of differentiation. This finding suggests correlation of acetaldehyde metabolism with the loss of stemness associated with spontaneous differentiation of hPSCs in 21% and 2% O_2.

Human mesenchymal stem cells represent an interesting source of adult stem cells for cell-based therapies and tissue engineering. The effects of different environmental oxygen

concentration on hMSCs have been studied previously, usually comparing air oxygen tension to a single oxygen concentration of physioxia. The controversial effects of physioxic condition on proliferation and differentiation of MSCs have been noted previously, these effects depend on several parameters; including oxygen level, species source of MSCs derived, different tissues, cell density, exposure time to physioxia (Das et al., 2010; Tsai et al., 2012). Under the experimental setting in this chapter, the metabolites were sampled and analysed at different time points during MSCs isolation while comparing between air oxygen (21% O_2) condition and two physioxic conditions (2% O_2 and 2% O_2 WS). In addition, the metabolites of osteogenic induction of MSCs *in vitro* were analysed at different time points during the differentiation.

Acetaldehyde at day 0 was consumed by bone marrow cells in all studied groups, but was the most consumed in 2% O_2 WS. Acetaldehyde was consumed at day 7 in intermittent and uninterrupted physioxia, whereas it was released in 21% O_2. At day 14 cells in 2% O_2 WS consumed acetaldehyde, while it was released in 21% and 2% O_2, but was released more in 21% O_2 than in 2% O_2. For adherent MSCs acetaldehyde was consumed in 2% O_2 WS, while it was released in 21% O_2 and 2% O_2. Conversely, for suspended MSCs, acetaldehyde was changed, being consumed in 21% and 2% O_2 while released in 2% O_2 WS. The changes in acetaldehyde level among different oxygen environments indicate the changes in metabolic pathways of acetaldehyde.

Throughout the time-course of osteo-induction of MSCs the acetaldehyde level in 21% O_2 increased and the difference between MSCs and osteo-induced MSCs increased as well. For both MSCs and osteo-induced MSCs in 2% O_2 acetaldehyde was changed along the time-course, being released at an early time-point and consumed at a late time-point.

Acetaldehyde in 2% O_2 WS was consumed in a fluctuating manner by both cells during the time-course. Indeed, it was shown that, in undifferentiated MSCs, lower consumption occurs at early and middle time-points but higher consumption occurs at a later time-point as compared with osteo-induced MSCs.

During the SIFT-MS measurements, several compounds aside from acetaldehyde were also measured during the analysis. Dimethyl sulphide and/or ethanethiol belong to volatile sulphur compounds were identified and detected in the headspace of cell culture samples. The production of sulphur-containing compounds in humans is attributed to the metabolisation of the sulphur-containing amino acids methionine and cysteine in the transamination pathway (Mochalski et al., 2013). Dimethyl sulphide can be produced via methylation of methanethiol by thiol S-methyl transferase (Tangerman, 2009). The origin of ethanethiol is currently unknown. The results of these experiments showed that SHEF1-hESCs produced are equivalent amount of dimethyl sulphide and/or ethanethiol in both oxygen conditions, whereas SHEF2-hESCs and ZK2012L-hiPSCs produced more dimethyl sulphide and/or ethanethiol in 21% O_2 than in 2% O_2. Thus environmental oxygen influences the amount of detected dimethyl sulphide and/or ethanethiol for both SHEF2-hESCs and ZK2012L-hiPSCs. Thus, the explanation for high level of dimethyl sulphide production may be an increase in enzyme thiol S-methyl transferase activity in 21% O_2.

Dimethyl sulphide and/or ethanethiol were correlated with the differentiation of hPSCs. The activity of the metabolic pathways for releasing or consuming dimethyl sulphide and/or ethanethiol were reduced or activated, respectively, at the beginning of

differentiation. This finding suggests correlation of DMS and/or ethanethiol levels with the loss of stemness associated with spontaneous differentiation in 21% and 2% O_2.

DMS and/or ethanethiol at day 0 was consumed by bone marrow cells in all three groups, but the highest consumption was seen in 2% O_2 WS and the lowest consumption was in 21% O_2. DMS and/or ethanethiol at day 7 was released in 21% O_2, whereas it was consumed in both physioxia groups (2% O_2 and 2% O_2 WS), with more consumption in 2% O_2 WS than in 2% O_2. At day 14 cells consumed DMS and/or ethanethiol in 2% O_2 WS with release in 21% O_2 and 2% O_2, more so in 21% O_2 than 2% O_2. For adherent MSCs DMS and/or ethanethiol was consumed in 2% O_2 WS with release in the other two groups. For suspended MSCs DMS and/or ethanethiol was consumed in all three groups, but consumption was lower in 2% O_2 WS than in 21% O_2 and 2% O_2. The changes in DMS and/or ethanethiol level among different oxygen environment may indicates the changes in metabolic pathways' rate of DMS and/or ethanethiol.

Throughout the time-course of osteo-induction of MSCs the DMS and/or ethanethiol level in 21% O_2 fluctuated and the difference between MSCs and osteo-induced MSCs increased at middle and late time-points. For both MSCs and osteo-induced MSCs in 2% O_2 DMS and/or ethanethiol fluctuated along the time-course. DMS and/or ethanethiol in 2% O_2 WS was changed in a fluctuating manner for osteo-induced MSCs during the time-course, while undifferentiated MSCs showed release it at early time-point and consumption at middle and late time-point. Indeed, it was shown that there are significant differences between undifferentiated MSCs and osteo-induced MSCs at early and late time-points. Further work would be needed to clarify whether proliferation changes or if changes to metabolism could be behind the change in DMS and/or ethanethiol levels.

In conclusion, analysis of volatile organic compounds seems promising in comparing the metabolic pathway of stem cells in normoxic versus physioxic conditions *in vitro*. Furthermore, it seems that VOCs can be used as a distinguishing characteristic profile in the characterisation of stem cells and their progenitor cells.

Chapter 6-Discussion

6.1 Discussion:

Stem cells present great potential in the regeneration of diseased or damaged tissue. In order to best exploit them, knowledge of self-renewal is of special interest over differentiation (Avior et al., 2016). Recent advances in metabolomics analysis will increase our understanding of stem cell self-renewal and differentiation status. Metabolomics has also been utilised to highlight differences in the metabolic profile of different stem cells. Given the differential responses of stem cells to differentiation under normoxic and hypoxic conditions, it would seem appropriate to characterise the metabolic profile of stem cells under a variety of oxygen conditions, to facilitate understanding the metabolism of stem cells self-renewal and differentiation status.

This study has revealed for the first time the utility of a novel, non-invasive sampling method using SIFT-MS for the analysis of two hESC lines and one hiPSC line cultured in two oxygen tensions. Volatile organic compound profile differentiation was achieved between hPSCs cultured in air oxygen (21% O_2) and physioxia (2% O_2) ($p<0.05$).

Each metabolite profile reflects the compounds in the headspace of culture media of cells cultured in different oxygen levels. Therefore, OPLS-DA showed 21% O_2 samples separated from 2% O_2 samples, indicating that the environmental conditions affect the overall metabolic profile of hPSCs. The environmental oxygen affects the metabolic profile of different cells. The metabolic profile of cells gives an indication of the cellular activity and can be thought of as a snapshot of cellular state when cultured in physioxic condition. Variables (m/z) unique to each sampling area were identified, with evidence of important variables from VIP values ≥1. Although variable (m/z) cannot be defined as specific biomarker, most variables attributed to more than one volatile organic species. The

alterations in the overall metabolite profile rather than individual metabolite or a specific metabolic pathway will give a global snapshot of the metabolic status of hPSCs.

Key stages in ethanol metabolism are oxidation catalysed by alcohol dehydrogenase (ADH) and cytochrome P450 2E1 (CYP2E1) (Manzo-Avalos et al., 2010). Based on the SIFT-MS results presented here, ethanol levels were higher for hPSCs in 21% O_2 than those in 2%, while acetaldehyde levels were higher for cells in 2% than those in 21% O_2. Both ADH and CYP2E1 convert ethanol into acetaldehyde (Tuma and Casey, 2003). The presence of ADH and CYP2E1 in hPSCs, cultured in physioxia (2% O_2) and air oxygen (21% O_2), used in this study has been confirmed by RT-PCR. It is possible that 4-methyl pyrazole (4-MP) inhibits the action of these enzymes (Zimatkin et al., 2006). The combined inhibition of ADH and CYP2E1 has affected the activity of these enzymes leading to decreased acetaldehyde levels and increased ethanol levels in the media, although SHEF2 in 21% O_2 did not decrease the acetaldehyde level. Thus, ethanol and/or acetaldehyde compounds are proposed to be volatile biomarkers to discriminate between hPSCs cultured in physioxia and air oxygen conditions.

Stem cell separation techniques rely on the expression of specific surface proteins. As a result, isolation of MSCs requires the combination of several antibodies (Dominici et al., 2006). Although previous report has indicated that MSCs are reside within the hypoxic niches in the bone marrow (Eliasson and Jonsson, 2010), this characteristic has not been exploited for identification of unique metabolic properties of MSCs.

Considering the varying of the environmental oxygen, the metabolic impacts of oxygen on bone marrow cells (BMCs) and mesenchymal stem cells (MSCs) was evaluated. This demonstrated that SIFT-MS metabolomics can discriminate responses of BMCs and MSCs

exposed to different environmental oxygen. Current techniques for assessment and comparison of oxygen rely on the study of the metabolome of BMCs and MSCs.

Each metabolite profile reflects the compounds in the headspace of culture media of cells cultured in different oxygen conditions. Therefore, OPLS-DA showed 21% O_2 samples separated from 2% O_2 samples, indicating that the environmental conditions affect the overall metabolic profile of BMCs and MSCs. Variables (m/z) unique to each sampling area were identified, with evidence of important variables from VIP values ≥1. Due to limitation of the SIFT-MS technique most variables (m/z) cannot be defined as specific biomarker because most variables are attributable to more than one volatile organic species. The changes in the overall metabolite profile rather than individual metabolite or a specific metabolic pathway will give a global snapshot of the metabolic profile of BMCs and MSCs.

The occurrence of metabolic changes was investigated over the 21 days of osteo-induction. The multivariate analysis of metabolite of MSCs during osteo-induction detected changes of metabolite according to MSCs differentiation. Metabolomics examination of hMSCs during the differentiation course yielded a large amount of data. Variables (m/z) unique to each sampling area were identified, with evidence of important variables from VIP values ≥1. Although variable (m/z) cannot be defined as specific biomarker, most variables attributed to more than one volatile organic species. The changes in the overall metabolite profile rather than individual metabolite or a specific metabolic pathway will give a global snapshot of the metabolic status of MSCs and osteo-induced MSCs.

Further investigation showed that many variables (m/z) were downregulated and upregulated during the time-course of differentiation. These putative metabolites were taken forward to narrow down the focus of the analysis.

Utilising of metabolomics profiles as biomarkers of MSCs during the time-course of osteogenic differentiation was also monitored by Surrati et al. (Surrati et al., 2016) who used LC-MS. Nevertheless, that approach is limited due to the fact that extracellular metabolites give only a rough approximation of intracellular metabolism.

Chapter 7-Conclusions and future works

7.1 Conclusions:

The research work presented in this thesis employed a non-invasive online technique for monitoring human cell cultures; particularly those clinically relevant to the field of regenerative medicine. The series of metabolomics experiment carried out is based, is Selected Ion Flow Tube-Mass Spectrometry (SIFT-MS), which is capable of rapidly and accurately measuring the concentration of trace compounds in the headspace of cell cultures media to parts per billion by volume (ppbv) levels. The potential and power of the SIFT-MS technique in the field of medicine, particularly in breath analysis, has been demonstrated by numerous previous studies (Spanel et al., 2011).

In the metabolomics approach a combination of both supervised and unsupervised methods for spectra data analysis have been demonstrated. PCA was employed first to build up a picture of sample variances and determine the outlier samples. Definitive PCA models have then been used for a supervised method, OPLS-DA, for the identification of samples.

SIFT-MS was used for the analysis of the headspace above hPSCs cultured in physioxia (2% O_2) and air oxygen (21% O_2) conditions to investigate how changes to this oxygen environment affected VOCs above the cells. Differences were observed between the SIFT-MS spectra obtained from the headspace cell cultures and the culture media alone, and between cell cultures of 2% O_2 and 21% O_2. A subset of variables and proposed compounds found to be the most responsible for the variation between the two conditions for each hPSCs has been identified. In addition, only acetaldehyde and DMS and/or ethanethiol were found to be changed significantly. The influence of the intracellular alcohol dehydrogenase (ADH) and cytochrome P450 2E1 (CYP 2E1) on the observed acetaldehyde change was investigated in hPSCs (hESCs and hiPSCs) by adding the ADH and CYP2E1 inhibitor 4-methyl pyrazole (4-MP) to the culture media and observing the

increase in the concentration of ethanol and decrease in the concentration of acetaldehyde in the headspace of treated cells when compared with non-treated cells. Indeed the application of the ADH and CYP2E1 inhibitor compound did not change the acetaldehyde level for SHEF2-hESCs in 21% O_2, in some cases causing the acetaldehyde level to increase above the treated cells as a result of catalase mediated oxidation of ethanol to acetaldehyde, a reaction which was not affected by 4-MP. The same chapter continued to investigate VOCs above hPSCs throughout spontaneous differentiation. This measurement was conducted before and during the differentiation of hPSCs. The findings were then exploited for the purpose of monitoring the level of compounds (biomarkers) in the gas phase above the cell culture media of hPSCs and their progenitors. The cultures were monitored at four time-points of the differentiation time-course with the concentration of acetaldehyde and DMS and/or ethanethiol seen to rise in undifferentiated cells and then decline from the first time-point onwards. In addition, the metabolite profiles of the cells were investigated over the time-course of 20 days. The OPLS-DA provided a separation of the cells culture media at different time-points and control media. A subset of variables and proposed compounds were found to be the most responsible for the variation between samples for each hPSC and condition.

SIFT-MS was applied for the analysis of the bone marrow cells over the time course of MSCs isolation in three environmental oxygen as well as isolated hMSCs from bone marrow cells in those conditions. The cultures were monitored at each time-point of the isolation time-course showing changes in the levels of VOCs between cells in different culture conditions. The OPLS-DA provided a separation of the cells culture media at each time-point and for each control media. A subset of variables and proposed compounds were found to be the most responsible for the variation between samples for each time-point over the time-course of isolation.

SIFT-MS was applied to the study of VOCs from hMSCs at different time-points during hMSCs osteo-induction *in vitro*. The OPLS-DA analysis from MSCs in undifferentiated and osteo-induced state provided clear separation between media samples from undifferentiated and osteo-induced cultures at day 14 and 21 in intermittent physioxia (2% O_2) and uninterrupted physioxia (2% O_2 WS) but not in air oxygen (21% O_2). A subset of variables and proposed compounds were found to be the most responsible for the variation between samples for each time-point over the time-course of differentiation. Individual OPLS-DA score plots revealed the metabolic profile of MSCs and osteo-induced MSCs during the time-course of differentiation.

7.2 Future works:

Studies described in this thesis have been conducted with small number of samples as compared to large scale metabolomics studies. Using a large number of samples would minimise the variation, which could potentially otherwise mask the detection of meaningful compounds change linked to the environmental condition and stem cell state.

However, SIFT-MS used for on-line and real-time detection and quantification of volatile compounds without the need for modification of biological samples in headspace analysis, offers immediate analyses. Though GC/LC-MS will remain important techniques for volatile compounds analysis, extensive sample preparation is required before analysis. This limits their potential applications within the biological setting and prevents a bio-sample being analysed in its natural state. The limitations of the SIFT-MS technique are the relatively small number of volatile compounds that can be measured in real-time while; isomeric separation is not feasible. Further combined GC-MS and SIFT-MS experiments to study VOCs above stem cells culture will surely be beneficial in the investigation of biomarkers.

In conclusion, the thesis has answered a majority of the aims for each chapter. This study employed SIFT-MS as a non-invasive and economical technique, confirming the power of SIFT-MS to study the VOCs in the headspace of stem cells and their progenitors. Combined SIFT-MS and stable isotope probing could be used in the future to quantify intracellular metabolites involved at specific stages of differentiation and to investigate specific pathways identified by this study.

Appendices

Appendix 1. Scores plot from OPLS-DA discrimination of SIFT-MS spectra of incubated and unincubated culture media. a) DMEM score plot. b) KO-DMEM score plot. c) Essential 8 Medium score plot. d) DMEM/F12 score plot. for each score plot X-axis, t[2] and Y-axis, t[1], indicate the second and first principal component, respectively. Ellipses represent the 95% confidence intervals for each OPLS-DA score plot. The unincubated media group (n=3), unincubated hypoxic conditioned media group (n=3) are shown as circles and squares, respectively. The 21% O_2 incubated media group (n=3), 2% O_2 incubated media group (n=3), and 2% O_2 incubated hypoxic conditioned media group (n=3) are shown as triangles, inverted triangles and diamonds, respectively.

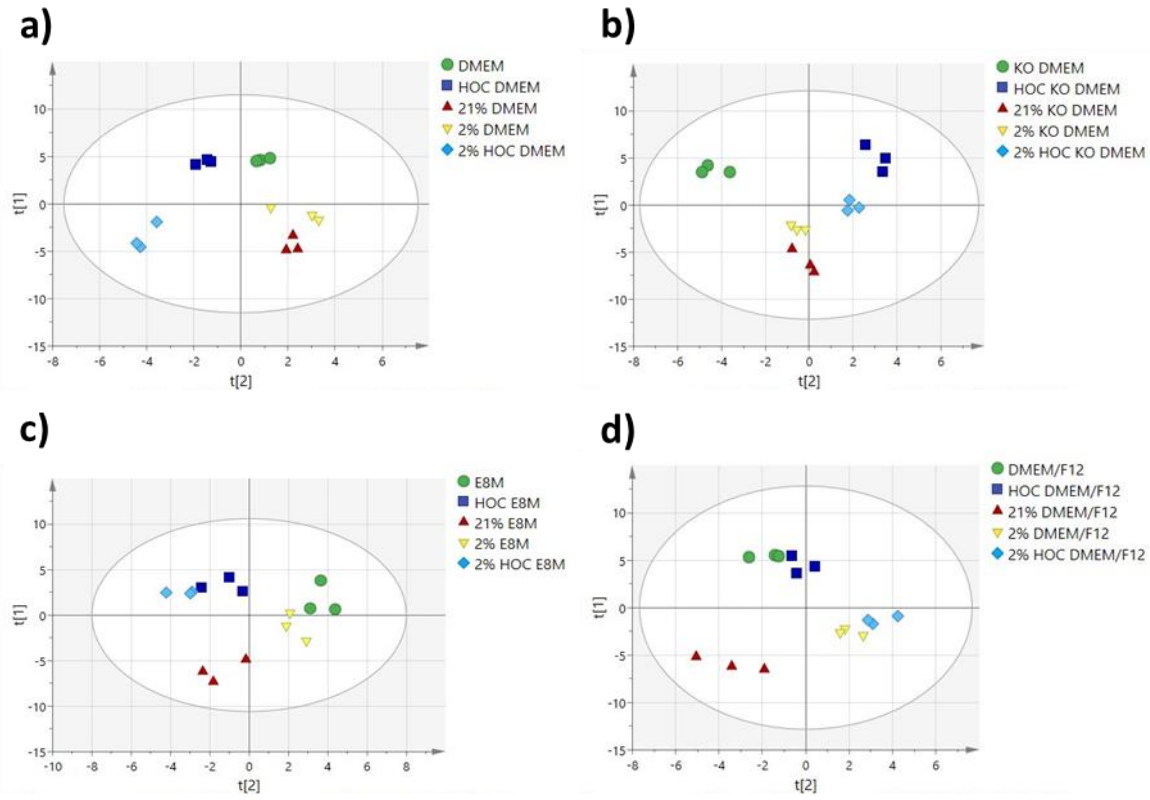

Appendix 2. Tables of quantified VOCs in the headspace of cell culture media

VOCs	Media	Unincubated media (Mean ± SD)	21% O_2 Incubated media (Mean ± SD)	2% O_2 Incubated media (Mean ± SD)	21% O_2 Vs. Control (P-Value)	2% O_2 Vs. Control (P-Value)
Acetone	DMEM	82 ± 48	22.8 ± 0.4	23.6 ± 0.6	0.44	0.66
	KO DMEM	321.4 ± 37.2	46.7 ± 0.8	45.3 ± 5.5	0.006	0.006
	E8M	25 ± 3.1	25.9 ± 5.7	17.5 ± 2.9	0.63	0.02
	DMEM/F12	35.9 ± 7	32.2 ± 1.4	27 ± 12.3	0.4	0.5
Acetaldehyde	DMEM	245.5 ± 55.1	104.1 ± 0.8	102.6 ± 2.5	0.85	0.04
	KO DMEM	589.8 ± 95	94.2 ± 16.1	69.6 ± 10	0.009	0.01
	E8M	119.1 ± 42.8	69.2 ± 14.3	51.3 ± 38.5	0.09	0.01
	DMEM/F12	346.1 ± 33.1	146.3 ± 11.7	62.1 ± 34.1	0.01	0.01
Ethanol	DMEM	1043.6 ±121.3	37516.5 ± 1982.1	29282.9 ± 10587.5	0.001	0.04
	KO DMEM	1148.3 ± 365.2	29059.9 ± 13370.2	11565.6 ± 6427.8	0.07	0.11
	E8M	1191.3 ± 764.5	27816.8 ± 12992	10125.3 ± 6508.9	0.06	0.11
	DMEM/F12	1713.3 ± 182.9	53935.4 ± 9604.7	43696.5 ± 18681.1	0.01	0.06
Butanol	DMEM	131.2 ± 93.9	114.1 ± 72.9	132.4 ± 100.8	0.86	0.98
	KO DMEM	2.5 ± 2.8	39.9 ± 69.1	2.5 ± 4.3	0.46	0.96
	E8M	7.1 ± 12.3	42.4 ± 65	0 ± 0	0.48	0.42
	DMEM/F12	136.8 ± 35.1	311.2 ± 70.8	266.6 ± 258.7	0.08	0.43
Pentanol	DMEM	14.4 ± 6.5	20.1 ± 4.2	17.4 ± 2.7	0.11	0.62
	KO DMEM	19.7 ± 3.6	21.9 ± 14.5	17.5 ± 9.1	0.76	0.58
	E8M	8.2 ± 2.2	19.7 ± 12.9	10.6 ± 6.2	0.2	0.41
	DMEM/F12	4.9 ± 4.8	29.3 ± 5.5	22.6 ± 18.5	0.001	0.16
DMS/Ethanethiol	DMEM	352.4 ± 162.4	260.1 ± 112	160.7 ± 8.5	0.47	0.16
	KO DMEM	402.1 ± 39.3	95.6 ± 30	81.6 ± 21.8	0.001	0.001
	E8M	95.2 ± 15.2	78.2 ± 9.5	62.3 ± 26.3	0.04	0.04
	DMEM/F12	282.5 ± 15.3	157.9 ± 35.1	81.7 ± 22	0.01	0.004
Hexanal	DMEM	12.9 ± 3.9	217.5 ± 44.8	110.4 ± 23.7	0.01	0.01
	KO DMEM	20.5 ± 3.8	464.9 ± 393.4	190.7 ± 166	0.18	0.21
	E8M	20.2 ± 16.8	455.1 ± 392.6	162.2 ± 144.7	0.18	0.19
	DMEM/F12	15.4 ± 7.3	735 ± 74.5	639 ± 466.6	0.004	0.14
Butyric acid	DMEM	5.1 ± 3.5	14.2 ± 3.5	10.8 ± 3.4	0.14	0.11
	KO DMEM	6.9 ± 3.1	12.9 ± 9.9	10.7 ± 4.9	0.28	0.35
	E8M	3.1 ± 2	11.6 ± 8.7	6.3 ± 4.5	0.25	0.34
	DMEM/F12	1.2 ± 0.4	23.2 ± 7.7	16.4 ± 18.3	0.03	0.28
Pentene	DMEM	10.3 ± 4.5	6.3 ± 5.3	7.4 ± 4.6	0.2	0.5
	KO DMEM	14.2 ± 2.6	9.8 ± 5.3	7.3 ± 5.4	0.21	0.12
	E8M	5.6 ± 3.2	8.8 ± 4.6	4.6 ± 2	0.09	0.64
	DMEM/F12	4.1 ± 5	6.3 ± 3.4	6.6 ± 1	0.67	0.5
Putresceine	DMEM	9.1 ± 5.9	13.2 ± 11.2	5.2 ± 5.9	0.71	0.62
	KO DMEM	7.4 ± 0.78	6.8 ± 2.3	6.3 ± 4.1	0.66	0.69
	E8M	2.4 ± 1.5	6.4 ± 4	5.5 ± 2.3	0.28	0.15
	DMEM/F12	1.8 ± 1.9	10.2 ± 3.8	15.6 ± 22.1	0.02	0.41

VOCs	Media	Unincubated media (Mean ± SD)	2% O2 Incubated media (Mean ± SD)	2% O2 Vs. Control (P-Value)
Acetone	HOC DMEM	35.8 ± 2	39.4 ± 11.7	0.64
	HOC KO DMEM	342.8 ± 81.8	114.6 ± 17.9	0.03
	HOC E8M	32.1 ± 4.4	30.8 ± 11.9	0.81
	HOC DMEM/F12	29.3 ± 9.5	32 ± 7.6	0.51
Acetaldehyde	HOC DMEM	351.1 ± 61.6	99.5 ± 26.4	0.01
	HOC KO DMEM	859.6 ± 52.9	263.1 ± 24.2	0.004
	HOC E8M	222.1 ± 33.2	95.5 ± 33.4	0.01
	HOC DMEM/F12	249.9 ± 44.4	55.9 ± 34	0.03
Ethanol	HOC DMEM	2102.1 ± 772.9	32010.5 ± 5626.8	0.008
	HOC KO DMEM	2157.1 ± 396.7	14421.1 ± 3262.7	0.02
	HOC E8M	2946.4 ± 764.9	17820.4 ± 4923.7	0.03
	HOC DMEM/F12	1448.4 ± 28.8	49735.3 ± 22978.6	0.06
Butanol	HOC DMEM	108.8 ± 22.2	164 ± 68.7	0.35
	HOC KO DMEM	61.8 ± 48.6	77.2 ± 13.5	0.52
	HOC E8M	63.1 ± 5.1	58.5 ± 36.4	0.82
	HOC DMEM/F12	50.1 ± 37.2	340.3 ± 296.8	0.22
Pentanol	HOC DMEM	20.5 ± 9.5	25.4 ± 4.8	0.55
	HOC KO DMEM	31.3 ± 3.7	32 ± 13	0.93
	HOC E8M	20 ± 6.6	26.1 ± 10.3	0.13
	HOC DMEM/F12	9.8 ± 4.3	34 ± 10.8	0.02
DMS/Ethanethiol	HOC DMEM	275.3 ± 57.1	142.7 ± 27.6	0.05
	HOC KO DMEM	476.4 ± 17	153 ± 39.2	0.001
	HOC E8M	173 ± 33.3	78.5 ± 20.6	0.09
	HOC DMEM/F12	223.6 ± 15	105.1 ± 24.4	0.006
Hexanal	HOC DMEM	22.9 ± 6.5	218.9 ± 18.5	0.005
	HOC KO DMEM	24.5 ± 13.1	91.6 ± 38.8	0.04
	HOC E8M	28.5 ± 18.6	105 ± 33.1	0.06
	HOC DMEM/F12	16.6 ± 5.3	571.1 ± 299.9	0.08
Butyric acid	HOC DMEM	9.9 ± 3.8	13.5 ± 2.8	0.25
	HOC KO DMEM	15.1 ± 2.3	14.9 ± 9.1	0.97
	HOC E8M	17.1 ± 5.2	21.9 ± 11.7	0.32
	HOC DMEM/F12	4.7 ± 4.4	14.7 ± 6.9	0.02
Pentene	HOC DMEM	11.7 ± 6.4	13.1 ± 3.9	0.82
	HOC KO DMEM	17.8 ± 3	18.8 ± 4.5	0.46
	HOC E8M	2.9 ± 1.5	4.2 ± 3.9	0.69
	HOC DMEM/F12	5.6 ± 2.3	21.4 ± 4.5	0.02
Putresceine	HOC DMEM	6.2 ± 4	3.8 ± 3.3	0.6
	HOC KO DMEM	12.5 ± 4.2	16.5 ± 15.1	0.65
	HOC E8M	29 ± 22.5	9.5 ± 12.8	0.32
	HOC DMEM/F12	6.6 ± 5.7	6.2 ± 4.1	0.94

References

ABAFFY, T., MÖLLER, M., RIEMER, D., MILIKOWSKI, C. and DEFAZIO, R., 2013. Comparative analysis of volatile metabolomics signals from melanoma and benign skin: a pilot study. Metabolomics, 9(5), pp. 998-1008.

ABEYTA, M.J., CLARK, A.T., RODRIGUEZ, R.T., BODNAR, M.S., PERA, R.A.R. and FIRPO, M.T., 2004. Unique gene expression signatures of independently-derived human embryonic stem cell lines. Human molecular genetics, 13(6), pp. 601-608.

ADAMS, N. and SMITH, D., 1976. The selected ion flow tube (SIFT); a technique for studying ion-neutral reactions. International Journal of Mass Spectrometry and Ion Physics, 21(3-4), pp. 349-359.

AFLATOONIAN, B., RUBAN, L., SHAMSUDDIN, S., BAKER, D., ANDREWS, P. and MOORE, H., 2010. Generation of Sheffield (Shef) human embryonic stem cell lines using a microdrop culture system. In Vitro Cellular & Developmental Biology-Animal, 46(3-4), pp. 236-241.

ALLEGRUCCI, C. and YOUNG, L., 2006. Differences between human embryonic stem cell lines. Human reproduction update, 13(2), pp. 103-120.

ALLEN, J., DAVEY, H.M., BROADHURST, D., HEALD, J.K., ROWLAND, J.J., OLIVER, S.G. and KELL, D.B., 2003. High-throughput classification of yeast mutants for functional genomics using metabolic footprinting. Nature biotechnology, 21(6), pp. 692.

ALSALAMEH, S., AMIN, R., GEMBA, T. and LOTZ, M., 2004. Identification of mesenchymal progenitor cells in normal and osteoarthritic human articular cartilage. Arthritis & Rheumatology, 50(5), pp. 1522-1532.

ARNOLD, J.M., CHOI, W.T., SREEKUMAR, A. and MALETIC-SAVATIC, M., 2015. Analytical strategies for studying stem cell metabolism. Frontiers in biology, 10(2), pp. 141-153.

AVIOR, Y., SAGI, I. and BENVENISTY, N., 2016. Pluripotent stem cells in disease modelling and drug discovery. Nature reviews.Molecular cell biology, 17(3), pp. 170.

BAKKENIST, C.J., DRISSI, R., WU, J., KASTAN, M.B. and DOME, J.S., 2004. Disappearance of the telomere dysfunction-induced stress response in fully senescent cells. Cancer research, 64(11), pp. 3748-3752.

BARAN, R., REINDL, W. and NORTHEN, T.R., 2009. Mass spectrometry based metabolomics and enzymatic assays for functional genomics. Current opinion in microbiology, 12(5), pp. 547-552.

BARRY, F., BOYNTON, R.E., LIU, B. and MURPHY, J.M., 2001. Chondrogenic differentiation of mesenchymal stem cells from bone marrow: differentiation-dependent gene expression of matrix components. Experimental cell research, 268(2), pp. 189-200.

BIANCO, P., 2011. Minireview: the stem cell next door: skeletal and hematopoietic stem cell “niches” in bone. Endocrinology, 152(8), pp. 2957-2962.

BOCK, C., KISKINIS, E., VERSTAPPEN, G., GU, H., BOULTING, G., SMITH, Z.D., ZILLER, M., CROFT, G.F., AMOROSO, M.W. and OAKLEY, D.H., 2011. Reference Maps of human ES and iPS cell variation enable high-throughput characterization of pluripotent cell lines. Cell, 144(3), pp. 439-452.

BOESTEN, D.M., DE VOS-HOUBEN, J.M., TIMMERMANS, L., DEN HARTOG, G.J., BAST, A. and HAGEMAN, G.J., 2013. Accelerated aging during chronic oxidative stress: a role for PARP-1. Oxidative medicine and cellular longevity, 2013, pp. 680414.

BOULTING, G.L., KISKINIS, E., CROFT, G.F., AMOROSO, M.W., OAKLEY, D.H., WAINGER, B.J., WILLIAMS, D.J., KAHLER, D.J., YAMAKI, M. and DAVIDOW, L., 2011. A functionally characterized test set of human induced pluripotent stem cells. Nature biotechnology, 29(3), pp. 279-286.

BOURIN, P., BUNNELL, B.A., CASTEILLA, L., DOMINICI, M., KATZ, A.J., MARCH, K.L., REDL, H., RUBIN, J.P., YOSHIMURA, K. and GIMBLE, J.M., 2013. Stromal cells from the adipose tissue-derived stromal vascular fraction and culture expanded adipose tissue-derived stromal/stem cells: a joint statement of the International Federation for Adipose Therapeutics and Science (IFATS) and the International Society for Cellular Therapy (ISCT). Cytotherapy, 15(6), pp. 641-648.

BROWN, M.A., WALLACE, C.S., ANAMELECHI, C.C., CLERMONT, E., REICHERT, W.M. and TRUSKEY, G.A., 2007. The use of mild trypsinization conditions in the detachment of endothelial cells to promote subsequent endothelialization on synthetic surfaces. Biomaterials, 28(27), pp. 3928-3935.

CAMARASA, M.V., GALVEZ, V.M., BRISON, D.R. and BACHILLER, D., 2012. Optimized protocol for derivation of human embryonic stem cell lines. Stem Cell Reviews and Reports, 8(3), pp. 1011-1020.

CAPUANO, R., SPITALIERI, P., TALARICO, R.V., DOMAKOSKI, A.C., CATINI, A., PAOLESSE, R., MARTINELLI, E., NOVELLI, G., SANGIUOLO, F. and DI NATALE, C., 2017. A preliminary analysis of volatile metabolites of human induced pluripotent stem cells along the in vitro differentiation. Scientific reports, 7(1), pp. 1621-017-01790-5.

CAVALLO, C., CUOMO, C., FANTINI, S., RICCI, F., TAZZARI, P.L., LUCARELLI, E., DONATI, D., FACCHINI, A., LISIGNOLI, G. and FORNASARI, P.M., 2011.

Comparison of alternative mesenchymal stem cell sources for cell banking and musculoskeletal advanced therapies. Journal of cellular biochemistry, 112(5), pp. 1418-1430.

CEZAR, G.G., QUAM, J.A., SMITH, A.M., ROSA, G.J., PIEKARCZYK, M.S., BROWN, J.F., GAGE, F.H. and MUOTRI, A.R., 2007. Identification of small molecules from human embryonic stem cells using metabolomics. Stem cells and development, 16(6), pp. 869-882.

CHEN, H., KUO, H., CHEN, W., WU, F., YANG, Y. and HO, H., 2008. A reduced oxygen tension (5%) is not beneficial for maintaining human embryonic stem cells in the undifferentiated state with short splitting intervals. Human reproduction, 24(1), pp. 71-80.

CHEN, X., 2010. Extracellular matrix provides an optimal niche for the maintenance and propagation of mesenchymal stem cells. Birth Defects Research Part C: Embryo Today: Reviews, 90(1), pp. 45-54.

CHENG, A., KAPACEE, Z., PENG, J., LU, S., LUCAS, R.J., HARDINGHAM, T.E. and KIMBER, S.J., 2014. Cartilage repair using human embryonic stem cell-derived chondroprogenitors. Stem cells translational medicine, 3(11), pp. 1287-1294.

CHIPPENDALE, T.W., HU, B., EL HAJ, A.J. and SMITH, D., 2012. A study of enzymatic activity in cell cultures via the analysis of volatile biomarkers. Analyst, 137(20), pp. 4677-4685.

CHRISTENSEN, D.R., CALDER, P.C. and HOUGHTON, F.D., 2014. Effect of oxygen tension on the amino acid utilisation of human embryonic stem cells. Cellular physiology and biochemistry : international journal of experimental cellular physiology, biochemistry, and pharmacology, 33(1), pp. 237-246.

CICIONE, C., MUINOS-LOPEZ, E., HERMIDA-GOMEZ, T., FUENTES-BOQUETE, I., DIAZ-PRADO, S. and BLANCO, F.J., 2013. Effects of severe hypoxia on bone marrow mesenchymal stem cells differentiation potential. Stem cells international, 2013, pp. 232896.

CORREIA, C., SERRA, M., ESPINHA, N., SOUSA, M., BRITO, C., BURKERT, K., ZHENG, Y., HESCHELER, J., CARRONDO, M.J. and ŠARIĆ, T., 2014. Combining hypoxia and bioreactor hydrodynamics boosts induced pluripotent stem cell differentiation towards cardiomyocytes. Stem Cell Reviews and Reports, 10(6), pp. 786-801.

DAS, R., JAHR, H., VAN OSCH, G.J. and FARRELL, E., 2009. The role of hypoxia in bone marrow–derived mesenchymal stem cells: considerations for regenerative medicine approaches. Tissue Engineering Part B: Reviews, 16(2), pp. 159-168.

DATTA, N., HOLTORF, H.L., SIKAVITSAS, V.I., JANSEN, J.A. and MIKOS, A.G., 2005. Effect of bone extracellular matrix synthesized in vitro on the osteoblastic differentiation of marrow stromal cells. Biomaterials, 26(9), pp. 971-977.

DAVIES, S., ŠPANEL, P. and SMITH, D., 2001. A new ‘online’method to measure increased exhaled isoprene in end-stage renal failure. Nephrology Dialysis Transplantation, 16(4), pp. 836-839.

DAWN, B. and BOLLI, R., 2005. Adult bone marrow–derived cells: regenerative potential, plasticity, and tissue commitment. Basic research in cardiology, 100(6), pp. 494-503.

DELANY, A.M., AMLING, M., PRIEMEL, M., HOWE, C., BARON, R. and CANALIS, E., 2000. Osteopenia and decreased bone formation in osteonectin-deficient mice. The Journal of clinical investigation, 105(7), pp. 915-923.

DELLATORE, S.M., GARCIA, A.S. and MILLER, W.M., 2008. Mimicking stem cell niches to increase stem cell expansion. Current opinion in biotechnology, 19(5), pp. 534-540.

DENERY, J.R., NUNES, A.A., HIXON, M.S., DICKERSON, T.J. and JANDA, K.D., 2010. Metabolomics-based discovery of diagnostic biomarkers for onchocerciasis. PLoS neglected tropical diseases, 4(10), pp. e834.

DENG, C., LI, N. and ZHANG, X., 2004. Development of headspace solid-phase microextraction with on-fiber derivatization for determination of hexanal and heptanal in human blood. Journal of Chromatography B, 813(1), pp. 47-52.

DIGIROLAMO, C.M., STOKES, D., COLTER, D., PHINNEY, D.G., CLASS, R. and PROCKOP, D.J., 1999. Propagation and senescence of human marrow stromal cells in culture: a simple colony-forming assay identifies samples with the greatest potential to propagate and differentiate. British journal of haematology, 107(2), pp. 275-281.

DOMINICI, M., LE BLANC, K., MUELLER, I., SLAPER-CORTENBACH, I., MARINI, F., KRAUSE, D., DEANS, R., KEATING, A., PROCKOP, D. and HORWITZ, E., 2006. Minimal criteria for defining multipotent mesenchymal stromal cells. The International Society for Cellular Therapy position statement. Cytotherapy, 8(4), pp. 315-317.

DUNN, W.B., BROADHURST, D.I., ATHERTON, H.J., GOODACRE, R. and GRIFFIN, J.L., 2011. Systems level studies of mammalian metabolomes: the roles of mass spectrometry and nuclear magnetic resonance spectroscopy. Chemical Society Reviews, 40(1), pp. 387-426.

ECKFELDT, C.E., MENDENHALL, E.M. and VERFAILLIE, C.M., 2005. The molecular repertoire of the'almighty'stem cell. Nature reviews.Molecular cell biology, 6(9), pp. 726.

EFIMENKO, A., STAROSTINA, E., KALININA, N. and STOLZING, A., 2011. Angiogenic properties of aged adipose derived mesenchymal stem cells after hypoxic conditioning. Journal of translational medicine, 9(1), pp. 10.

ELIASSON, P. and JÖNSSON, J., 2010. The hematopoietic stem cell niche: low in oxygen but a nice place to be. Journal of cellular physiology, 222(1), pp. 17-22.

ERICES, A., CONGET, P. and MINGUELL, J.J., 2000. Mesenchymal progenitor cells in human umbilical cord blood. British journal of haematology, 109(1), pp. 235-242.

EVANS, M.J. and KAUFMAN, M.H., 1981. Establishment in culture of pluripotential cells from mouse embryos. Nature, 292(5819), pp. 154-156.

EZASHI, T., DAS, P. and ROBERTS, R.M., 2005. Low O_2 tensions and the prevention of differentiation of hES cells. Proceedings of the National Academy of Sciences of the United States of America, 102(13), pp. 4783-4788.

FERNANDES, T.G., DIOGO, M.M., FERNANDES-PLATZGUMMER, A., DA SILVA, C.L. and CABRAL, J.M., 2011. Effect of hypoxia on proliferation and neural commitment of embryonic stem cells at different stages of pluripotency, Bioengineering (ENBENG), 2011. ENBENG 2011. 1st Portuguese Meeting in 2011, IEEE, pp. 1-4.

FICKERT, S., FIEDLER, J. and BRENNER, R., 2003. Identification, quantification and isolation of mesenchymal progenitor cells from osteoarthritic synovium by fluorescence automated cell sorting. Osteoarthritis and cartilage, 11(11), pp. 790-800.

FIEHN, O., 2001. Combining genomics, metabolome analysis, and biochemical modelling to understand metabolic networks. Comparative and Functional Genomics, 2(3), pp. 155-168.

FILIPIAK, W., MOCHALSKI, P., FILIPIAK, A., AGER, C., CUMERAS, R., E DAVIS, C., AGAPIOU, A., UNTERKOFLER, K. and TROPPMAIR, J., 2016. A Compendium of Volatile Organic Compounds (VOCs) Released By Human Cell Lines. Current medicinal chemistry, 23(20), pp. 2112-2131.

FILIPIAK, W., SPONRING, A., FILIPIAK, A., AGER, C., SCHUBERT, J., MIEKISCH, W., AMANN, A. and TROPPMAIR, J., 2010. TD-GC-MS analysis of volatile metabolites of human lung cancer and normal cells in vitro. Cancer epidemiology, biomarkers & prevention : a publication of the American Association for Cancer Research, cosponsored by the American Society of Preventive Oncology, 19(1), pp. 182-195.

FOLMES, C.D., NELSON, T.J., MARTINEZ-FERNANDEZ, A., ARRELL, D.K., LINDOR, J.Z., DZEJA, P.P., IKEDA, Y., PEREZ-TERZIC, C. and TERZIC, A., 2011. Somatic oxidative bioenergetics transitions into pluripotency-dependent glycolysis to facilitate nuclear reprogramming. Cell metabolism, 14(2), pp. 264-271.

FORRISTAL, C.E., CHRISTENSEN, D.R., CHINNERY, F.E., PETRUZZELLI, R., PARRY, K.L., SANCHEZ-ELSNER, T. and HOUGHTON, F.D., 2013. Environmental oxygen tension regulates the energy metabolism and self-renewal of human embryonic stem cells. PloS one, 8(5), pp. e62507.

FORRISTAL, C.E., WRIGHT, K.L., HANLEY, N.A., OREFFO, R.O.C. and HOUGHTON, F.D., 2010. Hypoxia inducible factors regulate pluripotency and proliferation in human embryonic stem cells cultured at reduced oxygen tensions. Reproduction (Cambridge, England), 139(1), pp. 85-97.

FORSYTH, N.R., MUSIO, A., VEZZONI, P., SIMPSON, A.H., NOBLE, B.S. and MCWHIR, J., 2006. Physiologic oxygen enhances human embryonic stem cell clonal

recovery and reduces chromosomal abnormalities. Cloning And Stem Cells, 8(1), pp. 16-23.

FREZZA, C., ZHENG, L., TENNANT, D.A., PAPKOVSKY, D.B., HEDLEY, B.A., KALNA, G., WATSON, D.G. and GOTTLIEB, E., 2011. Metabolic profiling of hypoxic cells revealed a catabolic signature required for cell survival. PloS one, 6(9), pp. e24411.

FRIDMAN, E. and PICHERSKY, E., 2005. Metabolomics, genomics, proteomics, and the identification of enzymes and their substrates and products. Current opinion in plant biology, 8(3), pp. 242-248.

FRIEDMAN, M.S., LONG, M.W. and HANKENSON, K.D., 2006. Osteogenic differentiation of human mesenchymal stem cells is regulated by bone morphogenetic protein-6. Journal of cellular biochemistry, 98(3), pp. 538-554.

FRIEEDENSTEIN, A., PETRAKOVA, K., KUROLESOVA, A. and FROLOVA, G., 1968. Hetrotopic of bone marrow. Analysis of precursor cells for osteogenic and hematopoetic tissue. Transplantacion., 6(2), pp. 230.

FUJIMAKI, S., MACHIDA, M., HIDAKA, R., ASASHIMA, M., TAKEMASA, T. and KUWABARA, T., 2013. Intrinsic ability of adult stem cell in skeletal muscle: an effective and replenishable resource to the establishment of pluripotent stem cells. Stem cells international, 2013, pp. 420164.

GANG, E.J., JEONG, J.A., HONG, S.H., HWANG, S.H., KIM, S.W., YANG, I.H., AHN, C., HAN, H. and KIM, H., 2004. Skeletal myogenic differentiation of mesenchymal stem cells isolated from human umbilical cord blood. Stem cells, 22(4), pp. 617-624.

GUZY, R.D. and SCHUMACKER, P.T., 2006. Oxygen sensing by mitochondria at complex III: the paradox of increased reactive oxygen species during hypoxia. Experimental physiology, 91(5), pp. 807-819.

HAASTERS, F., PRALL, W.C., ANZ, D., BOURQUIN, C., PAUTKE, C., ENDRES, S., MUTSCHLER, W., DOCHEVA, D. and SCHIEKER, M., 2009. Morphological and immunocytochemical characteristics indicate the yield of early progenitors and represent a quality control for human mesenchymal stem cell culturing. Journal of anatomy, 214(5), pp. 759-767.

HAKIM, F., KAITSUKA, T., RAEED, J.M., WEI, F.Y., SHIRAKI, N., AKAGI, T., YOKOTA, T., KUME, S. and TOMIZAWA, K., 2014. High oxygen condition facilitates the differentiation of mouse and human pluripotent stem cells into pancreatic progenitors and insulin-producing cells. The Journal of biological chemistry, 289(14), pp. 9623-9638.

HANAI, Y., SHIMONO, K., MATSUMURA, K., VACHANI, A., ALBELDA, S., YAMAZAKI, K., BEAUCHAMP, G.K. and OKA, H., 2012. Urinary volatile compounds as biomarkers for lung cancer. Bioscience, biotechnology, and biochemistry, 76(4), pp. 679-684.

HASS, R., KASPER, C., BÖHM, S. and JACOBS, R., 2011. Different populations and sources of human mesenchymal stem cells (MSC): a comparison of adult and neonatal tissue-derived MSC. Cell Communication and Signaling, 9(1), pp. 12.

HENDERSON, A.R., 1969. Biochemistry of hypoxia: current concepts. I. An introduction to biochemical pathways and their control. British journal of anaesthesia, 41(3), pp. 245-250.

HERBIG, U., JOBLING, W.A., CHEN, B.P., CHEN, D.J. and SEDIVY, J.M., 2004. Telomere shortening triggers senescence of human cells through a pathway involving ATM, p53, and p21 CIP1, but not p16 INK4a. Molecular cell, 14(4), pp. 501-513.

HERNÁNDEZ, J.A., LÓPEZ-SÁNCHEZ, R.C. and RENDÓN-RAMÍREZ, A., 2016. Lipids and oxidative stress associated with ethanol-induced neurological damage. Oxidative medicine and cellular longevity, 2016.

HOFFMAN, L.M. and CARPENTER, M.K., 2005. Characterization and culture of human embryonic stem cells. Nature biotechnology, 23(6), pp. 699.

HOLLYWOOD, K., BRISON, D.R. and GOODACRE, R., 2006. Metabolomics: current technologies and future trends. Proteomics, 6(17), pp. 4716-4723.

HOLZWARTH, C., VAEGLER, M., GIESEKE, F., PFISTER, S.M., HANDGRETINGER, R., KERST, G. and MÜLLER, I., 2010. Low physiologic oxygen tensions reduce proliferation and differentiation of human multipotent mesenchymal stromal cells. BMC cell biology, 11(1), pp. 11.

HOLZWARTH, C., VAEGLER, M., GIESEKE, F., PFISTER, S.M., HANDGRETINGER, R., KERST, G. and MÜLLER, I., 2010. Low physiologic oxygen tensions reduce proliferation and differentiation of human multipotent mesenchymal stromal cells. BMC cell biology, 11(1), pp. 11.

HU, B.Y., WEICK, J.P., YU, J., MA, L.X., ZHANG, X.Q., THOMSON, J.A. and ZHANG, S.C., 2010. Neural differentiation of human induced pluripotent stem cells follows developmental principles but with variable potency. Proceedings of the National Academy of Sciences of the United States of America, 107(9), pp. 4335-4340.

HU, C., FAN, L., CEN, P., CHEN, E., JIANG, Z. and LI, L., 2016. Energy Metabolism Plays a Critical Role in Stem Cell Maintenance and Differentiation. International Journal Of Molecular Sciences, 17(2), pp. 253-253.

HUBACEK, J. and POLEDNE, R., 1999. The Common cDNA and Amino Acid Sequences of the CD14 (Myeloid Cell-Specific Leucine-Rich Glycoprotein) Receptor.

HUNG, S., POCHAMPALLY, R.R., HSU, S., SANCHEZ, C., CHEN, S., SPEES, J. and PROCKOP, D.J., 2007. Short-term exposure of multipotent stromal cells to low oxygen increases their expression of CX3CR1 and CXCR4 and their engraftment in vivo. PloS one, 2(5), pp. e416.

IM, G., 2015. Stem cells for reutilization in bone regeneration. Journal of cellular biochemistry, 116(4), pp. 487-493.

IN 'T ANKER, P.S., NOORT, W.A., SCHERJON, S.A., KLEIJBURG-VAN DER KEUR, C., KRUISSELBRINK, A.B., VAN BEZOOIJEN, R.L., BEEKHUIZEN, W., WILLEMZE, R., KANHAI, H.H. and FIBBE, W.E., 2003. Mesenchymal stem cells in human second-trimester bone marrow, liver, lung, and spleen exhibit a similar immunophenotype but a heterogeneous multilineage differentiation potential. Haematologica, 88(8), pp. 845-852.

IN 'T ANKER, P.S., SCHERJON, S.A., KLEIJBURG-VAN DER KEUR, C., DE GROOT-SWINGS, G.M., CLAAS, F.H., FIBBE, W.E. and KANHAI, H.H., 2004. Isolation of mesenchymal stem cells of fetal or maternal origin from human placenta. Stem cells (Dayton, Ohio), 22(7), pp. 1338-1345.

JAISWAL, N., HAYNESWORTH, S.E., CAPLAN, A.I. and BRUDER, S.P., 1997. Osteogenic differentiation of purified, culture-expanded human mesenchymal stem cells in vitro. Journal of cellular biochemistry, 64(2), pp. 295-312.

JANG, M., CHUN, S., MUN, C., HONG, K.S. and SHIN, J., 2013. Evaluation of metabolomic changes as a biomarker of chondrogenic differentiation in 3D-cultured human mesenchymal stem cells using proton (1H) nuclear magnetic resonance spectroscopy. PloS one, 8(10), pp. e78325.

JEŽ, M., ROŽMAN, P., IVANOVIĆ, Z. and BAS, T., 2015. Concise review: the role of oxygen in hematopoietic stem cell physiology. Journal of cellular physiology, 230(9), pp. 1999-2005.

JIANG, B.H., SEMENZA, G.L., BAUER, C. and MARTI, H.H., 1996. Hypoxia-inducible factor 1 levels vary exponentially over a physiologically relevant range of O_2 tension. The American Journal of Physiology, 271(4), pp. C1172-C1180.

JING, D., WOBUS, M., POITZ, D.M., BORNHAUSER, M., EHNINGER, G. and ORDEMANN, R., 2012. Oxygen tension plays a critical role in the hematopoietic microenvironment in vitro. Haematologica, 97(3), pp. 331-339.

KAY, A.G., DALE, T.P., AKRAM, K.M., MOHAN, P., HAMPSON, K., MAFFULLI, N., SPITERI, M.A., EL HAJ, A.J. and FORSYTH, N.R., 2015. BMP2 repression and optimized culture conditions promote human bone marrow-derived mesenchymal stem cell isolation. Regenerative medicine, 10(2), pp. 109-125.

KHOSLA, S., WESTENDORF, J.J. and OURSLER, M.J., 2008. Building bone to reverse osteoporosis and repair fractures. The Journal of clinical investigation, 118(2), pp. 421-428.

KIM, J.Y., PARK, J.Y., KIM, O.Y., HAM, B.M., KIM, H., KWON, D.Y., JANG, Y. and LEE, J.H., 2010. Metabolic profiling of plasma in overweight/obese and lean men using ultra performance liquid chromatography and Q-TOF mass spectrometry (UPLC− Q-TOF MS). Journal of proteome research, 9(9), pp. 4368-4375.

KIM, J., KIM, S., PARK, S., KIM, Y., KIM, J., LEE, M. and RYU, H., 2004. Mesenchymal progenitor cells in the human umbilical cord. Annals of Hematology, 83(12), pp. 733-738.

KINNER, B., ZALESKAS, J. and SPECTOR, M., 2002. Regulation of smooth muscle actin expression and contraction in adult human mesenchymal stem cells. Experimental cell research, 278(1), pp. 72-83.

KOLF, C.M., CHO, E. and TUAN, R.S., 2007. Mesenchymal stromal cells: biology of adult mesenchymal stem cells: regulation of niche, self-renewal and differentiation. Arthritis research & therapy, 9(1), pp. 204.

KONDOH, H., LLEONART, M., BERNARD, D. and GIL, J., 2007. Protection from oxidative stress by enhanced glycolysis; a possible mechanism of cellular immortalization. Histology and histopathology, 22(1/3), pp. 85.

KONDOH, H., LLEONART, M.E., GIL, J., WANG, J., DEGAN, P., PETERS, G., MARTINEZ, D., CARNERO, A. and BEACH, D., 2005. Glycolytic enzymes can modulate cellular life span. Cancer research, 65(1), pp. 177-185.

KONIGSBERG, M., PEREZ, V., RIOS, C., LIU, Y., LEE, S., SHI, Y. and VAN REMMEN, H., 2013. Effect of oxygen tension on bioenergetics and proteostasis in young and old myoblast precursor cells. Redox biology, 1(1), pp. 475-482.

KRAUSE, D.S., SCADDEN, D.T. and PREFFER, F.I., 2013. The hematopoietic stem cell niche—home for friend and foe? Cytometry Part B: Clinical Cytometry, 84(1), pp. 7-20.

KULTERER, B., FRIEDL, G., JANDROSITZ, A., SANCHEZ-CABO, F., PROKESCH, A., PAAR, C., SCHEIDELER, M., WINDHAGER, R., PREISEGGER, K. and TRAJANOSKI, Z., 2007. Gene expression profiling of human mesenchymal stem cells derived from bone marrow during expansion and osteoblast differentiation. BMC genomics, 8(1), pp. 70.

KUMAR, D., DALE, T.P., YANG, Y. and FORSYTH, N.R., 2015. Self-renewal of human embryonic stem cells on defined synthetic electrospun nanofibers. Biomedical Materials, 10(6), pp. 065017.

LAPPALAINEN, R.S., SALOMÄKI, M., YLÄ-OUTINEN, L., HEIKKILÄ, T.J., HYTTINEN, J.A., PIHLAJAMÄKI, H., SUURONEN, R., SKOTTMAN, H. and NARKILAHTI, S., 2010. Similarly derived and cultured hESC lines show variation in their developmental potential towards neuronal cells in long-term culture. Regenerative medicine, 5(5), pp. 749-762.

LE BLANC, K., TAMMIK, C., ROSENDAHL, K., ZETTERBERG, E. and RINGDÉN, O., 2003. HLA expression and immunologic propertiesof differentiated and undifferentiated mesenchymal stem cells. Experimental hematology, 31(10), pp. 890-896.

LEES, J.G., RATHJEN, J., SHEEDY, J.R., GARDNER, D.K. and HARVEY, A.J., 2015. Distinct profiles of human embryonic stem cell metabolism and mitochondria identified by oxygen. Reproduction (Cambridge, England), 150(4), pp. 367-382.

LEÓN, Z., GARCÍA-CAÑAVERAS, J.C., DONATO, M.T. and LAHOZ, A., 2013. Mammalian cell metabolomics: experimental design and sample preparation. Electrophoresis, 34(19), pp. 2762-2775.

LI, B., RYAN, P.W., RAY, B.H., LEISTER, K.J., SIRIMUTHU, N. and RYDER, A.G., 2010. Rapid characterization and quality control of complex cell culture media solutions using Raman spectroscopy and chemometrics. Biotechnology and bioengineering, 107(2), pp. 290-301.

LI, N., LIU, W., LI, W., LI, S., CHEN, X., BI, K. and HE, P., 2010. Plasma metabolic profiling of Alzheimer's disease by liquid chromatography/mass spectrometry. Clinical biochemistry, 43(12), pp. 992-997.

LIESENER, A. and KARST, U., 2005. Monitoring enzymatic conversions by mass spectrometry: a critical review. Analytical and bioanalytical chemistry, 382(7), pp. 1451-1464.

LIN, L., HUANG, Z., GAO, Y., YAN, X., XING, J. and HANG, W., 2011. LC-MS based serum metabonomic analysis for renal cell carcinoma diagnosis, staging, and biomarker discovery. Journal of proteome research, 10(3), pp. 1396-1405.

LODI, D., IANNITTI, T. and PALMIERI, B., 2011. Stem cells in clinical practice: applications and warnings. Journal of Experimental & Clinical Cancer Research, 30(1), pp. 9.

LUND, P., PILGAARD, L., DUROUX, M., FINK, T. and ZACHAR, V., 2009. Effect of growth media and serum replacements on the proliferation and differentiation of adipose-derived stem cells. Cytotherapy, 11(2), pp. 189-197.

MA, T., GRAYSON, W.L., FRÖHLICH, M. and VUNJAK-NOVAKOVIC, G., 2009. Hypoxia and stem cell-based engineering of mesenchymal tissues. Biotechnology progress, 25(1), pp. 32-42.

MAKINO, S., FUKUDA, K., MIYOSHI, S., KONISHI, F., KODAMA, H., PAN, J., SANO, M., TAKAHASHI, T., HORI, S., ABE, H., HATA, J., UMEZAWA, A. and OGAWA, S., 1999. Cardiomyocytes can be generated from marrow stromal cells in vitro. The Journal of clinical investigation, 103(5), pp. 697-705.

MANZO-AVALOS, S. and SAAVEDRA-MOLINA, A., 2010. Cellular and mitochondrial effects of alcohol consumption. International journal of environmental research and public health, 7(12), pp. 4281-4304.

MAROM, R., SHUR, I., SOLOMON, R. and BENAYAHU, D., 2005. Characterization of adhesion and differentiation markers of osteogenic marrow stromal cells. Journal of cellular physiology, 202(1), pp. 41-48.

MARTIN, G.R., 1981. Isolation of a pluripotent cell line from early mouse embryos cultured in medium conditioned by teratocarcinoma stem cells. Proceedings of the National Academy of Sciences of the United States of America, 78(12), pp. 7634-7638.

MEIRELLES, L.D.S. and NARDI, N.B., 2003. Murine marrow-derived mesenchymal stem cell: isolation, in vitro expansion, and characterization. British journal of haematology, 123(4), pp. 702-711.

MICCHELI, A.T., MICCHELI, A., DI CLEMENTE, R., VALERIO, M., COLUCCIA, P., BIZZARRI, M. and CONTI, F., 2006. NMR-based metabolic profiling of human hepatoma cells in relation to cell growth by culture media analysis. Biochimica et Biophysica Acta (BBA)-General Subjects, 1760(11), pp. 1723-1731.

MILLMAN, J.R., TAN, J.H. and COLTON, C.K., 2009. The effects of low oxygen on self-renewal and differentiation of embryonic stem cells. Current opinion in organ transplantation, 14(6), pp. 694-700.

MITALIPOV, S. and WOLF, D., 2009. Totipotency, pluripotency and nuclear reprogramming. Engineering of stem cells. Springer, pp. 185-199.

MOCHALSKI, P., SPONRING, A., KING, J., UNTERKOFLER, K., TROPPMAIR, J. and AMANN, A., 2013. Release and uptake of volatile organic compounds by human hepatocellular carcinoma cells (HepG2) in vitro. Cancer cell international, 13(1), pp. 72.

MOHYELDIN, A., GARZÓN-MUVDI, T. and QUIÑONES-HINOJOSA, A., 2010. Oxygen in stem cell biology: a critical component of the stem cell niche. Cell stem cell, 7(2), pp. 150-161.

MORRISON, S.J. and SPRADLING, A.C., 2008. Stem cells and niches: mechanisms that promote stem cell maintenance throughout life. Cell, 132(4), pp. 598-611.

MOUSSAVI-HARAMI, F., DUWAYRI, Y., MARTIN, J.A., MOUSSAVI-HARAMI, F. and BUCKWALTER, J.A., 2004. Oxygen effects on senescence in chondrocytes and mesenchymal stem cells: consequences for tissue engineering. The Iowa orthopaedic journal, 24, pp. 15-20.

MUÑOZ, N., KIM, J., LIU, Y., LOGAN, T.M. and MA, T., 2014. Gas chromatography–mass spectrometry analysis of human mesenchymal stem cell metabolism during proliferation and osteogenic differentiation under different oxygen tensions. Journal of Biotechnology, 169, pp. 95-102.

MURAGLIA, A., CANCEDDA, R. and QUARTO, R., 2000. Clonal mesenchymal progenitors from human bone marrow differentiate in vitro according to a hierarchical model. Journal of cell science, 113 (Pt 7)(Pt 7), pp. 1161-1166.

NAKAMURA, A.J., CHIANG, Y.J., HATHCOCK, K.S., HORIKAWA, I., SEDELNIKOVA, O.A., HODES, R.J. and BONNER, W.M., 2008. Both telomeric and non-telomeric DNA damage are determinants of mammalian cellular senescence. Epigenetics & chromatin, 1(1), pp. 6.

NÄRVÄ, E., PURSIHEIMO, J., LAIHO, A., RAHKONEN, N., EMANI, M.R., VIITALA, M., LAURILA, K., SAHLA, R., LUND, R. and LÄHDESMÄKI, H., 2013. Continuous hypoxic culturing of human embryonic stem cells enhances SSEA-3 and MYC levels. PloS one, 8(11), pp. e78847.

NICHOLSON, J.K., LINDON, J.C. and HOLMES, E., 1999. 'Metabonomics': understanding the metabolic responses of living systems to pathophysiological stimuli via multivariate statistical analysis of biological NMR spectroscopic data. Xenobiotica, 29(11), pp. 1181-1189.

NIEBRUEGGE, S., BAUWENS, C.L., PEERANI, R., THAVANDIRAN, N., MASSE, S., SEVAPTISIDIS, E., NANTHAKUMAR, K., WOODHOUSE, K., HUSAIN, M. and KUMACHEVA, E., 2009. Generation of human embryonic stem cell-derived mesoderm and cardiac cells using size-specified aggregates in an oxygen-controlled bioreactor. Biotechnology and bioengineering, 102(2), pp. 493-507.

NIU, D., KONDO, T., NAKAZAWA, T., OISHI, N., KAWASAKI, T., MOCHIZUKI, K., YAMANE, T. and KATOH, R., 2012. Transcription factor Runx2 is a regulator of

epithelial-mesenchymal transition and invasion in thyroid carcinomas. Laboratory investigation, 92(8), pp. 1181.

OHLSTEIN, B., KAI, T., DECOTTO, E. and SPRADLING, A., 2004. The stem cell niche: theme and variations. Current opinion in cell biology, 16(6), pp. 693-699.

OLIVER, S.G., WINSON, M.K., KELL, D.B. and BAGANZ, F., 1998. Systematic functional analysis of the yeast genome. Trends in biotechnology, 16(9), pp. 373-378.

OSAFUNE, K., CARON, L., BOROWIAK, M., MARTINEZ, R.J., FITZ-GERALD, C.S., SATO, Y., COWAN, C.A., CHIEN, K.R. and MELTON, D.A., 2008. Marked differences in differentiation propensity among human embryonic stem cell lines. Nature biotechnology, 26(3), pp. 313.

OTTE, A., BUCAN, V., REIMERS, K. and HASS, R., 2013. Mesenchymal stem cells maintain long-term in vitro stemness during explant culture. Tissue Engineering Part C: Methods, 19(12), pp. 937-948.

OTTOSEN, L.D., HINDKJÆR, J., HUSTH, M., PETERSEN, D.E., KIRK, J. and INGERSLEV, H.J., 2006. Observations on intrauterine oxygen tension measured by fibre-optic microsensors. Reproductive biomedicine online, 13(3), pp. 380-385.

PANOPOULOS, A.D., YANES, O., RUIZ, S., KIDA, Y.S., DIEP, D., TAUTENHAHN, R., HERRERIAS, A., BATCHELDER, E.M., PLONGTHONGKUM, N., LUTZ, M., BERGGREN, W.T., ZHANG, K., EVANS, R.M., SIUZDAK, G. and IZPISUA BELMONTE, J.C., 2012. The metabolome of induced pluripotent stem cells reveals metabolic changes occurring in somatic cell reprogramming. Cell research, 22(1), pp. 168-177.

PASINI, P., POWAR, N., GUTIERREZ-OSUNA, R., DAUNERT, S. and RODA, A., 2004. Use of a gas-sensor array for detecting volatile organic compounds (VOC) in chemically induced cells. Analytical and bioanalytical chemistry, 378(1), pp. 76-83.

PATTAPPA, G., THORPE, S.D., JEGARD, N.C., HEYWOOD, H.K., DE BRUIJN, J.D. and LEE, D.A., 2012. Continuous and uninterrupted oxygen tension influences the colony formation and oxidative metabolism of human mesenchymal stem cells. Tissue Engineering Part C: Methods, 19(1), pp. 68-79.

PENG, L., JIA, Z., YIN, X., ZHANG, X., LIU, Y., CHEN, P., MA, K. and ZHOU, C., 2008. Comparative analysis of mesenchymal stem cells from bone marrow, cartilage, and adipose tissue. Stem cells and development, 17(4), pp. 761-774.

PERA, M.F., REUBINOFF, B. and TROUNSON, A., 2000. Human embryonic stem cells. Journal of cell science, 113 (Pt 1)(Pt 1), pp. 5-10.

PITTENGER, M.F., MACKAY, A.M., BECK, S.C., JAISWAL, R.K., DOUGLAS, R., MOSCA, J.D., MOORMAN, M.A., SIMONETTI, D.W., CRAIG, S. and MARSHAK, D.R., 1999. Multilineage potential of adult human mesenchymal stem cells. Science (New York, N.Y.), 284(5411), pp. 143-147.

RAJALA, K., VAAJASAARI, H., SUURONEN, R., HOVATTA, O., SKOTTMAN,H., 2011. Effects of the physiochemical culture environment on the stemness and pluripotency of human embryonic stem cells. Stem Cell Studies, 1(1),.

RICHARDSON, J.D., NELSON, A.J., ZANNETTINO, A.C., GRONTHOS, S., WORTHLEY, S.G. and PSALTIS, P.J., 2013. Optimization of the cardiovascular therapeutic properties of mesenchymal stromal/stem cells–taking the next step. Stem Cell Reviews and Reports, 9(3), pp. 281-302.

RIEKSTINA, U., CAKSTINA, I., PARFEJEVS, V., HOOGDUIJN, M., JANKOVSKIS, G., MUIZNIEKS, I., MUCENIECE, R. and ANCANS, J., 2009. Embryonic stem cell marker expression pattern in human mesenchymal stem cells derived from bone marrow, adipose tissue, heart and dermis. Stem Cell Reviews and Reports, 5(4), pp. 378-386.

ROBERTS, L.D., SOUZA, A.L., GERSZTEN, R.E. and CLISH, C.B., 2012. Targeted metabolomics. Current protocols in molecular biology, , pp. 30.2. 1-30.2. 24.

RODESCH, F., SIMON, P., DONNER, C. and JAUNIAUX, E., 1992. Oxygen measurements in endometrial and trophoblastic tissues during early pregnancy. Obstetrics & Gynecology, 80(2), pp. 283-285.

ROSOVA, I., DAO, M., CAPOCCIA, B., LINK, D. and NOLTA, J.A., 2008. Hypoxic preconditioning results in increased motility and improved therapeutic potential of human mesenchymal stem cells. Stem cells, 26(8), pp. 2173-2182.

ROWAN, D.D., 2011. Volatile metabolites. Metabolites, 1(1), pp. 41-63.

RUDNICKA, J., KOWALKOWSKI, T., LIGOR, T. and BUSZEWSKI, B., 2011. Determination of volatile organic compounds as biomarkers of lung cancer by SPME–GC–TOF/MS and chemometrics. Journal of Chromatography B, 879(30), pp. 3360-3366.

RUTTER, A.V., CHIPPENDALE, T.W., YANG, Y., ŠPANĚL, P., SMITH, D. and SULÉ-SUSO, J., 2013. Quantification by SIFT-MS of acetaldehyde released by lung cells in a 3D model. Analyst, 138(1), pp. 91-95.

SAEED, H., AHSAN, M., SALEEM, Z., IQTEDAR, M., ISLAM, M., DANISH, Z. and KHAN, A.M., 2016. Mesenchymal stem cells (MSCs) as skeletal therapeutics–an update. Journal of Biomedical Science, 23(1), pp. 41.

SATO, Y., ARAKI, H., KATO, J., NAKAMURA, K., KAWANO, Y., KOBUNE, M., SATO, T., MIYANISHI, K., TAKAYAMA, T., TAKAHASHI, M., TAKIMOTO, R., IYAMA, S., MATSUNAGA, T., OHTANI, S., MATSUURA, A., HAMADA, H. and NIITSU, Y., 2005. Human mesenchymal stem cells xenografted directly to rat liver are differentiated into human hepatocytes without fusion. Blood, 106(2), pp. 756-763.

SCHRAUFSTATTER, I.U., DISCIPIO, R.G. and KHALDOYANIDI, S., 2011. Mesenchymal stem cells and their microenvironment. Frontiers in bioscience (Landmark edition), 16, pp. 2271-2288.

SEVERINI, A. and MORGAN, A.R., 1991. An assay for proteinases and their inhibitors based on DNA/ethidium bromide fluorescence. Analytical Biochemistry, 193(1), pp. 83-89.

SHEEHY, E.J., BUCKLEY, C.T. and KELLY, D.J., 2012. Oxygen tension regulates the osteogenic, chondrogenic and endochondral phenotype of bone marrow derived mesenchymal stem cells. Biochemical and biophysical research communications, 417(1), pp. 305-310.

SHESTIVSKA, V., ANTONOWICZ, S.S., DRYAHINA, K., KUBIŠTA, J., SMITH, D. and ŠPANĚL, P., 2015. Direct detection and quantification of malondialdehyde vapour in humid air using selected ion flow tube mass spectrometry supported by gas chromatography/mass spectrometry. Rapid Communications in Mass Spectrometry, 29(11), pp. 1069-1079.

SHI, S. and GRONTHOS, S., 2003. Perivascular niche of postnatal mesenchymal stem cells in human bone marrow and dental pulp. Journal of bone and mineral research, 18(4), pp. 696-704.

SHIN, H., UMBER, B.J., MEINARDI, S., LEU, S., ZALDIVAR, F., BLAKE, D.R. and COOPER, D.M., 2009. Acetaldehyde and hexanaldehyde from cultured white cells. Journal of translational medicine, 7(1), pp. 31.

SHUI, C., SPELSBERG, T.C., RIGGS, B.L. and KHOSLA, S., 2003. Changes in Runx2/Cbfa1 expression and activity during osteoblastic differentiation of human bone marrow stromal cells. Journal of Bone and Mineral Research, 18(2), pp. 213-221.

SILVA, W.A., COVAS, D.T., PANEPUCCI, R.A., PROTO-SIQUEIRA, R., SIUFI, J.L., ZANETTE, D.L., SANTOS, A.R. and ZAGO, M.A., 2003. The profile of gene expression of human marrow mesenchymal stem cells. Stem cells, 21(6), pp. 661-669.

SILVA, C.L., PASSOS, M. and CAMARA, J.S., 2011. Investigation of urinary volatile organic metabolites as potential cancer biomarkers by solid-phase microextraction in combination with gas chromatography-mass spectrometry. British journal of cancer, 105(12), pp. 1894-1904.

SIMON, M.C. and KEITH, B., 2008. The role of oxygen availability in embryonic development and stem cell function. Nature reviews.Molecular cell biology, 9(4), pp. 285-296.

SMITH, D. and ADAMS, N., 1988. The selected ion flow tube (SIFT): studies of ion-neutral reactions. Advances in atomic and molecular physics, 24, pp. 1-49.

SMITH, D. and ADAMS, N.G., 1980. Elementary plasma reactions of environmental interest. Plasma Chemistry I. Springer, pp. 1-43.

SMITH, D., PYSANENKO, A. and ŠPANĚL, P., 2009. Ionic diffusion and mass discrimination effects in the new generation of short flow tube SIFT-MS instruments. International Journal of Mass Spectrometry, 281(1), pp. 15-23.

SMITH, D. and SPANEL, P., 1995. Ions in the terrestrial atmosphere and in interstellar clouds. Mass spectrometry reviews, 14(4-5), pp. 255-278.

SMITH, D. and ŠPANĚL, P., 2005. Selected ion flow tube mass spectrometry (SIFT-MS) for on-line trace gas analysis. Mass spectrometry reviews, 24(5), pp. 661-700.

SMITH, D. and ŠPANĚL, P., 1996. Application of ion chemistry and the SIFT technique to the quantitative analysis of trace gases in air and on breath. International Reviews in Physical Chemistry, 15(1), pp. 231-271.

SMITH, D., WANG, T., SULÉ-SUSO, J., ŠPANĚL, P. and HAJ, A.E., 2003. Quantification of acetaldehyde released by lung cancer cells in vitro using selected ion flow tube mass spectrometry. Rapid communications in mass spectrometry, 17(8), pp. 845-850.

SMITH, D., SPANEL, P. and DAVIES, S., 1999. Trace gases in breath of healthy volunteers when fasting and after a protein-calorie meal: a preliminary study. Journal of applied physiology (Bethesda, Md.: 1985), 87(5), pp. 1584-1588.

SONG, L. and TUAN, R.S., 2004. Transdifferentiation potential of human mesenchymal stem cells derived from bone marrow. FASEB journal : official publication of the Federation of American Societies for Experimental Biology, 18(9), pp. 980-982.

SPANEL, P., HALL, E., WORKMAN, C. and SMITH, D., 2004. A directly coupled monolithic rectangular resonator forming a robust microwave plasma ion source for SIFT-MS. Plasma Sources Science and Technology, 13(2), pp. 282.

ŠPANĚL, P. and SMITH, D., 1996a. Selected ion flow tube: a technique for quantitative trace gas analysis of air and breath. Medical and Biological Engineering and Computing, 34(6), pp. 409-419.

ŠPANĚL, P., DRYAHINA, K., REJŠKOVÁ, A., CHIPPENDALE, T.W. and SMITH, D., 2011. Breath acetone concentration; biological variability and the influence of diet. Physiological Measurement, 32(8), pp. N23.

ŠPANĚL, P., PAVLIK, M. and SMITH, D., 1995. Reactions of H3O and OH− ions with some organic molecules; Applications to trace gas analysis in air. International journal of mass spectrometry and ion processes, 145(3), pp. 177-186.

SPANEL, P. and SMITH, D., 1995. Reactions of hydrated hydronium ions and hydrated hydroxide ions with some hydrocarbons and oxygen-bearing organic molecules. The Journal of physical chemistry, 99(42), pp. 15551-15556.

ŠPANĚL, P. and SMITH, D., 2011. Progress in SIFT-MS: Breath analysis and other applications. Mass spectrometry reviews, 30(2), pp. 236-267.

ŠPANĚL, P. and SMITH, D., 2000. Selected ion flow tube mass spectrometry analyses of stable isotopes in water: isotopic composition of H 3 O and H 3 O (H 2 O) 3 ions in exchange reactions with water vapor. Journal of the American Society for Mass Spectrometry, 11(10), pp. 866-875.

ŠPANĚL, P. and SMITH, D., 1996b. A selected ion flow tube study of the reactions of NO and O 2 ions with some organic molecules: The potential for trace gas analysis of air. The Journal of chemical physics, 104(5), pp. 1893-1899.

SPOONER, A.D., BESSANT, C., TURNER, C., KNOBLOCH, H. and CHAMBERS, M., 2009. Evaluation of a combination of SIFT-MS and multivariate data analysis for the diagnosis of Mycobacterium bovis in wild badgers. Analyst, 134(9), pp. 1922-1927.

STOVER, A.E., HERCULIAN, S., BANUELOS, M.G., NAVARRO, S.L., JENKINS, M.P. and SCHWARTZ, P.H., 2016. Culturing Human Pluripotent and Neural Stem Cells

in an Enclosed Cell Culture System for Basic and Preclinical Research. Journal of visualized experiments : JoVE, (112). doi(112), pp. 10.3791/53685.

SULÉ-SUSO, J., PYSANENKO, A., ŠPANĚL, P. and SMITH, D., 2009. Quantification of acetaldehyde and carbon dioxide in the headspace of malignant and non-malignant lung cells in vitro by SIFT-MS. Analyst, 134(12), pp. 2419-2425.

SURRATI, A., LINFORTH, R., FISK, I.D., SOTTILE, V. and KIM, D., 2016. Non-destructive characterisation of mesenchymal stem cell differentiation using LC-MS-based metabolite footprinting. Analyst, 141(12), pp. 3776-3787.

TAKAHASHI, K., TANABE, K., OHNUKI, M., NARITA, M., ICHISAKA, T., TOMODA, K. and YAMANAKA, S., 2007. Induction of pluripotent stem cells from adult human fibroblasts by defined factors. Cell, 131(5), pp. 861-872.

TAKAHASHI, K. and YAMANAKA, S., 2006. Induction of pluripotent stem cells from mouse embryonic and adult fibroblast cultures by defined factors. Cell, 126(4), pp. 663-676.

TANGERMAN, A., 2009. Measurement and biological significance of the volatile sulfur compounds hydrogen sulfide, methanethiol and dimethyl sulfide in various biological matrices. Journal of Chromatography B, 877(28), pp. 3366-3377.

TARTE, K., GAILLARD, J., LATAILLADE, J.J., FOUILLARD, L., BECKER, M., MOSSAFA, H., TCHIRKOV, A., ROUARD, H., HENRY, C., SPLINGARD, M., DULONG, J., MONNIER, D., GOURMELON, P., GORIN, N.C., SENSEBE, L. and SOCIETE FRANCAISE DE GREFFE DE MOELLE ET THERAPIE CELLULAIRE, 2010. Clinical-grade production of human mesenchymal stromal cells: occurrence of aneuploidy without transformation. Blood, 115(8), pp. 1549-1553.

TCHIRKOV, A. and LANSDORP, P.M., 2003. Role of oxidative stress in telomere shortening in cultured fibroblasts from normal individuals and patients with ataxia–telangiectasia. Human molecular genetics, 12(3), pp. 227-232.

TEMTEM, M., SILVA, L.M., ANDRADE, P.Z., DOS SANTOS, F., DA SILVA, C.L., CABRAL, J.M., ABECASIS, M.M. and AGUIAR-RICARDO, A., 2009. Supercritical CO 2 generating chitosan devices with controlled morphology. Potential application for drug delivery and mesenchymal stem cell culture. The Journal of Supercritical Fluids, 48(3), pp. 269-277.

THOMSON, J.A., ITSKOVITZ-ELDOR, J., SHAPIRO, S.S., WAKNITZ, M.A., SWIERGIEL, J.J., MARSHALL, V.S. and JONES, J.M., 1998. Embryonic stem cell lines derived from human blastocysts. Science (New York, N.Y.), 282(5391), pp. 1145-1147.

THOMSON, J.A., KALISHMAN, J., GOLOS, T.G., DURNING, M., HARRIS, C.P., BECKER, R.A. and HEARN, J.P., 1995. Isolation of a primate embryonic stem cell line. Proceedings of the National Academy of Sciences of the United States of America, 92(17), pp. 7844-7848.

TOIVONEN, S., OJALA, M., HYYSALO, A., ILMARINEN, T., RAJALA, K., PEKKANEN-MATTILA, M., ÄÄNISMAA, R., LUNDIN, K., PALGI, J. and WELTNER, J., 2013. Comparative analysis of targeted differentiation of human induced pluripotent stem cells (hiPSCs) and human embryonic stem cells reveals variability associated with incomplete transgene silencing in retrovirally derived hiPSC lines. Stem cells translational medicine, 2(2), pp. 83-93.

TOMITA, R., TODOROKI, K., MARUOKA, H., YOSHIDA, H., FUJIOKA, T., NAKASHIMA, M., YAMAGUCHI, M. and NOHTA, H., 2016. Amino acid metabolomics

using LC-MS/MS: assessment of cancer-cell resistance in a simulated tumor microenvironment. Analytical Sciences, 32(8), pp. 893-900.

TSAI, C.C., YEW, T.L., YANG, D.C., HUANG, W.H. and HUNG, S.C., 2012. Benefits of hypoxic culture on bone marrow multipotent stromal cells. American journal of blood research, 2(3), pp. 148-159.

TUMA, J. and CASEY, C.A., 2003. Dangerous byproducts of alcohol breakdown-focus on adducts. Alcohol Research and Health, 27, pp. 285-290.

TURNER, C., ŠPANĚL, P. and SMITH, D., 2006. A longitudinal study of ethanol and acetaldehyde in the exhaled breath of healthy volunteers using selected-ion flow-tube mass spectrometry. Rapid communications in mass spectrometry, 20(1), pp. 61-68.

TURNER, J., QUEK, L., TITMARSH, D., KRÖMER, J.O., KAO, L., NIELSEN, L., WOLVETANG, E. and COOPER-WHITE, J., 2014. Metabolic profiling and flux analysis of MEL-2 human embryonic stem cells during exponential growth at physiological and atmospheric oxygen concentrations. PloS one, 9(11), pp. e112757.

ULLAH, I., SUBBARAO, R.B. and RHO, G.J., 2015. Human mesenchymal stem cells - current trends and future prospective. Bioscience reports, 35(2), pp. 10.1042/BSR20150025.

USSHER, J.R., ELMARIAH, S., GERSZTEN, R.E. and DYCK, J.R., 2016. The emerging role of metabolomics in the diagnosis and prognosis of cardiovascular disease. Journal of the American College of Cardiology, 68(25), pp. 2850-2870.

VILLAS-BÔAS, S.G., MAS, S., ÅKESSON, M., SMEDSGAARD, J. and NIELSEN, J., 2005. Mass spectrometry in metabolome analysis. Mass spectrometry reviews, 24(5), pp. 613-646.

VILLAS-BÔAS, S.G., NOEL, S., LANE, G.A., ATTWOOD, G. and COOKSON, A., 2006. Extracellular metabolomics: a metabolic footprinting approach to assess fiber degradation in complex media. Analytical Biochemistry, 349(2), pp. 297-305.

WANG, D., WANG, C., PI, X., GUO, L., WANG, Y., LI, M., FENG, Y., LIN, Z., HOU, W. and LI, E., 2016. Urinary volatile organic compounds as potential biomarkers for renal cell carcinoma. Biomedical reports, 5(1), pp. 68-72.

WANG, L., LI, Z., WANG, Y., WU, Z. and YU, B., 2015. Dynamic expression profiles of marker genes in osteogenic differentiation of human bone marrow-derived mesenchymal stem cells. Chinese Medical Sciences Journal, 30(2), pp. 108-113.

WANG, L.D. and WAGERS, A.J., 2011. Dynamic niches in the origination and differentiation of haematopoietic stem cells. Nature reviews.Molecular cell biology, 12(10), pp. 643-655.

WERT, G.D. and MUMMERY, C., 2003. Human embryonic stem cells: research, ethics and policy. Human reproduction, 18(4), pp. 672-682.

WHITTLE, C.L., FAKHARZADEH, S., EADES, J. and PRETI, G., 2007. Human breath odors and their use in diagnosis. Annals of the New York Academy of Sciences, 1098(1), pp. 252-266.

WU, S.M. and HOCHEDLINGER, K., 2011. Harnessing the potential of induced pluripotent stem cells for regenerative medicine. Nature cell biology, 13(5), pp. 497-505.

XIE, G.X., CHEN, T.L., QIU, Y.P., SHI, P., ZHENG, X.J., SU, M.M., ZHAO, A.H., ZHOU, Z.T. and JIA, W., 2012. Urine metabolite profiling offers potential early diagnosis of oral cancer. Metabolomics, 8(2), pp. 220-231.

XUE, R., DONG, L., ZHANG, S., DENG, C., LIU, T., WANG, J. and SHEN, X., 2008. Investigation of volatile biomarkers in liver cancer blood using solid-phase microextraction and gas chromatography/mass spectrometry. Rapid communications in mass spectrometry, 22(8), pp. 1181-1186.

YAMANAKA, S. and BLAU, H.M., 2010. Nuclear reprogramming to a pluripotent state by three approaches. Nature, 465(7299), pp. 704-712.

ZHANG, A., SUN, H., WANG, P., HAN, Y. and WANG, X., 2012. Modern analytical techniques in metabolomics analysis. Analyst, 137(2), pp. 293-300.

ZHANG, J., YAN, L., CHEN, W., LIN, L., SONG, X., YAN, X., HANG, W. and HUANG, B., 2009. Metabonomics research of diabetic nephropathy and type 2 diabetes mellitus based on UPLC–oaTOF-MS system. Analytica Chimica Acta, 650(1), pp. 16-22.

ZHAO, Q., REN, H. and HAN, Z., 2016. Mesenchymal stem cells: Immunomodulatory capability and clinical potential in immune diseases. Journal of Cellular Immunotherapy, 2(1), pp. 3-20.

ZHAO, E., XU, H., WANG, L., KRYCZEK, I., WU, K., HU, Y., WANG, G. and ZOU, W., 2012. Bone marrow and the control of immunity. Cellular & molecular immunology, 9(1), pp. 11-19.

ZIMATKIN, S.M., PRONKO, S.P., VASILIOU, V., GONZALEZ, F.J. and DEITRICH, R.A., 2006. Enzymatic mechanisms of ethanol oxidation in the brain. Alcoholism: Clinical and Experimental Research, 30(9), pp. 1500-1505.

ZUK, P.A., ZHU, M., MIZUNO, H., HUANG, J., FUTRELL, J.W., KATZ, A.J., BENHAIM, P., LORENZ, H.P. and HEDRICK, M.H., 2001. Multilineage cells from

human adipose tissue: implications for cell-based therapies. Tissue engineering, 7(2), pp. 211-228.